Hot Mix Asphalt Surface Characteristics

Bernard Igbafen Izevbekhai, Principal Investigator
Office of Materials & Roads Research
Minnesota Department of Transportation

August 2014

Technical Report Documentation Page

1. Report No. MN/RC 2014-28	2.	3. Recipients Accession No.	
4. Title and Subtitle Hot Mix Asphalt Surface Characteristics		5. Report Date August 2014	
		6.	
7. Author(s) Bernard Izevbekhai, Mark Watson, Tim Clyne, and ManShean (Sharon) Wong		8. Performing Organization Report No.	
9. Performing Organization Name and Address Minnesota Department of Transportation Office of Materials & Road Research 1400 Gervais Avenue Maplewood, MN 55109		10. Project/Task/Work Unit No.	
		11. Contract (C) or Grant (G) No. LAB 868	
12. Sponsoring Organization Name and Address Minnesota Department of Transportation Research Services & Library 395 John Ireland Boulevard, MS 330 St. Paul, Minnesota 55155-1899		13. Type of Report and Period Covered Final Report	
		14. Sponsoring Agency Code	
15. Supplementary Notes http://www.lrrb.org/pdf/201428.pdf			

16. Abstract (Limit: 250 words)

This report presents results of the research that examined various asphalt pavement surfaces in the MnROAD facility. It covers the fundamentals of surface profilometry, describes the construction of the textures and elucidates the performance trends of the various surface parameters. The variables examined include friction, measured with the lock wheel skid truck, smoothness, measured with the light weight profiler, mean profile depth measured by the circular track meter, sound absorption measured by the acoustic impedance tube and Tire-Pavement-Interaction-Noise measured by the on board sound intensity device.

Traffic difference was found to be a significant variable in the friction trend of the asphalt surfaces when the low-volume road inside lane of the cells were compared to the corresponding outside lane and when the mainline driving and passing lanes were compared. Based on the Wilcoxon Rank sum, Wilcoxon Sign Rank, and the T-test, traffic levels affected skid resistance. Additionally, the frictional-time series appeared to follow the half-life equation typical of disintegrating materials. A similar test on tire-pavement-noise difference found traffic to be insignificant within the five years of monitored performance of the same test tracks.

This study found that certain surface characteristics change with time regardless of traffic while others change with time and traffic. As the study found friction to be related to traffic, periodic measurements of friction can be performed when practicable, otherwise the half-life model developed in this study may be a rough predictor. In the deduced model, friction degradation appeared to be a function of the initial friction number and traffic-induced decay factor. In the low-volume road, there was hardly any evidence of effect of traffic on friction from a comparison of the traffic and environmental lanes. However, at higher traffic levels, (mainline driving versus passing lanes) traffic appeared to affect noise and friction.

The study also proposes a temperature-based correction algorithm for Tire-Pavement-Interaction-Noise. From distress mapping, IRI, and permeability measurements, there were no noticeable trends within the five years of study. Additionally, this research performed advanced data analysis, identified significant variables and accentuated intrinsic relationships between them. Additionally, the "on board sound intensity" (OBSI)-Temperature correlation exhibited a negative polynomial relationship indicating the higher importance of temperature to OBSI relationship in asphalt than published characteristics of concrete pavements. It ascertained that texture mean profile depth was not as significant as texture skewness in predicting surface properties. Smoothness measurements indicated that most asphalt surfaces are not associated with laser-induced anomalous IRI reading errors. The major properties affecting ride in most asphalt surfaces were evidently extraneous to the surface texture features.

17. Document Analysis/Descriptors Asphalt pavements, texture, smoothness, mean profile depth, surface friction, texture half life, skewness, sound absorption		18. Availability Statement No restrictions. Document available from: National Technical Information Services, Alexandria, Virginia 22312	
19. Security Class (this report) Unclassified	20. Security Class (this page) Unclassified	21. No. of Pages 188	22. Price

Hot Mix Asphalt Surface Characteristics

Final Report

Prepared by:

Bernard Igbafen Izevbekhai
Mark Watson
Tim Clyne
ManShean (Sharon) Wong
Minnesota Department of Transportation
Office of Materials & Road Research

August 2014

TABLE OF CONTENTS

LIST OF FIGURES IN TEXT

LIST OF TABLES

ACKNOWLEDGEMENTS

Bernard Igbafen Izevbekhai, P.E., Ph.D.

Research Operations Engineer

Minnesota Department of Transportation

1400 Gervais Avenue Maplewood MN 55109

E-mail: Bernard.izevbekhai@state.mn.us

Phone: 651 3665454 Fax: 6513665461

July 2014

CHAPTER 1
INTRODUCTION & DEFINITIONS

STUDY OBJECTIVES AND RESEARCH OVERVIEW

Study Objectives

Prior to this study, MnDOT needed to know how various asphalt surface types perform over time. It therefore initiated this study to evaluate frictional properties, texture configurations, texture durability, ride quality, acoustic impedance and noise characteristics of asphalt surfaces. Study was aimed at ascertaining optimal and economic textures or surfaces that optimize durability, quietness, friction and ride quality. While 4 years were not considered sufficient to accomplish all the objectives particularly in long terms, it aims at accentuating the short-term properties for extrapolations where tenable. Additionally, this study served at the barest minimum as a springboard for continuation of research on asphalt surfaces.

Research Overview

The work done in this research is best accentuated through the tasks outlined and performed. Task 1 performed a literature review detailing state-of-the-practice and state-of-the-art techniques for measuring, analyzing, and modeling pavement surface characteristics. The interrelationships between noise, texture, ride, friction, and durability will be reviewed.

Task 2 described test section construction and initial monitoring Construction on several MnROAD test cells used for this study took place during the summer of 2008. Immediately after construction texture, friction, noise and ride measurements were performed. This served as baseline measurements for comparison in subsequent data collection efforts. Several pieces of equipment and software acquired to assist in data collection and analysis in the study were discussed.
Deliverable for Task 2: PowerPoint presentation and summary report.

Task 3 involved Subcontracts for Additional Measurements and Analysis
Outside researchers/consultants will be hired to perform additional surface characteristic measurements that MnDOT is not currently equipped to perform. These measurements included statistical pass by (noise), sound absorption, Robotex (3-D surface texture), rolling resistance (fuel efficiency), and others. In addition, consultants may be hired to perform advanced data

analysis on certain surface characteristic measurements (e.g., the effect of texture on sound absorption). Reports were rendered for each task.

Task 4 performed and discussed seasonal measurements of surface characteristics (2009)
The surface characteristics measurements performed twice per year for four years quantified seasonal variation. Noise was measured with On Board Sound Intensity (OBSI) protocol and the sound absorption tube. Texture was measured with the sand volumetric technique or a laser device ASTM E-2157. Ride was measured with the triple and single laser of the lightweight profiler. Friction was measured with a skid trailer according to ASTM E 274 procedure, the dynamic friction tester, and other devices as they became available. Durability was assessed in terms of pavement raveling and cracking according to a MnDOT-modified LTPP distress survey.

Task 5 Performed and discussed Seasonal Measurements of Surface Characteristics (2010)

Task 6 performed and discussed Seasonal Measurements of Surface Characteristics (2011)

Task 7 performed and discussed Seasonal Measurements of Surface Characteristics (2012)

Task 8 was the analytical part of the study where the data from tasks 2-7 were analyzed mathematically and statistically. Among many other things, this task developed a process for extracting skewness from the texture data using a software PARSER and analyzed it to ascertain the importance of the skewness parameter in asphalt surfaces. Other analysis included the influence of traffic on Ride friction and noise. Additionally, friction degradation was examined in the light of analysis of experimental data. The field data collected during the project was analyzed graphically. Relationships between the various pavement surface characteristics will be identified and characterized. Deliverable for Task 8: PowerPoint presentation and summary report.

Task 9 performed a technical summary for Deployment and Implementation of the lessons learned in this study. This technical brief will be written and distributed to interested parties both locally and nationally. Where applicable, revised protocols and/or specifications will be

proposed for asphalt mixtures (MnDOT Bituminous Office) and noise mitigation techniques (MnDOT Office of Environmental Services).

Task 10 performed a compilation of the draft final report on this study. For the avoidance of redundancy, this final report included the background and state of the art in one chapter, construction of various textures in the next chapter followed by the fourth year performance report in the third chapter. It was not deemed necessary to enunciate the previous years' performance since these were reflected in the fourth year time series. The data analysis was the bulk of the final report and was presented in the 4th chapter. The 5th chapter presents the conclusion and recommendations.

BACKGROUND

Pavement surface characteristics are composed of several different interrelated parameters, which will be defined later. These parameters include texture, ride, friction, noise and durability. Often times the same measured parameter obtained using one device does not necessarily correlate with the same parameter measurements obtained using another device – this has led to recent efforts to harmonize results using international indexes such as the international friction index (IFI that combines friction value and a speed number) and the international ride index (IRI). These indexes have helped researchers to quantify and compare results obtained in different locations, with different equipment and under different conditions. Texture and ride are commonly evaluated using spectral analysis, which can be described using two parameters: a horizontal component, or wavelength (λ) and a vertical component, or amplitude (a). Figure 1.1 below shows typical influence of different texture wavelengths on pavement surface characteristics. Note that some characteristics such as noise, friction, and splash and spray are affected by the same wavelength.
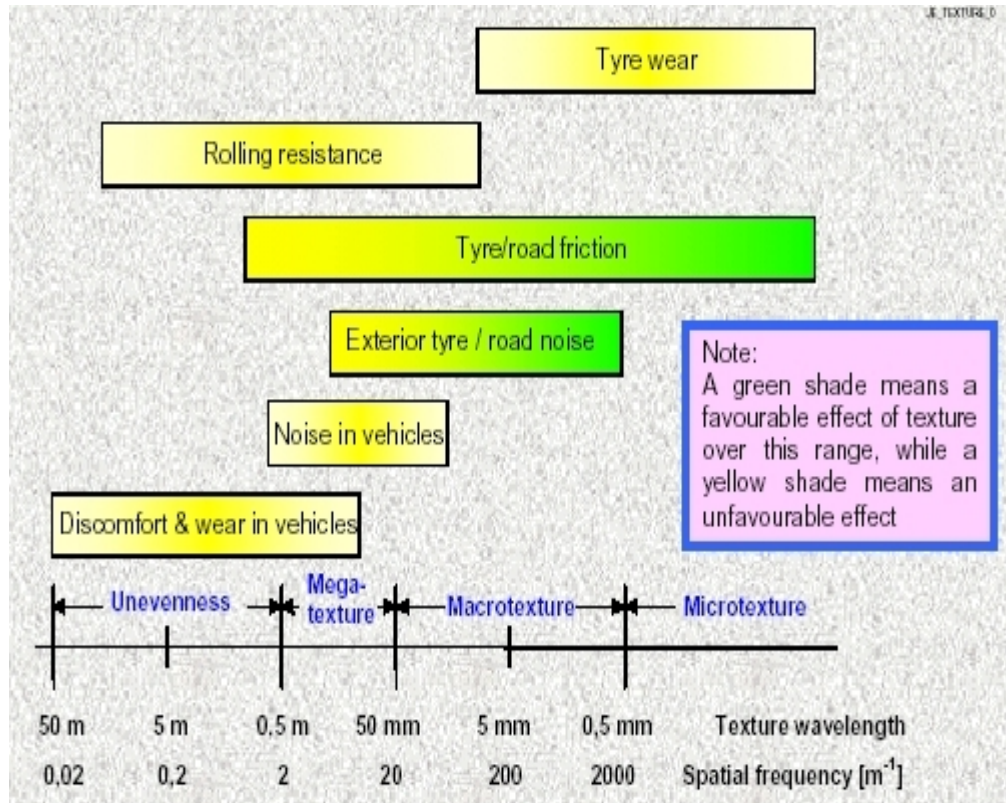
Figure 1.1 Texture Wavelength Influence on Surface Characteristics [2]

Skid Resistance:

Skid Resistance is the amount of force generated when a tire slides on a wet pavement [3]. The skid resistance is affected by both microtexture and macrotexture. It decreases with increasing speed.

Microtexture:

Microtexture has a relative horizontal wavelength (λ) of less than 0.5mm, and relative vertical amplitude (a) of less than 1 mm. This provides the direct contact between the tire and the pavement surface, as well as providing the adhesion component of friction [5].

Macrotexture:

Macrotexture results from the large aggregate particles and has a relative wavelength (λ) between 0.5-mm and 50-mm, and amplitude (a) of less than 10-mm. This allows for the drainage of water, which improves the contact between the tire and the pavement surface and reduces the

5

occurrence of hydroplaning [5]. It also provides the hysteresis component of friction [5]. Note that wavelengths larger than 0.5 mm are defined by the terms roughness, or evenness.
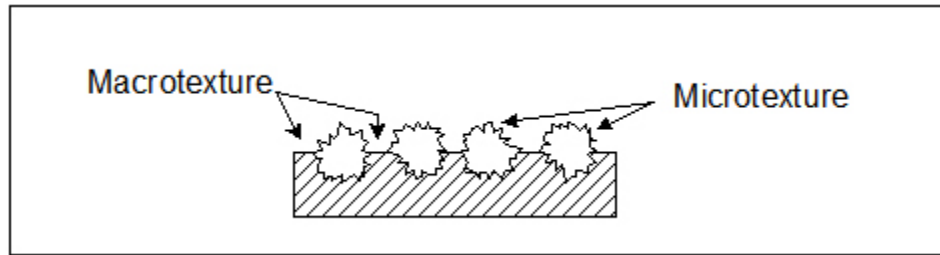
Figure 1.2: Microtexture vs. Macrotexture [1]

Megatexture:

Surface irregularities with wavelengths between 50-mm and 500-mm and vertical amplitudes between 0.1 and 50 mm imply megatexture [6]. Note that the wavelengths are of the same order of magnitude as the tire pavement interface and are responsible for low frequency noise generation and vehicle vibrations [6].

Mean Texture Depth (MTD):

ASTM defines the mean texture depth (MTD) as "The mean depth of the pavement surface macrotexture determined by the volumetric technique of ASTM method E 965" [7].

Mean Profile Depth (MPD):

ASTM defines the mean profile depth (MPD) as "The average of all the mean segment depths of all the segments of the profile" [7]. The PIARC international experiment [3, 9] discovered that the best parameter to describe the pavements macrotexture is the MPD. The MTD and MPD are related by equation 1 when the MTD was found using glass spheres of diameter 0.2mm. Note that when MPD predicts MTD the result is estimated texture depth (ETD). The coefficients of equation 1 change with different methods [3].

$$MTD = 0.79MPD + 0.23 \qquad (1)$$

International Friction Index:

The International Friction Index (IFI) is composed of a friction number (F60) and a speed constant (Sp) [3]. Sp relates to the macrotexture [1] while friction value and the speed constant [2] [3] generate F60.

$$S_p = a + b * TX \quad (1) \qquad F60 = A + B * FRS * e^{\frac{S-60}{S_p}} + C * TX \qquad (2)$$

Where:

- *a* and *b* are constants determined for each specific texture *TX*
- *FRS* is the measurement of friction by a specific device at speed *S*
- *A*, *B* and *C* are device specific constants tabulated in ASTM E-1960 [10]
- *C* is zero for smooth tires, and non-zero for ribbed, or patterned tires

International Ride Index (IRI):

A MnDOT report [8] defines the international Ride Index (IRI) as "The amount of vertical movement a vehicle would experience over a given horizontal stretch of road" [8]. A clearer definition actually reflects the vertical displacement as a function of vertical acceleration of the quarter car travelling on that profile at 50 miles per hour. An extremely rough spot on a smooth road would produce little change in IRI for a long analysis section.

MEASURING SURFACE CHARACTERISTICS

Often times it is insufficient to measure only one surface characteristic, and it becomes necessary to employ multiple tests to describe the pavement surface accurately [3]. In addition to measuring multiple characteristics, testing for surface characteristics must account for the changes due to temperature and seasons. There are also short-term changes, for example, when rain events wash off dust and oil accumulations from pavement surfaces, friction numbers (before and after this event) vary [3]. Special consideration must also be given to the equipment to ensure proper calibration. Often times it is difficult to compare measurements of the same characteristic made with two different devices. For instance, the Dynamic Friction Tester (DFT) generates a DFT number while the Lockwheel skid trailer generates a friction number (FN).

Correlation of one to the other for measurement taken on the same spot presents challenges. The next subsection describes some of the equipment and technologies used in this study.

SURFACE FRICTION

There currently is no system available to measure microtexture profiles at highway speeds [3] therefore these portable devices are used.

British Pendulum Tester (ASTM E 303-93):

The relatively simple portable device that has field and lab application has been in operation since 1960 [3]. A slider of known potential energy and low slip speed makes contact with the pavement over a fixed distance; the loss of energy due to the contact with the surface is due to friction. The results are reported in terms of a British Pendulum Number that can be used as a surrogate for microtexture. Preliminary measurements were made with this device but researchers were not certain of the repeatability of results are those were largely dependent on the condition of the plastic pads that often needed replacement.

Dynamic Friction Tester (DFT), ASTM E 1911:

The Dynamic Friction Tester (DFT) shown in Figure 1.3 below consists of three rubber sliders, positioned on a disk of diameter 13.75 in, that are suspended above the pavement surface. When the tangential velocity of the sliders reaches 90 km/hr water is applied to the surface and the sliders make contact with the pavement.
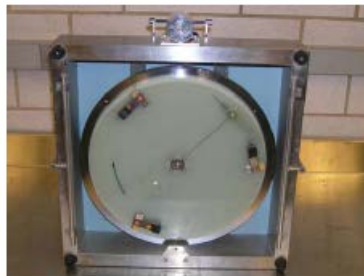
a) British Pendulum   b) DFT Contact Base   c) DFT Front/side View

Figure 1.3 MnDOT's Portable Friction Devices [23]

A computer takes friction measurements across a range of speeds as the sliders slow to a stop. A DFT value obtained at 20 km/hr, along with texture measurement provides a good indication of IFI [3].

Locked Wheel Skid Trailer Ribbed Tire (ASTM E 501) Smooth Tire (ASTM E 524):
The LWST test method is the most popular in the U.S. [3] (Figure 1.4). Both LWST testing methods are identical except in the specifications of the test tire; either a ribbed or a smooth tread tire can be used. The locked wheel system produces a slip speed (speed of the test tire relative to the speed of the vehicle) equal to that of the test vehicle (see Figure 1. 4), or a 100% slip condition. The brake is applied to the testing wheel and the resulting constant force is measured for an average of 1 second after the wheel is locked. Since the test does not give a continuous measurement, the Standard [11] requires at least five lockups in a uniform test section. The results are reported as a skid number, which is 100 times the friction value. Although most states use the ribbed tire, there has been an increased interest in use of the smooth tire. Furthermore, even though friction testing often times accompanies accident investigations, the friction values obtained from the tests are intended for comparison with other pavements, or to chart the change with time, and are insufficient to determine vehicle stopping distances [11]. The ribbed tire is primarily influenced by microtexture and the smooth tire is primarily influenced by macrotexture [3].

Figure 1.4-Locked Wheel Skid Trailer [23]

Fixed Slip Devices – Grip Tester (Figure 1.5) (No ASTM Available):

Although commonly used at airports, the Grip Tester device has not been widely applied on automotive pavements. This device operates at constant slip, but usually between 10 to 20%, not 100% as is the case with the LWST [3]. The Grip Tester, a common example, produces continuous measurements of low-speed friction opposed to the LWST, which produces spot measurements corresponding to a distance traveled by the vehicle in 1 second [3].

For fixed-slip and side-force, skid measurements at low tire slip speeds the effect of microtexture dominates, but at higher speeds, the effect of macrotexture dominates. Consequently, practitioners accompany friction with macrotexture measurement of macrotexture [3].

Figure 1.5: Grip Tester [4]

MACROTEXTURE

Sand Patch Test ASTM E 965-96:

This test reports the diameter (D) of a uniformly graded patch of sand or glass beads that is spread out to form a circle on the pavement surface (See Figure 1.6a). The volume of the material divided by the area is the mean texture depth (MTD) for a spot location on the pavement surface [12]. A National Aeronautic & Space Agency (NASA) variation of this method uses grease as a material, and a Japanese variation measures the length of glass spheres spread on the pavement surface over a fixed width with a linear track [3].

Circular Track Meter (CTMeter) ASTM E 2157-01:

This test, see Figure 1.6 b and c, is similar in concept to the sand patch (Figure 1.6a), except that the former uses lasers to measure the surface profile of a circle around a circumference. The

profile of this circle divided by the circumference yields a spot measurement of the MPD and a root mean square (RMS) value of the macrotexture profile [13].

| **(a) Sand Patch Process** | **(b) CTM Front View** | **(c) CTM Exposed Base** |

Figure 1.6 Measurement of Texture Depth [23]

Ultra-Light Inertial Profiler (ULIP) [14]:

A study conducted by de Fortier Smit and Waller [14] of the National Center for Asphalt Technology (NCAT) evaluated the ULIP in the measurement of macrotexture of different mixture types and surface textures at the test track. The macrotexture results correlated well with that of the sand patch and CTM measurements, the ULIP had the advantage of being able to take a continuous measurement (as opposed to a spot measurement) thus enabling the researchers to develop software to conduct a spectral analysis with the calculation of the L_4 and L_{63} ISO texture wavelength parameters.

The researchers cautioned that the device produced waviness pattern of 1.5 m from the tires of the SEGWAY® of which must be considered when conducting an analysis.

Outflow Meter:

The outflow meter characterizes the macrotexture of non-porous pavements effectively [3]. The time for the water level to fall by a fixed amount is the outflow time (OFT); this is highly correlated with both the MPD and the MTD [3].

MEGATEXTURE

RUGO Non-Contact Profilometer (developed by the French Laboratory of Roads and Bridges (Figure 1. 7) International Standard – ISO 5725:
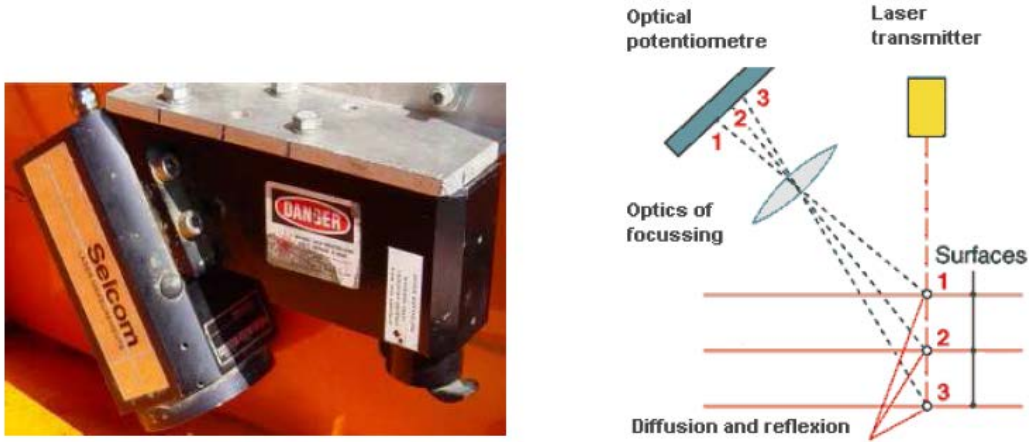
Figure 1.7: RUGO Device and Operating Principle [6]

Cerezo and Gothie [6] used the RUGO device by to characterize the megatexture of a pavement surface using the following formula:

$$L_{TX,\lambda} = 20 Log\left(\frac{a_\lambda}{a_{ref}}\right).$$

Where

a_λ is the mean square value of the vertical displacement of the surface profile

a_{ref} is 10^{-6}m

ai is the value obtained using a 1/3 octave band filter with center wavelength of i.

1. L_{ME} [dB]: Related to the whole of deformations (63 – 500mm). Is an overall assessment of pavement irregularities and is similar to a "mean value" of megatexture

2. L_{63} [dB]: Related to the shortest deformations (50, 63 and 80mm), which are responsible for the tire/pavement contact noise.

3. L_{500} [dB]: Related to the longest deformations (400, 500 and 630mm), which have an influence on vehicle vibrations.

Using the three parameters the researchers evaluated the repeatability and reproducibility of the megatexture measurements by conducting several tests on homogenous sections, at different speeds, sampling frequencies, and operators.

They found that the only parameter that influenced the measurements was the operator, as he chose the path of measurement. Small differences in this path led to differences in the megatexture values. Next the researchers performed a statistical analysis of the measured results

following ISO 5725-2 which led them to conclude that the megatexture measurement with the RUGO device had good accuracy. They noted that the next step in the research process was to correlate the megatexture measurements with noise measurements [6].

RIDE

Ride is typically measured using a profile device that characterizes the amount of vertical rise over a horizontal distance. This profile can be measured using lasers and accelerometers with van mounted pavement management vehicles for network level measurements, or with a light weight inertial surface analyzer device (LISA) for short distance, low speed measurements, see Figure 1.8 below [15]. It would be ideal for the profile to be measured with a straight laser line transverse to the pavement surface, however for practical reasons the point measurement (obtained with lasers) spaced at regular intervals are used. MnDOT pavement management vans utilize 5 lasers [8] (Figure 1.9) to obtain the profile and the current lightweight profile device in use by the department uses 3 lasers. In Sweden seventeen lasers are used to obtain the profile, while other countries use a single rotating laser to obtain numerous measurements.

Figure 1.8: Lightweight Inertial Surface Analyzer (LISA) [15]
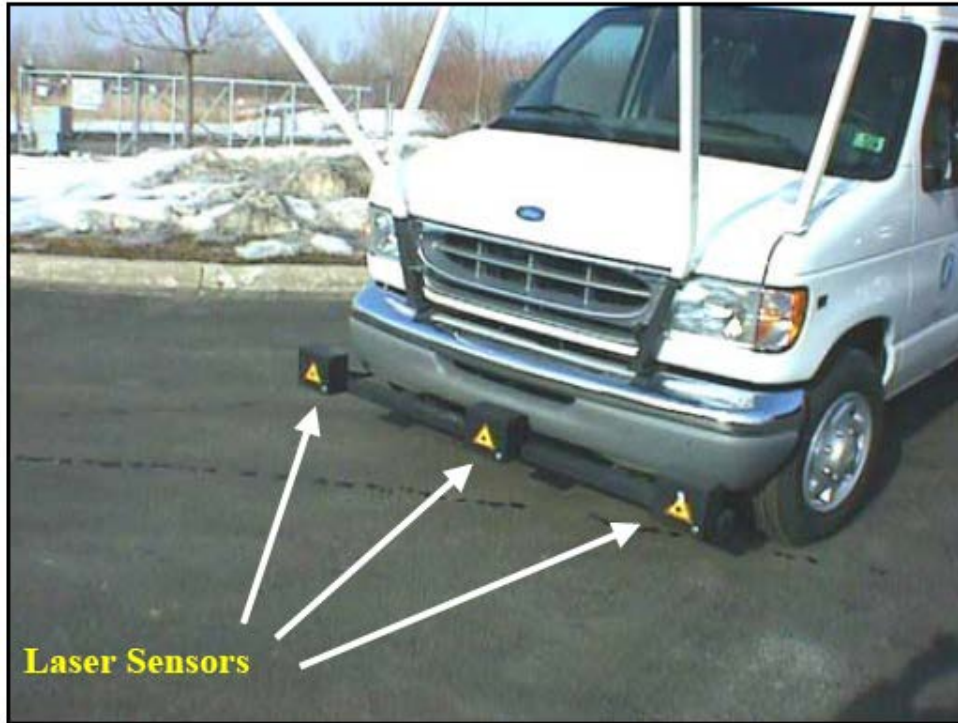
Figure 1.9: MnDOT Pavement Management Van [8]

As part of the NCHRP web document No 40, the FHWA identified the following devices in use to characterize smoothness for new HMA pavements by conducting a survey of State DOTs [15]. Note that the number in parentheses indicates the number of states using the device.

- Profilograph (24)
- Rolling Straight Edge (5)
- Straight edge (7)
- Mays Meter (3)
- Profiler (16)
- Rolling Dipstick (1)
- Hearne Straightedge (1)

The survey [15] also identified the unit of measurement to characterize ride, again the number in parentheses indicates the number of states responding.

- Profile Index (16)
- IRI (4)

14

- Straight Edge Variability (6)
- Other (6)

The Japanese developed two portable devices to quickly and accurately measure the profile of sidewalks: the Dekoboko Walk (DEK) and the DAM device, both of which are shown along with a dipstick in Figure 1.10 below. They found that the root mean square residuals (RMSE) of the devices were both the same and less than 6 mm for a section that was less than 10m in length.

Figure 1.10 DAM, DEK and Dipstick Profile Devices [15]

NOISE

Controlled Pass-by (CPB) and Statistical Pass-by (SPB):

Controlled Pass-by (CPB) measurements can be made with stationary microphones positioned near the road (usually 7.5m from the center of the measured lane at a height of 1.2m above the surface [17]) to obtain sound measurements. Controlling the number and types of vehicles that pass the microphones helps to control the random residuals [16]. Additionally vehicles can turn off the engine as they approach the microphone in order to measure the tire/road noise [17].

Statistical Pass-by (SPB) obtains sound measurements in the same manner as the CPB method; however the vehicles and tires are not controlled but are those in the free flowing traffic stream. Peak noise for a particular vehicle type is obtained along with the vehicle speed (usually

with a radar device), this information is then used to predict the average noise level of a particular vehicle group at a given reference speed within a certain confidence interval (determined by the sample size) [17].

Close Proximity (CPX) - On Board Sound Intensity (OBSI):

Close Proximity (CPX) methods usually obtain sound measurements while a vehicle is in motion using microphone(s) positioned very close to the tire pavement interaction [17]. The following is an excerpt from Izevbekhai [20] on the data collection process and operation of the on board sound intensity (OBSI) device shown in Figure 1.11. OBSI equipment consists of a Chevrolet Impala and eight intensity meters connected via four communication cables to a Bruel and Kjaer front-end collector connected to a dell laptop computer. The intensity meters are mounted on a rig system attached to a standard reference test tire that is installed at the rear left side of the vehicle and maintained at a temperature of 30 ˚C. After recording temperature, four intensity meters were plugged in to the B &K front-end unit, as well as 12v power supply and Ethernet (computer) cable. With this arrangement, the unit is capable of measuring repeatable tire-pavement-interaction noise of the tire-pavement contact-patch at a speed of 60 miles an hour, thus measuring approximately 440 ft within 5 seconds. It is mandatory to mount the rig on a non-dedicated vehicle and calibrate microphones. Durometer evaluation of the tire prior to measurement is also a required procedure, prior to data collection [20].

The report indicated that generally there was agreement between OBSI measurements taken by different operators, on different days.

Figure 1.11: MnDOT OBSI Set-Up [20]

16

Impedance Tube (ASTM E-1050 Modified) for In Situ Evaluation Sound Absorption:
MnDOT's BSWA 435 in-situ sound absorption measuring device consists mainly of a rigid impedance tube, capped by a white noise source, supported on a steady base and equipped with two microphones. The tube facilitates insulation from exterior sound source when the white noise source sends signals to the pavement surface. The 11 inch (100 mm) diameter tube accommodates two microphones that are connected to a frequency analyzer. These dimensions of the tube allow an analysis within a range of 20 and 800 Hertz. The separation of the incident noise from the reflected noise is accomplished by the transfer function method.

The sound absorption test is a process that measures the sound absorptiveness of a pavement surface. During the test, the sound analyzed is not generated by the interaction of the rolling tire with pavement surface but by noise source above the impedance tube. On the BSWA 425 device, a white noise source is used. White noise is a random audio signal with a flat power spectral density that contains noise at the same power at all frequencies. During the test, the impedance tube is placed on the pavement surface and a set of sensitive microphones are attached to the pre-installed housing at the lower end of the tube. These microphones are also connected to an analyzer. The noise source sends the incident sound energy (white noise) to the surface and the incident and reflected waves are captured by the two microphones. Software windows the reflected waves and converts the data to the 3rd octave sound absorption coefficient at 315, 400, 500, 750, 1000, 1250 and 1650 Hertz. Thus, the coefficients need to between one and zero where a value of one would mean that all of the sound is being absorbed.

Sound absorption output is generated as a function of frequency as shown in equation 1 (below). Ordinarily, the result is generated in a narrow band but 3rd octave band results are reported. Berengier et al discussed that the sound absorption coefficient (R_p) is expressed as a function of frequency:

$$|R_P(f)|^2 = 1 - \frac{1}{K_r^2}\left|\frac{P_r(f)}{P_d(f)}\right|^2 \tag{3}$$

Where: K_r is the spreading factor, P_r is the reflected sound energy and P_d is the incident sound energy [3]. The output of a sound absorption factor is typically in the form of the sound absorption at the seven frequencies defined earlier. This coefficient is therefore expressed as a function of frequency. With this information, the pervious or impervious surfaces can thoroughly be analyzed to evaluate acoustical properties.
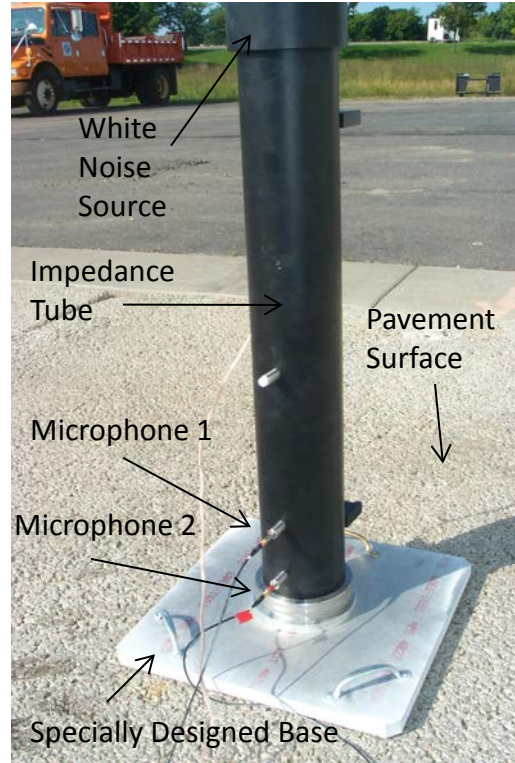
Figure 1.12 Impedance Tube

MULTIPLE PARAMETER DEVICES

High Speed Laser Systems:

 Recently Jackson [21] investigated the use of high-speed height-based sensor technology, as shown in Figure 1.13, to obtain friction and surface characteristics of asphalt pavement surfaces.

Figure 1.13: FDOT Unit High-Speed Laser System [21].

The researcher concluded that the device was able to accurately produce repeatable measures of the MPD. In addition, the relationship between the MTD and the MPD is similar to that in ASTM E 1845 which suggests that this device could be used to accurately obtain the MTD. The researcher provided an example as to how the FN40 data obtained from the device could be transformed to IFI. Finally, macrotexture appears to be a poor predictor of overall pavement friction, which is agrees with previous findings and recent industry pushes to adopt the IFI standard [21]. However this measurement of macrotexture at highway speeds could be combined with current friction measuring devices, such as a LWST, to obtain an IFI value.

Currently, Austria uses the RoadSTAR device, (Figure 1.14), to measure surface characteristics and road geometrics under normal traffic conditions (Table 1.1) [22].

Figure 1.14 RoadSTAR Device [22]

19

Table 1.1 Properties and Characteristics measured by RoadSTAR [22]

Skid Resistance

- 18 % Slip (Standard)
- blocked wheel
- Automatic Breaking System (ABS)
- Temperature of the road surface
- Temperature of the measuring tire

Macro-Texture

- MPD (Mean Profile Depth)
- ETD (Estimated Texture Depth)

Transverse Evenness

- Rut depth (left, right)
- Profile depth (left, right)
- Rut width
- Rut Volume
- theoretical waterfilm thickness
- Waterfilm width
- Waterfilm volume

Roughness

- IRI (International Roughness Index)
- RN (Ride Number)
- FFT-Analysis
- longitudinal profile

Road Geometry

- Curvature
- Crossfall
- Gradient
- height profile
- dGPS-co-ordinates

MODELS AND ANALYSES OF SURFACE CHARACTERISTICS

The Penn State Model [3] describes the relationship between friction μ and slip speed S using an exponential equation (3). Note in equation 4 that S_p is a speed constant.

$$\mu = \mu_0 * e^{-\frac{S}{S_P}} \tag{4}$$

The PIARC model (equation 5) is identical to the Penn State Model, but the intercept was shifted from 0 to 60 km/hr. Note that $F(S)$ is the friction obtained at a slip speed S, and $F60$ is the friction obtained at 60 km/hr.

$$F(S) = F60 * e^{\frac{60 - S}{S_p}} \tag{5}$$

The Rado model assumes that as the tire transitions from the free rolling to the locked wheel position, the friction increases from 0 to a peak value, then decreases to the locked wheel friction as shown in (equation 6) [3].

$$\mu(S) = \mu_{peak} * e^{-\left[\frac{\ln\left(S/S_{peak}\right)}{C}\right]^2} \tag{6}$$

Both the Penn State and the Rado Models [3] can be related to vehicle braking in emergencies.

In 2008, Khasawneh and Liang [23] published the results of their study to relate the surface characteristics of four different pavements. Friction results were obtained from the locked wheel skid trailer (LWST) and the dynamic friction tester (DFT) at different speeds, texture results were quantified using the mean profile depth (MPD) obtained from the circular texture meter (CTM). Rigorous statistical analysis consisting of simple linear regression among: Skid number (SN) obtained from LWST at 64 km/hr, Fn obtained from DFT at 64 and 20 km/hr, and MPD obtained from CTM was performed. In addition three models of linear regression were developed in an effort to predict SN (64) (skid number obtained at 64 km/hr using the LWST) from:

1. DFT at 64 km/hr and MPD,

2. DFT at 64 km/hr and DFT at 20 km/hr

3. DFT at 64 km/hr, DFT at 20 km/hr, and MPD.

Note that DFT at 64 km/hr was included to account for the effect of macrotexture and DFT at 20 km/hr was to account for the effect of microtexture. Normality and constant variance checks were performed on the residuals as these are important assumptions in linear regression. The results from the analysis were validated using analysis of variance (ANOVA) techniques.

The researchers concluded from the simple linear regression models that SN obtained at 64 km/hr was correlated to DFT at 64 and 20 km/hr. However the prediction of 20 km/hr was much lower and was attributed to the speed effect. There was a low coefficient of determination (R^2) between SN at 64 km/hr and MPD. This was attributed to the ribbed tire being insensitive to macrotexture. The multiple linear regressions revealed that MPD, and DFT at 20 km/hr did not add much to the regression model. DFT at 64 km/hr predicts SN at 64 km/hr [23].

In 2000, Roo and Gerretsen [24] developed a simulation model (RODAS) to predict the physical characteristics (texture, profile, porosity, specific flow resistance and acoustical structure factor) from the HMA pavement material specifications of aggregate shape and gradation, amount and type of binder, as well as the percentage of sand and filler. The RODAS model was designed to be a module in the larger TRIAS (Tire Road Interaction Acoustical Simulation) model to use road surface characteristics to aid in the design of quiet pavements.

They found that RODAS can predict the acoustical characteristics of pavement surfaces with reasonable accuracy, the absorption model delivers a prediction inaccuracy (small enough to distinguish different pavement types), and the texture prediction model needs to be improved as it is not very accurate.

Berengier and Anfosso-Ledee [16] investigated the effect of road noise barriers on the propagation of road noise and the interaction with porous surfaces using numerical models. They also rated different pavement types as shown in Table 1.2, by using the controlled pass-by technique (CPB) which measured the sound generated from control vehicles traveling at control speeds from a receiver placed near the road.

Table 1.2 Classification of Different Pavement Categories using CPB

Type of pavement	Number of samples	Minimum L_{Amax} (dB(A))	Maximum L_{Amax} (dB(A))	Mean L_{Amax} (dB(A))	Standard deviation (dB(A))
0/6 Porous asphalt	3	68.7	71.9	70.1	1.7
0/10 Porous asphalt	71	69.5	77.4	73.4	1.5
0/6 Very thin asphalt concrete	52	70.4	78.4	73.8	1.8
0/6 Ultra thin asphalt concrete	10	73.5	76.1	74.6	0.8
0/14 Porous asphalt	37	73.3	78.1	75.6	1.4
0/10 Asphalt concrete	10	73.7	78.1	76.2	1.4
Cold-applied slurry surfacing	7	75.2	82.0	77.3	2.5
0/10 Very thin asphalt concrete	10	74.9	79.1	77.4	1.4
0/10 Ultra thin asphalt concrete	16	74.7	78.8	77.5	1.1
Surface dressing	15	75.4	82.5	78.9	1.8
Cement concrete	5	77.1	80.0	79.0	1.2
0/14 Asphalt concrete	5	77.7	81.1	79.4	1.4
0/14 Very thin asphalt concrete	2	78.7	81.5	80.1	2.0
0/14 Ultra thin asphalt concrete	1	80.4	80.4	80.4	-

In 2004 Lee et al [25] used a three-dimensional finite element model to model the complex interaction between the British pendulum tester and the pavement surface. They were

able to obtain to obtain a skid resistance value and other contact information based on the surface type without having to perform the physical test.

Trifiro et al [26] analyzed different pavement sections at the Virginia Smart Road by measuring the friction with different devices, at different speeds and obtaining an international friction index value, IFI, as defined by PIRAC. The researchers found that the repeatability of the locked wheel skid trailers (LWST) was good, as were LWST tests of using the same tire at different speeds. However the ribbed tire did not correlate with the smooth tire, and there were discrepancies among the IFI values calculated using the different devices.

McGhee et al [27] performed continuous texture measurements using laser-based devices as a possible tool to aid in detecting segregation and non-uniformity of HMA mixtures. The researchers concluded that the method "holds great promise".

NCHRP Web Document No. 42 [15] presented the issues related to pavement smoothness and highlighted the main concerns related to pavement smoothness including:

- Accuracy and repeatability of equipment
- Reproducibility of equipment
- Use of profile data for corrective action
- Knowledge and understanding of equipment and measures
- Relating smoothness to cost and performance
- Identifying and appropriate index for smoothness
- Lack of standard guide specifications
- Future use of profile data
- Using smoothness index to monitor pavement performance

INTERRELATIONSHIPS AMONG SURFACE CHARACTERISTICS

National Cooperative Highway Research Program (NCHRP) Synthesis No. 291 [3] reviewed the current state of the art for measuring and characterizing pavement surface characteristics by surveying national and international agencies and by conducting a literature review. The report noted the following relationships between pavement design parameters and surface characteristics:

- Splash and spray was reduced and skid resistance improved with an increase in macrotexture, especially porous pavements.
- Exterior noise levels increase with increasing macrotexture, however the range of macrotexture also influences the skid resistance.
- In vehicle noise was affected by higher wavelengths of macrotexture and megatexture.
- The relationship between tire wear and microtexture was not deemed important by agencies, and no models could be found in literature

The report also commented on the surface characteristics of the following asphalt surfaces and maintenance treatments.

- Stone Mastic Asphalt (SMA) pavements tend to have great macrotexture properties and the ability retain these properties under heavy truck traffic
- Superpave pavements are designed to combat rutting which reduces the tendency to hydroplane, there is no consideration given to surface texture or skid resistance.
- Microsurfacing Treatments are durable treatments that restore macrotexture treatments and to some degree, ride quality to asphalt pavements; many proprietary products have been applied in Europe and the U.S.
- Seal Coats typically provide similar macrotexture benefits as Microsurfacing treatments, but use more conventional materials.

FRICTION & HMA DESIGN PARAMETERS

Flintsch et al [45] recently investigated the relationship between the International Friction Index (IFI), HMA design characteristics, and certain testing conditions at the Virginia Smart Road. The different HMA mixes studied included five different Superpave mixes, a stone mastic asphalt (SMA) and an open graded friction course (OGFC). The surface characteristics were

measured using an LWST, a British Pendulum Tester and laser texture devices while considering the test tire, the vehicle test speed, and the grade.

The researchers found that the friction measurements were dependent upon texture, age and temperature. They noted that past studies demonstrated that "aggregate type and structure significantly influence microtexture and macrotexture, thus influencing the skid resistance of a paved surface (Henry and Dahir, 1979; Forster, 1989; Kandhal and Frazier, 1998)". They investigated the effect of the HMA design parameters of speed constant (Sp) and the normalized friction value (F60) of IFI using a stepwise regression analysis. The results of the analysis (shown below) indicate that SP can be predicted from NMS and VMA, and that friction increases with voids, percent passing the No. 200, and with the use of modified binders.

$$Sp=-270.0+28.3*NMS+6.79*VMA \tag{7}$$

Where:

NMA: nominal aggregate maximum size

VMA: voids in the mineral aggregate

$$\mathbf{F60=0.38189-0.02962*Tire+0.01295*Binder+0.00911*PP200+0.00897*VTM} \tag{8}$$

Where:

Tire: type of tire used in testing, a categorical variable with 0 for smooth and 1 for ribbed tire)

Binder: Binder Code (PG64-22=-1, PG70-22=0, PG76-22=1)

PP200: Percent Passing No. 200 sieve

VTM: Total voids in the mixture

Boscaino et al [18] recently investigated "the ability of texture indicators to influence and represent surface performance" [18]. They found that the extrinsic properties of drainability, friction, and sound absorption were all correlated to surface texture and geometry; however the nature of the correlations were very different for each of the extrinsic properties.
In 2004, Nagelhout et al [19] reported on the use of laser texture meters to quantify the amount of raveling in an HMA pavement surface. They noted the importance of raveling because it negatively affects the noise, friction, and rolling resistance of the pavement. The study found that there is a possibility of using the device to detect raveling and that the results were much more repeatable than visual condition surveys by trained inspectors [19].

TEXTURE & NOISE

In 2006 Ongel et al [28] sought to find correlations between tire/pavement noise and various pavement parameters including, but not limited to surface characteristics and surface type. Their report was part of a long-term study initiated by the California Department of Transportation (CalTrans) that monitored the noise reduction properties, quality, durability, ride and safety of open graded mixes in comparison to other asphalt surface types. The surface types investigated are shown in Table 1.3, and the measured data as well as the test used to obtain the data are shown in Table 1.4.

Table 1.3 Pavement Test Sections Used in CalTrans Study

Site Location	Surface Types	Construction Season	AADT	AADTT
Yolo 80	30-mm OGAC	Summer 1998	134,000	8,991
Sacramento (SAC) 5	30-mm RAC-O	Summer 2004	122,000	16,116
Los Angeles (LA) 138	30-mm OGAC 75-mm OGAC 30-mm RAC-O 30-mm BWC 30-mm DGAC	Spring 2002	4,300	606
Fresno (FRE) 33	45-mm RAC-G 90-mm RAC-G 45-mm RUMAC-GG 90-mm RUMAC-GG 45-mm Type-G MB 90-mm Type-G MB 45-mm Type-D MB 90-mm Type-D MB 90-mm DGAC	Summer 2004	7,575	1,439
San Mateo (SM) 280	40-mm RAC-O	Fall 2002	110,000	2,552
Los Angeles (LA) 19	35-mm European (EU) Gap Graded Asphalt Concrete	May 2005	36,500	1,861

Notes: OGAC: Open-graded Asphalt Concrete
                RAC-O: Rubberized Open-graded Asphalt Concrete
                BWC: Bonded Wearing Course
                RAC-G: Rubberized Gap-graded Asphalt Concrete (wet process)
                RUMAC-GG: Rubber-modified Asphalt Concrete (dry process)
                Type-D MB: Dense-graded Rubberized Asphalt Concrete (terminal blend)
                Type-G MB: Gap-graded Rubberized Asphalt Concrete (terminal blend)
                DGAC: Dense-graded Asphalt Concrete

Table 1.4 Data Collection and Tests

	Type of Data	Specific Test/Sampling
Sampling and testing during traffic closures	Pavement cores	100 mm and 150 mm in diameter
	Condition survey	Caltrans condition survey manual
	Microtexture	British Pendulum, ASTM E303
	Permeability	Falling Head Method
Testing at normal highway speeds	Tire/pavement noise	On-Board Sound Intensity (OBSI)
	Roughness	IRI from laser profilometer, ASTM E1926
	Macrotexture	Laser profilometer, ASTM E1845

The researchers found good repeatability using the onboard sound intensity (OBSI) for sound measurement with a 0.4 dBA average difference and a standard deviation of 0.3 dBA for three runs, therefore the researchers used the average of the three runs for analysis. They tried to correlate the A-weighted sound levels to the following pavement parameters: air void content, permeability, MPD, RMS, BPN, IRI, NMAS, thickness, and age. Permeability, air void, roughness, and friction at the right wheel path were used in the correlation.

The researchers concluded from OBSI measurements open graded mixes can reduce Tire-Pavement-Interaction-Noise by up to 4.5 dB (A), in addition they found that these mixes also had higher macrotexture (MPD) than other mixes. They found a moderate correlation between noise level and the product of surface layer thickness and air void content, increasing either parameter may reduce pavement noise. MPD and RMS were highly correlated, and both were positively correlated with air void and permeability [1.4.].

De Fortier Smit and Waller [14] also sought to find a relationship between the MPD, ISO texture parameters of L_4, L_{63} and sound measurements obtained using the NCAT close proximity trailer (CPX) with two different test-tires. The researchers used ANOVA analysis and concluded that no single texture factor significantly affected the noise measurements; however a poor correlation was found using the texture parameters and interactions of the factors indicating that noise was influenced by more than just macrotexture. According to de Fortier Smit and Waller [14], "The traffic volume of the sections prior to noise and texture testing varied depending on reconstruction and rehabilitation efforts at the track. A consequence of this is that the material and roughness characteristics of the section mixtures were not "as constructed". This explains the difficulties and complexities in relating macrotexture measurements to sound.

The density of the sections would likely have increased, the open graded friction courses were possibly clogged, aggregate degradation is a possibility, surface macrotexture may have decreased and the roughness of the sections would have increased with trafficking" [14].

The researchers also suggested warming the test tires for at least twenty minutes prior to testing to ensure test repeatability in sound pressure measurements.

CHAPTER CONCLUDING REMARKS

Many different methods can be used to characterize the pavement's several interrelated surface characteristics. These surface characteristics are affected by not only short term and long term seasonal and temperature effects, but also are dependent upon the device being used. This necessitates the frequent testing of sections and calibration of equipment and further complicates correlation of measured results with other devices. Recent advances in laser technology and computing are improving the ease, frequency and repeatability with which measurements can be taken, especially in facilitating the analysis of the spectral content of the surface characteristics.

Many pavement practitioners have expressed interest in IFI which is hoped to harmonize friction measurements by incorporating both a macrotexture and a normalized friction measurement into the value. This would make it easier to compare results obtained from different devices and accurately characterize the pavement's surface.

There has been limited success in relating different pavement surface characteristics with design parameters in an attempt to optimize properties and better characterize behavior. Often times optimizing one characteristic such as friction causes an increase in another characteristic such as noise; however porous pavements have good macrotexture qualities and absorb sound relatively well when compared with other HMA pavement types.

Literature shows that there may be predictive models relating asphalt surface properties. This underscores the need to perform, data analysis to ascertain if some correlation trends may exist or if some of those postulated are valid. However, they are susceptible to " drain down" and raveling.

CHAPTER 2

CONSTRUCTION AND INITIAL TESTING OF VARIOUS TEST CELLS

CHAPTER INTRODUCTION

The Minnesota Road Research Project (MnROAD) was constructed by the Minnesota Department of Transportation (MnDOT) in 1990-1993 as a full-scale accelerated pavement testing facility, with traffic opening in 1994. Located near Albertville, Minnesota (40 miles northwest of St. Paul-Minneapolis), MnROAD is one of the most sophisticated, independently operated pavement test facilities of its type in the world. Its design incorporates thousands of electronic in-ground sensors and an extensive data collection system that provide opportunities to study how traffic loadings and environmental conditions affect pavement materials and performance over time. MnROAD consists of two unique road segments located parallel to Interstate 94 as shown in Figure 2. 1 as described below:

- A 3.5-mile Mainline interstate roadway carrying "live" traffic averaging 28,500 vehicles per day with 12.7 % trucks.
- A 2.5-mile closed-loop Low Volume Road carrying a MnROAD-operated 18-wheel, 5-axle, 80,000-lb tractor-semi-trailer to simulate the conditions of rural roads.
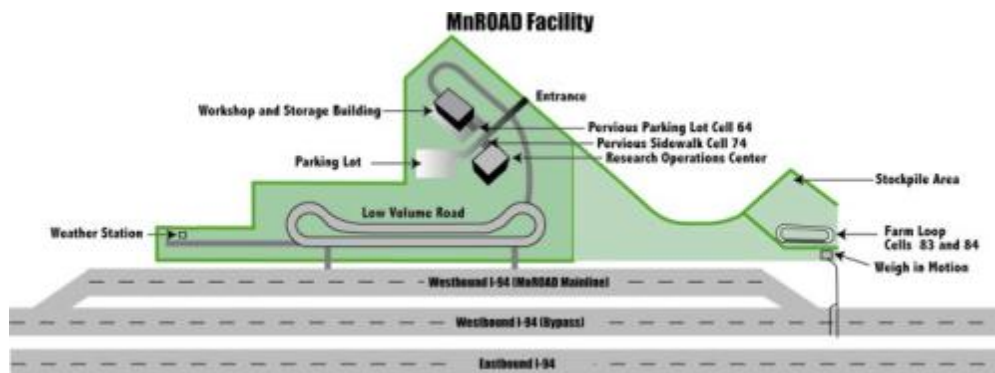
Figure 2.1 MnROAD Facility Map

During the summer and fall of 2008 MnROAD was undergoing its phase 2-construction project (SP 8680-157) to reconstruct or rehabilitate many of its existing cells. Many of these reconstructed cells had unique characteristics and incorporated innovative technologies that were relatively new to MnDOT.

Figure 2.2 and 2.3 show the relative location of the test cells of interest located on the mainline and low volume road respectively.
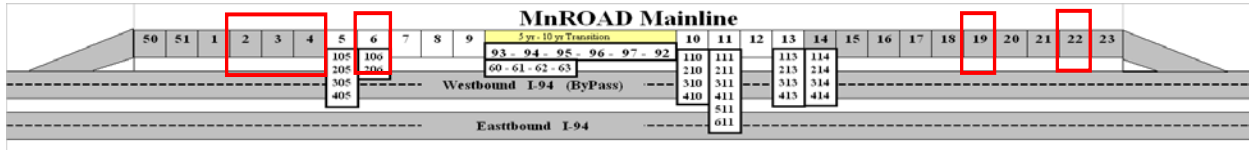
Figure 2.2 Location of Test Cells on MnROAD Mainline (ML)
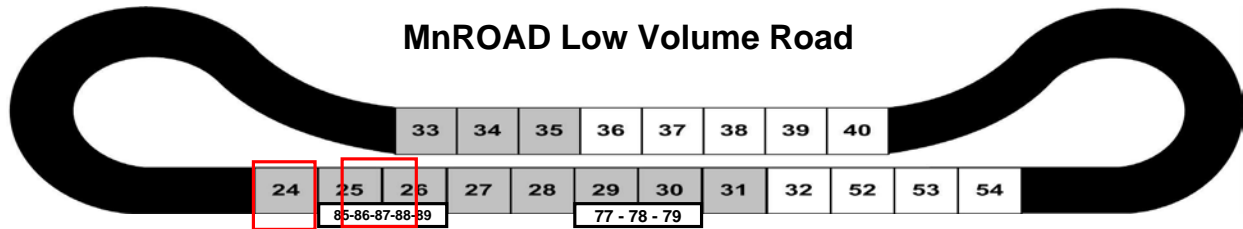
Figure 2.3 Locations of Test Cells on MnROAD Low Volume Road (LVR)

CHAPTER OBJECTIVES

This chapter briefly summarizes the construction and initial materials testing of the surface layers included in this study. It does not focus on construction details or testing that is not directly related to the surface layer. Next, the results of various surface characteristics tests designed to measure: texture, friction, ride, sound, permeability and durability are presented in graphical and tabular format. Data analysis is reserved for chapter 4.

CELL CONSTRUCTION

INTRODUCTION

The surface characteristics study includes ten test cells on both the MnROAD ML and LVR. These test cells have unique surface mixture types that include different gradations (gap graded, coarse dense graded and fine dense graded), different binder types, different levels of binder aging (Warm Mix Asphalt and Aging Study) and different amounts and gradations (Fractionated) of recycled asphalt pavement (RAP). Figures show the typical sections of the ML and LVR test cells respectively. Note the thickness and type of surface, base (FDR denotes Full Depth Reclamation) and subgrade materials. Note also that test cell 24 is part of the aging study and 100' sections of the cell will receive a fog seal surface treatment of CRS-2p(d) in one year increments starting in 2009 and ending in 2012, note that the fog seal treatment in 2008 was a CSS-1h(d). Detailed mix design worksheets for the surface layers can be found in Appendix.

Table 2.1 shows the details of the surface wear course of the cells which were tested as a part of this study. Note the RAP content and that cells numbered less than 24 (<24) are located on the mainline, denoted ML, and the remaining cells are located on the low volume road, denoted (LVR). Note also that the HMA surface mixture types are denoted according to MnDOT's 2008 specifications [29] and can be summarized as follows: All mixtures, except for the Ultra-Thin Bonded Wearing Course (UTBWC) were Superpave or Gyratory design (denoted SP) and all had a maximum aggregate size of 19.0 mm (nominal maximum size of 12.5 mm) denoted by "B". The mixtures on the LVR were based on 20 year design of 1 to < $3*10^6$ ESALS, denoted by "3" where those on the ML were based on 3 to <$10*10^6$ ESALS denoted by "4". All mixtures had target air voids of 4.0% denoted by "40". Finally the last letter indicates the binder Performance Grade (PG): F (64-34), C (58-34), H (70-28) or B (58-28). Table 2.2 shows the paving dates of the HMA cells, which were all paved in fall 2008 starting on September 10, 2008 and continuing through October 30, 2008.

Table 2.1 Location HMA Surface Allocation

Cell (Loc)	HMA Surface Mix Type	PG Grade, %RAP	Description
2 (ML)	UTBWC	64-34, 0%	Ultra-Thin Bonded Wearing Course **(UTBWC)**
3 (ML)	UTBWC	64-34, 0%	Ultra-Thin Bonded Wearing Course **(UTBWC)**
4 (ML)	SPWEB440F	64-34, 0%	Level 4 12.5 mm Dense Graded Superpave **(-34, 0% RAP)**
6 (ML)	SPWEB440F Special	64-34, 0%	4.75 mm Taconite HMA **(4.75)**
19 (ML)	SPWEB440C Special	58-34, 20%	Warm Mix Asphalt 12.5 mm Dense Graded Superpave **(WMA)**
22 (ML)	SPWEB440C Special	58-34, 30%	Fractionated RAP 12.5 mm Dense Graded Superpave **(FRAP)**
24 (LVR)	SPWEB440C	58-34, 20%	Warm Mix 12.5 mm Dense Graded Superpave **(WMA Control)**
86 (LVR)	SPWEB440H Special 1	70-28, 0%	Porous HMA on Sand **(Porous)**
87 (LVR)	SPWEB340B	58-28, 20%	Level 3 12.5 mm Dense Graded Superpave **(Porous Control)**
88 (LVR)	SPWEB440H Special 1	70-28, 0%	Porous HMA on Clay **(Porous)**

Table 2.2 2008 HMA Paving Dates

Date	Cell Number	Description
10-Sep-08	22	Fractionated RAP wear (FRAP)
17,18-Sep-08	19	WMA wear (WM)
29-Sep-08	2, 3	Ultra-thin Bonded Wearing Course (UTBWC)
	4	Superpave (SP,64-34,0%RAP)
15-Oct-08	86, 87, 88	Porous HMA (POROUS) & Superpave (POROUS-CTRL)
16-Oct-08	24	WMA Control (WM-CTRL)
30-Oct-08	6	4.75 mm Taconite HMA (4.75)

Figure 2.4 Typical Sections of Mainline (ML) Test Cells

86	87	88	24
25	25-26	26	24
5" Perv HMA	4" Control	5" Perv HMA	3" 58-34
4" RR Ballast	4" Mesabi Ballast	4" RR Ballast	4" Cl6sp
			Sand
10" CA-15	11" CA-15	10" CA-15	100' Fog Seal 2008 100' Fog Seals 2008 2009 2010 2011 2012
Type V Geo-Textile	Type V Geo-Textile	Type V Geo-Textile	
Sand	Clay Sand	Clay	
Oct 08	Oct 08	Oct 08	Oct 08
Current	Current	Current	Current

Figure 2.5 Typical Sections of Mainline (ML) Test Cells

MAINLINE CELLS

Cells 2 and 3 on mainline each were constructed using a ⅝ - ¾" ultra-thin bonded wearing course (UTBWC) surface. The UTBWC is a thin, gap graded, wearing course constructed with a heavy polymer modified AC, (Figure 2.4 and 2.5). The tack coat was applied directly in front of the mixture with a spray paver note the circled apparatus applies the tack coat (Figure 2.7). The UTBWC was constructed over 2" of level 4 Superpave and 6" of full depth reclaimed layer treated with an engineered emulsion [29]. The surface course of Cell 4 was 3" of the same level 4 Superpave that was under the UTBWC, and was paved with the same spray paver Figures (2.6&2.7)

34

Figure 2.6: Nova Chip Paver

Figure 2.7 UTBWC (Left) and X-Section of Porous HMA (Right)

Cell 6 is part of a National Center for Asphalt Technology (NCAT) study on the use of fine graded mixtures. Cell 6 is a 4.75 mm Superpave mix composed of taconite aggregates and 7.4% binder content of PG 64-34, see Figure 2.**7.** This cell is the only cell included in this study that is a thermally insulated pavement, which is a new HMA surface course constructed over a new Portland Cement Concrete (PCC) pavement. This is a finer mix, has higher binder content and is more rut resistant than the standard coarse, dense graded SuperPave mixes used by MnDOT. This mixture does not incorporate any recycled asphalt pavement (RAP). This mixture is

designed to be a thin high quality surface wearing course. The Taconite tailings are a Minnesota iron bearing ore, which are denser than granite aggregates and are in great abundance (more than 2,000,000 tons) in the northern regions of MN.

Figure 2.8: Nova Chip Surface (Left) and Warm Mix Surface (Right)

Cell 19 is a standard Superpave mixture consisting of PG 58-34 binder, 20% RAP constructed over gravel base material using warm mix asphalt (WMA) technology, (Figure 2.8). This innovative WMA technology lowers the mixing temperature of the asphalt mixture which lowers the energy costs at the plant and has the purported benefit of less aging of the binder. This may make the pavement less stiff and probably less noisy; but the addition of RAP would increase the stiffness of the mixture. Other benefits of the technology include fewer fumes at the worksite and the same density with less compactive effort when compared to the same non-WM mixture. The WMA technology alone is not expected to have a dramatic effect on the surface characteristics.

Cell 22 is a standard coarse, dense graded Superpave mixture consisting of 30% RAP, fractionated (FRAP) into 20% RAP fines and 10% RAP coarse. This cell used 3.7% new or virgin PG 58-34 AC.

LOW VOLUME ROAD CELLS

Cell 24 is the warm mix control cell (did not utilize warm mix technology) but had the same binder PG grade 58-34 and 20% RAP content. This cell is part of a study investigating the

effects of aging, which means that a surface treatment will be applied to the cell in 100'
increments annually until the entire cell is treated (about 5 years or 2012).

Cells 86 and 88 on the low volume road were constructed of 5" porous HMA with PG 70-28
binder, see Figure 2.7. These cells were constructed over coarse aggregate bases over either a
sand or a clay subgrade respectively. These cells had very high void content and connectivity as
they were designed to allow water to drain through the pavement. This unique design is also
expected to have benefits on noise abatement as well. Cell 87 is the porous asphalt control cell,
which is composed of a coarse, dense graded level 3 Superpave mix and a binder PG grade of
58-28.

Table 2.3 show the average % density and air voids of the HMA cells. Note that MnDOT
specifies a minimum mat density of 92.0%. The Table does not include the densities of the
longitudinal joint as most constructed joints were warm joints and not reflective of cold joints
which MnDOT typically encounters.

Table 2.3 2008 Average Density and Air Void Results for HMA Cores

Cell	Description	% Density	Air Voids
6	4.75 mm taconite	93.1	6.9
15-19, 23	WMA wear	92.0	8.0
22	Fract. RAP wear	93.6	6.4
24	WMA control	91.4	8.6
87	porous control	93.2	6.8
88	porous HMA	82.0	18.0

EXPERIMENTAL TESTING

Table 2.4 shows the various tests that were used in this project to quantify and compare the
various surface characteristics of the different HMA mixtures used at the MnROAD test facility.
The initial results of these tests, as well as a short description of the methodology and results are
included.

Table 2.4 Tests Used to Characterize Initial HMA Surface Characteristics

Test Name (ASTM No)	Measured Property Value (units)	Frequency of Test
Sand Patch (E965)	Texture (Macro) Mean Texture Depth (MTD)	Twice Annually (Spring and Fall)
Circular Texture Meter (E 2157)	Texture (Macro) Mean Profile Depth (MPD)	Twice Annually (Spring and Fall)
Locked Wheel Skid Trailer (ASTM E 274)	Friction Skid No (SN) = 100*Friction No	Twice Annually (Spring and Fall)
Grip Tester	Friction Grip No.	Four Times Annually (Seasonally)
Light Weight Profiler (LISA) No ASTM	Ride IRI (m/Km or in/mi)	Twice Annually (Spring and Fall)
Impedance Tube (No ASTM)	Sound Absorption	
On Board Sound Intensity (OBSI)	Noise (Sound Intensity)	Four Times Annually (Seasonally)
Permeability (No ASTM)	Hydraulic Conductivity, K (cm/sec)	Varies
LTTP Distress Survey	Visible Distresses	Twice Annually

TEXTURE

Sand Patch Test:

The sand patch test (ASTM E 965) reports the diameter (D) of a uniformly graded patch of glass beads that is spread out to form a circle on the pavement surface. The volume of the material divided by the area is the mean texture depth (MTD) for a spot location on the pavement surface as shown by equation 9 [30]. Figure 2.9 shows the test schematics; note that the diameter is the average of four measurements. The sand patch test was performed during October 2008 on all

HMA study cells except 2 and the porous (cells 86 and 88) during the month of November. This test was performed at 4 locations: 2, 4, 6 and 8 feet from the edge line for each cell, see Figure 2.9, 4 feet east of FWD point No. 9. These locations were marked with PK nails to ensure that subsequent measurements would be in the same location. Figure 2.9 show the average of these four macro texture measurements taken for each cell. As expected, the UTBWC (cell 3) has the highest MTD, at least twice the value of the dense graded cells. The 4.75 taconite mixture (cell 6) had an MTD result similar to more coarse graded mixtures, and it appears that the remaining cells including the WMA (cell 19) and the use of FRAP (cell 22) had similar MTD results.
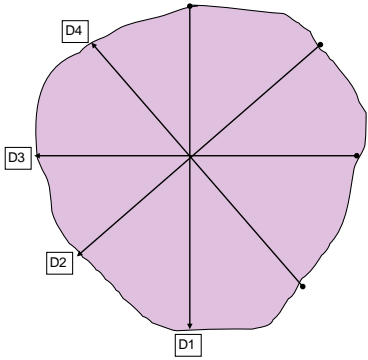
Calibrated Bottle Volume (V)	Patches with Glass beads (of Known Volume)	Average Diameter of Patch (Davg.)

Figure 2.9 Sand Patch Field Tests (LEFT) and Test Schematic (RIGHT)

$$\textbf{Davg} = \frac{\sum_{i=1}^{n} D_i}{n} \tag{9a}$$

$$\textbf{Davg} = \frac{4V}{\pi D^2} \tag{9b}$$

$$\tag{9}$$
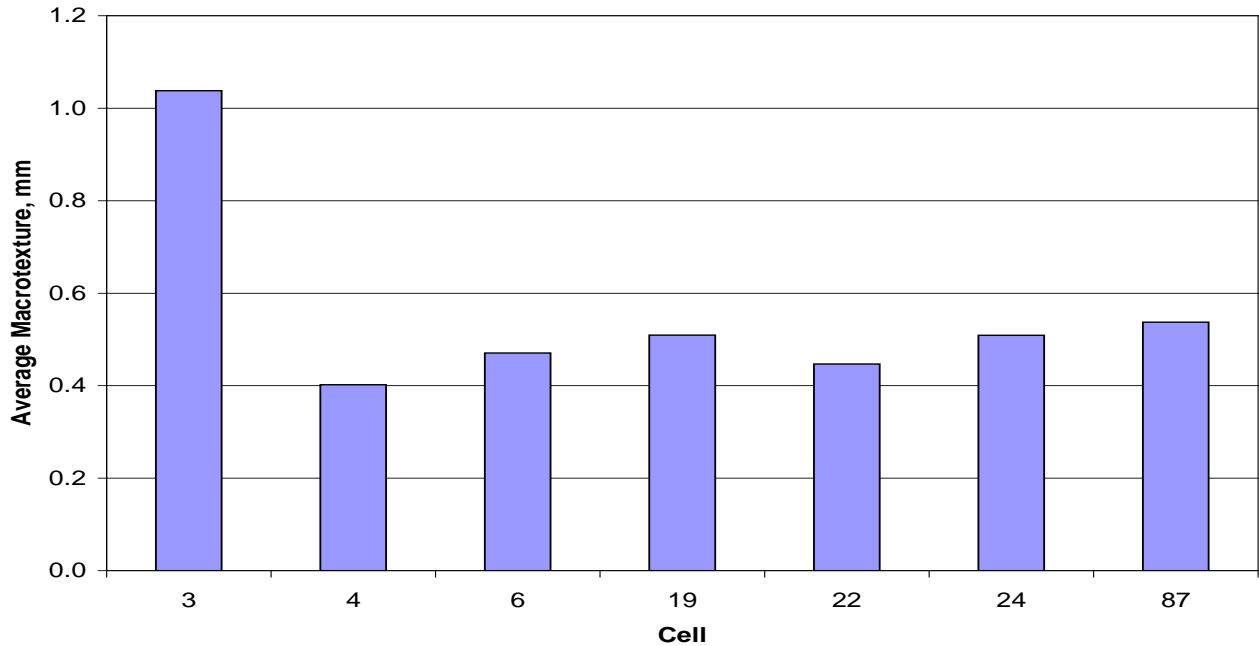
Figure 2.10 October 2008 Sand Patch Test Results
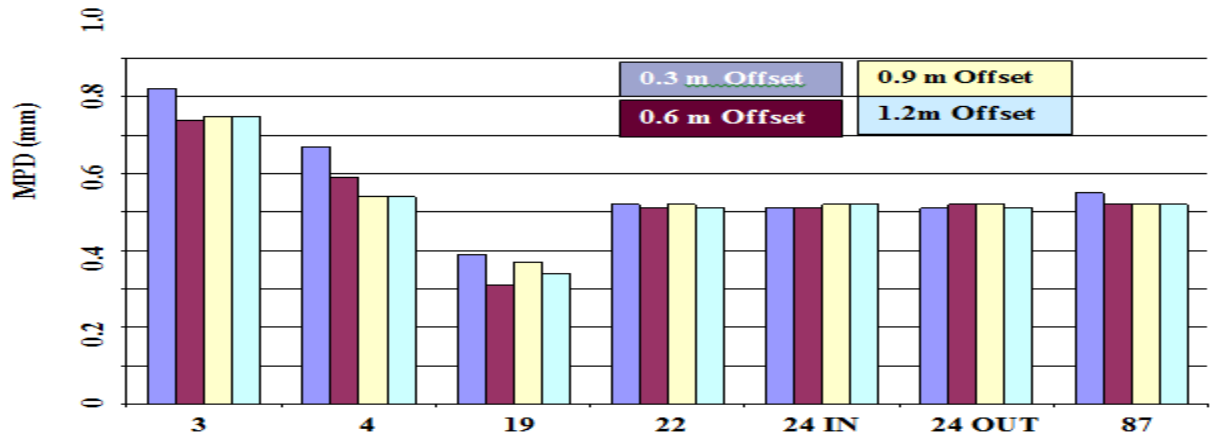
Figure 2.11 October 2008 CTM Test Results

The team used the circular track meter (CTMeter) to measure mean profile depth MPD. According to Abe et al (13) the MPD values are extremely highly correlated with the MTD values, equation 10 shows the recommended relationship between MTD and MPD. Figures 2.10 and 2.11 show how correlated the sand patch test is to the CTM The test reports both the MPD and the root mean square (RMS) values of the macro texture profile [31].

Figure 2.12 shows the preliminary results for the test cells, which were taken in April 2009. This test was performed at same the 4 locations as the sand patch test: 2, 4, 6 and 8 feet

from the fog line (shoulder edge line) for each cell. Although the CTMeter and sand patch results cannot be compared directly due to the difference in testing dates (and most likely temperature), it is interesting to note that the results generally agree with the sand patch results. The UTBWC (cell 3) surface has the greatest texture, however the difference between the UTBWC and the remaining cells appear to be smaller, and the WMA (cell 19) has much lower texture results than other similarly dense graded mixtures. A correlation of the sand Patch and the CTM follows the equation $MTD = 0.947 * MPD + 0.069$ (10)
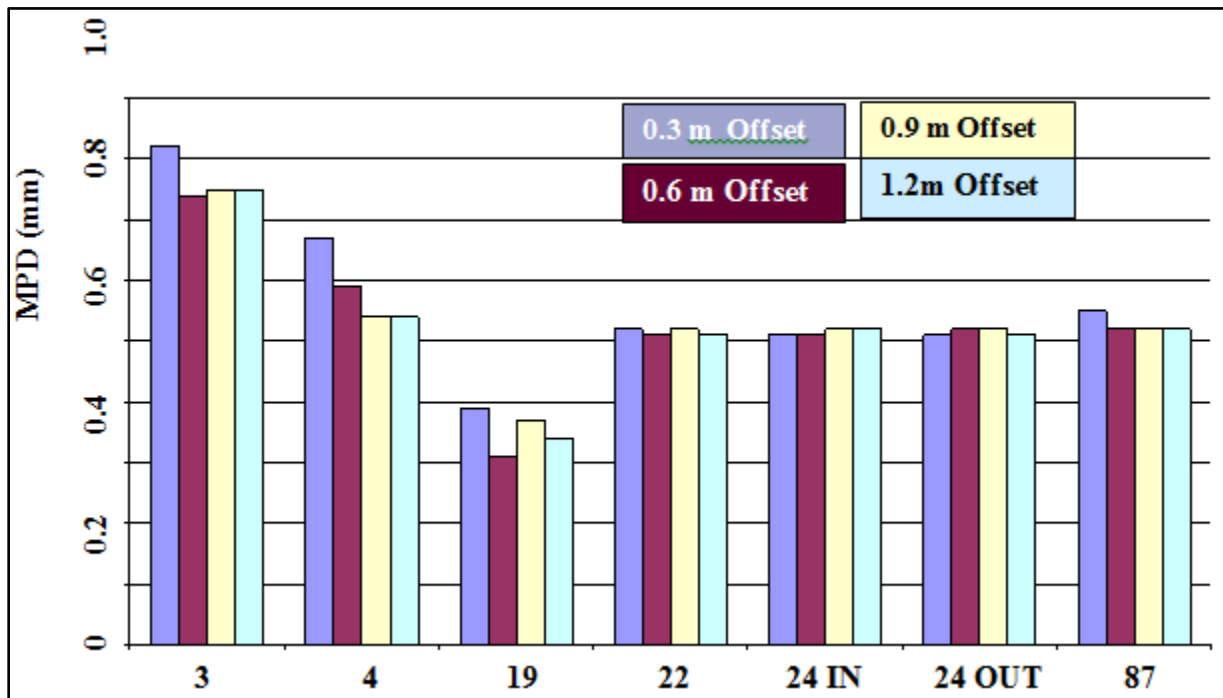
Figure 2.5 Circular Track Meter Outside Lane (LVR) or Driving Lane Mainline (CTM) Spring 2009 Results

FRICTION

Locked Wheel Skid Trailer (LWST):

The locked wheel skid trailer (LWST) was performed in accordance with ASTM E 247 [37], and is shown in Figure 1.3. This test is one of the most common methods employed by state DOTs to obtain a measure of friction.

41

Figure 2.13 summarize the skid numbers from LWST testing conducted on MnROAD test cells on October 2008. The air temperature was 68ºF and the pavement surface temperatures ranged from 63ºF to 83ºF as shown in Table 2.5. The 4.75mm Aggregate Asphalt (cell 6) appears to have the lowest values, but these results must be taken with caution as there was gravel present in the test cell during the test. The WMA (cell 19) appears to have the highest results of both ribbed and smooth with the UTBWC (cells 2 & 3) close behind. The -34, 0%RAP (cell 4), the FRAP (cell 22) and the WM-CTRL (cell 24) had the most pronounced differences between the ribbed and smooth tires and the UTBWC (cell 3), the 4.75 (cell 6) and WMA (cell 19) had the smallest differences. Figure 2.14 summarizes the LWST results collected on June 2009 in the driving lane of the ML and the inside lane of LVR. Figure 2.15 summarizes the LWST results collected on June 2009 in the passing lane of the ML and the outside lane of LVR. These tests were conducted when the air temperature was 68ºF and the pavement surface temperatures ranged from 85.8ºF to 119.2ºF as shown in table 2.6 and 2.7. The UTBWC cells (2 & 3) had consistently relatively high values, and low differences between results, for both the ribbed and smooth tires in both the driving and the passing lanes. The WMA control (cell 24) had the highest ribbed tire result in the inside lane (with a relatively average smooth tire result), and the highest ribbed and smooth tire result, with a low difference between the results, on the outside lane. The porous (cells 86 and 88) displayed ribbed and smooth tire results lower than the UTBWC, consistent between the inside and outside lanes and a low difference between the smooth and ribbed tire results. The 4.75 (cell 6) had among the highest ribbed tire results and the lowest smooth tire results.

It appears that, in general, the fine, dense graded mixtures displayed the greatest variability in the difference between ribbed and smooth tire results and in the difference between lanes, followed by the coarse dense graded mixtures (excluding cell 19).

Table 2.5 October 2008 LWST Results ML-Driving, LVR-Inside Lane

CELL	FN	PEAK	SPEED	AIR TEMP	PVMT TEMP	TIRE TYPE	MIN FN	MAX FN	SLIP
3	55.6	89.41	39.1	68	79.3	Ribbed	53	58	13
4	53.1	81.77	42.5	68	78.6	Ribbed	51	55	16
6	41.8	66.88	40.8	68	80.3	Ribbed	39	47	22
19	57	82.96	39.5	68	77.5	Ribbed	55	59	12
22	56	78.98	39.4	68	76.8	Ribbed	53	59	13
24	51.6	77.79	41.4	68	63.3	Ribbed	48	54	13
3	52.2	97.17	39.3	68	79.8	Smooth	46	57	12
4	39.7	54.46	39.6	68	78.8	Smooth	25	49	25
6	35.9	53.55	40	68	83.3	Smooth	31	39	14
19	58	78.68	39.6	68	80.1	Smooth	56	62	8
22	39.9	51.15	39.5	68	76.6	Smooth	30	56	16
24	41.6	62.01	41.4	68	64.6	Smooth	35	46	13
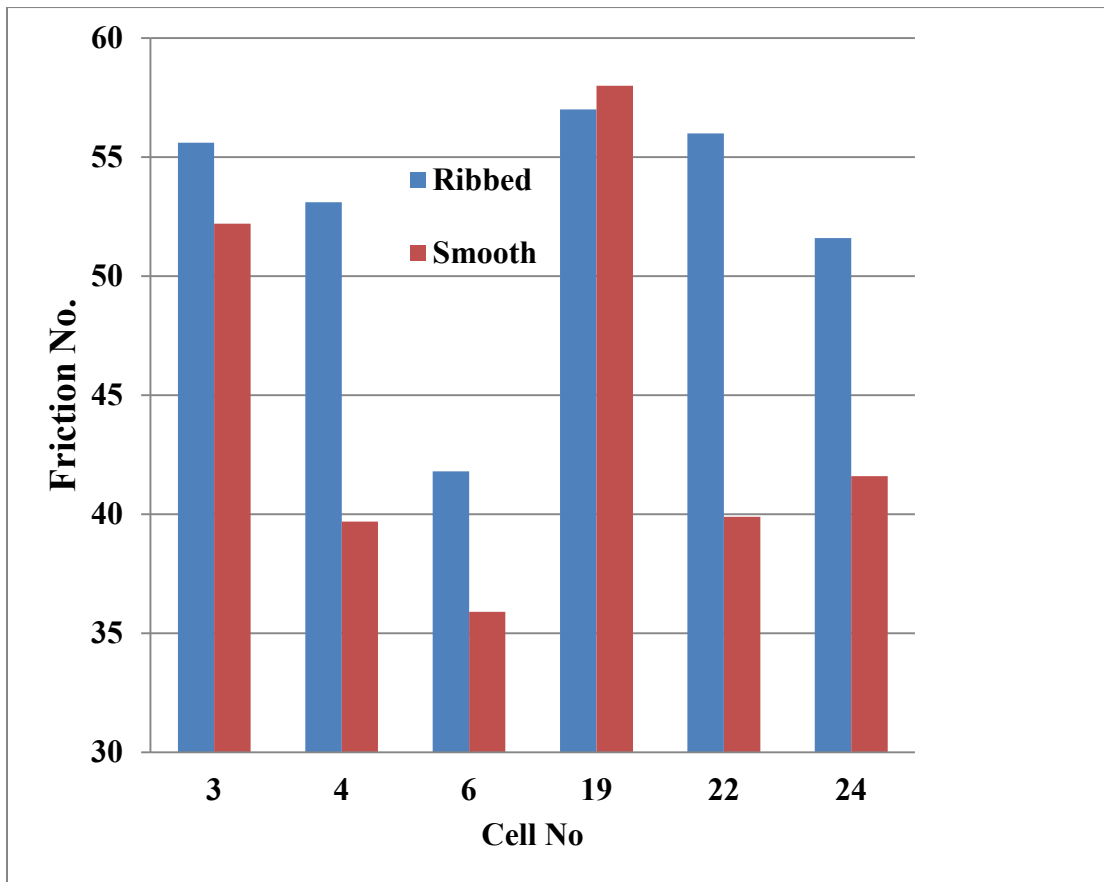
Figure 2.13 October 2008 MnROAD LWST Results for ML-Driving, LVR-Inside Lane

43

Table 2.6 June 2009 LWST Results

CELL	LANE	FN	PEAK	AIR TEMP	PVMT TEMP	TIRE TYPE	MIN FN	MAX FN	SLIP
2	Drive	57.5	85.85	68	90.7	Ribbed	56	59	18
3	Drive	57.2	87.58	68	88.7	Ribbed	56	59	16
4	Drive	55.8	79.57	68	98.2	Ribbed	54	58	17
6	Drive	60.6	85.79	68	98.5	Ribbed	58	63	17
19	Drive	58.9	79.01	68	96.7	Ribbed	57	61	11
22	Drive	54.3	78.02	68	97.7	Ribbed	52	56	14
24	IN	61.8	83.21	68	109	Ribbed	59	65	16
86	IN	43.8	80.6	68	110.9	Ribbed	40	62	19
87	IN	57.2	77.9	68	106.9	Ribbed	54	61	7
88	IN	45.3	78.3	68	112.1	Ribbed	43	48	19
2	Pass	56.2	82.19	68	88.5	Ribbed	55	58	10
3	Pass	54.8	85.26	68	88.3	Ribbed	52	59	19
4	Pass	53.9	73.37	68	93	Ribbed	51	57	11
6	Pass	63	81.61	68	93.8	Ribbed	60	66	11
19	Pass	52.5	75.96	68	93.8	Ribbed	51	54	19
22	Pass	50.2	72.39	68	94.5	Ribbed	49	52	9
24	OUT	64.9	79.91	68	114.2	Ribbed	63	67	14
86	OUT	44.3	82.49	68	116.9	Ribbed	41	47	11
87	OUT	57.7	73.29	68	111.2	Ribbed	55	60	12
88	OUT	46.5	85.86	68	116.9	Ribbed	41	52	13
2	Drive	57.5	87.3	68	92.5	Smooth	56	60	17
3	Drive	63	92.34	68	93	Smooth	59	65	17
4	Drive	48.2	69.52	68	97.5	Smooth	44	54	9
6	Drive	30	40.01	68	91.5	Smooth	26	33	11
19	Drive	42.6	58.78	68	98.5	Smooth	37	50	17
22	Drive	31.8	38.69	68	98.2	Smooth	24	51	10
24	IN	35.1	49.87	68	96.2	Smooth	30	45	14
86	IN	50.4	86.17	68	108.4	Smooth	44	61	4
87	IN	24.7	31.73	68	96	Smooth	20	29	21
88	IN	49	86.72	68	99.5	Smooth	45	53	12
2	Pass	59.8	88.45	68	85.8	Smooth	58	61	13
3	Pass	59.8	87.13	68	87.1	Smooth	57	61	11
4	Pass	40.2	52.85	68	95.3	Smooth	32	49	21

Table 2.7 (Cont'd) June 2009 LWST Results

CELL	LANE	FN	PEAK	AIR TEMP	PVMT TEMP	TIRE TYPE	MIN FN	MAX FN	SLIP
6	Pass	30.4	51.02	68	94.8	Smooth	28	33	5
19	Pass	48.3	66.84	68	94.5	Smooth	45	52	18
22	Pass	25.6	39.21	68	88.5	Smooth	22	30	20
24	Outside	65.2	76.99	68	104	Smooth	52	72	9
86	Outside	46.7	86.85	68	119.2	Smooth	43	50	12
87	Outside	42.6	42.82	68	106.2	Smooth	35	48	31
88	Outside	47.8	88.74	68	110.4	Smooth	45	51	10
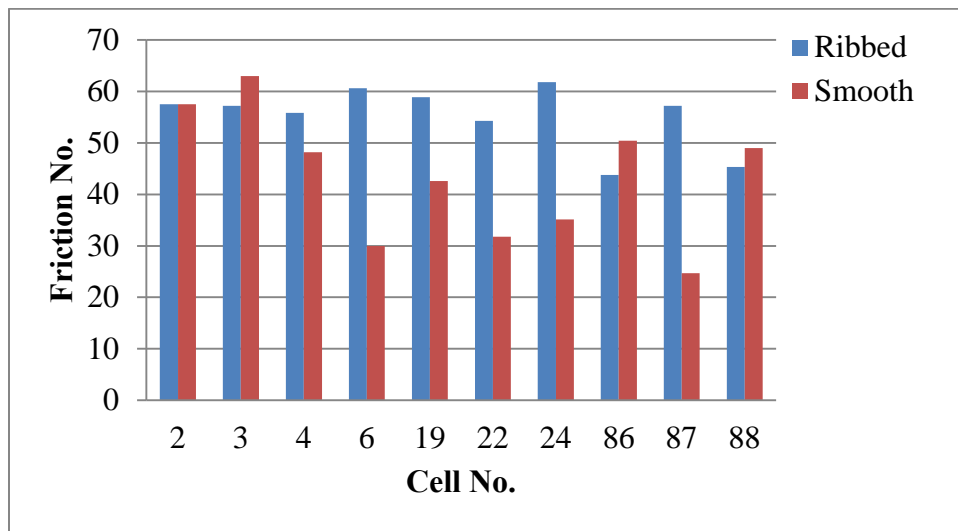
Figure 2.14 June 2009 MnROAD LWST Results for ML-Driving, LVR-Inside Lane
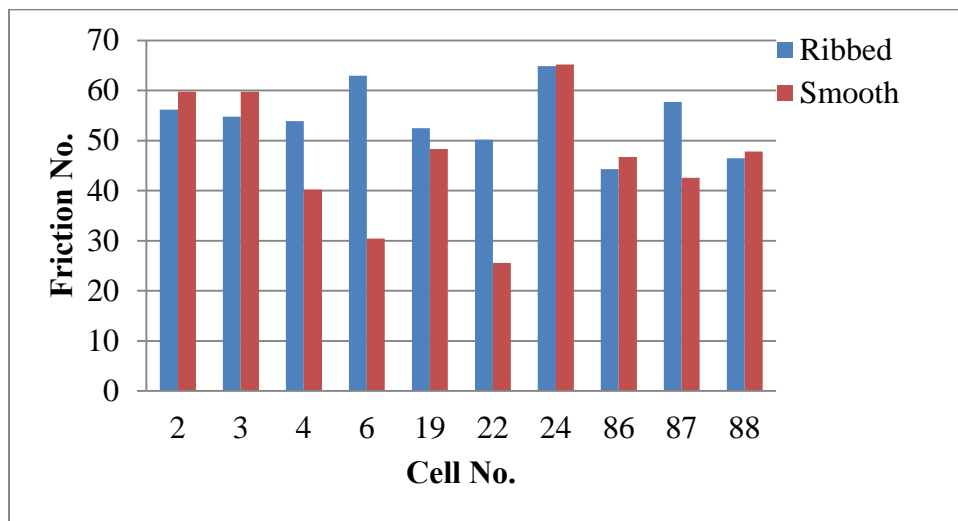
Figure 2.15 June 2009 MnROAD LWST Results for ML-Passing, LVR- Outside Lane

45

Grip Tester:

The Grip Tester shown in Figure **1.5** was provided through the Federal loans program. The test was conducted at 40 miles per hour in a standard pickup truck and operates at constant slip, usually between 10 to 20%, not 100% as is the case with the LWST. The Grip Tester produces continuous measurements of low-speed friction opposed to the LWST which produces spot measurements corresponding to a distance traveled by the vehicle in 1 second. For fixed-slip and side-force skid measurements at low tire slip speeds, the effect of micro texture dominates [34]. Higher grip numbers correspond to a higher micro texture.

Figure 2.16 and 2.17 summarize the average Grip Tester results obtained over the entire length of the MnROAD test cells. The cells were tested on throughout the day on April 20, 2009 in the wheel path, between the wheel paths and in the driving and passing lanes. The air temperature was between 5 – 8 ℉; and pavement subsurface (0.5" below the surface) temperatures ranged from 8 to 22 ℉, except for the porous cells which remained almost constant at 11℉ throughout the day. The UTBWC (cells 2 & 3) had the highest grip numbers followed closely by the porous (cells 86 & 88). The porous control (cell 87) had the lowest the grip numbers, and the highest difference between wheel paths in a single lane. The FRAP (cell 22) and WMA control (cell 24) displayed relatively low grip numbers compared with the -34, 0%RAP (cell 4), the 4.75 (cell 6) and the WMA (cell 19). Appendix B shows plots of continuous measurements obtained from Grip Tester in the passing lane.
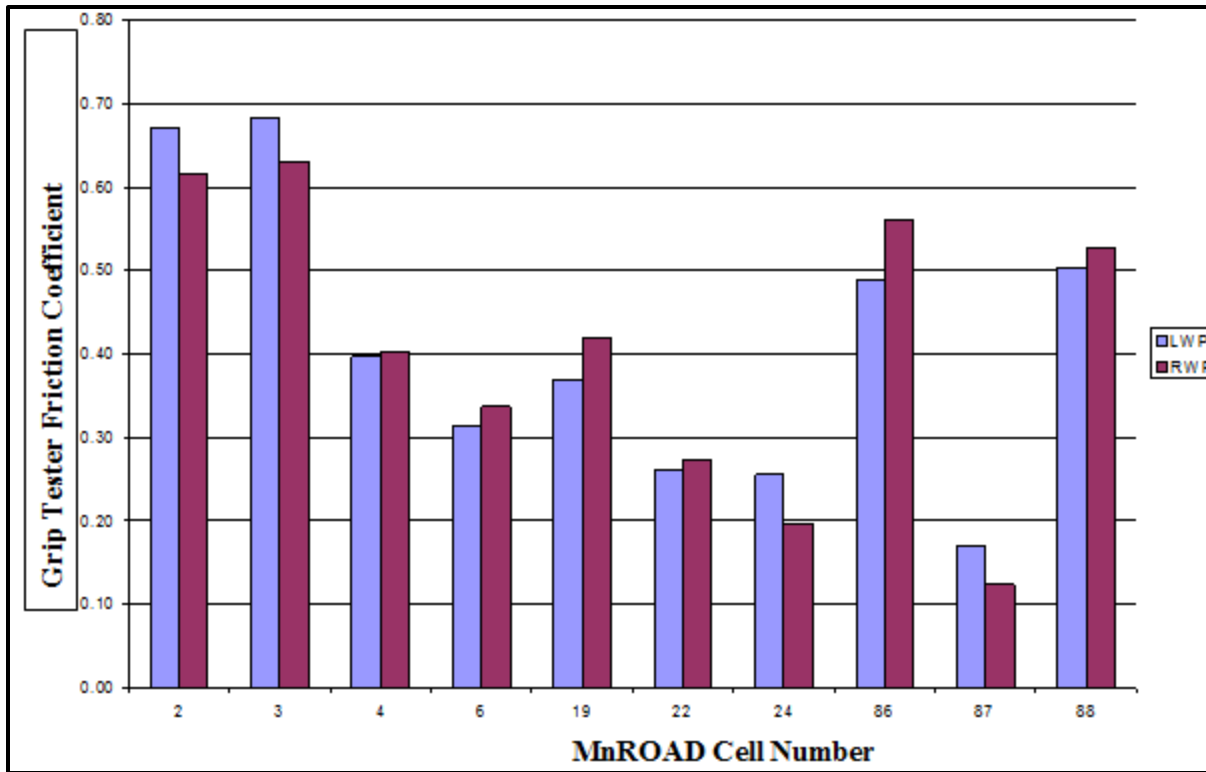
Figure 2.16 April 2009 MnROAD Grip Tester Results for ML-Driving, LVR-Inside Lane
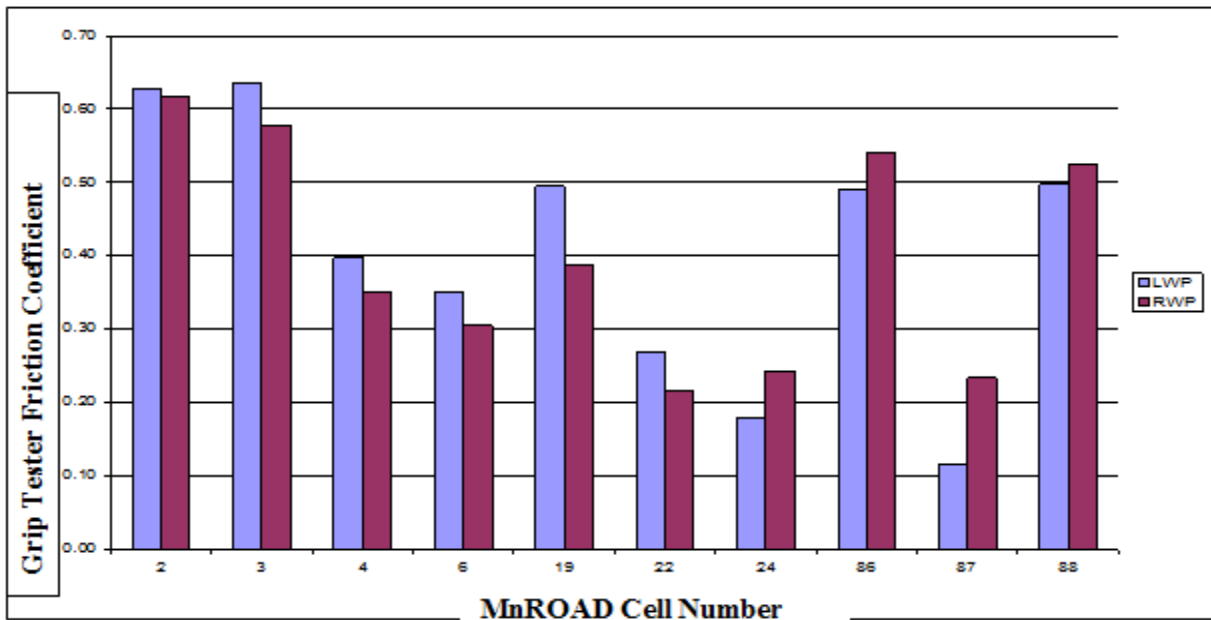
Figure 2.17 April 2009 MnROAD Grip Tester Results for ML-Passing, LVR-Outside Lane

Dynamic Friction Tester:

The Dynamic Friction Tester (DFT) consists of three rubber sliders, positioned on a disk of diameter 13.75 in, that are suspended above the pavement surface. When the tangential velocity of the sliders reaches 90 km/hr water is applied to the surface and the sliders make contact with the pavement. A computer takes friction measurements across a range of speeds as the sliders slow to a stop. This test was just recently acquired by MnDOT using project funds, and consequently measurements will be included in a later report.

RIDE

Ames Light Weight Profiler Measurements:

Ride was measured in both the left and right wheel paths of the driving and passing lanes using an Ames lightweight inertial surface analyzer (LISA) as shown in Figures 2.18 and 2.19. The testing took place on November 19, 2008 following construction. The results were separated into cells by cropping the start and end stations of each of the cells.

Figure 2.18 and 2.19 show a comparative plot of the average ride for the entire length of the study cells in terms of IRI (in/mi) for the driving and passing lanes respectively. In the driving lane, the UTBWC (cells 2 & 3) had the lowest IRI, followed by the FRAP (cell 22) and in the passing lane the WM (cell 19) and the FRAP (cell 22) had the lowest IRI. In the driving lane, the 4.75 (cell 6) appears to have the highest IRI, and in the passing lane, the -34, 0%RAP had the highest IRI followed by the 4.75 (cell 6) and the UTBWC (cells 2 & 3). The -34, 0%RAP (cell 4) and the WMA (cell 19) appear to have large differences between the LWP and RWP in the driving and passing lanes and large differences between the driving and passing lanes. Figure 2.20 shows the measured profile of cell 3, in the left wheel path of the driving lane; plots of the remaining cells: 4, 6, 19 and 22 can be found in Appendix 2.B. At this stage the lightweight profiler was equipped with a line laser and a triple spot laser which helped with evaluation of texture influence on IRI.
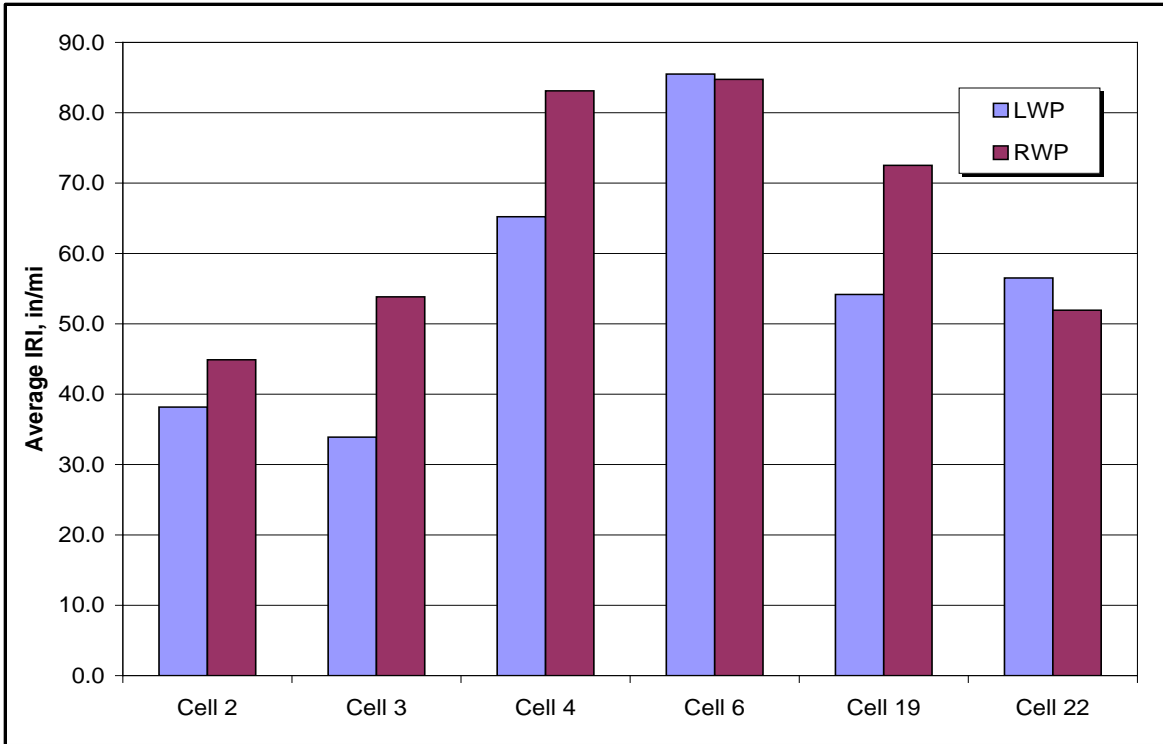
Figure 2.18 Plot of Average IRI for Driving Lane (in/mi), LISA Results
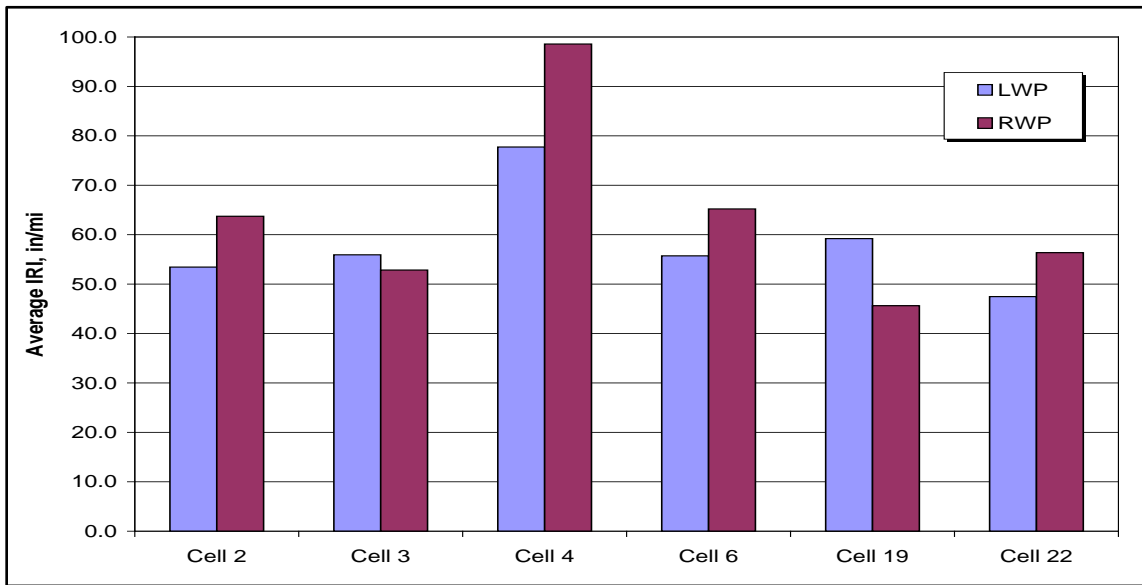
Figure 2.19 Plot of Average IRI for Passing Lane (in/mi), LISA Results
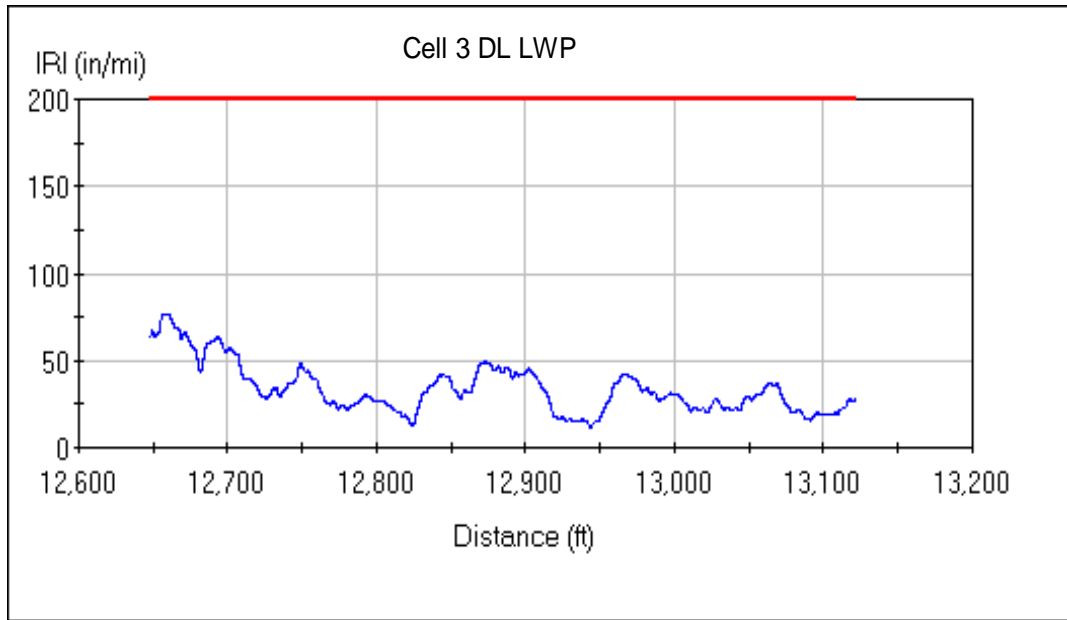
Figure 2.20 October 2008 Continuous Ride Results of Cell 3 (Driving Lane, Left Wheel Path)

SOUND

Absorption (Impedance Tube):

Figure 2.21 shows the initial impedance tube used in 2008. Subsequently, the Current tube acquired by MnDOT later in 2009 was subsequently used according to the standard already described [33]. Figure 2.22 shows the absorption ratios at different frequencies of selected HMA surfaces, which were measured on October 20, 2008 at a test temperature of 64ºF.

Not surprisingly, the porous cell (cell 86) consistently has significantly higher absorption coefficients than the other surfaces. The UTBWC (cell 3) consistently had a higher absorption ratio than the remaining other surfaces, although this difference was not as great as the porous and varied considerably at different frequencies. The 4.75 (cell 6) appears to have among the lowest absorption coefficients. The gradation of the HMA mix appears to have a great impact on sound impedance.

| Original (NCAT) Impedance Tube 2008 | MnDOT Improved Impedance Tube (Note Base enhanced with Circular Hollow Ring Housing a Hermetic Seal) |

Figure 2.21 Sound Impedance Tube
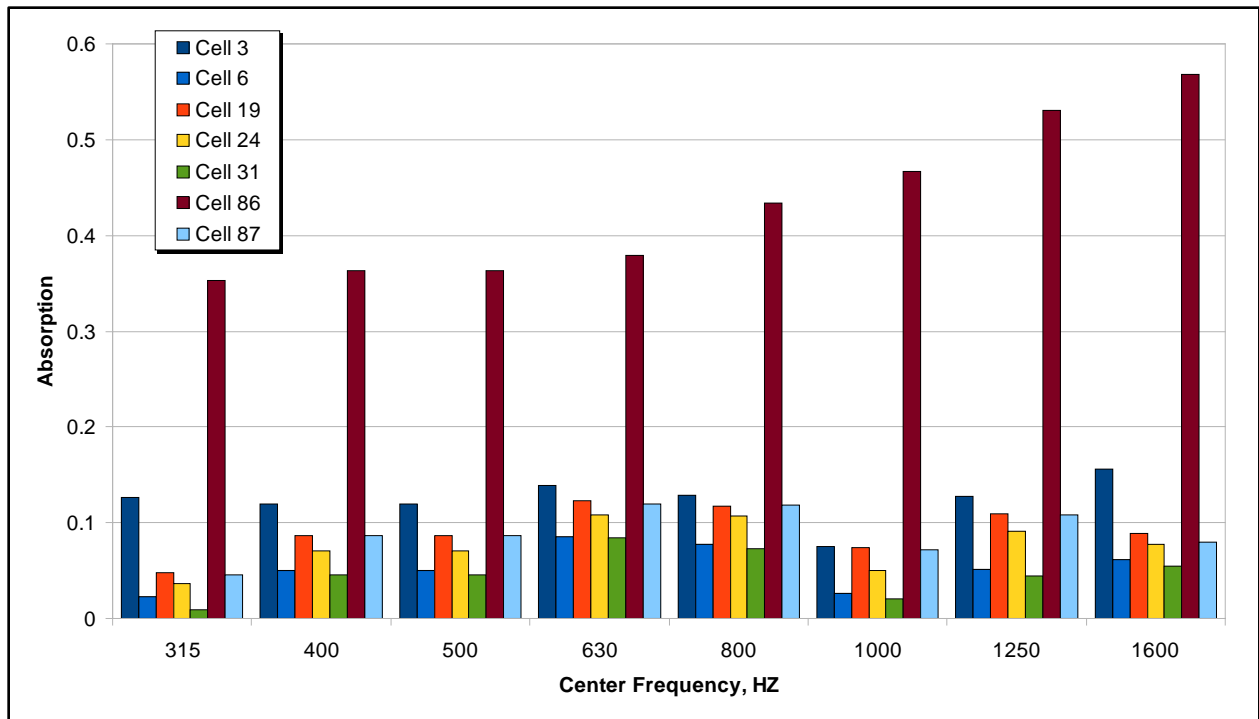
Figure 2.22 Absorption Ratios at different frequencies for selected HMA Surface Types

Intensity (OBSI):

Measurements were conducted according to the procedure already described in chapter 1 adhering to interim AASHTO standard TP 76-09). Monitoring involved three runs per lane thus generating OBSI and spectral details.

The FRAP (cell 22) had the highest A-weighted sound intensity, and the passing lane of the WMA (cell 19) was among the lowest. The UTBWC (cells 2 &3) did not provide the expected sound abatement advantage and had among the highest A-weighted sound intensities.

Figure 2.23 On Board Sound Intensity Test Setup and Microphone Close Up View

1/3 Octave Bands
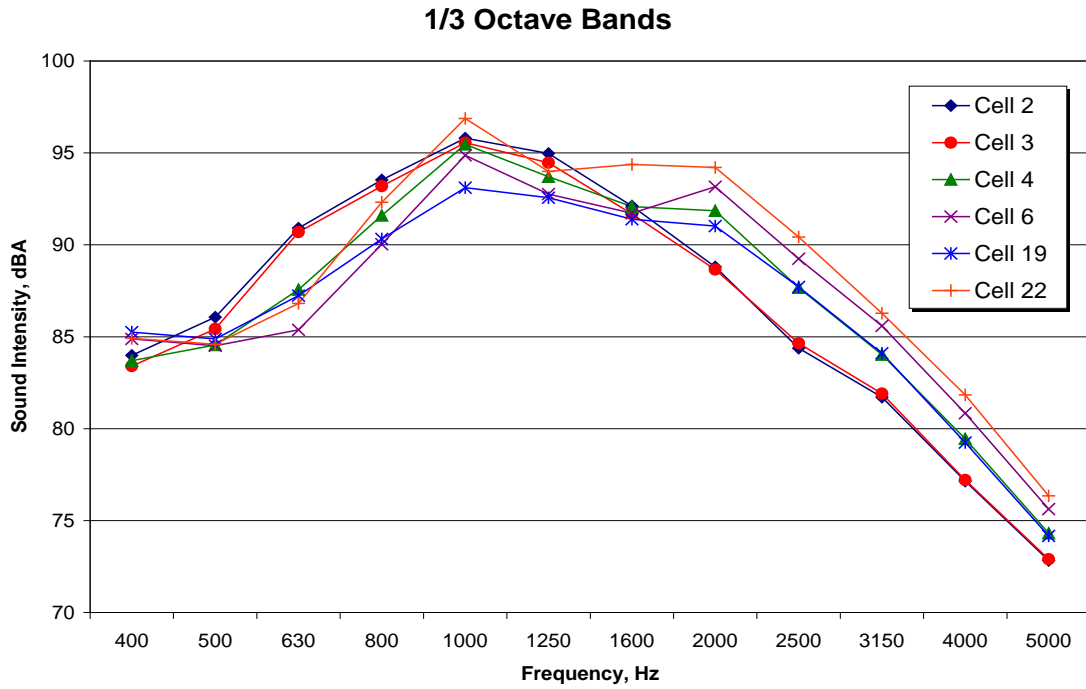
Figure 2.24 On Board Sound Intensity Test Results Passing Lane

1/3 Octave Bands
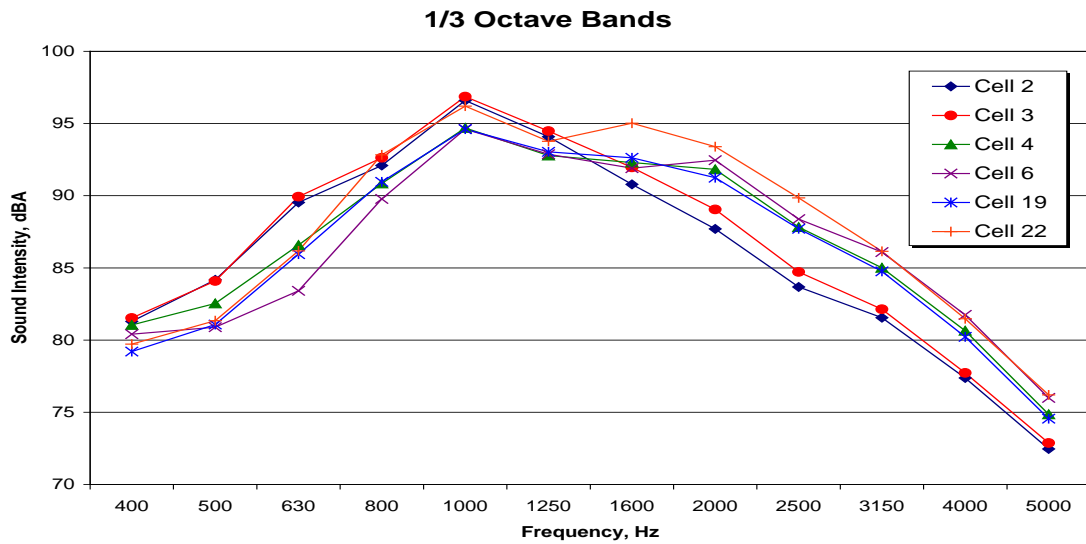
Figure 2.25 On Board Sound Intensity Test Results Driving Lane

53
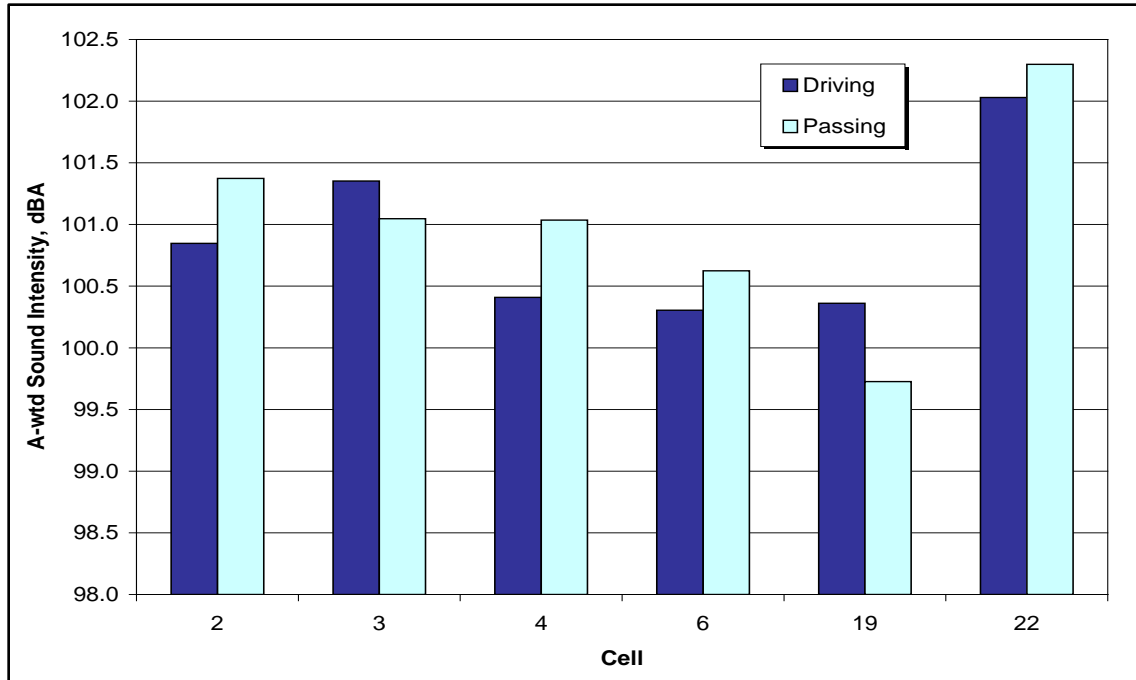
Figure 2.26 A-Weighted Sound Intensity

HYDRAULIC CONDUCTIVITY

Falling Head Permeameter:

The hydraulic conductivity was measured for non-porous HMA cells using a falling head Permeameter shown in Figure 2.27. The hydraulic conductivity was calculated based upon the falling head principle of permeability as shown in equation 4.

$$K = (aL / At)\ln(h_1 / h_2)$$

(11)

The measurements were taken on June 18 – 19, 2009 when the air temperature was between 65 and 82°F. Figure 2.28 shows the hydraulic conductivity measurements of these non-porous HMA cells. The UTBWC (cell 2) has hydraulic conductivity orders of magnitude greater than all other compared cells. The remaining cells have negligible hydraulic conductivity, and the 4.75 (cell 6) has essentially 0 conductivity.

The permeability was also measured for the porous cells using a modified Permeameter as shown in Figure 2. 27. Figure 2.29 shows the hydraulic conductivity measurements of the

porous HMA cells which seem to show a general decreasing trend in hydraulic conductivity. This may be an indication that the cells are becoming "clogged" with debris.

Figure 2.27 Cascaded Field Permeameter'
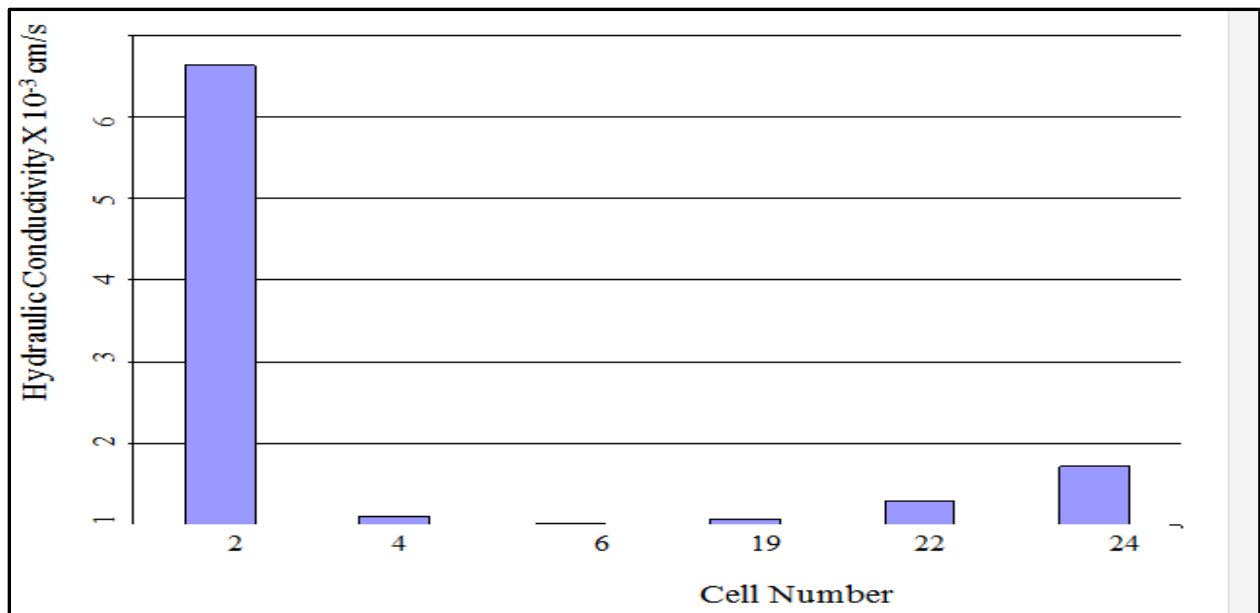
Figure 2.28 Hydraulic Conductivity of Non-Porous HMA
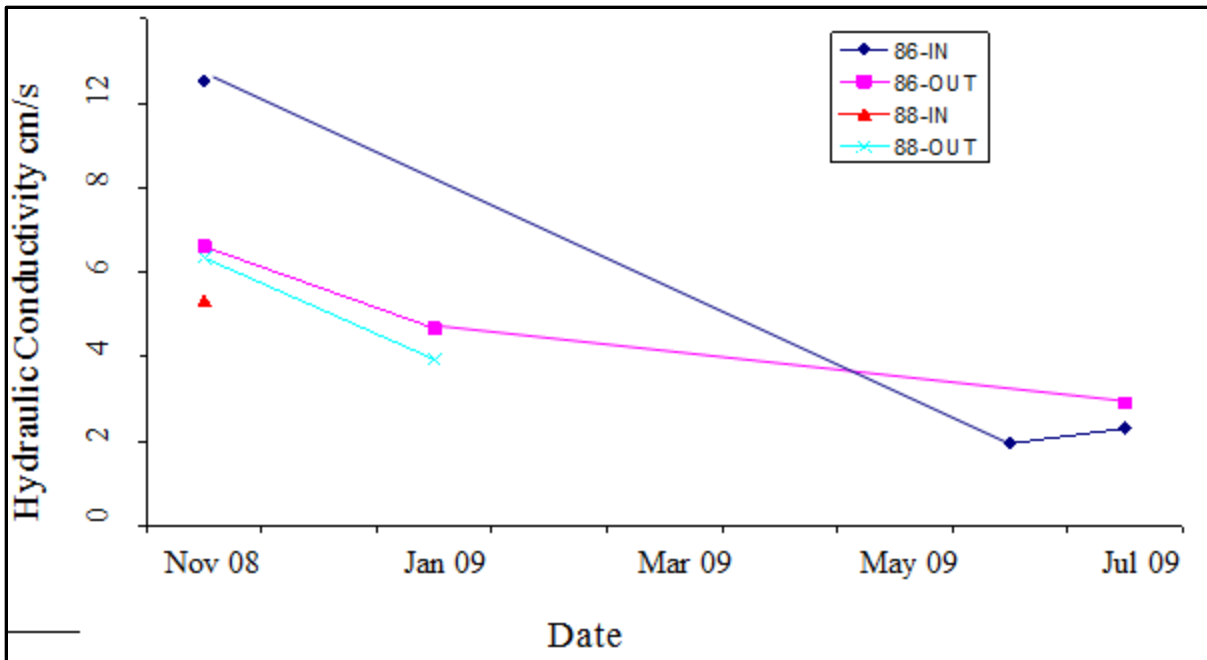
Figure 2.29 Hydraulic Conductivity of Porous HMA

DURABILITY

LTPP Distress Survey Strategy:

The durability of all test cells was evaluated by trained personnel using a rating system based upon the long-term pavement performance (LTPP) evaluation method.

Currently the only visible distresses are low severity raveling and low severity transverse cracking. Although this raveling may be more appropriately labeled asphalt binder drain down, this occurred during the construction process. Raveling, measured in ft^2 was present only in the porous HMA (cells 86 and 88 Figure 2.30). The transverse cracking is measured in lineal ft (12 ft) and present only in cell 6, see Figure 2.31. Forensic cores taken this spring indicate that the concrete layer underneath was also cracked and the HMA was bonded well to the concrete. The cracking in cell 6 was also over embedded sensors (denoted 'TREE'), which may have had an impact as well. Tables 2.8 and 2.9 present the results of the initial distress survey conducted in spring 2009. Note that the general format of the Table is distress type_measurement_severity, for example: "transverse_l_h" denotes transverse cracking, measured in lineal feet, high severity.

56

Figure 2.30 Porous HMA (Cell 86 LEFT, Cell 88 RIGHT), August 2009

Figure 2.31 4.75 mm Aggregate Asphalt (Cell 6), August 2009

Table 2.2: Distress Survey of Test Cells Using LTPP Procedure

	CELL NO.	2	2	3	3	4	4	6	6	19	19	22	22	24	24	86	86	87	87	88	88
	LANE	D	P	D	P	D	P	D	P	D	P	D	P	I	O	I	O	I	O	I	O
Distress	FATIGUE_A_L	0	0	0	0	0	0	0	0	0	0	0	0	0	0	0	0	0	0	0	0
	FATIGUE_A_M	0	0	0	0	0	0	0	0	0	0	0	0	0	0	0	0	0	0	0	0
	FATIGUE_A_H	0	0	0	0	0	0	0	0	0	0	0	0	0	0	0	0	0	0	0	0
	BLOCK_A_L	0	0	0	0	0	0	0	0	0	0	0	0	0	0	0	0	0	0	0	0
	BLOCK_A_M	0	0	0	0	0	0	0	0	0	0	0	0	0	0	0	0	0	0	0	0
	BLOCK_A_H	0	0	0	0	0	0	0	0	0	0	0	0	0	0	0	0	0	0	0	0
	EDGE_L_L	0	0	0	0	0	0	0	0	0	0	0	0	0	0	0	0	0	0	0	0
	EDGE_L_M	0	0	0	0	0	0	0	0	0	0	0	0	0	0	0	0	0	0	0	0
	EDGE_L_H	0	0	0	0	0	0	0	0	0	0	0	0	0	0	0	0	0	0	0	0
	LONG_WP_L_L	0	0	0	0	0	0	0	0	0	0	0	0	0	0	0	0	0	0	0	0
	LONG_WP_L_M	0	0	0	0	0	0	0	0	0	0	0	0	0	0	0	0	0	0	0	0
	LONG_WP_L_H	0	0	0	0	0	0	0	0	0	0	0	0	0	0	0	0	0	0	0	0
	LONG_WP_SEAL_L_L	0	0	0	0	0	0	0	0	0	0	0	0	0	0	0	0	0	0	0	0
	LONG_WP_SEAL_L_M	0	0	0	0	0	0	0	0	0	0	0	0	0	0	0	0	0	0	0	0
	LONG_WP_SEAL_L_H	0	0	0	0	0	0	0	0	0	0	0	0	0	0	0	0	0	0	0	0
	LONG_NWP_L_L	0	0	0	0	0	0	0	0	0	0	0	0	0	0	0	0	0	0	0	0
	LONG_NWP_L_M	0	0	0	0	0	0	0	0	0	0	0	0	0	0	0	0	0	0	0	0
	LONG_NWP_L_H	0	0	0	0	0	0	0	0	0	0	0	0	0	0	0	0	0	0	0	0
	LONG_NWP_SEAL_L_L	0	0	0	0	0	0	0	0	0	0	0	0	0	0	0	0	0	0	0	0
	LONG_NWP_SEAL_L_M	0	0	0	0	0	0	0	0	0	0	0	0	0	0	0	0	0	0	0	0
	LONG_NWP_SEAL_L_H	0	0	0	0	0	0	0	0	0	0	0	0	0	0	0	0	0	0	0	0
	TRANSVERSE_NO_L	0	0	0	0	0	0	1	1	0	0	0	0	0	0	0	0	0	0	0	0
	TRANSVERSE_L_L	0	0	0	0	0	0	12	12	0	0	0	0	0	0	0	0	0	0	0	0
	TRANSVERSE_NO_M	0	0	0	0	0	0	0	0	0	0	0	0	0	0	0	0	0	0	0	0
	TRANSVERSE_L_M	0	0	0	0	0	0	0	0	0	0	0	0	0	0	0	0	0	0	0	0
	TRANSVERSE_NO_H	0	0	0	0	0	0	0	0	0	0	0	0	0	0	0	0	0	0	0	0
	TRANSVERSE_L_H	0	0	0	0	0	0	0	0	0	0	0	0	0	0	0	0	0	0	0	0
	TRANSVERSE_SEAL_NO_L	0	0	0	0	0	0	0	0	0	0	0	0	0	0	0	0	0	0	0	0
	TRANSVERSE_SEAL_L_L	0	0	0	0	0	0	0	0	0	0	0	0	0	0	0	0	0	0	0	0
	TRANSVERSE_SEAL_NO_M	0	0	0	0	0	0	0	0	0	0	0	0	0	0	0	0	0	0	0	0
	TRANSVERSE_SEAL_L_M	0	0	0	0	0	0	0	0	0	0	0	0	0	0	0	0	0	0	0	0
	TRANSVERSE_SEAL_NO_H	0	0	0	0	0	0	0	0	0	0	0	0	0	0	0	0	0	0	0	0
	TRANSVERSE_SEAL_L_H	0	0	0	0	0	0	0	0	0	0	0	0	0	0	0	0	0	0	0	0
	PATCH_NO_L	0	0	0	0	0	0	0	0	0	0	0	0	0	0	0	0	0	0	0	0
	PATCH_A_L	0	0	0	0	0	0	0	0	0	0	0	0	0	0	0	0	0	0	0	0
	PATCH_NO_M	0	0	0	0	0	0	0	0	0	0	0	0	0	0	0	0	0	0	0	0
	PATCH_A_M	0	0	0	0	0	0	0	0	0	0	0	0	0	0	0	0	0	0	0	0
	PATCH_NO_H	0	0	0	0	0	0	0	0	0	0	0	0	0	0	0	0	0	0	0	0
	PATCH_A_H	0	0	0	0	0	0	0	0	0	0	0	0	0	0	0	0	0	0	0	0
	POTHOLES_NO_L	0	0	0	0	0	0	0	0	0	0	0	0	0	0	0	0	0	0	0	0
	POTHOLES_A_L	0	0	0	0	0	0	0	0	0	0	0	0	0	0	0	0	0	0	0	0
	POTHOLES_NO_M	0	0	0	0	0	0	0	0	0	0	0	0	0	0	0	0	0	0	0	0
	POTHOLES_A_M	0	0	0	0	0	0	0	0	0	0	0	0	0	0	0	0	0	0	0	0
	POTHOLES_NO_H	0	0	0	0	0	0	0	0	0	0	0	0	0	0	0	0	0	0	0	0
	POTHOLES_A_H	0	0	0	0	0	0	0	0	0	0	0	0	0	0	0	0	0	0	0	0
	SHOVING_NO	0	0	0	0	0	0	0	0	0	0	0	0	0	0	0	0	0	0	0	0
	SHOVING_A	0	0	0	0	0	0	0	0	0	0	0	0	0	0	0	0	0	0	0	0
	BLEEDING_A_L	0	0	0	0	0	0	0	0	0	0	0	0	0	0	0	0	0	0	0	0
	BLEEDING_A_M	0	0	0	0	0	0	0	0	0	0	0	0	0	0	0	0	0	0	0	0
	BLEEDING_A_H	0	0	0	0	0	0	0	0	0	0	0	0	0	0	0	0	0	0	0	0
	POLISH_AGG_A	0	0	0	0	0	0	0	0	0	0	0	0	0	0	0	0	0	0	0	0

	CELL NO.	2	2	3	3	4	4	6	6	19	19	22	22	24	24	86	86	87	87	88	88
	LANE	D	P	D	P	D	P	D	P	D	P	D	P	I	O	I	O	I	O	I	O
Distress	RAVELING_A_L	0	0	0	0	0	0	0	0	0	0	0	0	0	0	339	0	0	0	164	111
	RAVELING_A_M	0	0	0	0	0	0	0	0	0	0	0	0	0	0	0	0	0	0	0	0
	RAVELING_A_H	0	0	0	0	0	0	0	0	0	0	0	0	0	0	0	0	0	0	0	0
	PUMPING_NO	0	0	0	0	0	0	0	0	0	0	0	0	0	0	0	0	0	0	0	0
	PUMPING_L	0	0	0	0	0	0	0	0	0	0	0	0	0	0	0	0	0	0	0	0
	CONST_SHLD_JNT_SEAL_L	0	0	0	0	0	0	0	0	0	0	0	0	0	0	0	0	0	0	0	0
	CONST_SHLD_JNT_SEAL_M	0	0	0	0	0	0	0	0	0	0	0	0	0	0	0	0	0	0	0	0
	CONST_SHLD_JNT_SEAL_H	0	0	0	0	0	0	0	0	0	0	0	0	0	0	0	0	0	0	0	0
	CONST_SHLD_JNT_L	0	0	0	0	0	0	0	0	0	0	0	0	0	0	0	0	0	0	0	0
	CONST_SHLD_JNT_M	0	0	0	0	0	0	0	0	0	0	0	0	0	0	0	0	0	0	0	0
	CONST_SHLD_JNT_H	0	0	0	0	0	0	0	0	0	0	0	0	0	0	0	0	0	0	0	0
	CONST_CL_JNT_SEAL_L	0	0	0	0	0	0	0	0	0	0	0	0	0	0	0	0	0	0	0	0
	CONST_CL_JNT_SEAL_M	0	0	0	0	0	0	0	0	0	0	0	0	0	0	0	0	0	0	0	0
	CONST_CL_JNT_SEAL_H	0	0	0	0	0	0	0	0	0	0	0	0	0	0	0	0	0	0	0	0
	CONST_CL_JNT_L	0	0	0	0	0	0	0	0	0	0	0	0	0	0	0	0	0	0	0	0
	CONST_CL_JNT_M	0	0	0	0	0	0	0	0	0	0	0	0	0	0	0	0	0	0	0	0
	CONST_CL_JNT_H	0	0	0	0	0	0	0	0	0	0	0	0	0	0	0	0	0	0	0	0

P= passing lane. D= Driving lane: I = inside lane and O = Outside Lane

DISCUSSION ON INITIAL TESTING RESULTS OF CONSTRUCTED CELLS

The construction of different surface types that utilize a wide range of new technologies and materials in close proximity to each other, within a state of the art pavement-research test facility will provide a valuable insight into the influence of mixture, environmental and traffic properties on various surface characteristics.

The UTBWC (cells 2 & 3) had the lowest initial average IRI of the tested surfaces. The 4.75 (cell 6) and the -34, 0%RAP had among the highest average IRI followed by the WMA (cell 19) and the FRAP (cell 22). It is unclear at this time which mixture properties are influencing ride the most. Surface macro texture appeared to be heavily influenced by mixture gradation, with the UTBWC (cells 2 & 3) exhibiting high macro texture alone. However the fine, dense graded 4.75 (cell 6) exhibited little noticeable difference from the more coarse dense graded mixtures. Friction also appeared to be influenced by mixture gradation with the UTBWC (cells 2 & 3) and the Porous HMA (cells 86 & 88) exhibiting relatively high values and relatively low differences between ribbed and smooth tire results. The 4.75 (cell 6) exhibited relatively high ribbed tire results, but low smooth tire results. An exception to this gradation observation are results from the WMA control (cell 24) which showed the highest results (and low variability between smooth and ribbed tires) in June 2009 LWST testing, and the WMA (cell 19) which showed the highest results in October 2008 LWST testing (with low variability between smooth and ribbed tires).

The influence of mixture properties on noise is not readily apparent based upon visual observations alone, however, gradation appears to have an effect on the absorption ratios and binder properties and RAP content appear to have an effect on sound intensity levels. The porous HMA (cell 86) had significantly higher absorption coefficients followed by the UTBWC (cell 3), with the 4.75 (cell 6) exhibiting among the lowest absorption coefficients. The FRAP (cell 22) had the highest A-weighted sound intensity, and the passing lane of the WMA (cell 19) had among the lowest. This may suggest that the stiffness of the mixture may play a role in the high-speed sound intensities. It has been documented elsewhere [38] that HMA pavements become louder as they age. In addition a relatively flexible pavement that is allowed to vibrate is beneficial for noise abatement. The UTBWC (cells 2 &3) had among the highest A-weighted sound intensities. This mixture was expected to provide a sound abatement advantage because of the gap gradation, however this advantage may have been mitigated by the fact that the

UTBWC is a relatively stiff mixture and thus not able to vibrate as much as other mixtures.

Durability only appears to be an issue for the porous HMA (cells 86 & 88) as these sections are already experiencing raveling after their first winter. The 4.75 (cell 6) is the only cell experiencing cracking, but this crack is near embedded instrumentation and over a crack in the underlying PCC pavement, which may have influenced the crack development. The UTBWC (cells 2 & 3) had the lowest average IRI of the tested surfaces. The 4.75 (cell 6) and the -34, 0%RAP had among the highest average IRI followed by the WMA (cell 19) and the FRAP (cell 22). It is unclear at this time which mixture properties are influencing ride the most.

CHAPTER 3

SEASONAL MEASUREMENTS OF SURFACE: 4TH YEAR CHARACTERISTICS (2012)

PERFORMANCE OF SURFACE TREATMENTS

Chapter Objectives

This chapter discusses the 4th year monitoring and tests and results obtained as far as they include performance of the test cells in the prior 3 years.

Chronology of Surface Treatments

The surface characteristics study includes eleven test cells on both the MnROAD ML and LVR. These test cells have unique surface mixture types that include different gradations (gap graded, one-sized gradation, coarse dense graded and fine dense graded), different binder types, different levels of binder aging (Warm Mix Asphalt and Aging Study) and different amounts and gradations (Fractionated) of recycled asphalt pavement (RAP). Construction details, including mix design worksheets and other pertinent information are available in the Task 2 report of this study which documents construction and initial test results [40].

In 2011 cells 106 & 206 were reconstructed due to a failure of the concrete layer below the asphalt. Cell 24 received an additional fog seal over 100 ft in late August.

Figure 3.1 Typical Sections of Mainline (ML) Test Cells as at 2011

24	27	86	87	88
3" 58-34	2" 52-34 / 2" 58-34	5" Porous HMA	4" Control	5" Porous HMA
4" Class 6	6" Class 5	4" RR Ballast	4" Mesabi Ballast	4" RR Ballast
Sand	GCBD / 2009 Chip Seal	10" CA-15	11" CA-15	10" CA-15
100' Fog Seals 2008 2009 2010 2011 2012	7" Clay Borrow / Clay	Type V Geo-Textile	Type V Geo-Textile	Type V Geo-Textile
		Sand	Clay Sand	Clay
Oct 08	Aug 06	Oct 08	Oct 08	Oct 08
Current	Current	Current	Current	Current

Figure 3.2 Typical Sections of Low Volume Road (LVR) Test Cells as at 2011

Four cells had surface treatments placed over the HMA surface. These cells include 2, 3, 24 and 27 (Figures 3.1 &3.2). Cells 2 and 3 received an ultra-thin bonded wearing course (UTBWC), consisting of a high quality, gap graded aggregate and a highly polymer modified asphalt cement (AC). Cell 24 is part of a pooled fund aging study (TPF-5(153)) which required a different section of the cell to be sealed every year. The cell received a fog seal with CSS-1H or CRS-2p emulsion every year through 2012 (100 ft section per year). In September 2009, Cell 27 received a chip seal surface treatment consisting of a polymer modified CRS-2p emulsion followed by class A aggregate meeting the FA-2 (inside lane) and FA-3 (outside lane) gradations shown in Table 3.10.

A current pooled-fund study, TPF-5 (153) involves the Minnesota Local Road Research Board and the Maryland, Minnesota, Ohio, Texas, Wisconsin Departments of Transportation, and the Asphalt Institute as the study's principal investigator. The study explores how pavement preservation improves the performance of the existing asphalt pavements relative to aging to help determine the optimal timing for application of these treatments. Researchers are applying surface treatments to successive subsections of cell 24 throughout the pavement life – from immediately behind the paver to successive years – and taking field cores from each subsection every year to determine the material properties, especially related to aging. Monitoring activities also will include various distress surveys.

Micro Surfacing

MnROAD demonstrated the advancements in the effectiveness of traditional and flexible micro surfacing during the course of five maintenance projects starting with a single test cell in 1999. A 2006 MnROAD study involved treating four low-volume road (LVR) cells with flexible micro surfacing, which uses an PG grade 48-34 asphalt binder rigid enough for rut filling, but also flexible enough to inhibit low-temperature reflective cracking. The treatments showed promising results for reflective cracking and rut filling and led to a 2012 micro surfacing project MnROAD with Kraton and FHWA that used high-polymer modified emulsion on an interstate test cell. Results are showing that use of "softer" base asphalt (low temperature grade of -34 ^{0}C) should enhance the performance of micro surfacing in the colder northern climate states.

Thin Asphalt Overlay

Mill-and-fill is a commonly used repair in Minnesota, and study of a warm-mix asphalt (WMA) overlay at MnROAD revealed that lower plant temperatures for WMA might help extend the life due to less aging. In 2008, MnROAD placed a WMA overlay on an original MnROAD interstate cell that had poor ride, severe top-down cracking, and transverse cracking every 20 feet. Three inches were milled and four inches of WMA placed. The WMA modifier assisted the contractor in achieving compaction, with 40 percent of the cracking returning after four years of interstate service.

Ultra-Thin Bonded Wearing Course (UTBWC) with Full-Depth Recycling (FDR)

In partnership with Road Science, MnROAD constructed three stabilized FDR reclamation sections with varying pulverized asphalt concrete/granular base ratios on the I-94 mainline in 2008. The sections allow researchers to study the performance of full-depth reclaimed pavements that were stabilized with engineered emulsion over time. Surfacing for two cells consisted of a two-inch Superpave mix and a three-quarter-inch ultra-thin bonded wearing course (NovaChip). Another cell consisted of two-inch Superpave with one-inch of dense-graded mix placed with the spray paver. After 5 years of interstate high volume traffic, these test cells are performing well with good ride with very little to no rutting or cracking.

Table 3.1 Chip Seal Surface Treatment Gradation

Sieve Size	FA-1	FA-2	FA- 2 1/2	FA-3	FA-3 1/2	QC range
12.5 mm [**1/2 inch**]	100	100	100	100	100	
9.5 mm [**3/8 inch**]	100	100	100	100	90-100	±5%
6.3 mm [**1/4 inch**]	100	100	0-80	0-70	0-70	±7%
4.75 mm [**# 4**]	0-100	0-100	0-50	0-25	0-25	±7%
2.36 mm [**# 8**]	---	0-40	0-12	0-5	0-5	±4%
1.18 mm [**# 16**]	0-30	0-10	0-5	---	---	±4%
300 μm [**# 50**]	0-15	0-5		---	---	±4%
150 μm [**# 100**]	0-5	---		---	---	±4%
75 μm [**# 200**]	0.0-1.0	0.0-1.0	0.0-1.0	0.0-1.0	0.0-1.0	
Material Tests						
% Shale, max. Mn/DOT 1209	5	5	5	3	2	
Flakiness Index, max. %, FHL T 508[1]	N/A	25	25	25	25	
Los Angeles Rattler, max. % loss, AASHTO T 96 (Mn/DOT modified)				35	35	

[1] Aggregate retained on each sieve, which comprises at least 4 percent of the total sample shall be tested.

Figures 3.3 to 3.5 show the surface of selected study cells, including: ultrathin bonded wearing course (UTBWC), warm mix (WMA), 4.75mm (aggregate size) taconite, porous and Chip Seal, respectively.

Figure 3.3 Ultra-Thin Bonded Wearing Coarse [Left], Warm Mix Asphalt [Right]

Figure 3.4 4.75 Taconite [Left] and Cross-Section of Porous HMA [Right]

Figure 3.5 Chip Seal Surface

Figure 3.6 shows a history of mean profile depth values over time either on the driving or inside lane of each test section. Each marker on the graph represents an average of several texture measurements at a particular location. The porous asphalt surfaces (Cells 86 and 88) clearly have the most texture, followed by the chip seal surface (Cell 27) and then the UTBWC (Cells 2 and 3). The UTBWC surfaces showed a very slight increase in profile depth over time, while all of the other surfaces stayed relatively constant.
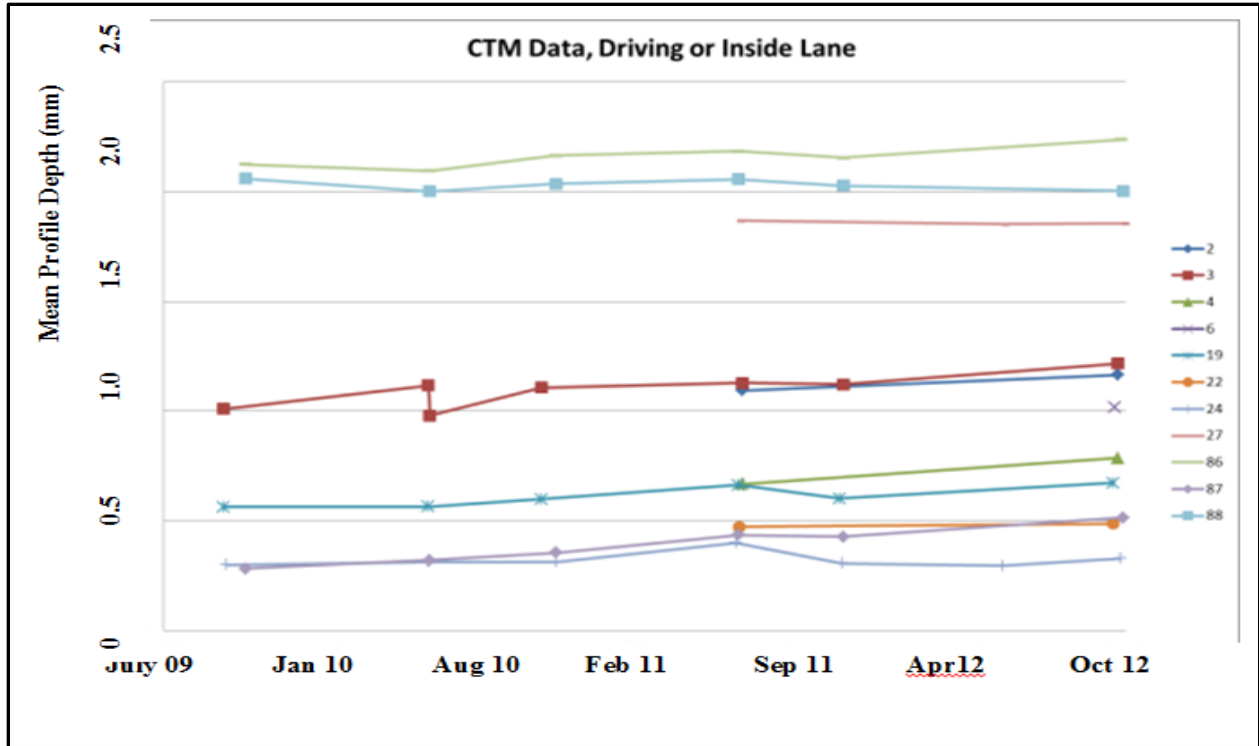
Figure 3.6 History of CTM Data (2009-2012)

Figure 3.7 through 3.12 show the mean profile depth for each cell by station. Each line on the graph represents a different season. The solid lines are the driving or inside lane, while the dotted lines are the passing or outside lane. In general, the driving/inside lane has a lower mean profile depth than the passing/outside lane, indicating that increased traffic degrades the surface texture of asphalt pavements. The plots also shown how uniform (or not) each pavement surface is throughout the length of the cell. Several of the plots also show that the fall measurements are slightly lower than the summer measurements.
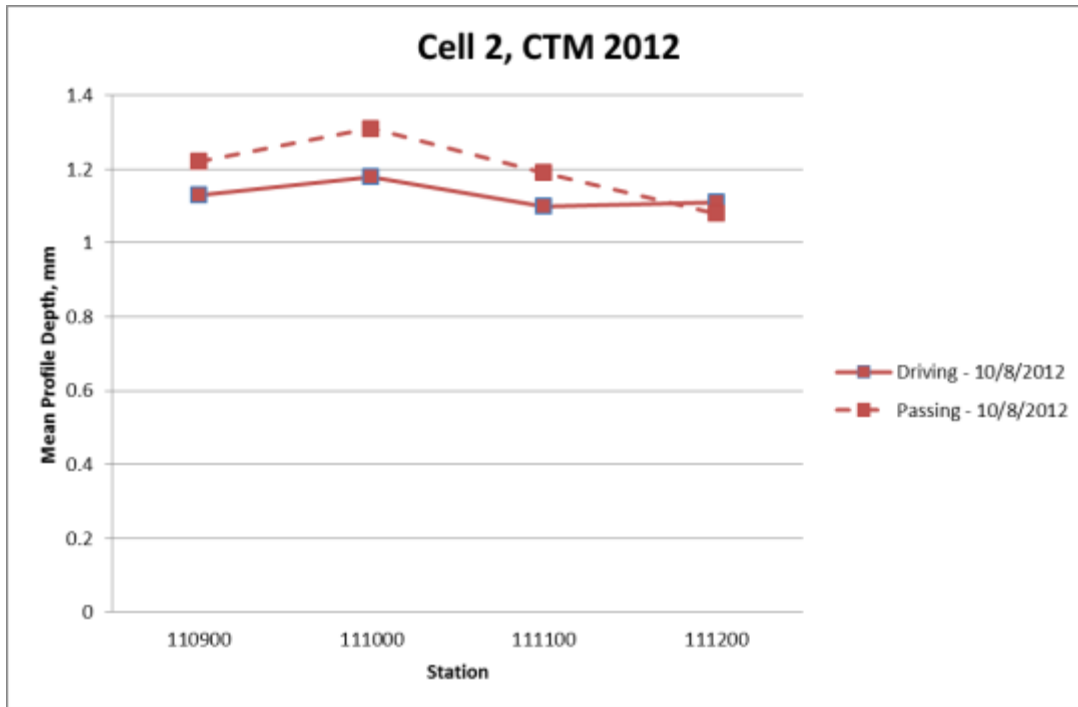
Figure 3.7 2012 Cell 2 CTM Data by Station (110900=1109+00)
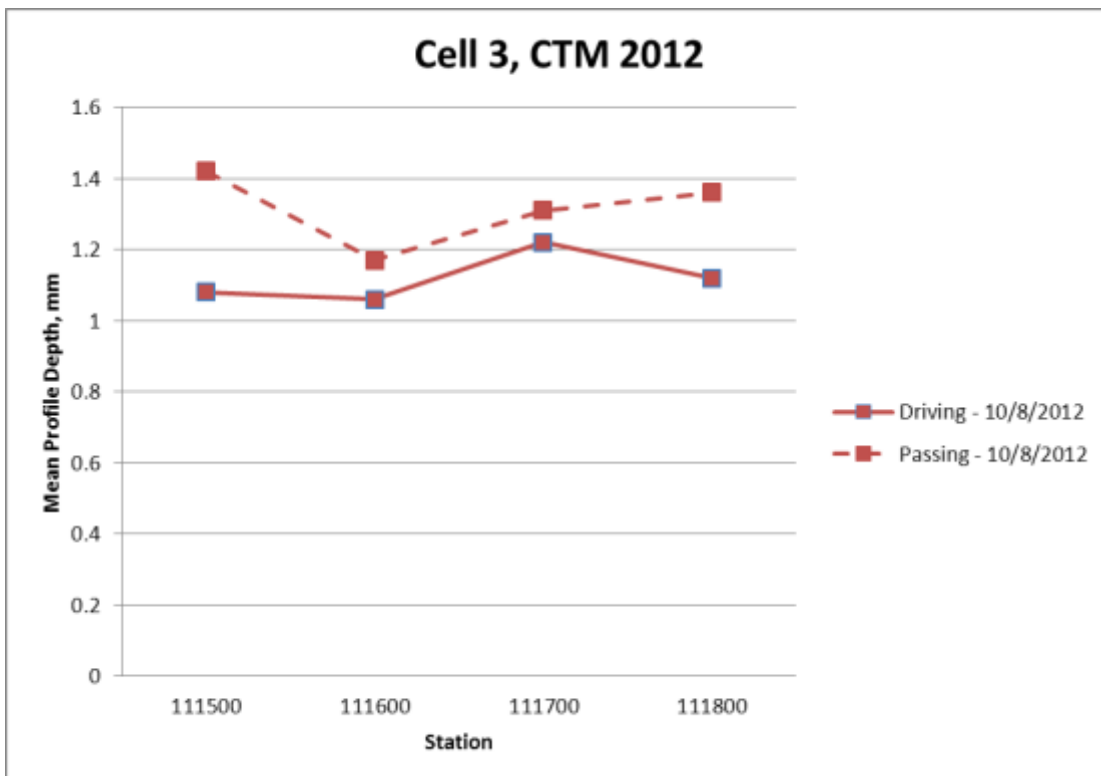
Figure 3.8 2012 Cell 3 CTM Data by Station (111500=1115+00)
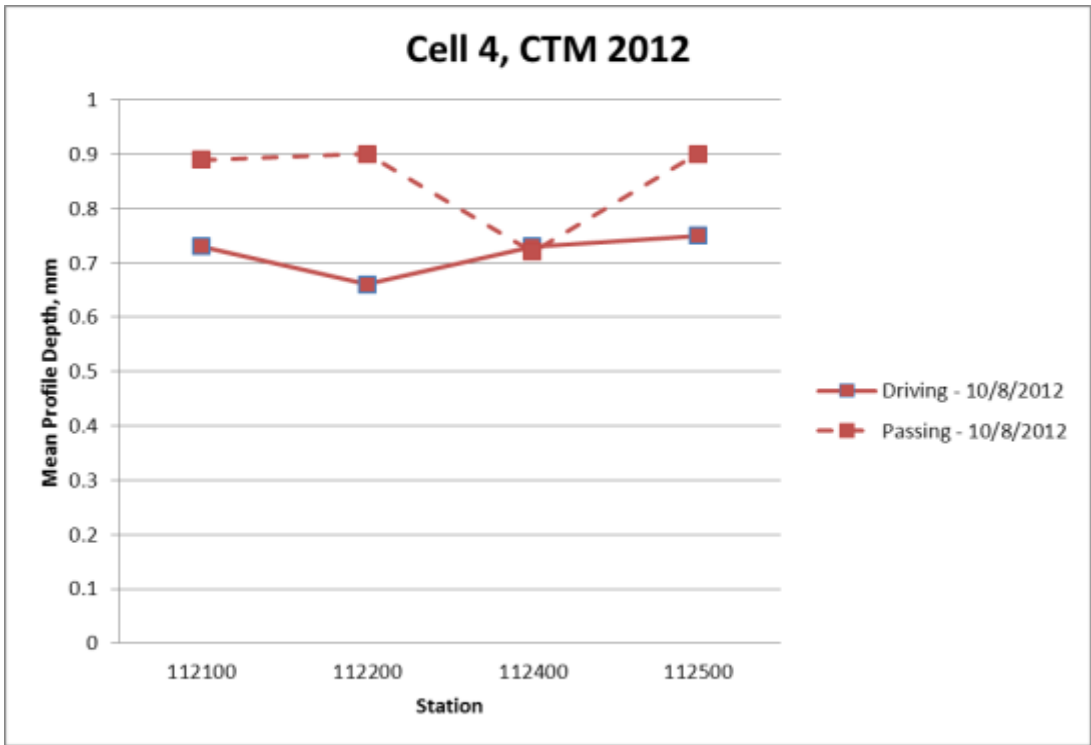
Figure 3.9 2012 Cell 4 CTM Data by Station (112100=1121+00)
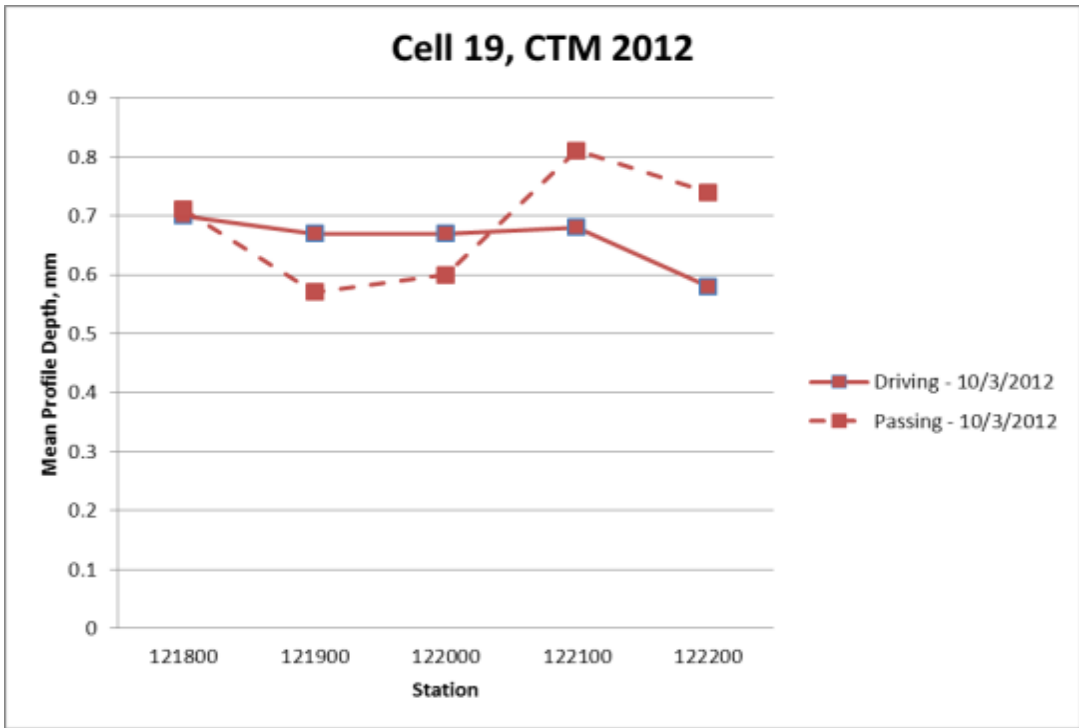
Figure 3.10 2012 Cell 19 CTM Data by Station (121800=1218+00)

70
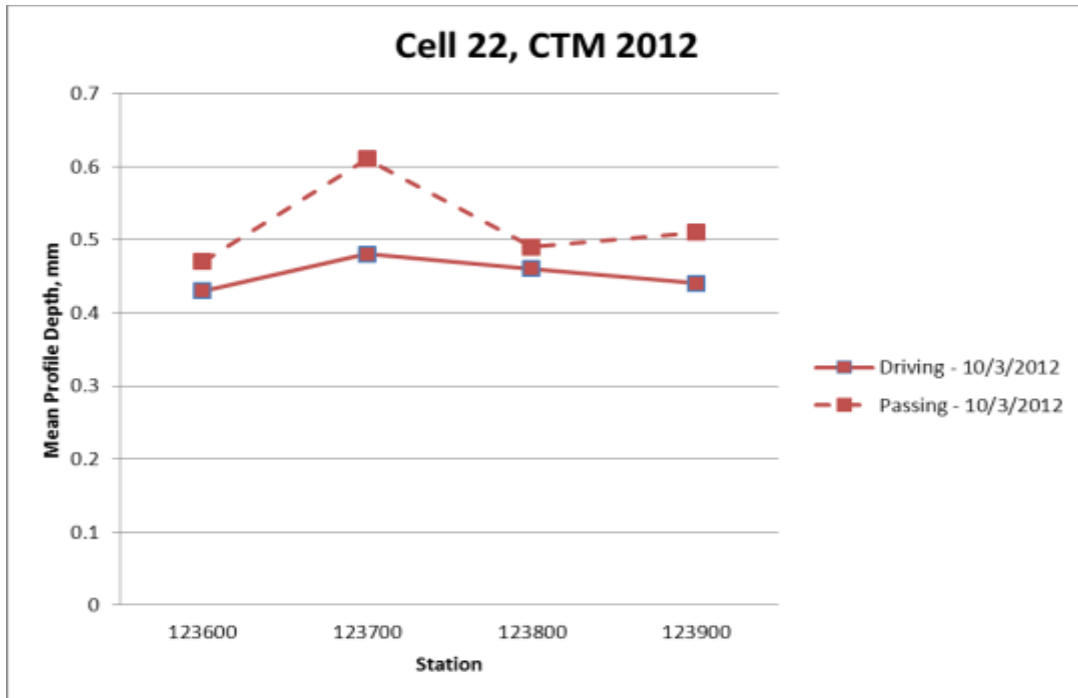
Figure 3.11 2012 Cell 22 CTM Data by Station (123600=236+00)
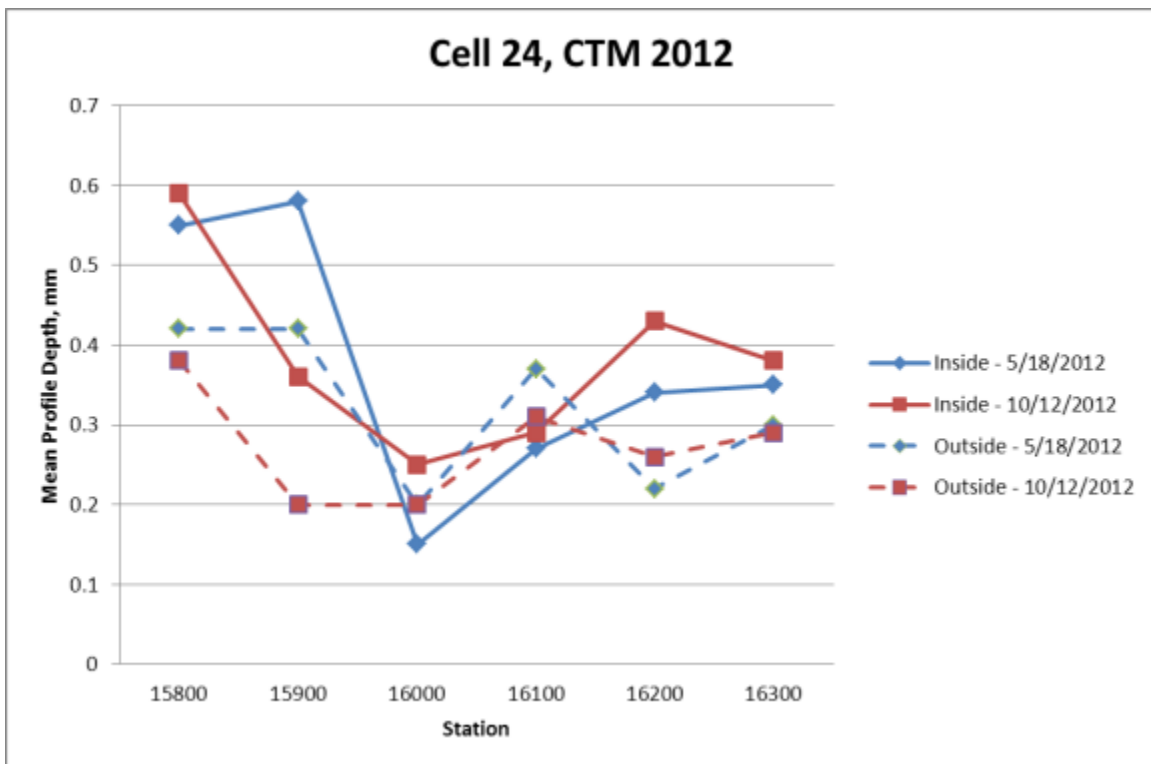
Figure 3.12 2012 Cell 24 CTM Data by Station (15800=158+00)

71
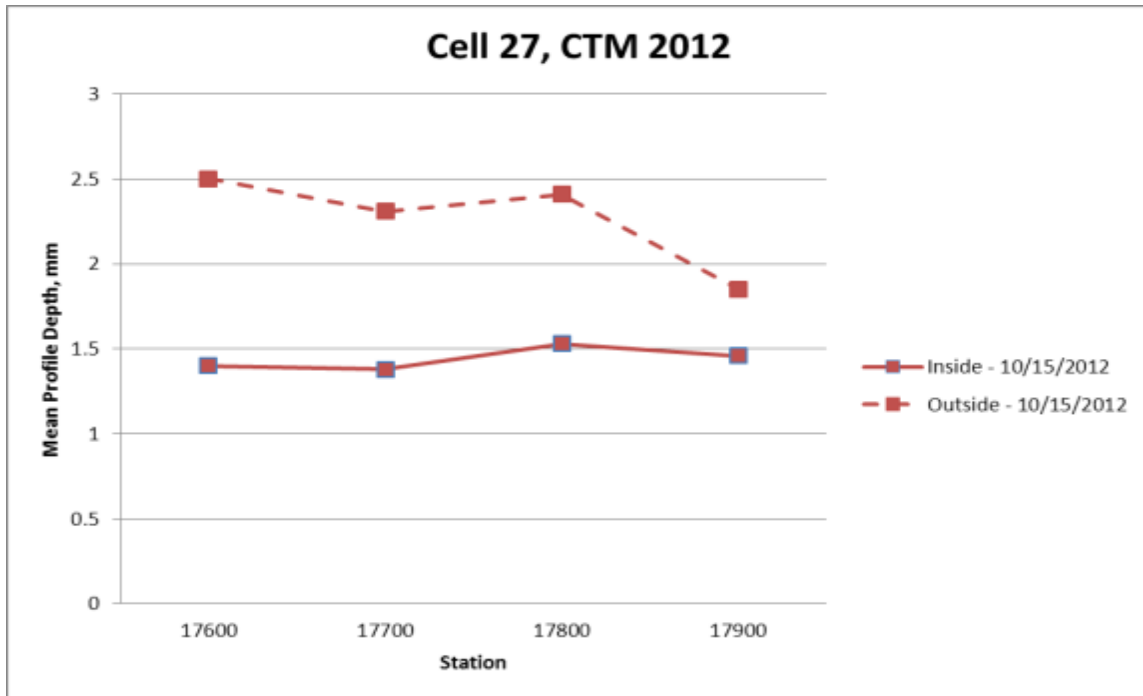
Figure 3.13 2012 Cell 27 CTM Data by Station (17600=176+00)
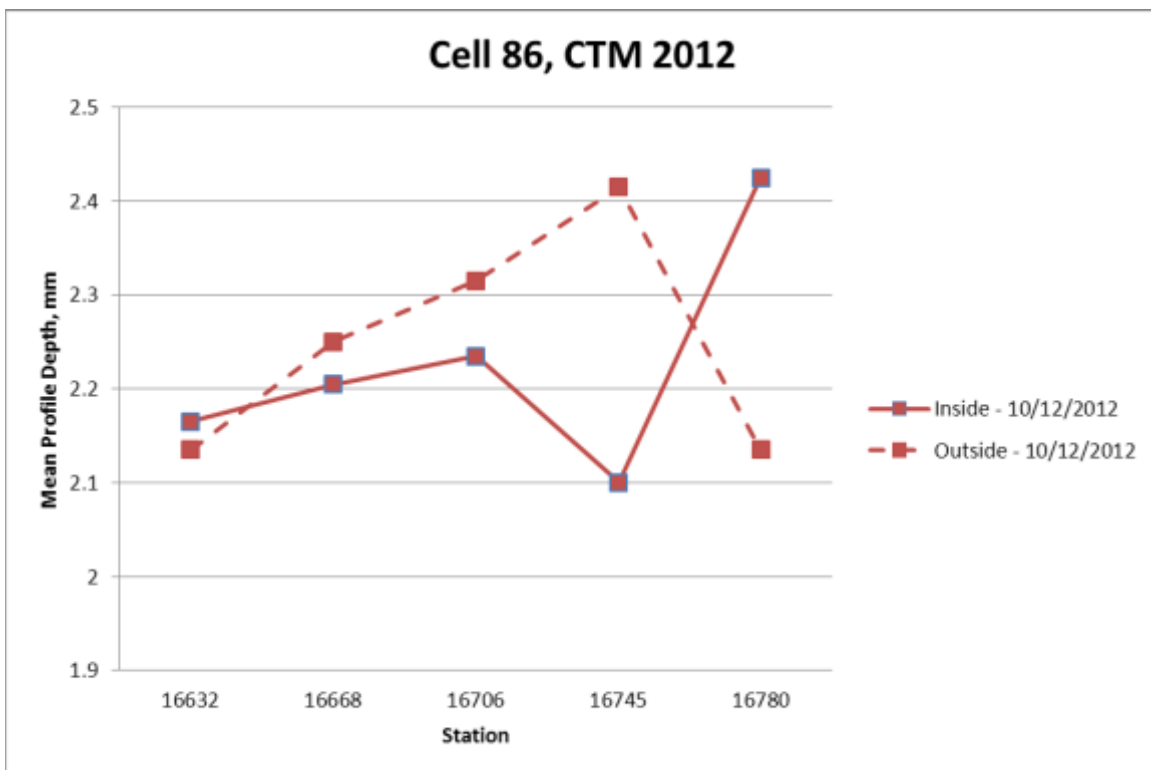
Figure 3.14: 2012 Cell 86 CTM Data by Station (16632=166+32)
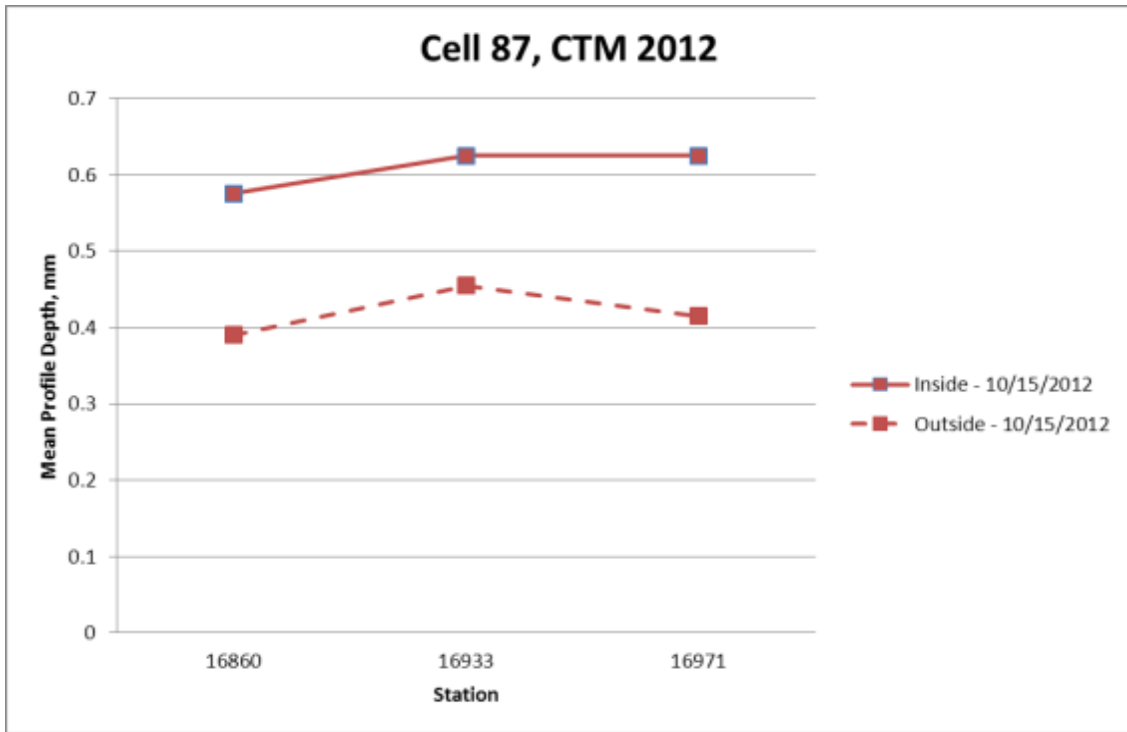
Figure 3.15: 2012 Cell 87 CTM Data by Station (16860=168+60)
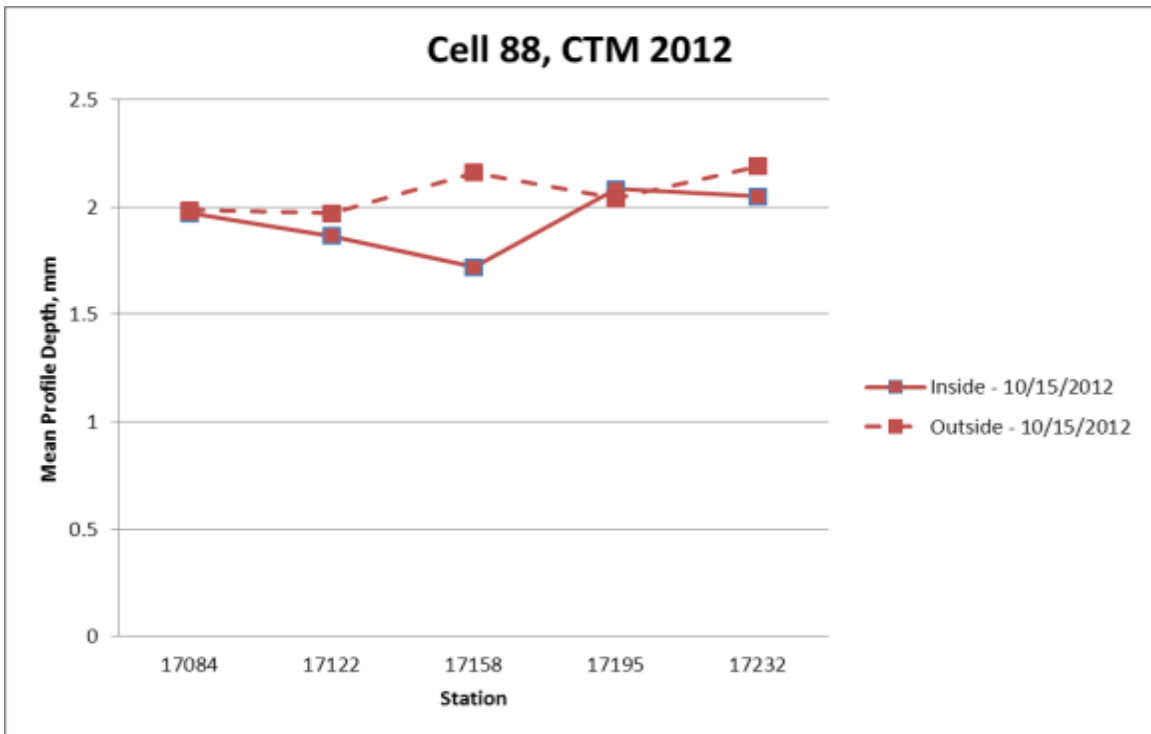
Figure 3.16: 2012 Cell 88 CTM Data by Station (17084=170+84)

73

FRICTION

Locked Wheel Skid Trailer (LWST):

Results of measurements performed are shown in Table 3.3

Table 3.3 Descriptive Statistics for Skid Trailer Data 2009-2012 (Ribbed Tire)

	2	3	4	19	22	24	27	86	87	88
Mean	58.5	59.8	41.9	41.2	29.2	21.4	56.0	53.6	38.2	50.7
Minimum	52.6	54.2	36.1	33.5	25.0	5.2	38.5	46.7	24.7	34.6
Maximum	62.2	63.2	49.2	50.7	37.0	65.2	65.6	60.4	45.8	57.7
Standard Deviation	2.9	2.8	4.4	4.9	3.1	19.2	9.1	4.0	6.5	5.8
Sample Variance	8.1	7.8	19.2	24.3	9.8	370.5	82.7	16.4	42.7	34.0
Count	13	13	13	14	14	12	13	12	12	12

Figure 3.17 shows a plot of all of the friction data collected with the skid trailer over time. The plot shows test results from the ribbed tire on the driving or inside lane. The friction numbers generally range from about 40 to 60. There is some variability in the measurements, which could in part be attributed to pavement surface and tire temperatures at the time of measurement. Some surfaces as the porous asphalt (Cells 86 and 88) and chip seal (Cell 27) appear to have a slight increase in friction number over time, while other surfaces remain relatively constant. Again, one can see the extremely low friction numbers in Cell 24 due to the fog seals that were placed just before (within one week) friction measurements.
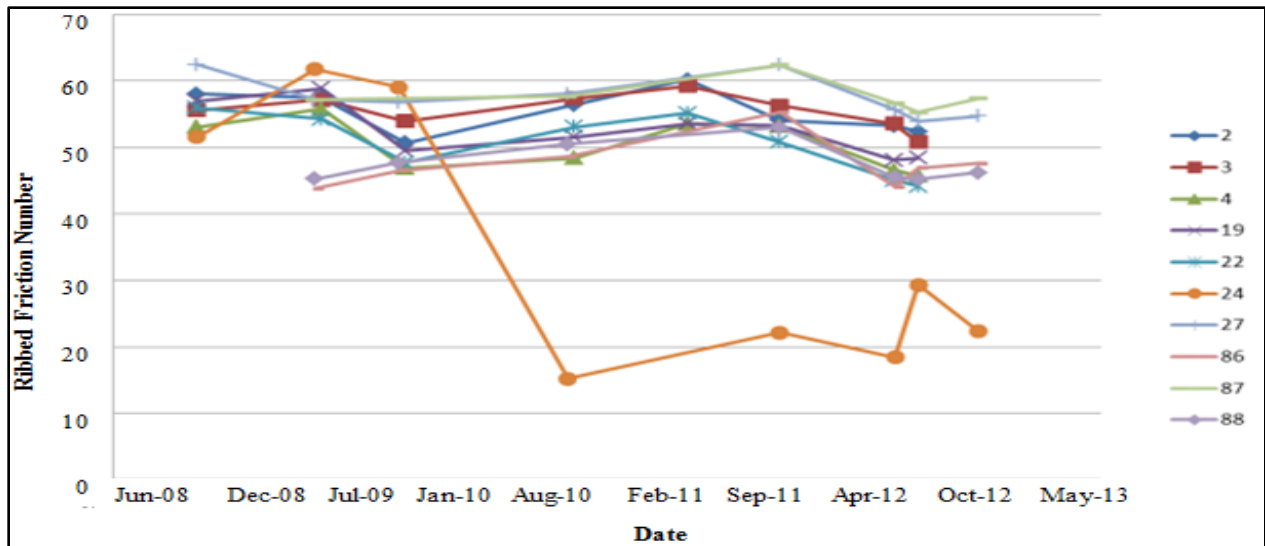
Figure 3. 17 History of Skid Trailer Data, Ribbed Tire

Figure 3.18 and 3.19 show 2012 skid data from the Mainline and Low Volume Road, respectively. The bar colors represent different combinations of tire type and lane. For the dense graded asphalt surfaces (Cells 4, 19, 22, 24, and 87) the ribbed tire has significantly higher friction numbers than the smooth tire. In these cases the microtexture of the mixture is the dominant component of the surface texture. For the more open, aggressive asphalt surfaces (Cells 2, 3, 27, 86, and 88) the ribbed and smooth tires give more similar values, with the smooth tire often exhibiting a higher friction number. In these cases the mixture macrotexture governs the friction properties of the pavement surface. In general the passing/outside lane has a higher friction number than the driving/inside lane, again demonstrating the effect of traffic on friction characteristics of asphalt pavements.
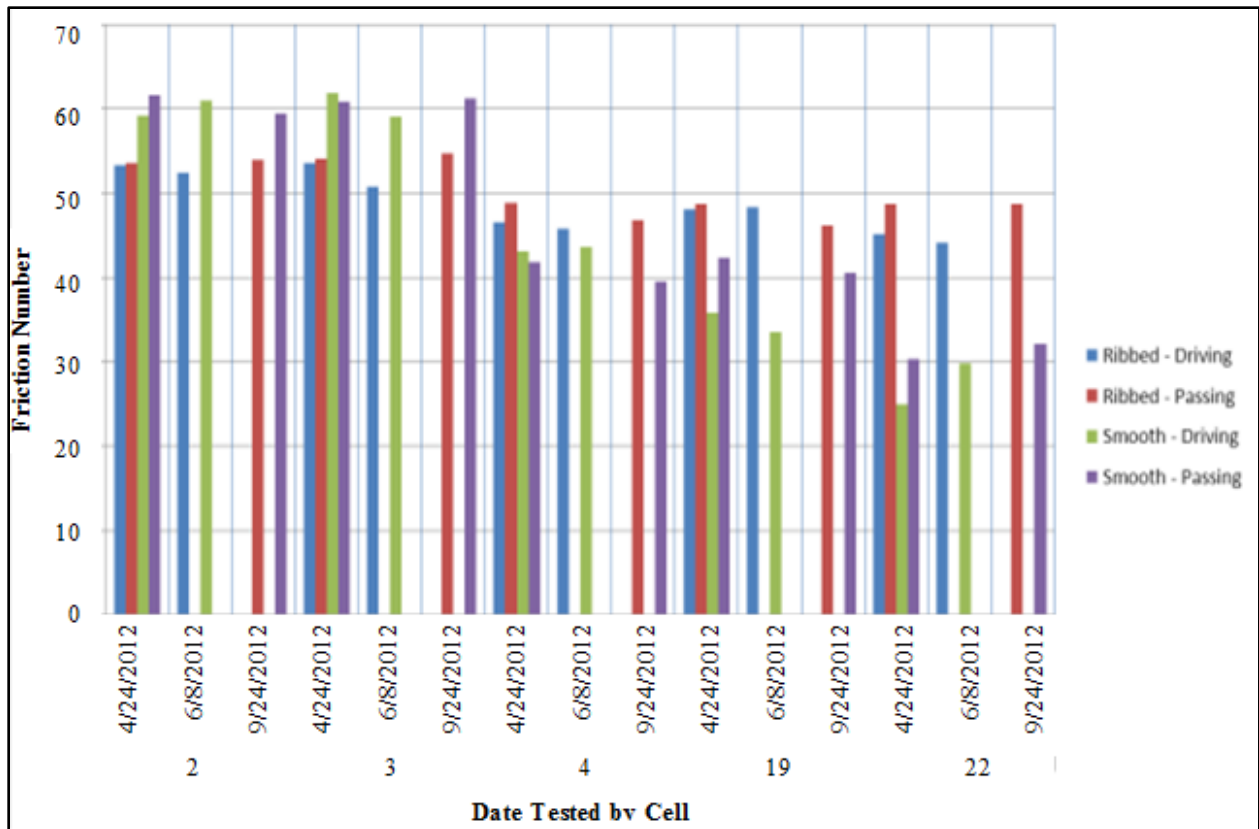
Figure 3.18 2012 Mainline Skid Trailer Data
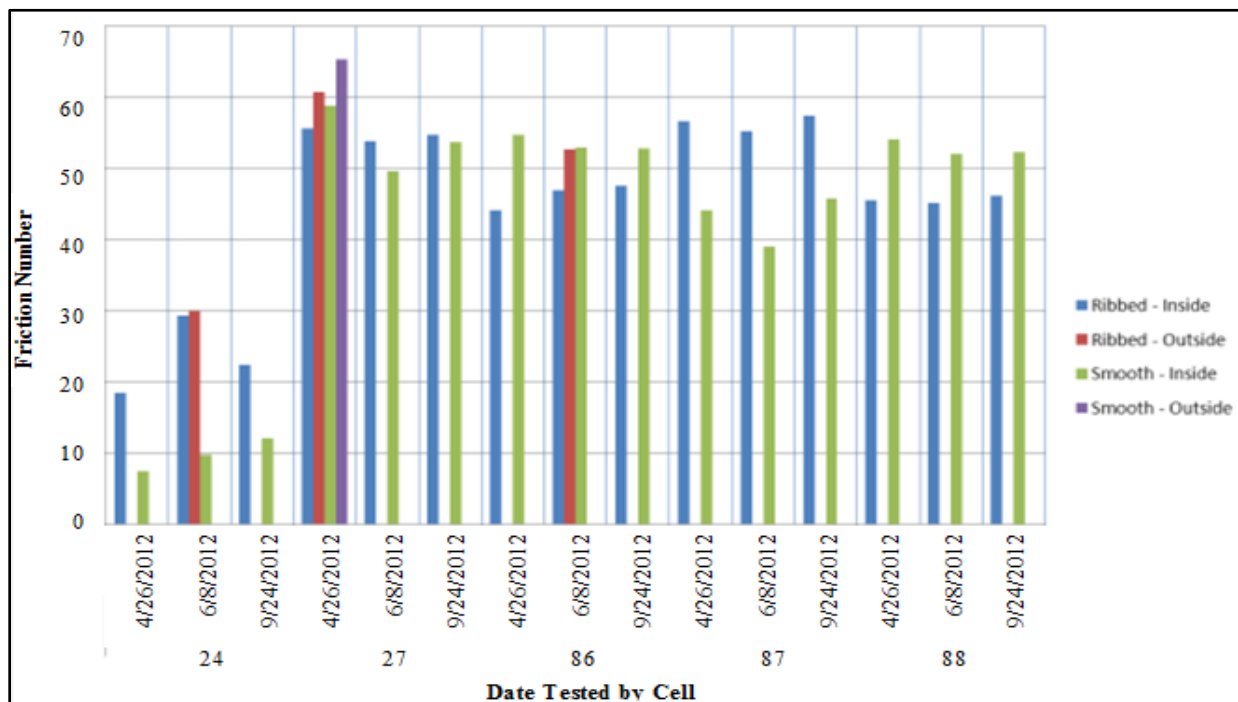
Figure 3.19 2012 Low Volume Road Skid Trailer Data

76

Dynamic Friction Tester:

Figure 3.20 shows the DFT data over time at 20 km/hr (12.5 mph) and 80 km/hr (50 mph), respectively. The slower the speed, the higher the friction. The UTBWC (Cell 3) and 4.75 mm taconite mixture (Cell 106) had the highest friction coefficients, while the dense graded Superpave mixtures (Cells 4, 19, and 22) were all about the same. The friction decreased slightly over the years on the UTBWC and 4.75 mm surfaces. Friction remained constant on the Superpave surfaces when measured at 20 km/hr, but showed an increase during year four when measured at 80 km/hr.

Figure 3.21 show the 2012 DFT data for the four Mainline cells measured. Again it can be seen that the coefficient of friction decreases as speed increases. In addition, the UTBWC surface had the highest coefficients at all speeds. At 60 km/hr (37 mph) the UTBWC was closely followed by Cell 4 and then the other two Superpave mixtures (Cells 19 and 22), which were identical. Below 40 km/hr Cell 4 interchanged with Cell 22. Figure 3.22 shows DFT data measured on Cell 24 in 2012 in various locations. This is the test section on the Low Volume Road where a fog seal was placed on successive 100-ft subsections every year since 2008. The subsection that received a fog seal in 2008 is an anomaly, where the friction coefficient is higher than the control (without fog seal). Otherwise the data clearly shows that with each successive fog seal application the coefficient of friction decreases. Researchers used increasingly higher application rates each year on the aging pavement. Additionally, older fog seals have been abraded by traffic loadings. While the goal of this test section was to study the aging characteristics of the asphalt mixture, the friction data indicates that the surface will require light sanding or chip seal would for the purposes of traffic safety.
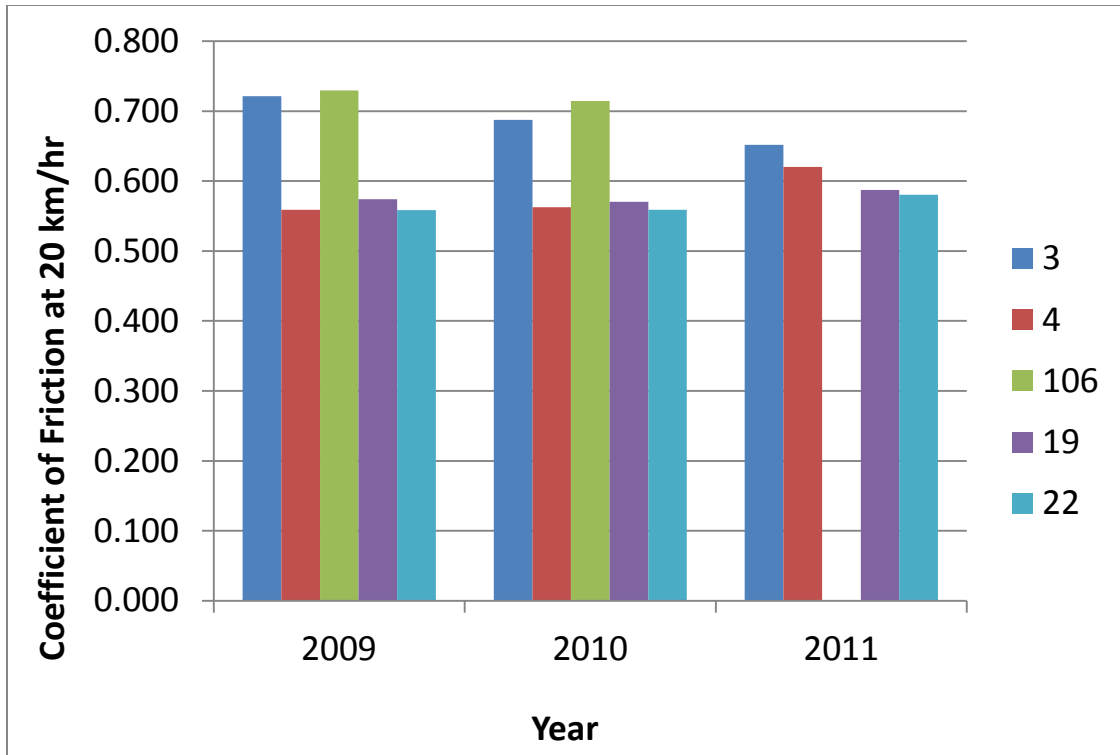
Figure 3.20 History of DFT Data at 20 km/hr
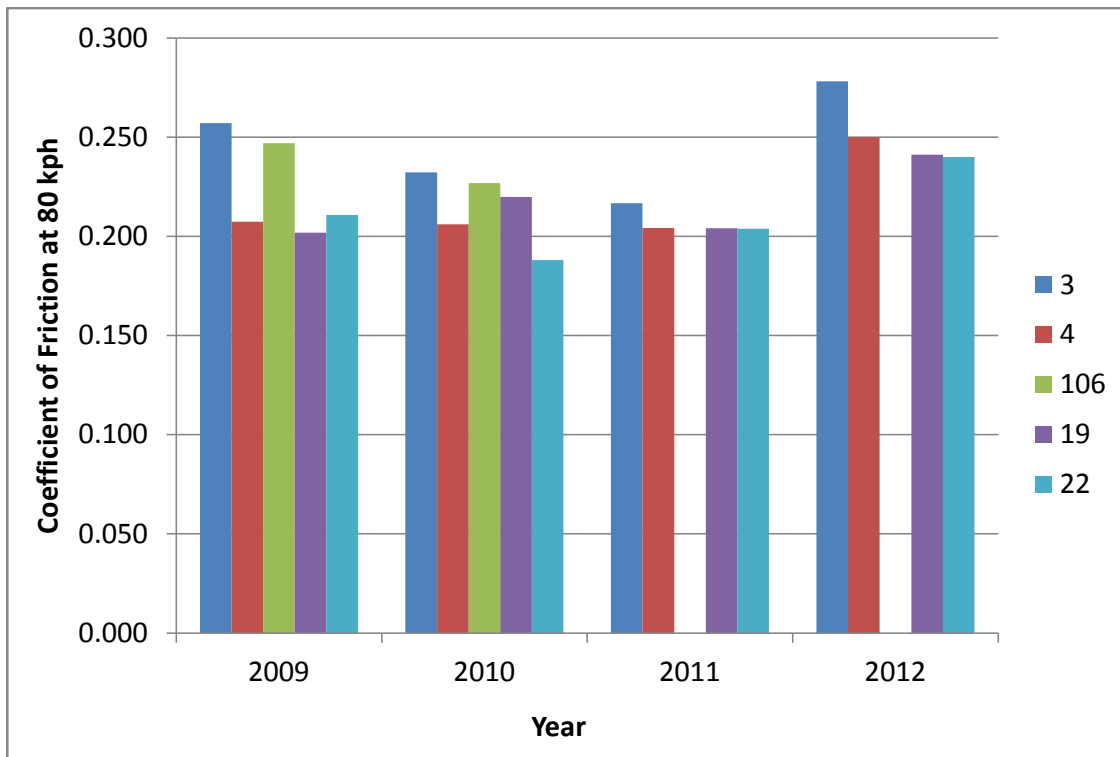
Figure 3.21 History of DFT Data at 80 km/hr

78
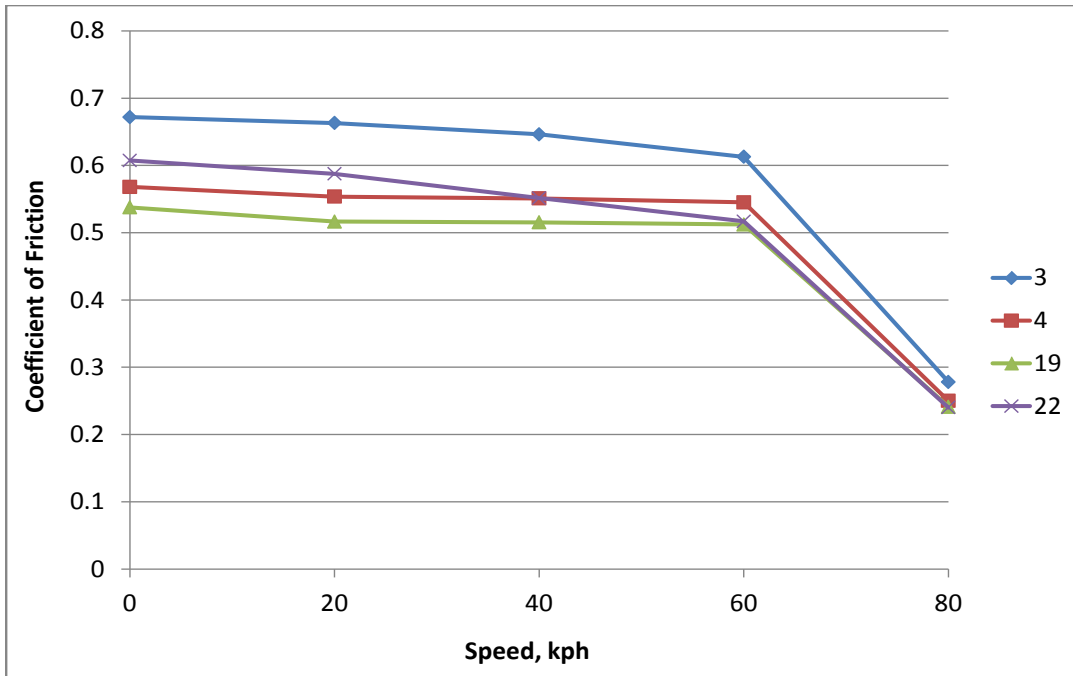
Figure 3.22 2012 DFT Data vs. Speed (1 mph=1.6 km/hr
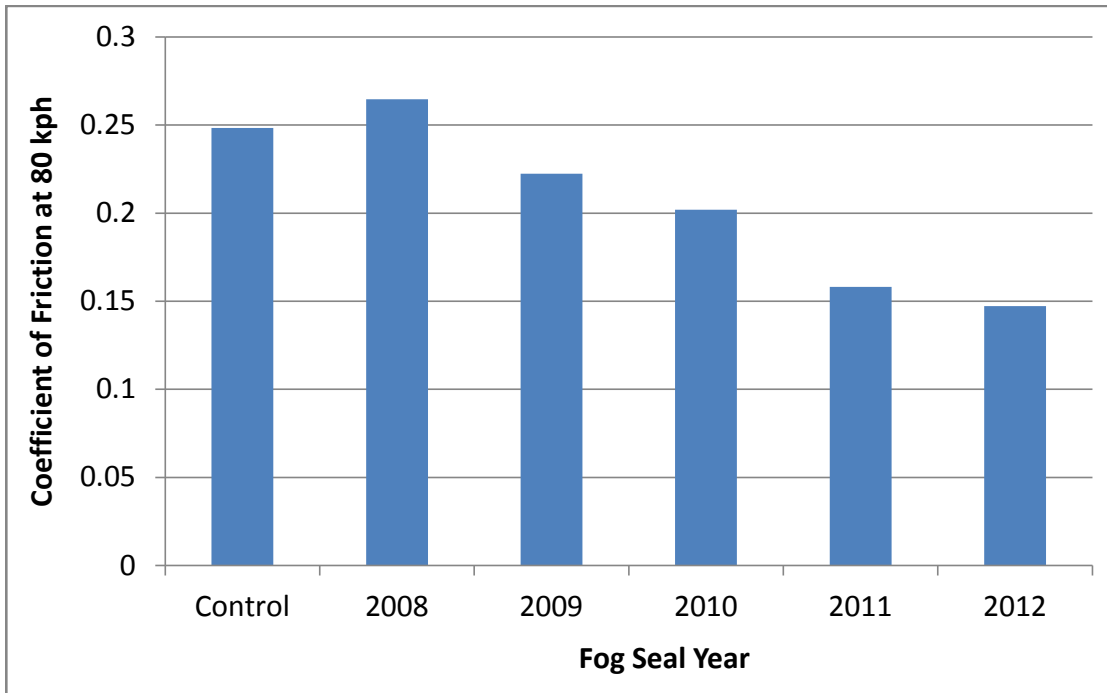
Figure 3.23 LVR Cell 24 DFT Data over Fog Seals

Figure 3.24 shows a plot of ride quality data collected with the LISA over time. The plot shows only the driving/inside lane, and each marker represents an average across several runs of the right and left wheel paths. The Figure 3.24 clearly shows that the porous asphalt (Cells 86 and 88) are the roughest while the UTBWC (Cells 2 and 3) are the smoothest. Each cell tends to follow a cyclic pattern throughout the year, with smooth values in the summer and fall and rough values in winter and spring. None of the cells appear to be getting significantly rougher over time.
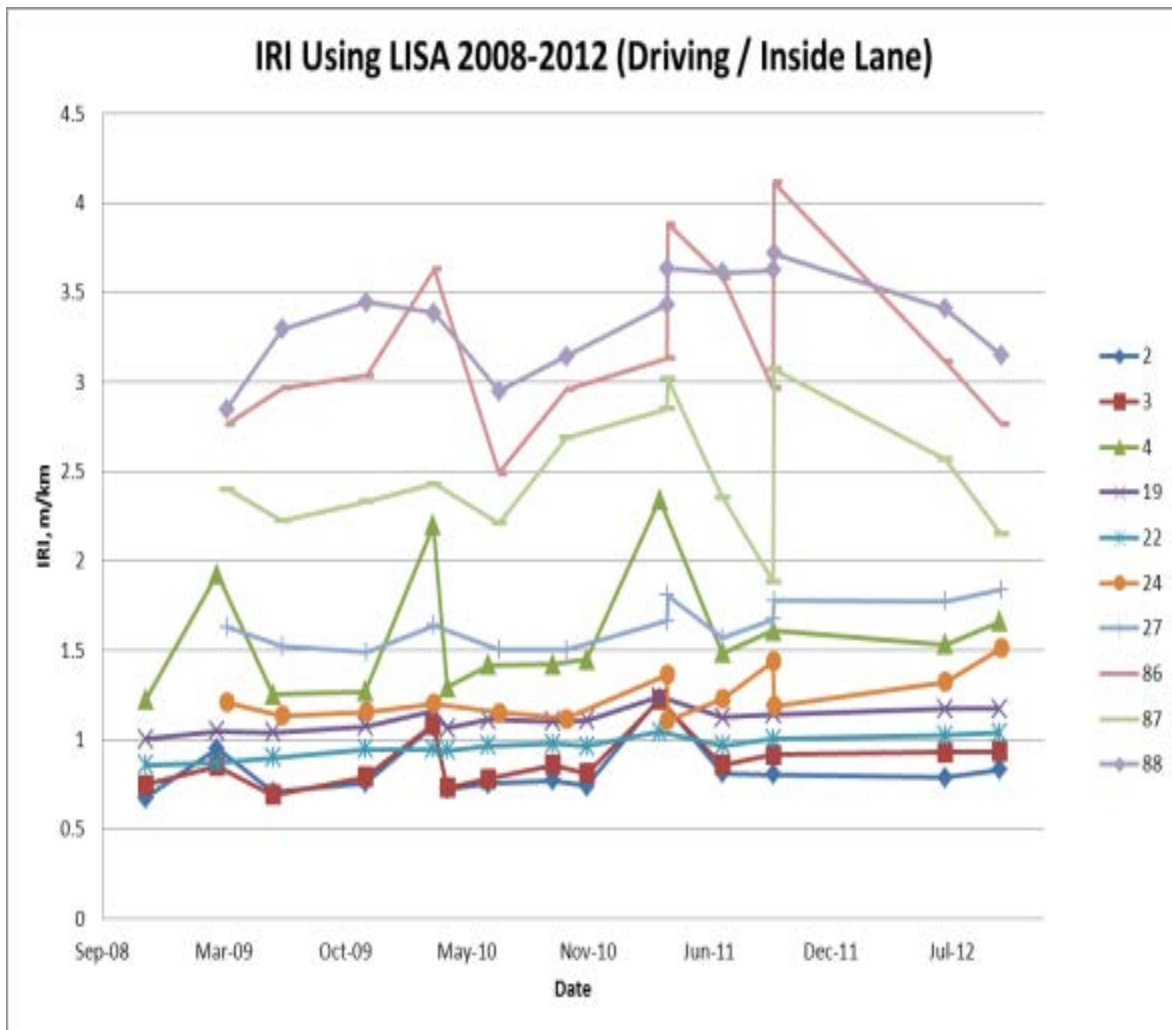
Figure 3.24 History of LISA Ride Quality Values (Driving/Inside Lane)

Figure 3.25 shows 2012 LISA data from the MnROAD Mainline. These cells again show that the pavement is the roughest in early spring while the unbound materials are thawing and then

gets smoother during the summer and fall when the subgrade has dried out. In most cases the left wheel path of the driving lane is the smoothest of the four paths in each cell. Often the right wheel path of the driving lane is the roughest, likely due to heavy truck traffic in that lane, and at times the right wheel path of the passing lane is the roughest.

On the Low Volume Road (Figure 3.26) the inside lane tends to be rougher than the outside lane, again due to the heavy traffic on the inside lane. The left wheel path of the inside lane tends to be rougher than the right wheel path, which is the opposite of what one might expect. For the outside lane the cells are about evenly split between which wheelpath (left or right) is smoother.
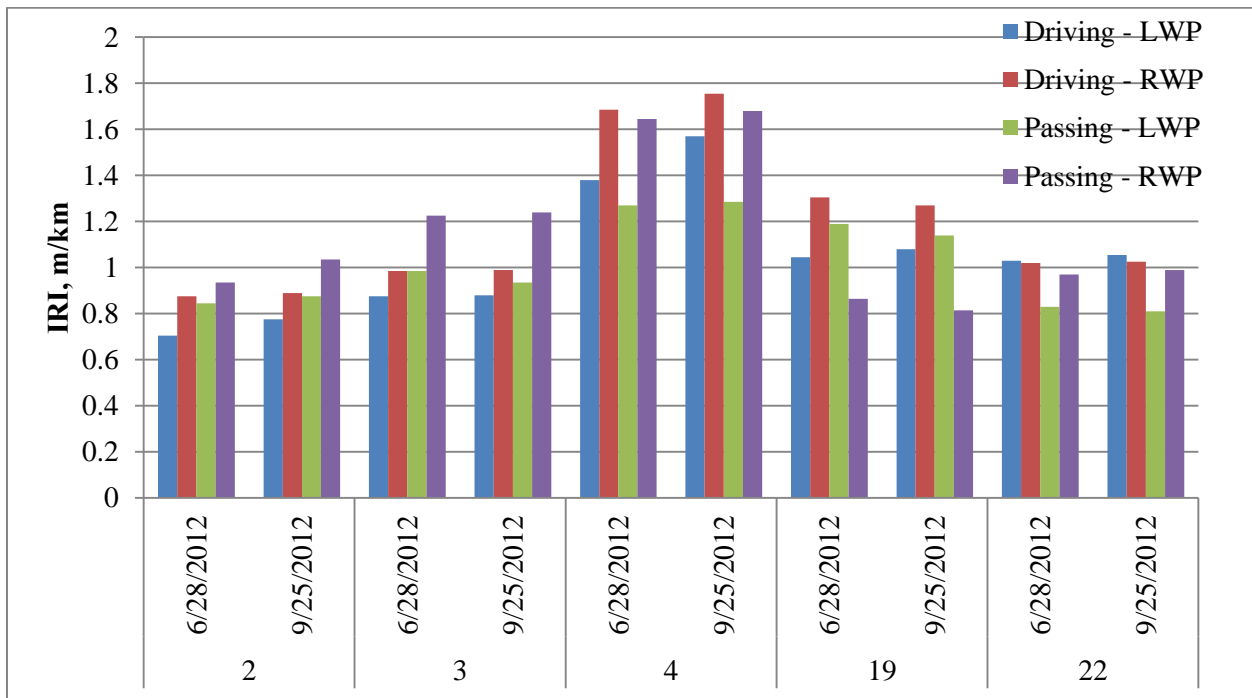
Figure 3.25 Mainline 2012 LISA Measurements
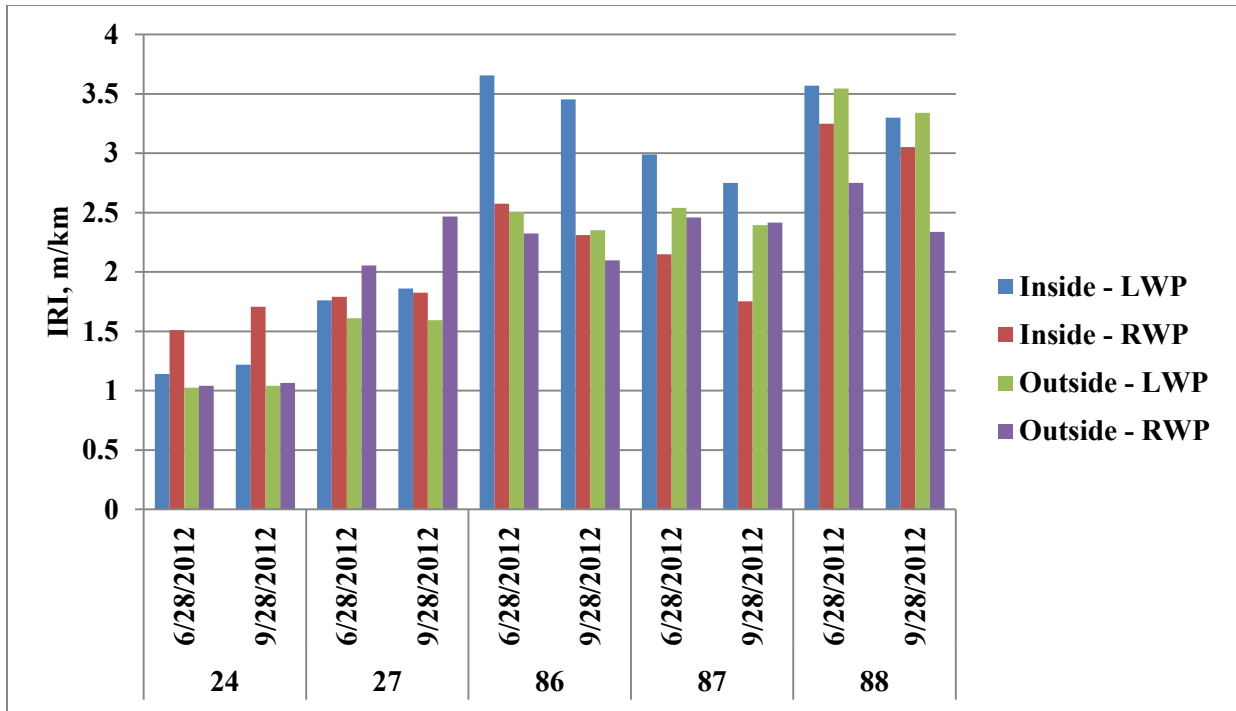
Figure 3.26 Low Volume Road 2012 LISA Measurements

Sound Intensity (OBSI):

Figure 3.27 shows the OBSI measurements over time on the driving/inside lane. There is a large spread in the noise levels from about 98 to 105 dBA. Interesting trends are noted in the Figure 3.27. The OBSI levels tend to be lowest in the summer when the pavement surface is warm and soft; they are highest in cold weather when the asphalt mixtures are stiff. There is a general upward trend of noise levels over time with the porous asphalt showing a more gradual trend and dense graded surfaces (Cells 4 and 24, for example) showing a sharper increase. Interestingly, the chip seal surface (Cell 27) shows a decrease in OBSI levels over time. It is possible that aggregates are being worn off the surface by truck traffic, leading to a less aggressive texture.
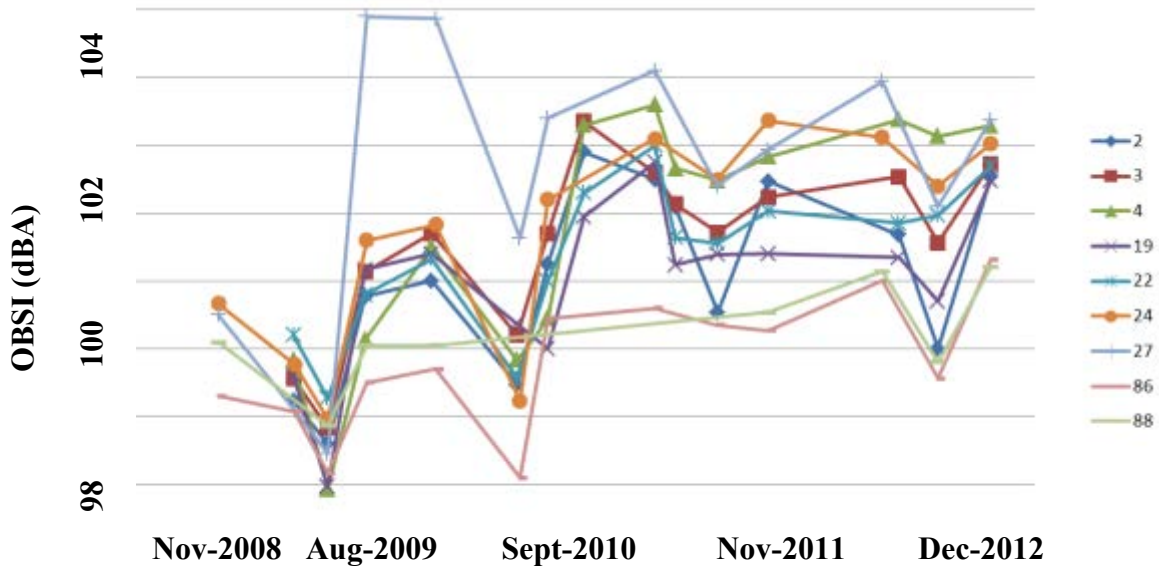
Figure 3. 27 History of OBSI Measurements (Driving/Inside Lane)

Figure 3.28 and 3.29 show bar charts of the OBSI data in 2012 for the Mainline and Low Volume Road, respectively. In most cases the driving/inside lane is louder than the passing/ outside lane, indicating that wear from heavy traffic leads to higher noise levels. The chip seal on Cell 27 is the exception, with a larger aggregate size on the outside lane leading to higher OBSI values. In some cases (e.g., UTBWC) the difference between cool and warm weather testing is quite dramatic, while in other cases (e.g. porous asphalt) the differences in OBSI levels between seasons are much less.
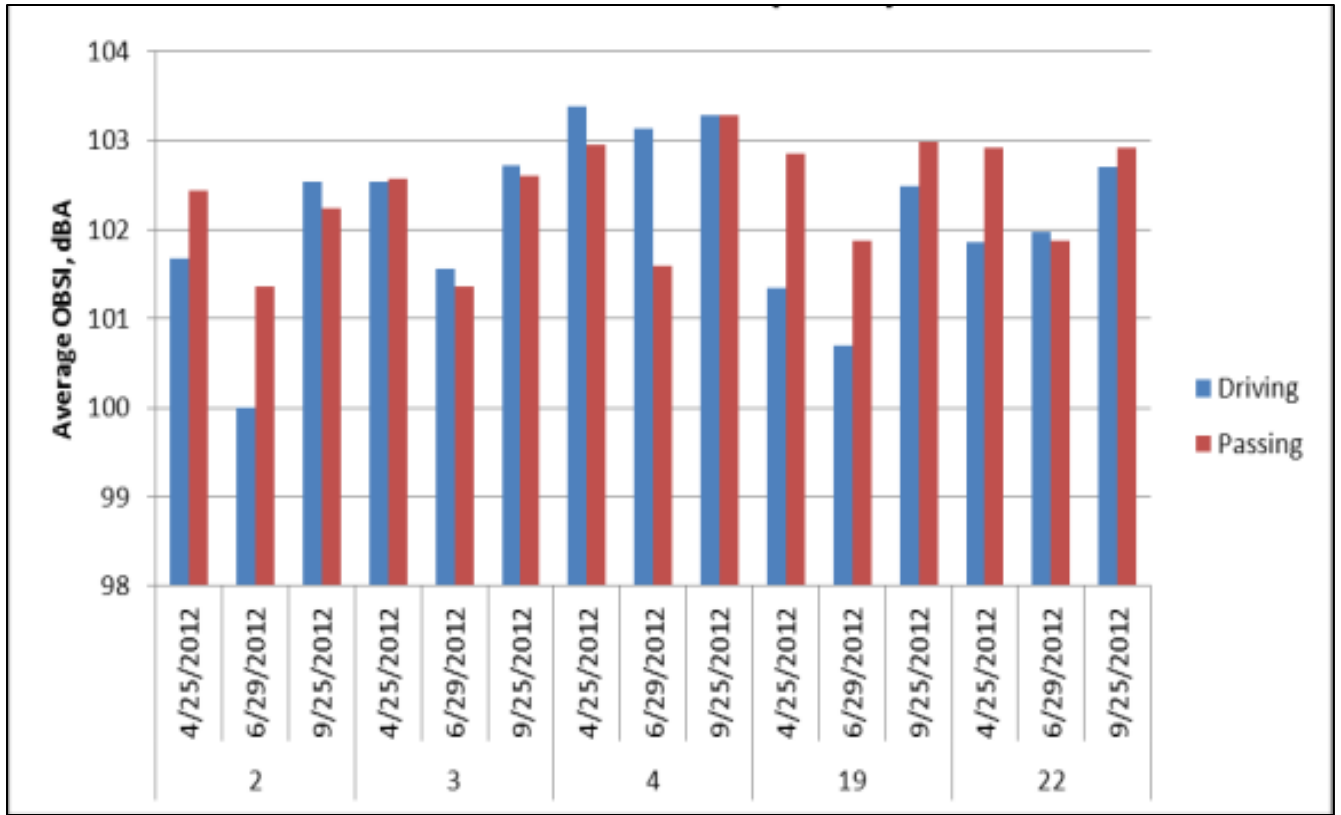
Figure 3.28 2012 Mainline OBSI Data
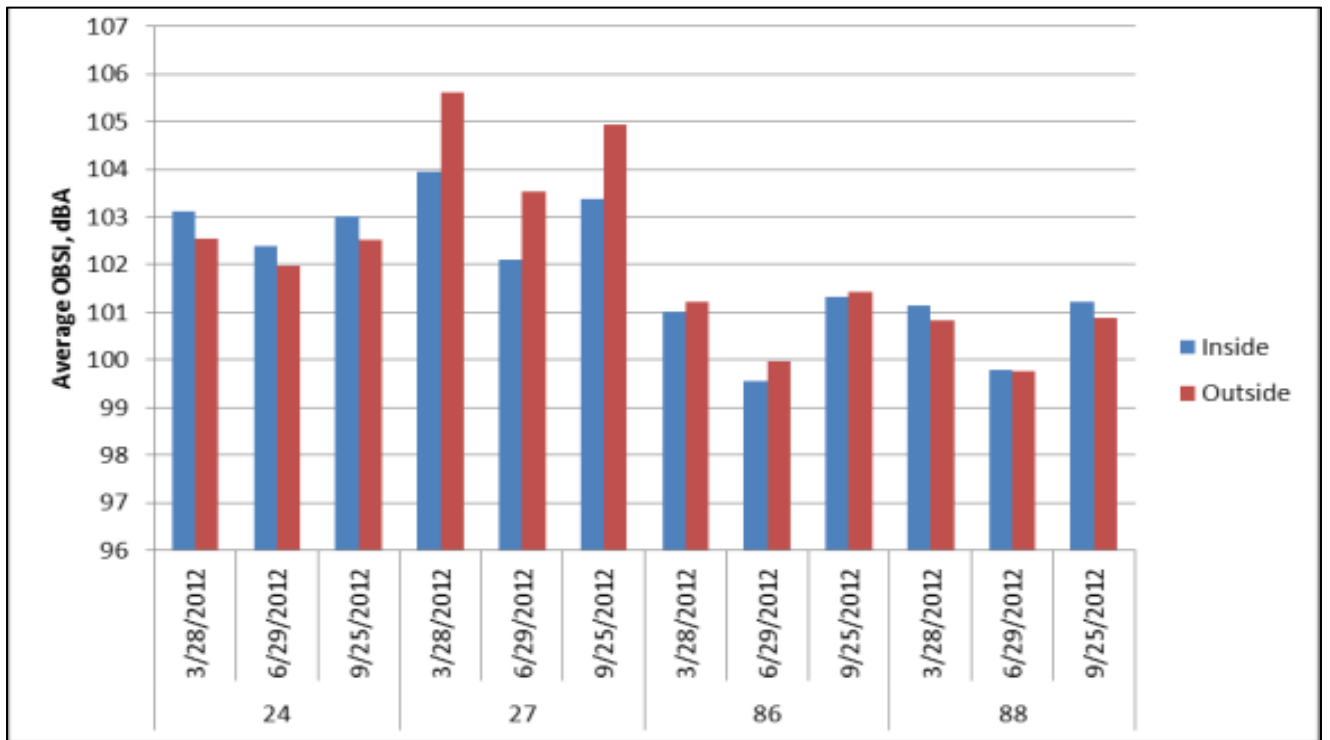
Figure 3.29 2012 Low Volume Road OBSI Data

HYDRAULIC CONDUCTIVITY

The hydraulic conductivity was also measured for the porous cells using a modified permeameter as shown in Figure 3.31. The hydraulic conductivity was found using equation 2.3.

$$k = \frac{T_P A_X}{A_X t} \ln\left[\frac{h_i + 2}{h_f + 2}\right]$$

$k = Hydraulic\_Conductivity, cm/\sec$

$T_P = Thickness\_Pavement, cm$

$A_x = Cross\_Sectional\_Area, cm^2$

$t = flow\_time, \sec$

$h_i = initial\_head, cm$

$h_f = final\_head, cm$

(2.14)

Figure 3.31 shows the hydraulic conductivity measurements of the porous HMA cells over time, which seem to show a general decreasing trend in hydraulic conductivity. Operational staff vacuumed the cells in late October of 2012 and the November 2012 data point reflected improved hydraulic conductivity. There is an increase in hydraulic conductivity.

Figure 3. 30 Field Permeameter
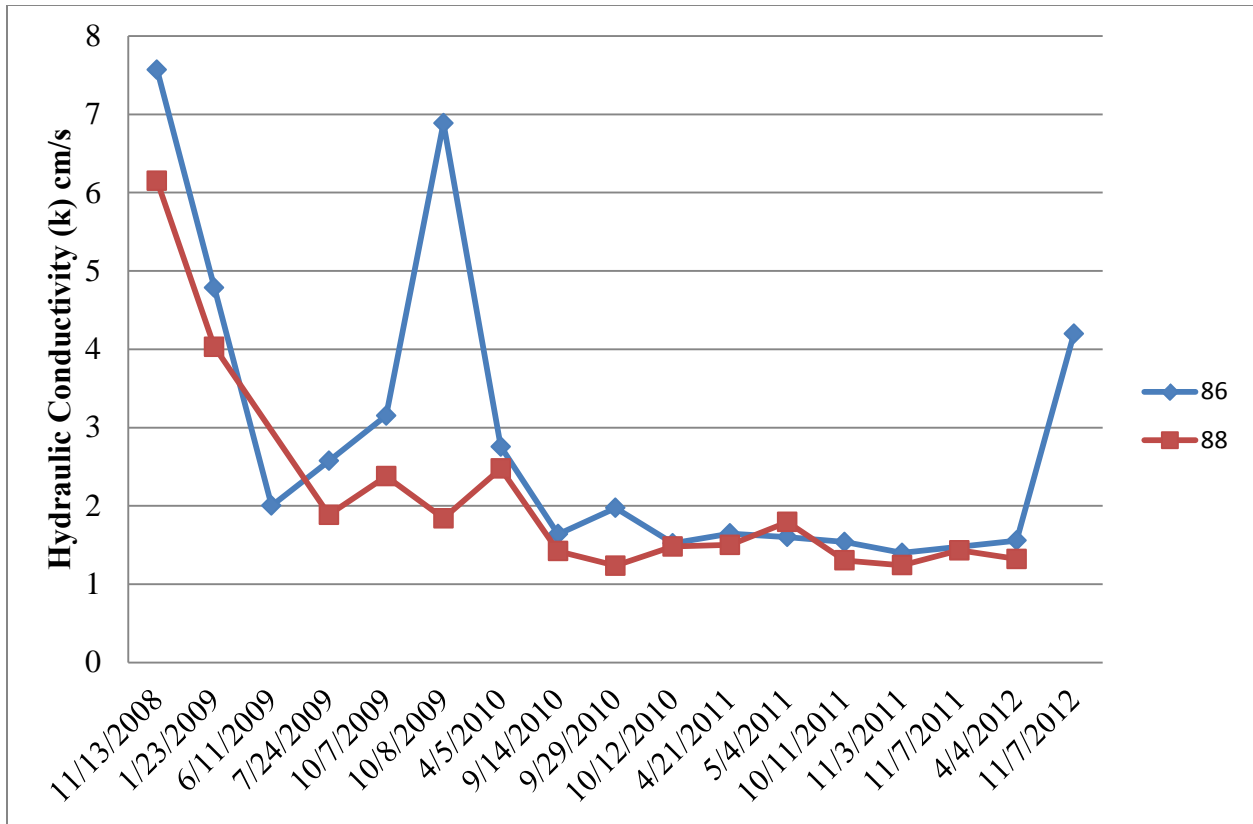
Figure 3.31 History of Permeability Measurements

Figure 3.32 and 3.33 show permeability measurements throughout 2012 categorized by cell, day, and wheelpath of the inside and outside lane, respectively. Not every location was measured during each data collection period. In most cases, the outer wheel path has higher permeability than the inner wheel path. In general the outside lane has slightly higher permeability values than the inside lane, indicating that truck traffic on the inside lane contributes to the clogging of the pores. Measurements were made in cell 86 in the fall after vacuuming the cells, removing debris.
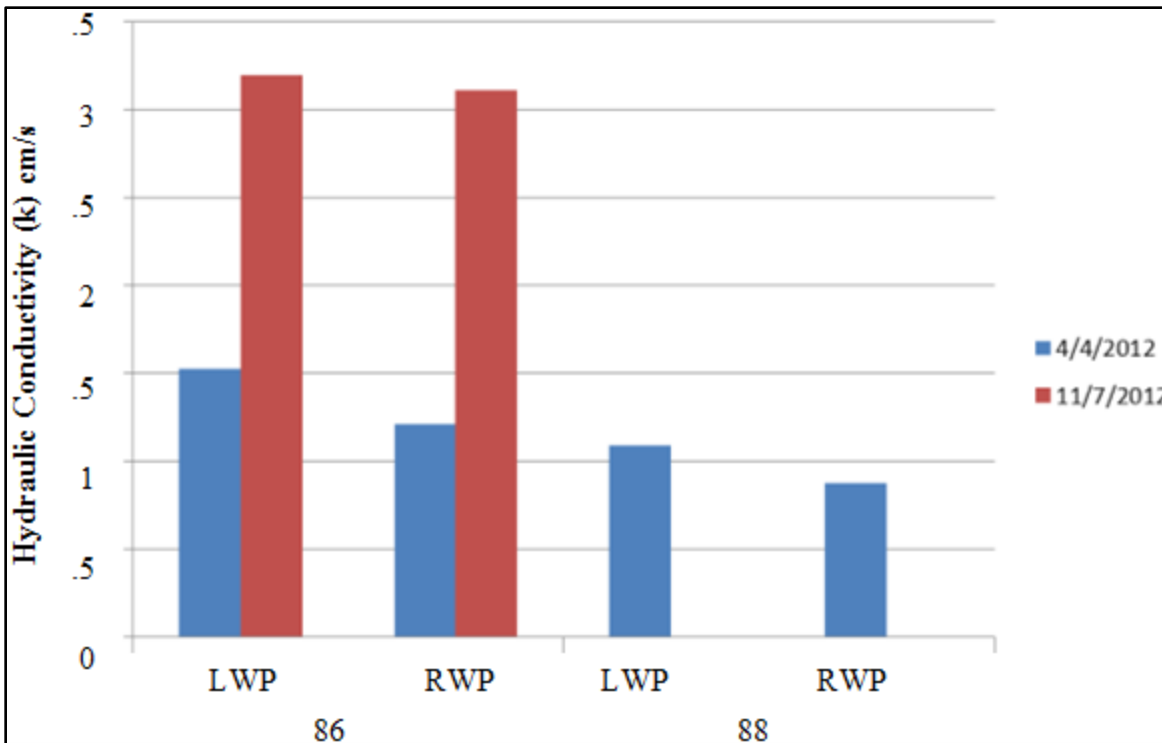
Figure 3.32 2012 Hydraulic Conductivity (Inside Lane)
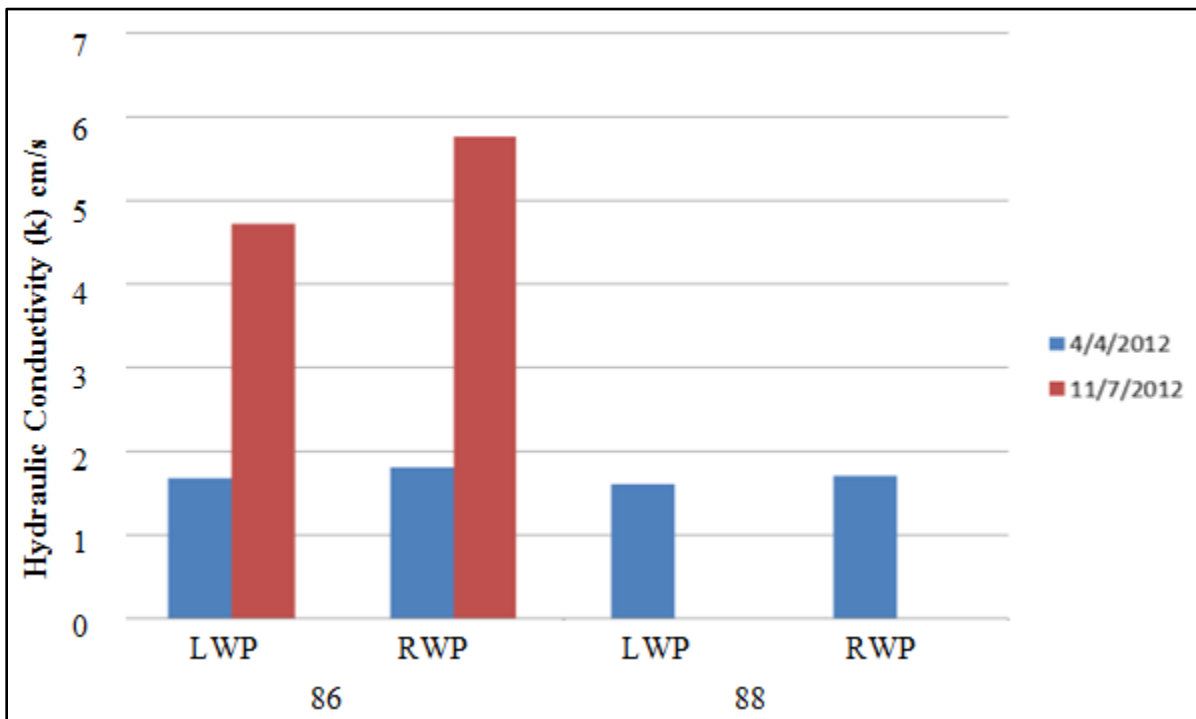
Figure 3.33 2012 Hydraulic Conductivity (Outside Lane)

DURABILITY

Visual Distress Survey (LTPP):

Trained personnel using the Long-Term Performing Pavement (LTPP)-based evaluation method
[52] evaluated the durability of all test cells. For 17 different distresses: cracking (9 types),
patching/potholes (2 types), surface deformation (2 types), surface defects (3 types) Operational
personnel visually evaluated the cells. Table 3.4 shows the distress name and type, how the
distress was measured, and the applicable severity levels. The test cells are surveyed in the
spring and fall of each year at MnROAD.

Table 3.4 LTPP Distress Ratings for Asphalt Concrete Surfaces

Distress	Unit of Measure	Severity (Levels)
Cracking		
Fatigue	Area	Yes (3)
Block Cracking	Area	Yes (3)
Edge	Length	Yes (3)
Longitudinal (Wheel Path)	Length	Yes (3)
Longitudinal (Non-Wheel Path)	Length	Yes (3)
Longitudinal Sealant Det.	Length	Yes (3)
Longitudinal Sealant Det.	Length	Yes (3)
Transverse Cracking	Number & Length	Yes (3)
Transverse Sealant Det.	Number & Length	Yes (3)
Patching/Potholes		
Patching	Number & Area	Yes (3)
Pot Holes	Number & Area	Yes (3)
Surface Deformation		
Rutting	Depth	No
Shoving	Number & Area	No
Surface Defects		
Bleeding	Area	No
Polished Aggregate	Area	No
Raveling	Area	Yes (3)
Other Distresses		
Pumping	Number & Length	No

Table 3.5 shows the distress names and types that are present in the study cells. There
are currently 4 distresses in 4 of the cells. Cells 106 and 206 are not included in this table, as

they were reconstructed in summer 2011 due to severe distress in the underlying concrete layer. The porous asphalt (Cells 86 and 88) show substantial raveling. The raveling is most likely due to a combination of construction defects, snowplow damage, and wear from heavy truck traffic; it has continued to increase over time, although the rate of increase seems to be slowing. Note that if the distresses are not shown in the table, then they were not observed in the cell at the time of the evaluation.

Table 3.5 Fall 2012 LTPP Distress Surveys

Distress	Measure, Severity	Cell, Lane
Cracking		
Centerline Joint	26 ft, Low	Cell 3, Driving
	47 ft, Low	Cell 19, Driving
	24 ft, Low	Cell 86, Inside
Transverse	1 (3 ft), Low	Cell 3, Driving
Shoulder Joint	203 ft, Low	Cell 22, Driving
	50 ft, Medium	Cell 22, Driving
Patching/Potholes		
Patching	2 (84 ft^2) Low	Cell 4, Driving
Surface Defects		
Raveling	20 ft^2, Low	Cell 2, Driving
	50 ft^2, Low	Cell 4, Driving
	2072 ft^2, Low	Cell 86, Inside
	1172 ft^2, Low	Cell 86, Outside
	2091 ft^2, Low	Cell 88, Inside
	1174 ft^2, Low	Cell 88, Outside

Rutting (ALPS):

Rutting can be defined as a longitudinal surface depression in the wheel path. Rutting is an important indicator of performance, as excessive rutting leads to shedding water and potential vehicle hydroplaning. Mixture rutting is influenced by insufficient compaction (i.e. high air voids), excessively high asphalt content, excessive mineral filler, or insufficient amount of angular particles [55]. The Automated Laser Profile System (ALPS), Figure 3.35, was used to characterize the rutting of all study cells. The ALPS collected rutting measurements in both wheel paths of both lanes, every ¼" transversely at 50-foot intervals within the cells. Rutting measurements are generally made on each cell in the spring and summer, or fall and summer of each year and fall of each year.

Figure 3.34 Automated Laser Profile System (ALPS)

Figure 3.35 and 3.36 show the average rut depths over time on the Mainline and Low Volume Road, respectively. Each point represents an average across both wheel paths over the length of the cell in the driving or inside lane. Each of the cells shows a gradual increase in average rut depth over time due to traffic loading. The increase in rut depth is sharpest in the first year while the asphalt is relatively soft, then at a slower rate in later years. The largest rut depth on the Mainline is about ¼" while rut depths on the Low Volume Road are approaching ½" on some cells. The 4.75 mm taconite mixture (Cell 106) showed the lowest rut depths, closely followed by some of the dense graded mixtures (Cells 22, 24, and 87). Surface rut measurements are unable to distinguish whether the rutting is primarily in the asphalt layer or in the underlying base and subgrade layers. Forensic investigations later in the pavements' lives will be able to more precisely determine the layer most responsible for rutting.
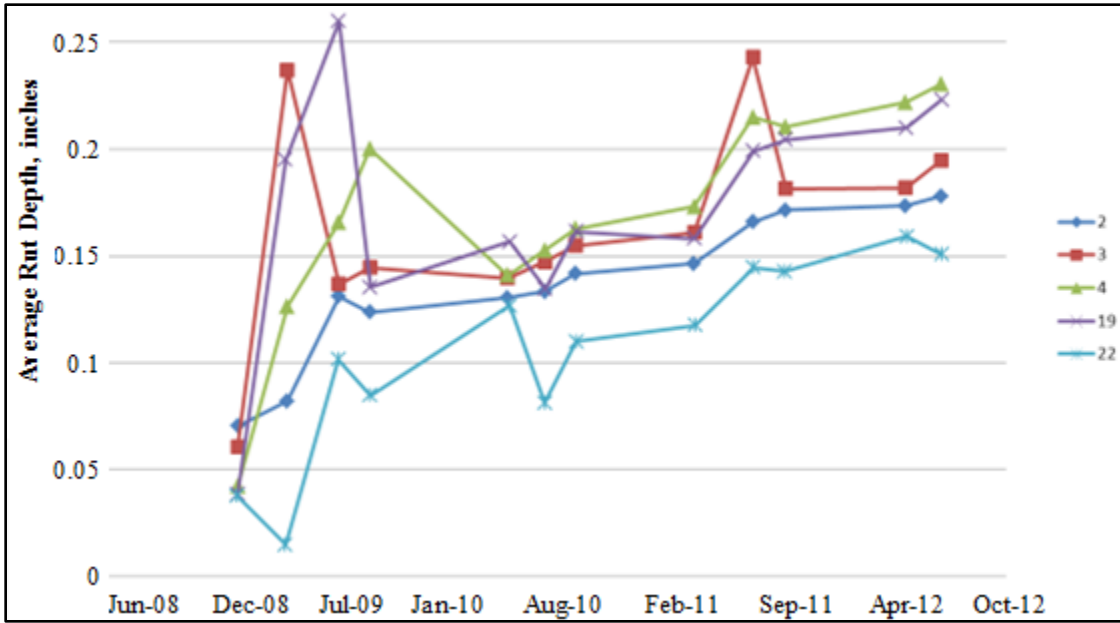
Figure 3.35 History of Average Mainline Rut Depths
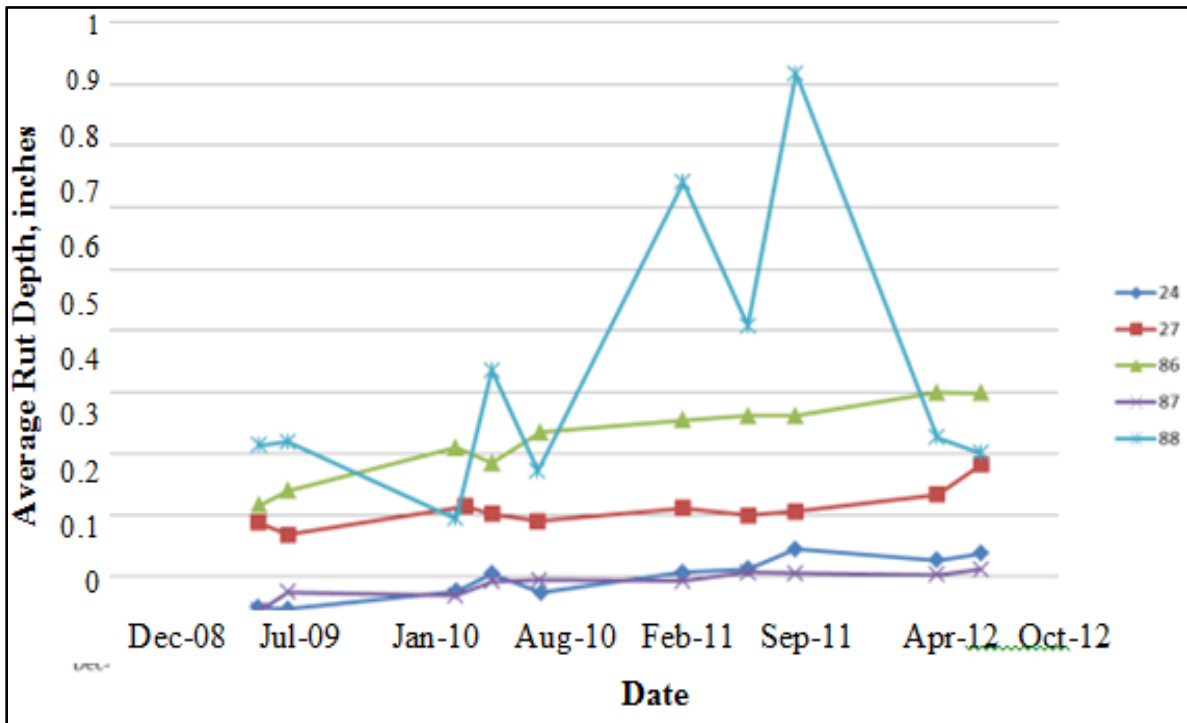
Figure 3.36 History of Average Low Volume Road Rut Depths

91

The construction of different surface types that utilize a wide range of mix designs and materials in close proximity to each other, within a state of the art pavement research facility will provide a valuable insight into the influence of mixture, environmental and traffic factors on various surface characteristics. This report documented the fourth completed annual cycle of measurements but did not provide in-depth analysis of the data. A contract was initiated in July 2011 with Purdue University to perform detailed data analysis of the various surface characteristics, ultimately resulting in a sophisticated noise model for asphalt pavements. Their work is in progress and will be completed in the winter of 2013.

SECTION CONCLUSION

The following are general observations and comparisons that can be made about the influence of the mixture properties on the surface characteristics of the various mixture types at MnROAD.

Ride

- The UTBWC surfaces (Cells 2 and 3) are the smoothest over time.
- The porous asphalt surfaces (Cells 86 and 88) are the roughest over time.
- Ride quality tends to be worst in the spring with frozen or thawing conditions and better in the summer and fall when the subgrade materials dry out.

Texture

- Aggressive, open graded surfaces (porous asphalt, chip seal, UTBWC) have the highest mean profile depth, while the 4.75 mm taconite mixture has the lowest profile depth.
- Texture values can be variable when measured at different stations and offsets within a cell.

Friction

- Friction numbers measured by the skid trailer were generally very good with the exception of Cell 24, which has received a fog seal treatment just before friction measurements the last three years.
- For the dense graded asphalt surfaces (Cells 4, 106, 19, 22, 24, and 87) the ribbed tire has significantly higher friction numbers than the smooth tire.

- For the more open, aggressive asphalt surfaces (Cells 2, 3, 27, 86, and 88) the ribbed and smooth tires give more similar values, with the smooth tire often exhibiting a higher friction number.

- In general the passing/outside lane has a higher friction number than the driving/inside lane, showing the effect of traffic on friction.

- The UTBWC (Cell 3) and 4.75 mm taconite (Cell 106) surfaces had the highest coefficient of friction values measured with the dynamic friction tester. The dense graded Superpave surfaces (Cells 4, 19, and 22) had approximately equal coefficients.

- On Cell 24 the coefficient of friction decreased with each successive application of fog seal, indicating that a light sanding or chip seal may be considered to maintain a safe driving surface.

Noise

- The porous asphalt surfaces (Cells 86 and 88) are the quietest, while the chip seal (Cell 27) and some of the dense graded asphalt mixtures (Cells 4 and 24) are the loudest.

- OBSI levels are lowest in the summer when the pavement surface is warm; they are highest in cold weather.

- There is a general upward trend of noise levels over time with the porous asphalt showing a more gradual trend and dense graded surfaces showing a sharper increase.

- In some cases (e.g., novachip) the difference between cool and warm weather test results were significant, while in other cases (e.g. porous asphalt) the differences in OBSI levels between seasons are much less.

- Porous asphalt surfaces (Cells 86 and 88) have the highest sound absorption coefficients; UTBWC surfaces (Cells 2 and 3) are a distant second.

- Dense graded asphalt mixtures have extremely low sound absorption coefficients, with the 4.75 mm taconite mixture (Cell 106) having the lowest.

- The sound absorption coefficients of the open graded surface textures (porous and UTBWC) decrease significantly over time, while this is not the case for the dense graded mixtures.

Durability

- The porous asphalt mixtures (Cells 86 and 88) show a substantial amount of raveling,

93

which is most likely due to a combination of construction defects, snowplow damage, and wear from heavy truck traffic.

- The largest rut depth on the Mainline is about ¼" while rut depths on the Low Volume Road are approaching ½" on some cells.

- The 4.75 mm taconite mixture (Cell 106) showed the lowest rut depths, closely followed by some of the dense graded mixtures (Cells 22, 24, and 87).

- The porous asphalt surfaces show the greatest rut depths.

CHAPTER 4
ADVANCED DATA ANALYSIS

BACKGROUND

Major analyses carried out in the study of flexible pavement surfaces include effects of texture skewness (a measure of the spikiness of the textured surface asperities), temperature and friction. Section one investigates if skewness compared to mean profile depth is a better indicator or predictor of Tire-Pavement-Interaction-Noise; section two is to observe the relationship between temperature and on-board sound intensity; and lastly section three is to observe frictional properties on asphalt pavements.

Section two discusses the relationship between pavement noise and temperature in asphalt pavements. In this study, temperature effect was studied with the data obtained from routine measurements as well as certain decays when OBSI was measured every hour in all the test cells. Section three discusses frictional properties of tire-pavement interaction in asphalt pavement surfaces. Friction is essential in pavement infrastructure as a primary indicator of skid resistance or safety. The data used in the analysis originated from multiple MnROAD asphalt test cells. This chapter reveals a significant degree of sensitivity of flexible pavements to temperature and shows the significance of spikiness. It also validated the theorem that friction degradation follows a pattern of decay, similar to the half-life equation. The rate of friction degradation is proportional to the value of the friction number.

EVALUATION OF SKEWNESS PROPERTIES SURFACES

Many authorities including Izevbekhai [58] discuss the relationship between road texture and pavement noise. In these articles, they suggest that road texture may have influence on pavement noise. Most pavement surfaces that have similar mean profile depth do not necessarily have similar sound intensity. Therefore, researchers are still searching for alternative measures that can more accurately predict pavement noise. In this project, skewness is investigated under an assumption that it may be a better approach in predicting the pavement noise than mean profile depth. Izevbekhai et al [58] showed that texture orientation (spikiness) another term for skewness was a significant variable in the prediction of Tire-Pavement-Interaction-Noise. The dependent variable of pavement noise is chosen because it is determined to be the most texture intensive component of the surface properties. Other measures such as IRI are affected more by the condition of the pavement structure than the surface textures.

This section discusses the feasibility of on-board sound intensity (OBSI) prediction by texture spikiness in asphalt pavement surfaces. Primarily, skewness indeed provides a better indicator to OBSI prediction compared to mean profile depth of road texture in concrete pavements. Therefore, the objective of this project is to investigate if the same conclusion applies to asphalt pavement surfaces. The most important step of the analysis is to collect sufficient data to analyze. Selection of test cells used is done by picking and choosing asphalt test cells at the MnROAD facility. The test cells chosen are cell 1 through 4, 19, 22, 70 from the mainline; cell 24, 27, 86, 88 from the low volume roadway (LVR). The asphalt test cells at MnROAD were selected based on the availability and completeness of raw data from both CTM and OBSI folders. After reviewing the files, the best choice of test cells were test cell 1 through 4, 19, 22 and 70 from the mainline (as shown in Figure 4.1.4); and test cell 24, 27, 86 and 88 from the LVR (as shown in Figure 4.1.44).

This section defines five essential terms, which are circular texture meter (CTM), skewness, PARSER program, on-board sound intensity (OBSI) and coefficient of determination (R^2).

Outputs given by the device is mean texture depth (MTD) of the eight segments. By using the software developed for CTMeter (as shown in Figure 4.1), mean profile depth (MPD) and root mean square (RMS) of MPD is then reported. CTM and Parser icons are shown below.

| CTM ICON | VBA Program for Skewness and Texture Wavelength Determination |
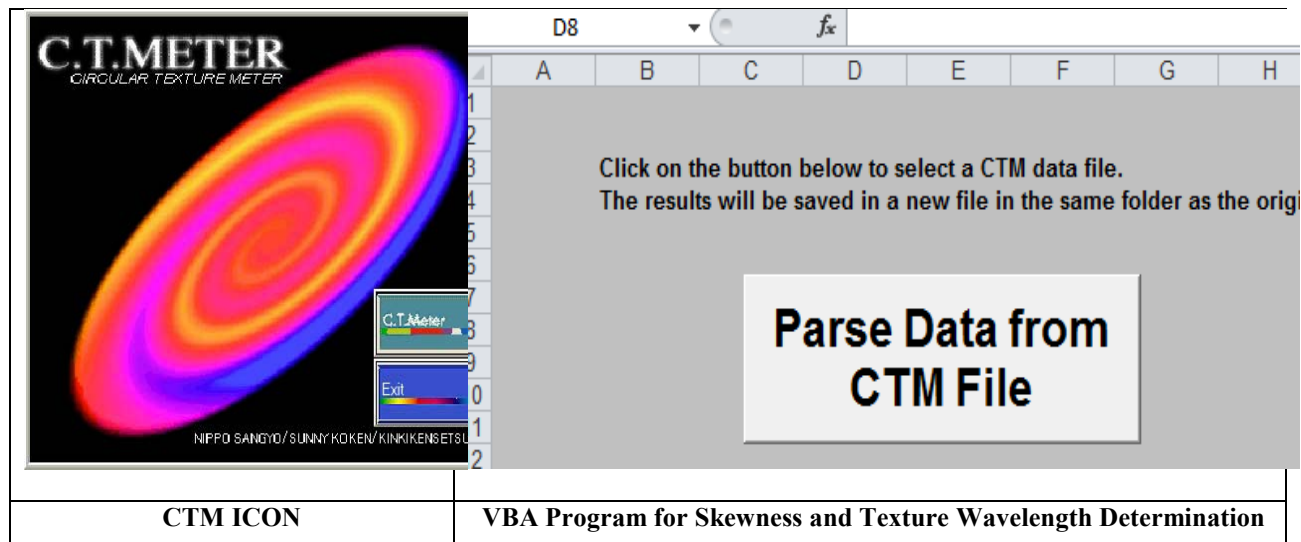
Figure 4.1 CTM and PARSER ICONS

Skewness is a measure of texture spikiness in pavement surfaces. Pavement surfaces are categorized into two sorts: spiky and non-spiky surfaces. The signature characteristic of a spiky surface is the sharp peaks and rounded valleys that indicates appearance of asperities projected above surface; while non-spiky surface has flat peaks and sharp valleys that indicates depressions in surface. Probability density function plotted by using frequency of peak heights shows that spiky surface has positively skewed distribution, and non-spiky surface has negatively skewed distribution. Therefore, it is correct to say that a spiky surface has positive skewness. In contrast, a non-spiky surface has negative skewness. Figure 4.2 illustrates a typical layout of the two texture orientations and the probability density function plots of both surfaces.
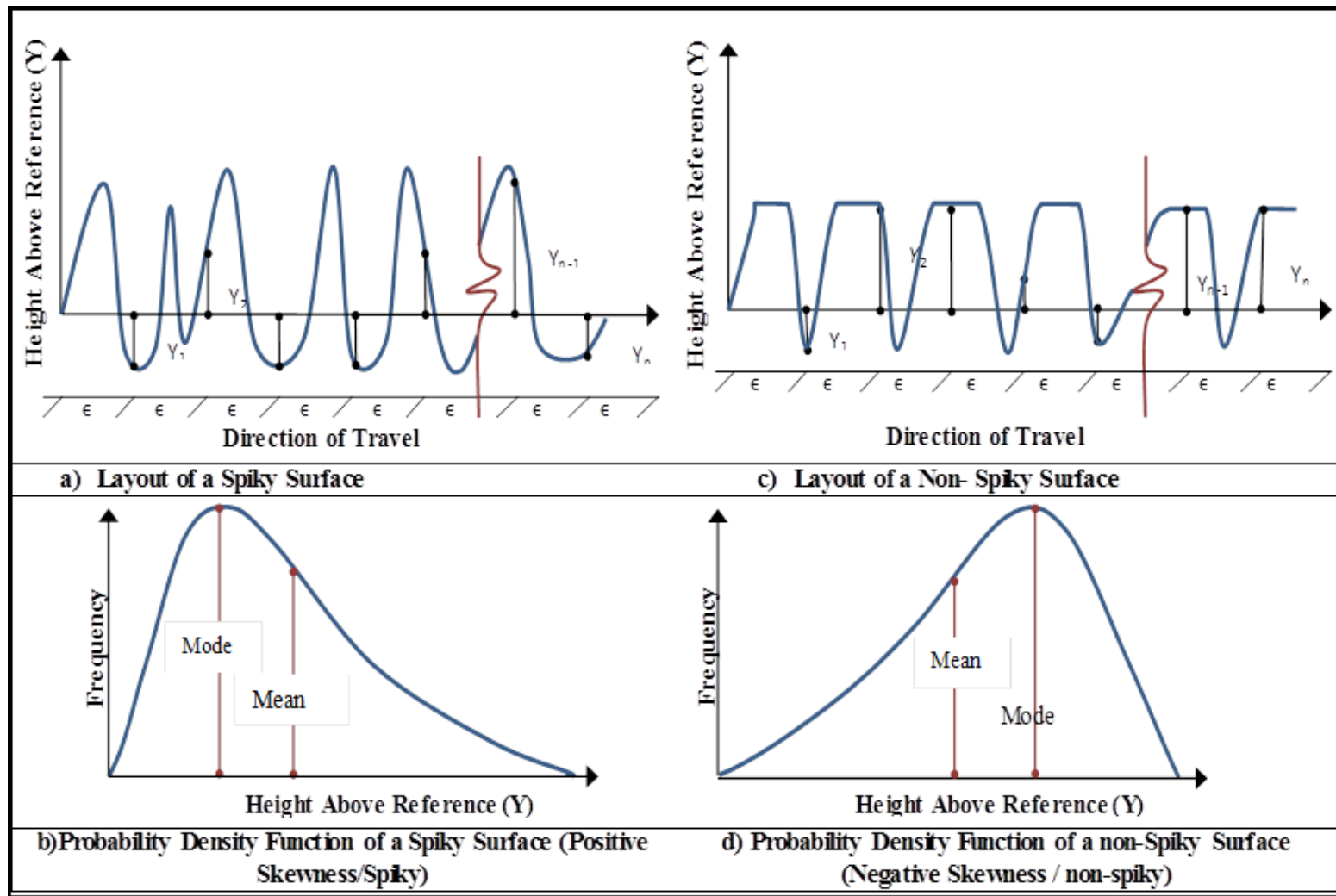
Figure 4.2 Layout Graphs and Probability Density Function Graphs [57]

In additional, skewness can also be mathematically computed by using the following formula [57]:

$$\text{Skewness} = \frac{\sum_{i=1}^{N}(Y_i-\overline{Y})^3}{(N-1)S^3} \qquad (12)$$

where Y = depth measured from reference

N = Sample size

S = Sample standard deviation

PARSER was developed by the MnDOT Concrete Road Research team to aid in extracting CTM raw data. After raw data files were parsed, results were automatically saved in a new excel spreadsheet. PARSER delivers 128 texture depth measurements for each segment for each of the three separate runs. This data is then used to calculate skewness with the formula above. This program thus facilitates computation of skewness.

Coefficient of determination (R^2) indicates how well data points fit a best-fitted line. A best-fitted line represents the ideal line based on least-squares minimization of residuals. In other words, a higher value of R^2 means a better correlation between independent variable and dependent variable.

All raw data was taken from the MnROAD OBSI data-collection folder. Due to the difficulty of matching or obtaining simultaneous data sets data sets for the same date, the data was retrieved from two different but compatible test operations. MPD and skewness data were from October 2012 while the OBSI data was from September 2012.

Intensity (OBSI):

OBSI raw data was retrieved from September 2012. The OBSI Super-Macro program is a program that analyzes data by extracting raw data from the PULSE software and separating all runs to correspond to the associated test section. Results are saved in a summary database filet. Before running the Macro, was preceded by some set-up.

Firstly, the process created a field data spreadsheet using the existing OBSI field data template. Run test numbers were filled into the associated cell numbers according to the written data sheet from the testing day. Next, test results given from the PULSE program were imported into Excel manually with a new sheet for each run. This step was done by copying each

measurement's result given by the PULSE program into the sheet with the same test run number. Lastly, the Macro program was initiated to get a summarized result for OBSI.

Mean Profile Depth (MPD):

The October 2012 the Macro program imported CTM raw data files into a new spreadsheet assembling information on the cell number, lane and station. Next, MPD and RMS of MPD values were entered manually by opening CTM raw data files with the CTM program one by one.

Skewness:

CTM raw data files were parsed using the PARSER software as introduced earlier on. As a result, the 1,024 texture depth measurements of the eight segments were generated in spreadsheet. Values were then used to plot graphs in order to identify visually which segment should be used to compute the skewness. Appropriate segment is chosen based on the graph plotted, where the lowest texture depth measurement (y-axis) and the second segment will be the opposing segment of it. For example, Figure 4.3 shows outcome given by PARSER program for test cell 1 (right-lane of the right- wheel-path). Segment chosen was segment 1 because the lowest texture depth measurement (circled in red) is at point 114, which is included in segment 1. After choosing the segments, skewness can be computed by using the data analysis tool in Excel.
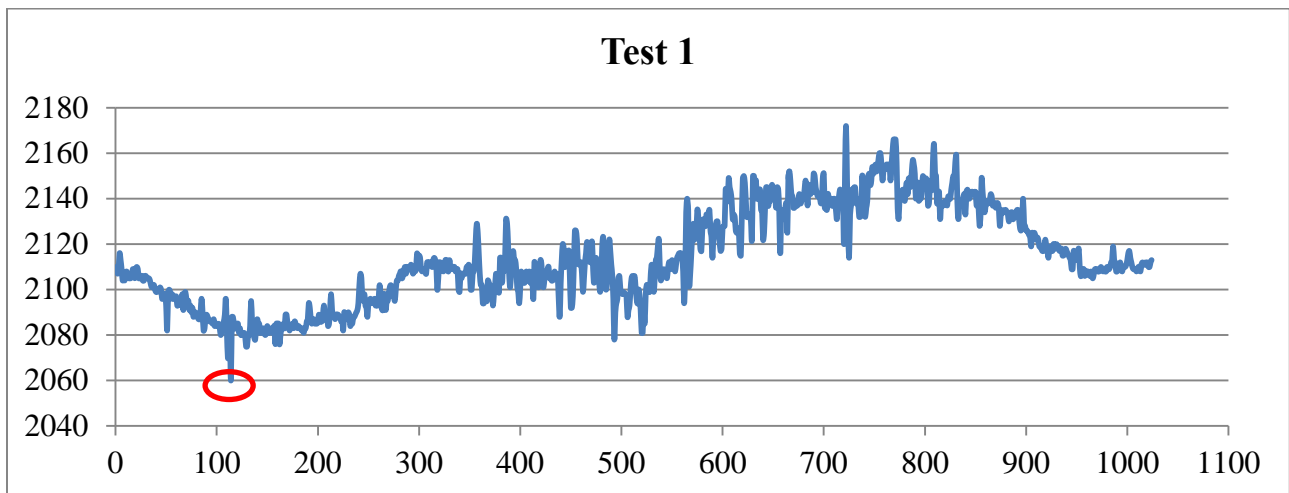
Figure 4.3 Example of graph plotted for determining the suitable segments

ANALYTICAL METHOD

The method used in the project was fairly straightforward and simple. The following sub-sections explain briefly of how each variable was organized.

Dependent Variable:

OBSI was the dependent variable in this analysis. The reason of it being chosen as the dependent variable was to evaluate the effectiveness of using independent variables such as MPD or skewness to accurately predict OBSI.

Independent Variables

MPD and skewness were the independent variables, where they were plotted in respected to OBSI. Choosing MPD and skewness as the independent variables allowed the use of the R^2 value computed to evaluate which property can more accurately predict OBSI. There were three CTM's measurements taken in each location with 2 segments of skewness to be computed for each of them. Consequently, there was large amount of skewness data for each test cell. Therefore, average approach was used. All variables' values were arranged into a spreadsheet to plot graphs of OBSI vs. MPD and OBSI vs. skewness. Lastly, a comparison of the R^2 value for both plots were observed in order to investigate which independent variables are the most suitable indicator for OBSI prediction in asphalt pavement surfaces.

Plots of OBSI vs. Mean Profile Depth:

Figure 4.4 through Figure 4.7 show plots of the OBSI vs. MPD for driving and passing lanes at both the mainline and LVR. Two significant observations based on the graphs are evident. Firstly, most data points are far apart from the best-fitted line. Secondly, R^2 values are relatively small and in the range of 0.05 to 0.241. Figure 4.1.47 shows compilation of data points for both lanes at mainline and LVR to get a better picture of the convergence of the readings.
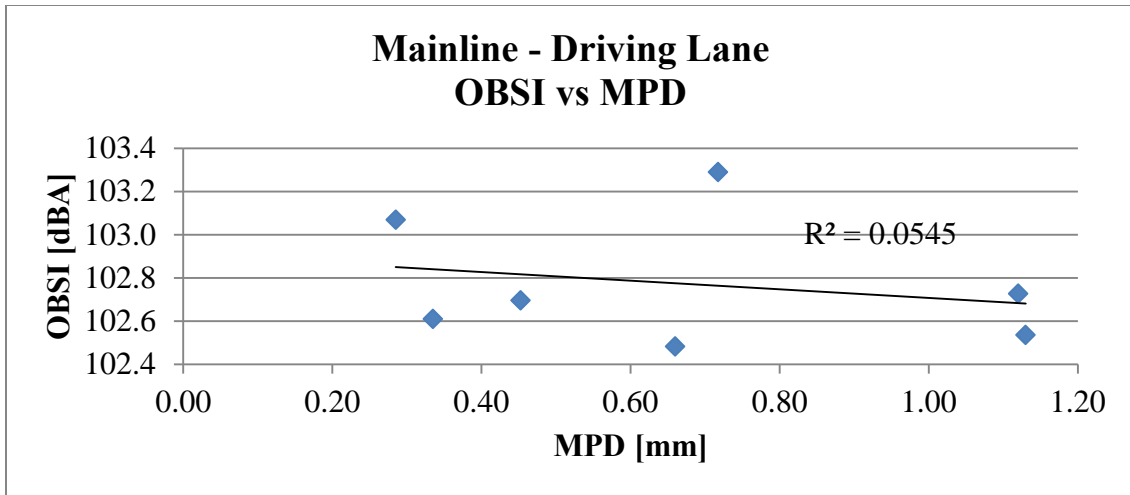
Figure 4.4 Plot of OBSI vs. MPD for driving lane at mainline
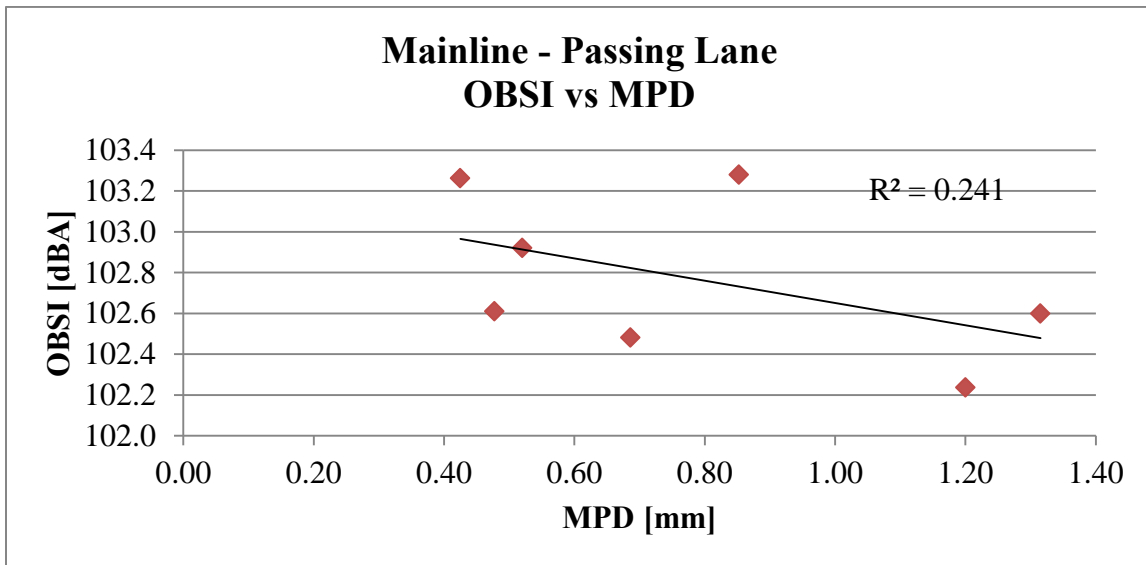
Figure 4.5 Plot of OBSI vs. MPD for passing lane at mainline
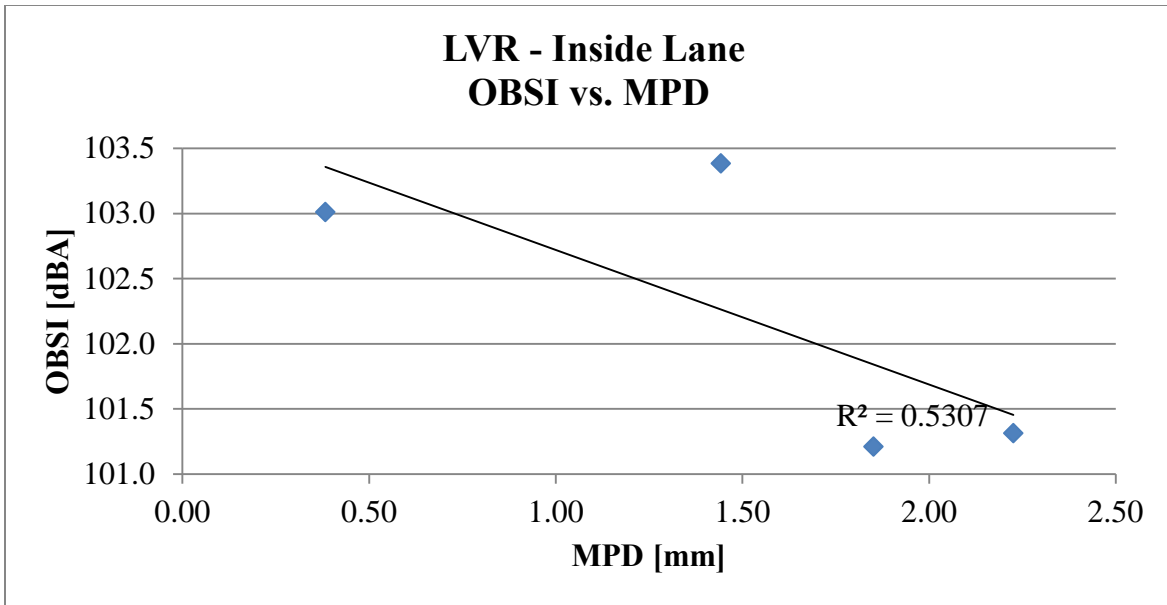
Figure 4.6 Plot of OBSI vs. MPD for inside lane at LVR
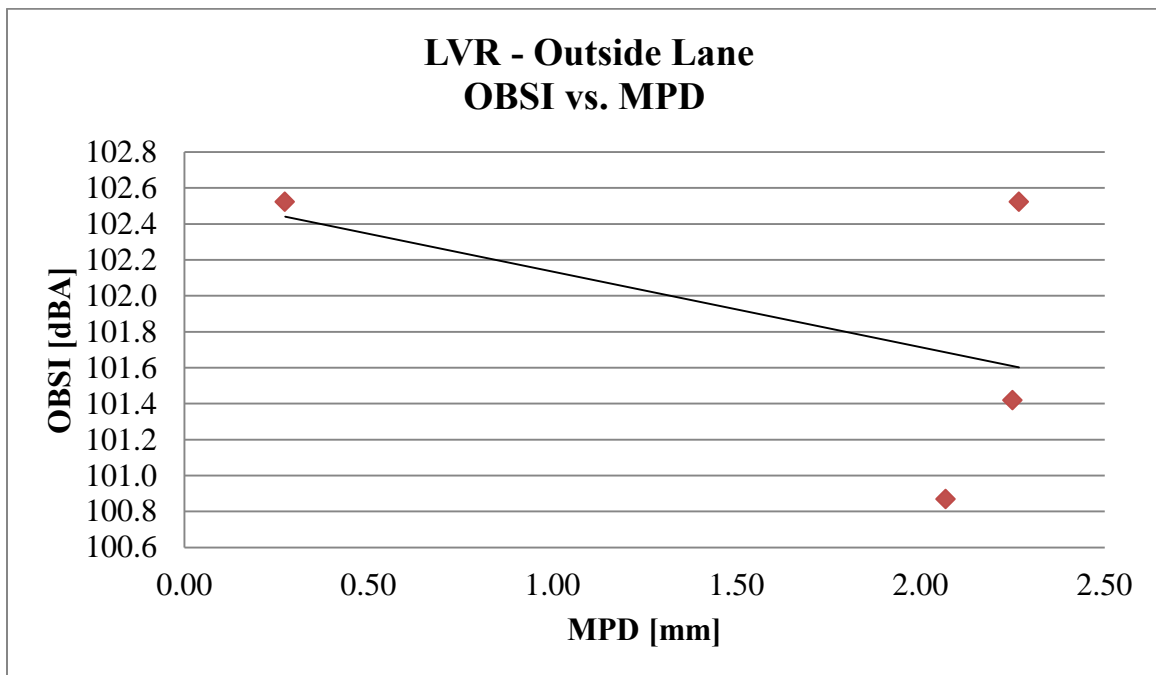
Figure 4.7 Plot of OBSI vs. MPD for outside lane at LVR
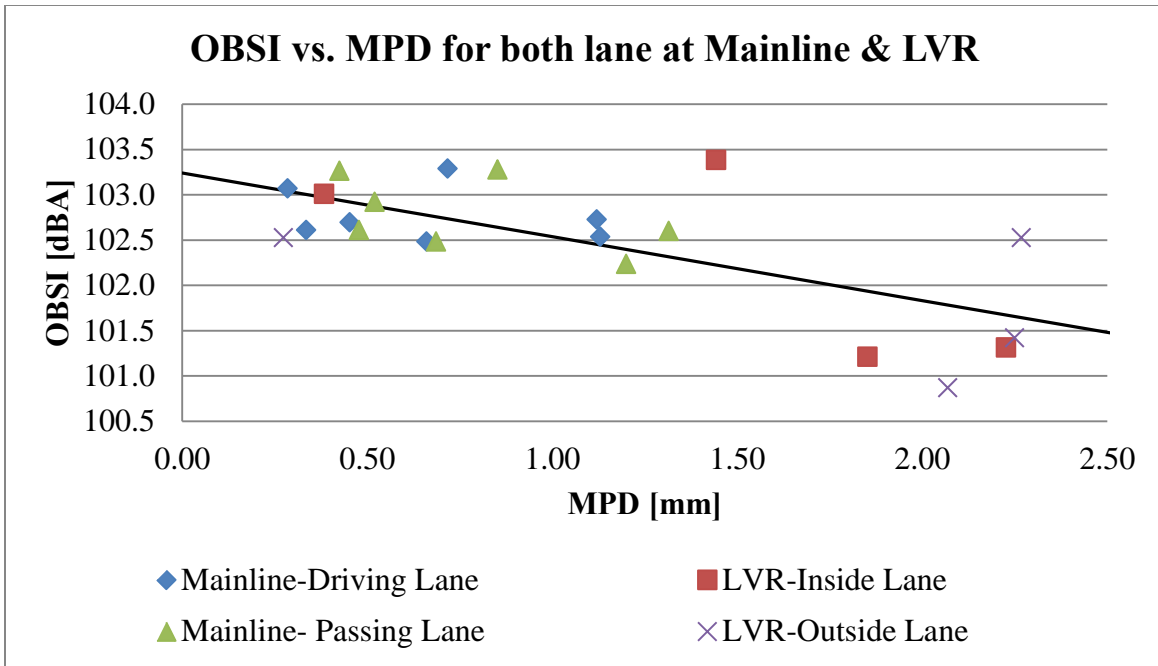
Figure 4.8 Plot of OBSI vs. MPD for both lane at mainline

Figures 4. 9 through Figure 4.12 illustrate plots of OBSI vs. skewness for both lanes on both roadways. Additionally, two noteworthy remarks are evident from the plots. First, majority of the data points are close to the best-fitted line; secondly, the graphs contain a moderate to high R^2 values in the range of 0.5 to 0.8.

Figure 4.13 shows compilation of data points for both lanes at both roadways: mainline and LVR to get a better idea of the convergence of readings.
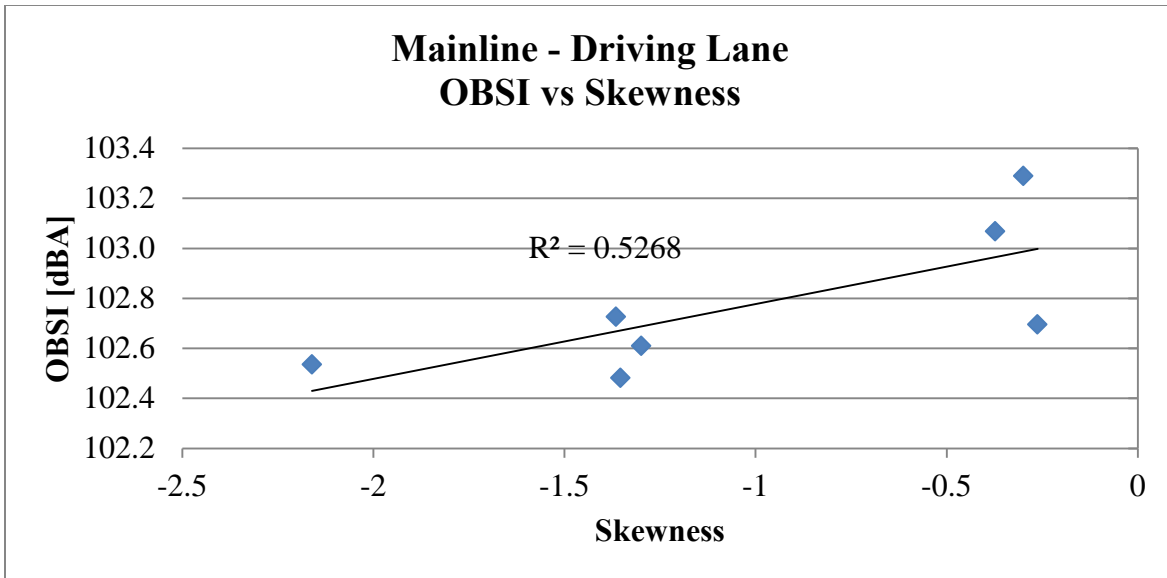
Figure 4.9 Plot of OBSI vs. Skewness for driving lane at mainline
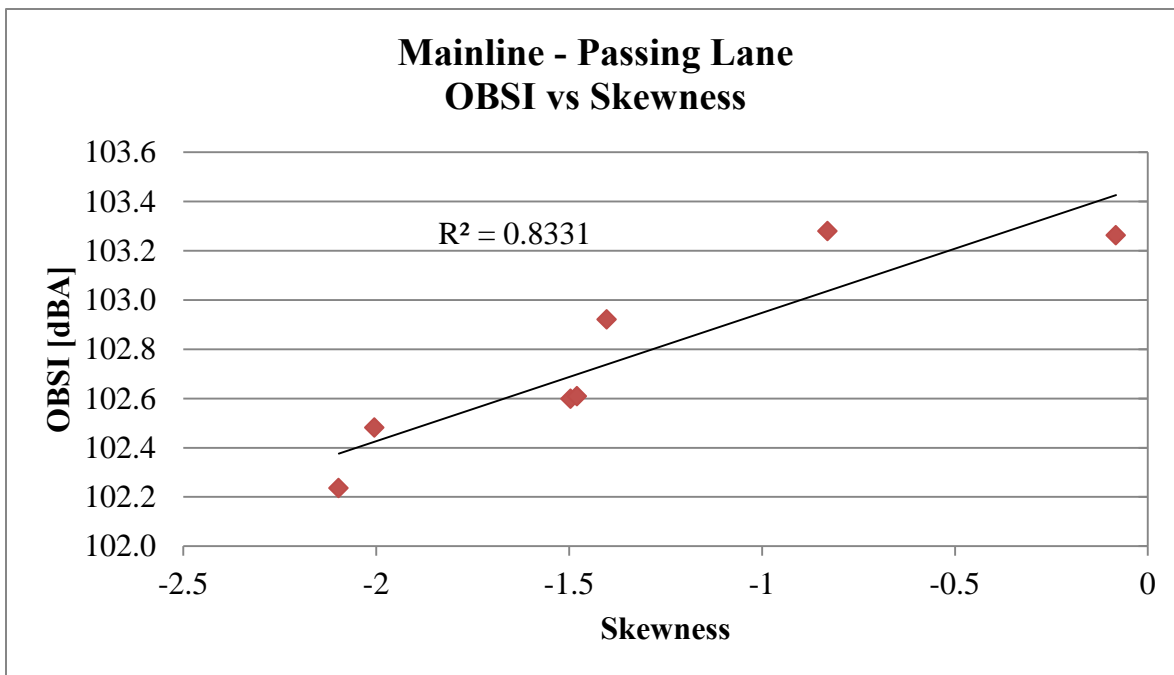
Figure 4.10 Plot of OBSI vs. Skewness for passing lane at mainline
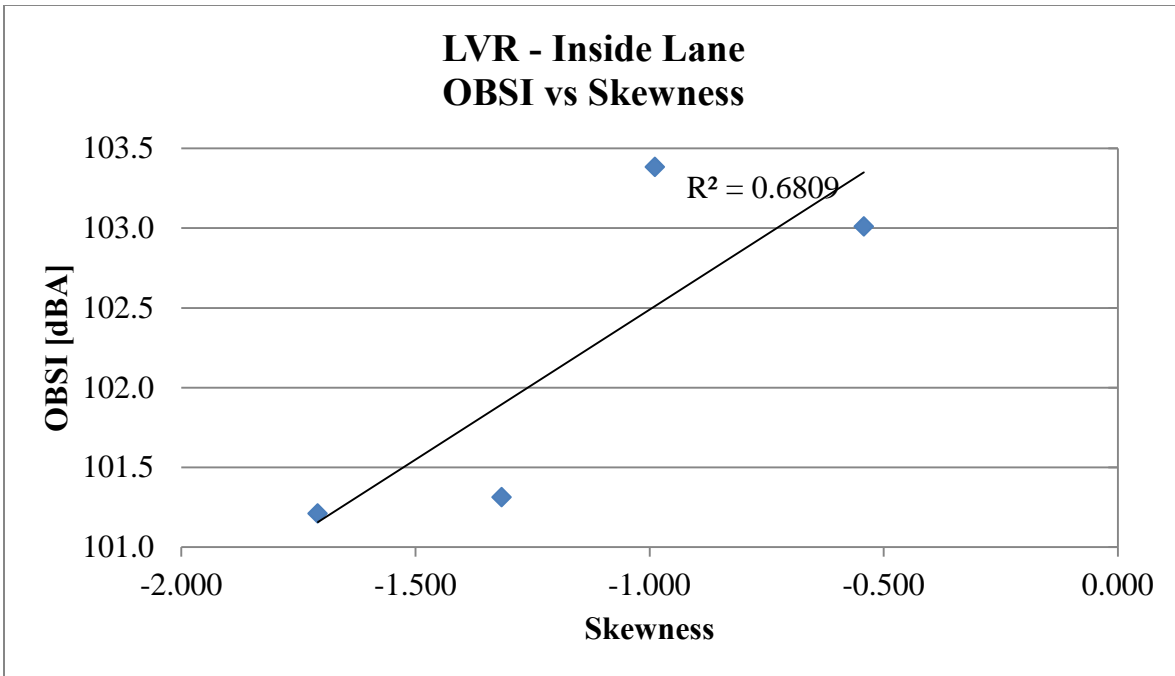
Figure 4.11 Plot of OBSI vs. Skewness for inside lane at LVR
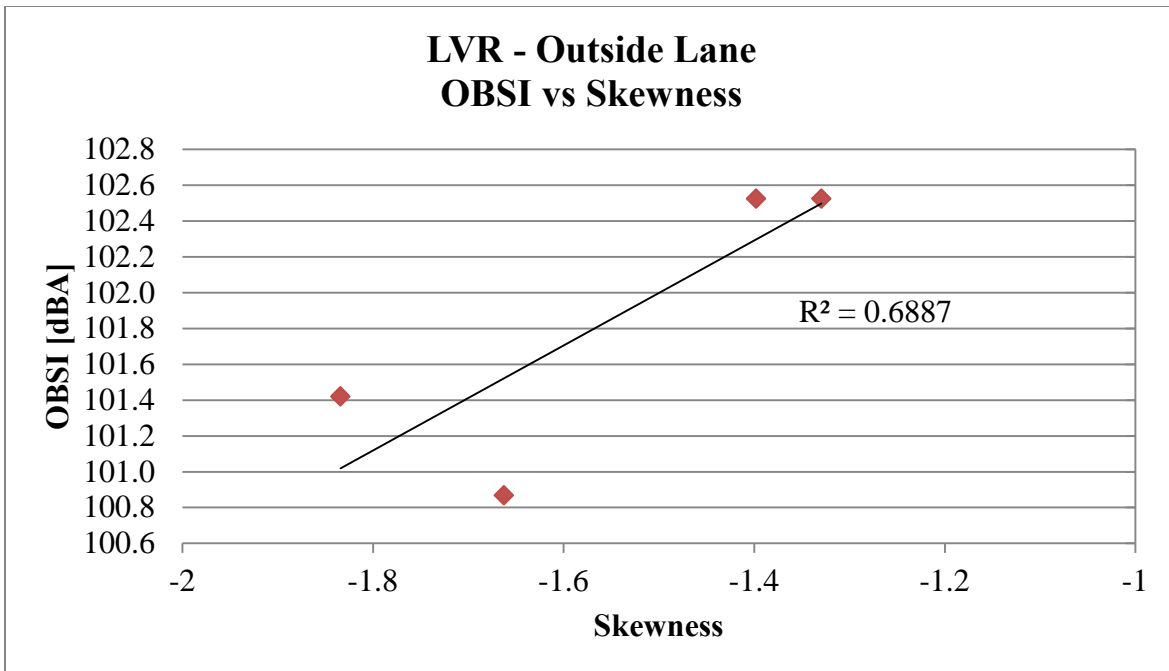
Figure 4.12 Plot of OBSI vs. Skewness for outside lane at LVR
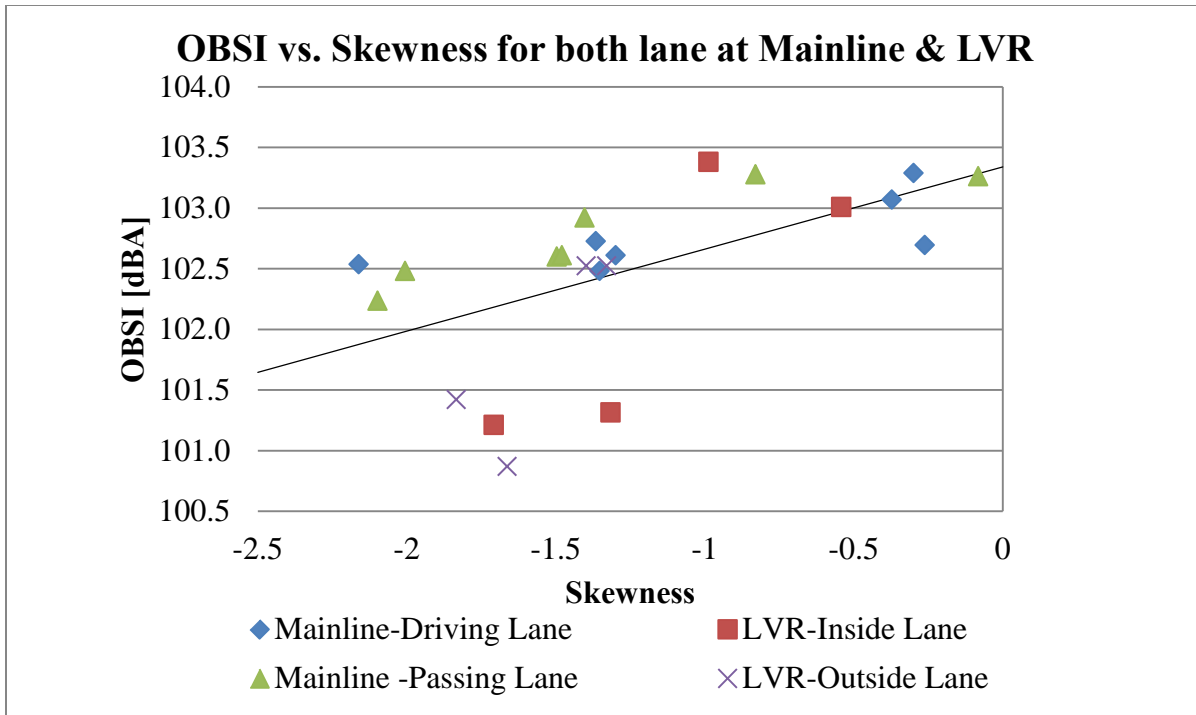
Figure 4.13 Plot of OBSI vs. MPD for both lane at mainline and LVR

Summary:

Observations made based on the results show that skewness is a better indicator for sound intensity prediction compared to MPD, based on a higher R^2 values for OBSI vs. skewness than OBSI vs. MPD (Table 4.1)

Table 4.1 R^2 value for mainline and LVR according to the lanes

Mainline	Coefficient of Determination (R^2)	
	Driving	Passing
OBSI vs. MPD	0.054	0.241
OBSI vs. Skewness	0.527	0.833
LVR	Coefficient of Determination (R^2)	
	Inside	Outside
OBSI vs. MPD	0.531	0.241
OBSI vs. Skewness	0.681	0.689

The same analysis was conducted by using data from June 2011 to investigate if the conclusion is consistent. Results did not clearly indicate the preponderance of skewness over MPD in OBSI prediction that was obtained in the previous 2012 Data. Evidently an in-depth study involving a larger sample space is recommended.

STUDY OF PAVEMENT NOISE VERSUS TEMPERATURE

INTRODUCTION

This section discusses the relationship between pavement noise and temperature for asphalt test cells. Unlike concrete, asphalt is a highly viscous liquid or semi-liquid form of petroleum. Therefore, the rates of changing (α-value) between both measurements vary depending on types of asphalt used in the mix and the temperature...

The selected test sections chosen for analysis include mainline cells 1, 2, 3, 4, 15, 19, 20, 22 and 70.

Two significant properties evaluated for correlation include temperature (independent variable) and the tire-pavement-interaction-noise (dependent variable). An hourly OBSI measurement conducted on 18th of April 2011 from 4 A.M. to 5 P.M. facilitated this aspect of the analysis. That day provided a large diurnal temperature range available in most spring days. There will be a brief discussion of temperature noise relationship followed by data analysis.

The speed of sound can be computed in respect to time with the following formula:

$$c = 331.3 + 0.6T \qquad (12)$$

$$\text{where} \quad c = \text{speed of sound}$$
$$T = \text{temperature in } °C$$

Speed of sound is associated to temperature linearly with positive slope. However for the purpose of modelling, the Kelvin absolute temperature scale is preferred because in retains an element of true mathematical proportionality that the Farenheit or Celsius scales do not have. This can be explain by the following: as temperature rises, the faster sound travels in a medium. In a hot medium, heat energy alters speed of the molecules collision by converting energy into kinetic energy. As molecules move faster due to the transmission of the kinetic energy, they

collide with each other rapidly. Hence, it is safe to say that the hotter the medium, the faster the sound travels.

Relationship between Density and Temperature:

According to the ideal gas law,

$$\rho = \frac{P}{RT} \tag{13}$$

where ρ = density of medium kg/m^3

P = pressure (N/m^2)

R = ideal gas constant = 8.314 JK^{-1}mol^{-1}

Temperature is indirectly proportional to density of medium. That is to say, the higher the temperature is, the denser the medium is. This can be explained by using the kinetic theory as well. As temperature rises, particles accelerate hence lead to a conversion of kinetic energy to a mass in a form of new particles. The addition in the mass will leads to denser medium as density is defined as the mass of the material per unit volume.

Definition of Sound Intensity:

Sound intensity is defined as sound power per unit area. It is a measurement of level differences in noise.

Sound intensity can be defined mathematically with the formula below:

$$SI = \rho c \tag{14}$$

where SI = sound intensity

ρ = density of medium

c = speed of sound

As can be observed in the equation, sound intensity can be related in respect to density of medium. By combining and substituting equation (12) and (13), we get a new relationship of sound intensity in respect to pressure, gas constant and temperature:

$$\text{Sound Intensity} == \frac{P}{R}\left[\frac{167}{T} + 0.6\right] \tag{15}$$

where T = temperature in K, Sound Intensity is in Watts/m^2

     P = pressure in N/m^2

     R = ideal gas constant = 8.314 JK^{-1}mol^{-1}

The adiabatic constant should play a role in this equation but the derivation does not set the stage for introduction of the adiabatic constant. However its presence or absence may not change the form of the model. This basic equation is not a straight line but it establishes that temperature and OBSI are inversely related. The model will now be validated with data.

Relationship between Sound Intensity and Temperature:

Figure 4.14 shows the relationship between temperature and sound intensity. As temperature rises, sound intensity decreases.
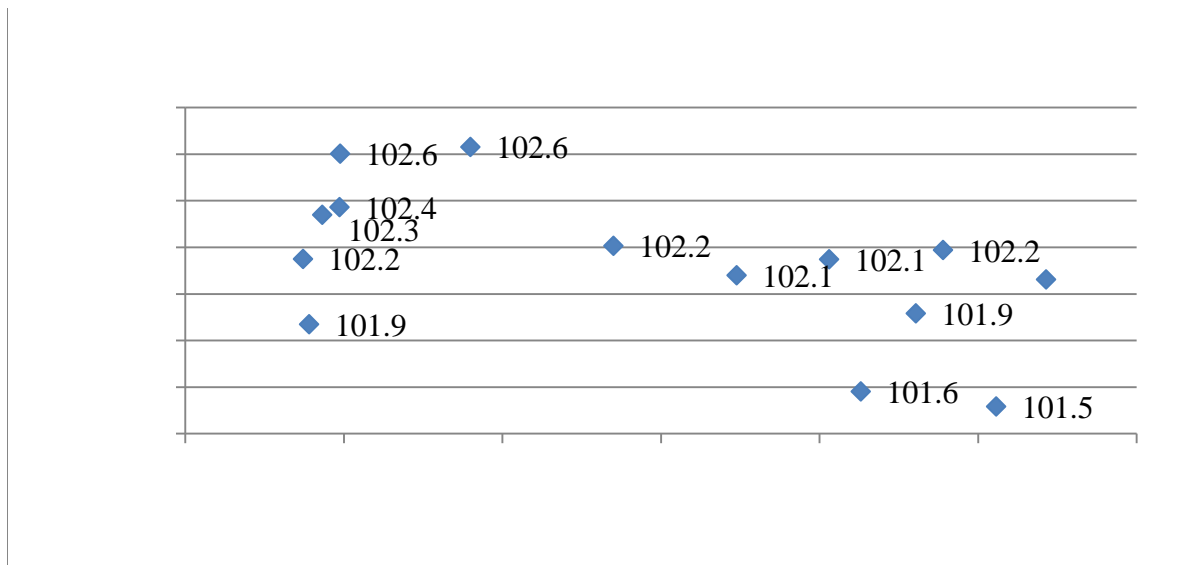
Figure 4.14: OBSI versus Temperature plot

Theoretically, the relationship between sound intensity and temperature is inversely proportional. From equation 32 general formula is of the form

$$SI = \frac{k}{T^{\propto}} \tag{16}$$

where SI =sound intensity

k= constant

T= temperature (°K)

α = Exponent (This was 1 for concrete [58]

APPROACH

For the study of the pavement noise versus temperature, two methods are used in the analysis. The first method directly uses the data given; while another uses solver tool in Excel. OBSI difference is used in the comparison instead of OBSI average given in the database. The both measurements are plotted in such a way that OBSI is the dependent variable (y-axis) and temperature is the independent variable (x-axis).

Direct Method:

In this method, OBSI measurements used are selected directly from the OBSI data collection database from 18th of April 2011. OBSI differences from 100 dBA are used instead of the given OBSI average in Excel spreadsheets. This method removes the rigor inherent in OBSI values, which relate mainly by difference. Note that an OBSI difference of 3 dBA is tantamount to a difference of 50 % of the noise source in watts/m2. After obtaining the OBSI difference for each temperature, it is plotted against temperature.

Solver Method:

Solver uses an iterative process to assign the model constants that will minimize the residuals of the equation=$\sum (Model\ OBSI\ difference - Measured\ OBSI\ difference)^2$

Solver is based on the Levenberg Marquardt method of seeking the least descent for or global and local minima in model fitting. (Figures 4.2 to 4.11).

Comparison of Data:

First Cell 1 data was used to compare the accuracy of both linear and power trend lines. This was repeated in the other test cells Next, graphs that comprised both methods were plotted for each test section to gain the equation of the data points. Lastly, compilation of all test cells data points was plotted.

T-Test: Paired Two Samples for Means:

The two-sample t- test determines if two sets of samples are significantly different from each other. The null hypothesis is that the two samples' mean are equal to one and another, while the alternative hypothesis will be the opposite. The t-value and p-value are determined with known mean and standard deviation. The general equation for t-value is such as below:

$$t = \frac{\overline{X_1} - \overline{X_2}}{\sqrt{\left(\frac{SD_1{}^2}{N_1} + \frac{SD_2{}^2}{N_2}\right)}} \tag{17}$$

where $\overline{X_1}, \overline{X_2}$ = average mean of both sample

SD_2 = standard deviations of both average

N_1, N_2 = number of samples

The P-value was determined by com

RESULTS

OBSI vs. Temperature:

This section shows graphs plotted by using OBSI values with the corresponding temperatures. Figure 4.15 shows the comparison of both linear and power trend lines to observe the most suitable equation that can describe the relationship between sound intensity and temperature. Figure 4.16 through Figure 4.24 show OBSI vs temperature relationship for each cell. Figure 4.25 compiles results of all test cells to show the relationship of equation to the asphalt's property. Lastly, Table 4.2 tabulates all the equations obtained through direct and solver methods. Linear trend line gave a coefficient of determination (R^2) of 0.9993, whereas power trend line provided a R^2 value of 1.
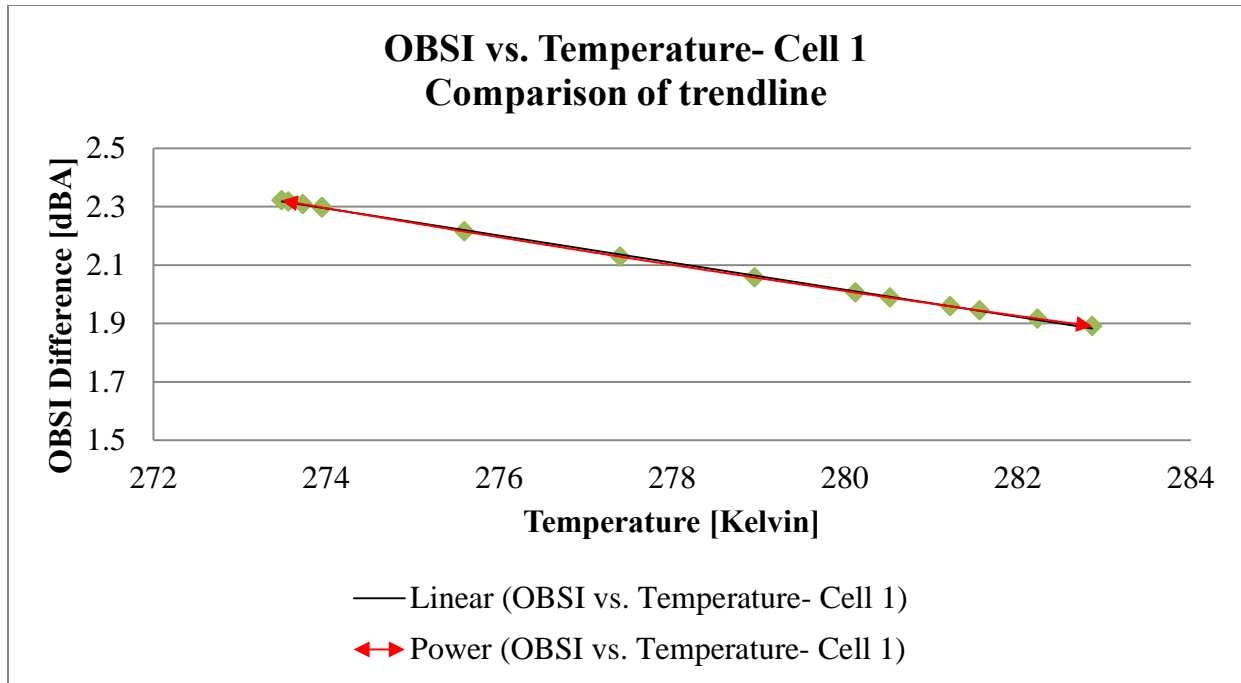
Figure 4.15: Comparison of Linear Trend line and Power Trend line for cell 1

Red data points are the data obtained from using solver method, whereas blue data points are the data gotten from using direct method.
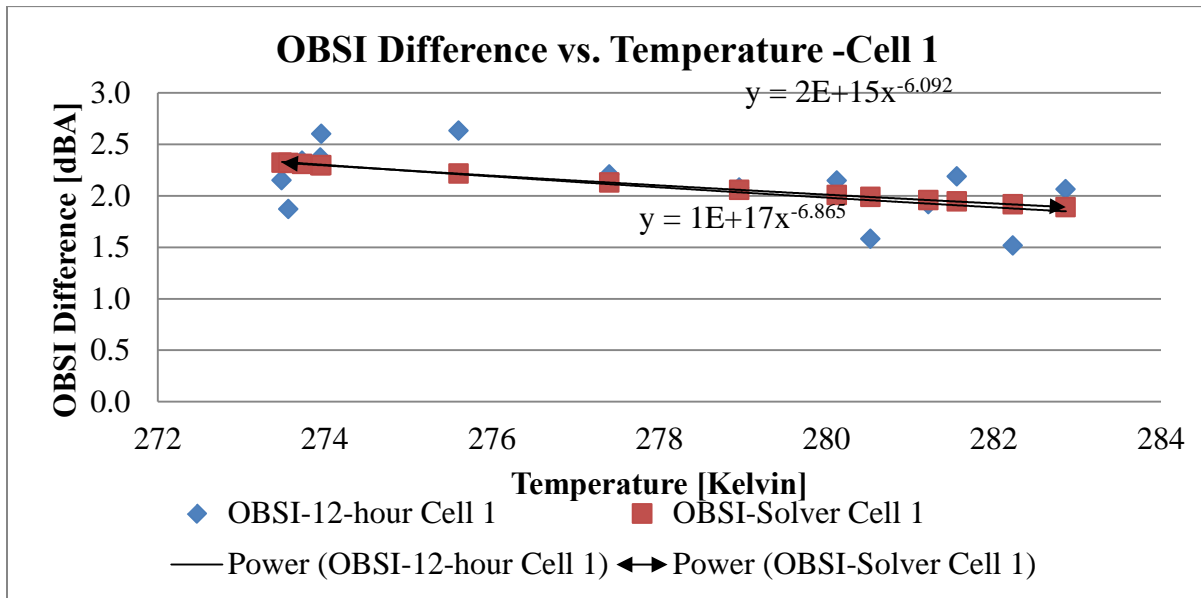
Figure 4.16 Plot of OBSI Difference versus Temperature for cell 1

114
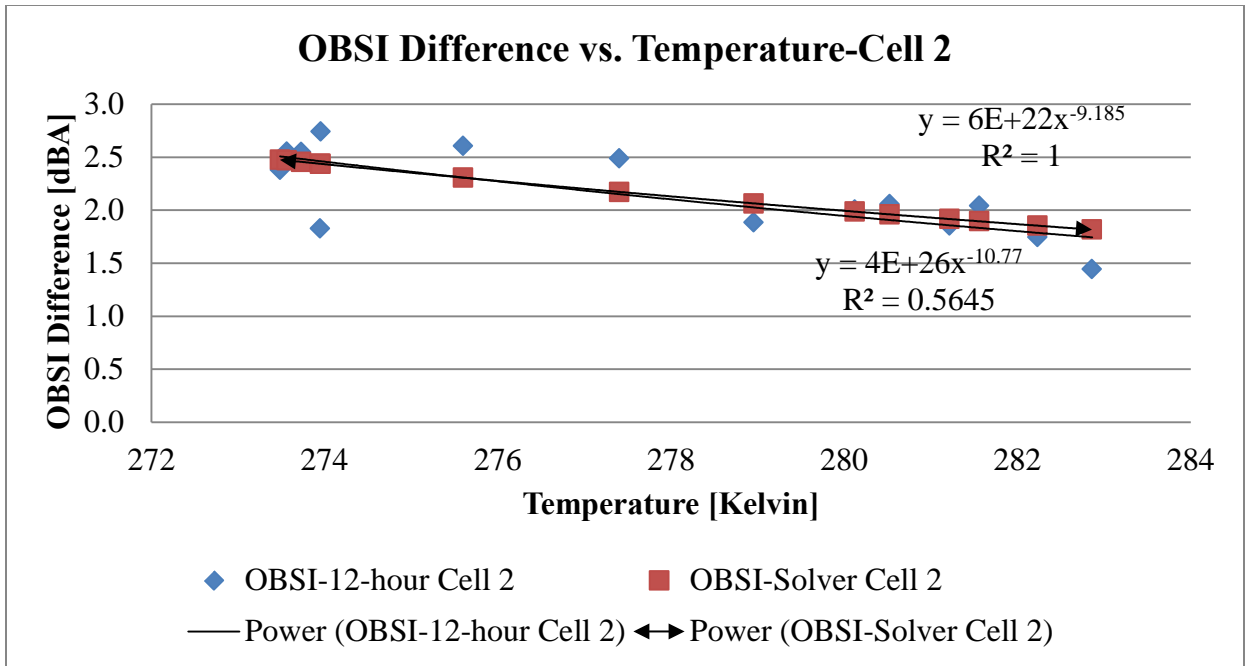
Figure 4.17 Plot of OBSI Difference versus Temperature for cell 2
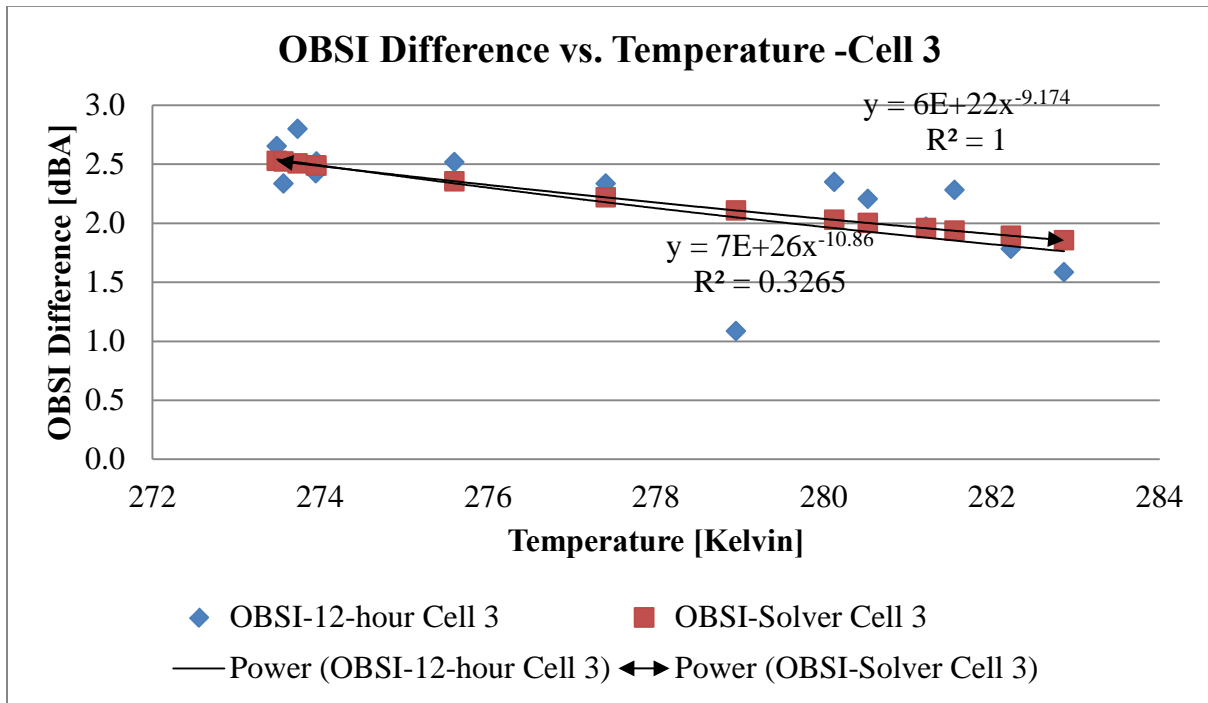
Figure 4.18 Plot of OBSI Difference versus Temperature for cell 3
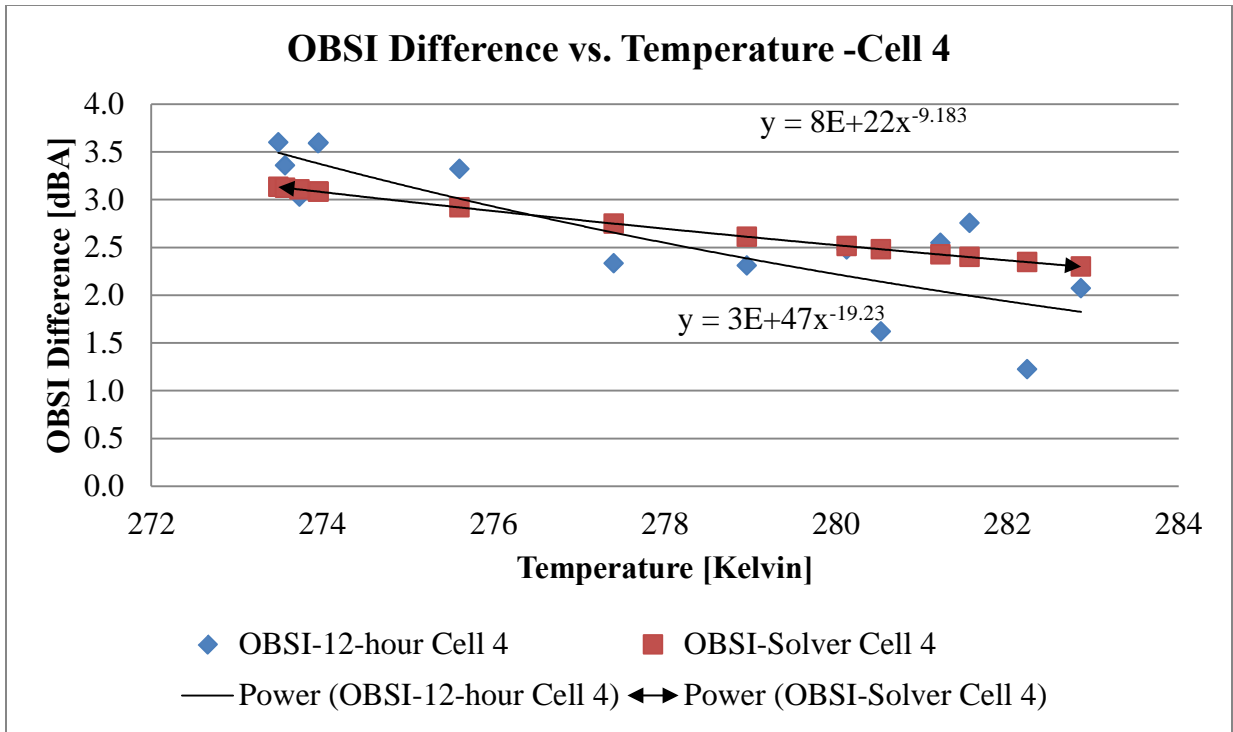
Figure 4.19 Plot of OBSI Difference versus Temperature for cell 4
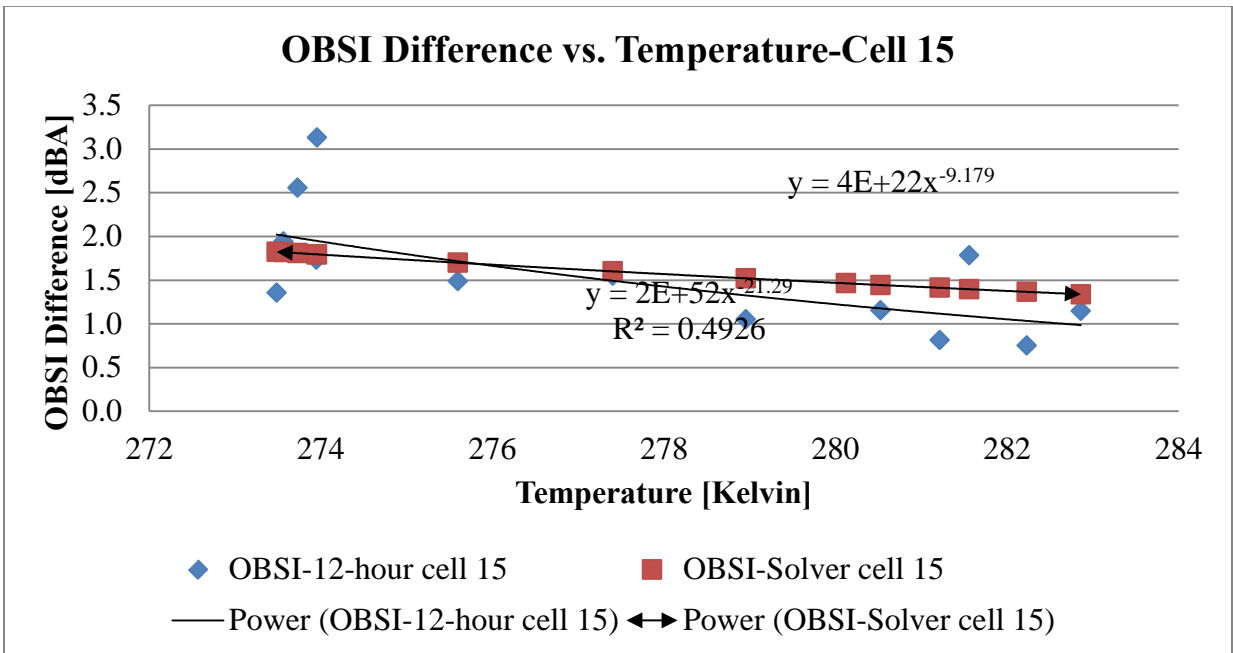
Figure 4.20 Plot of OBSI Difference versus Temperature for cell 15
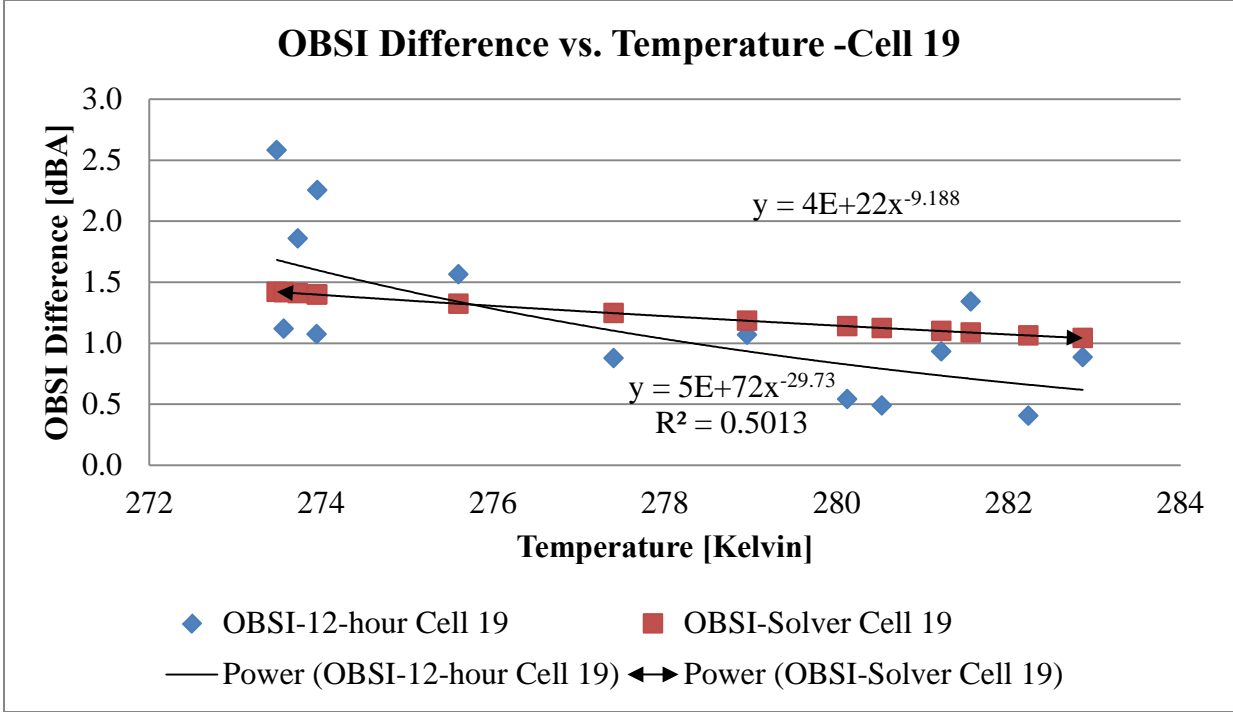
Figure 4.21 Plot of OBSI Difference versus Temperature for cell 19
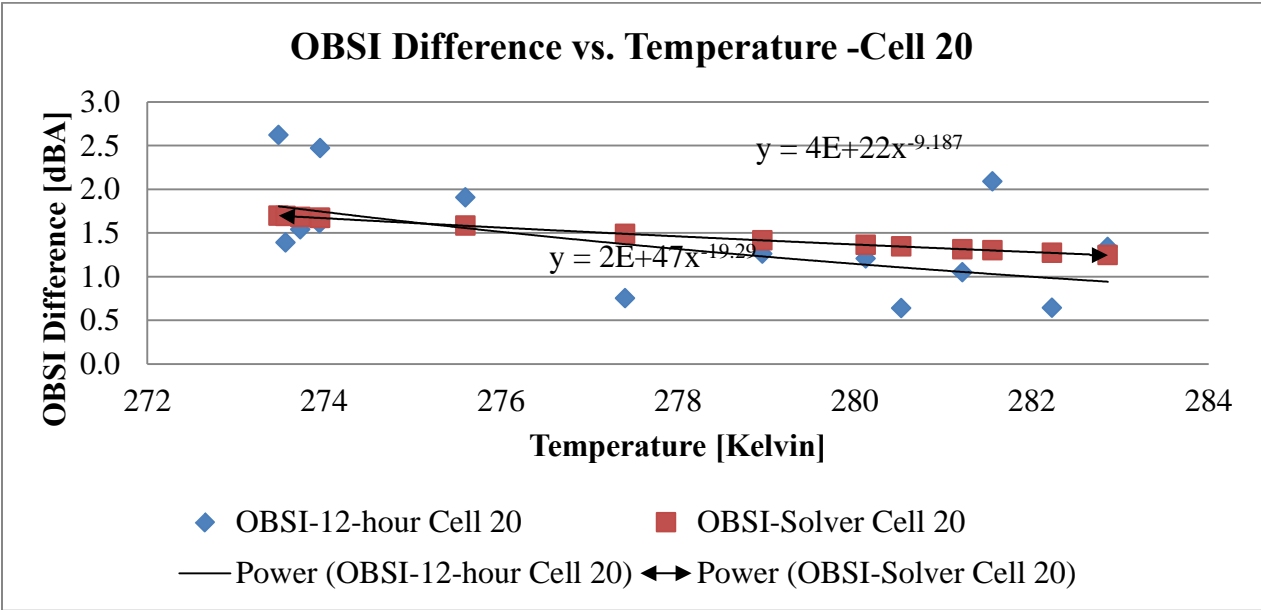
Figure 4.22 Plot of OBSI Difference versus Temperature for Cell 20

117
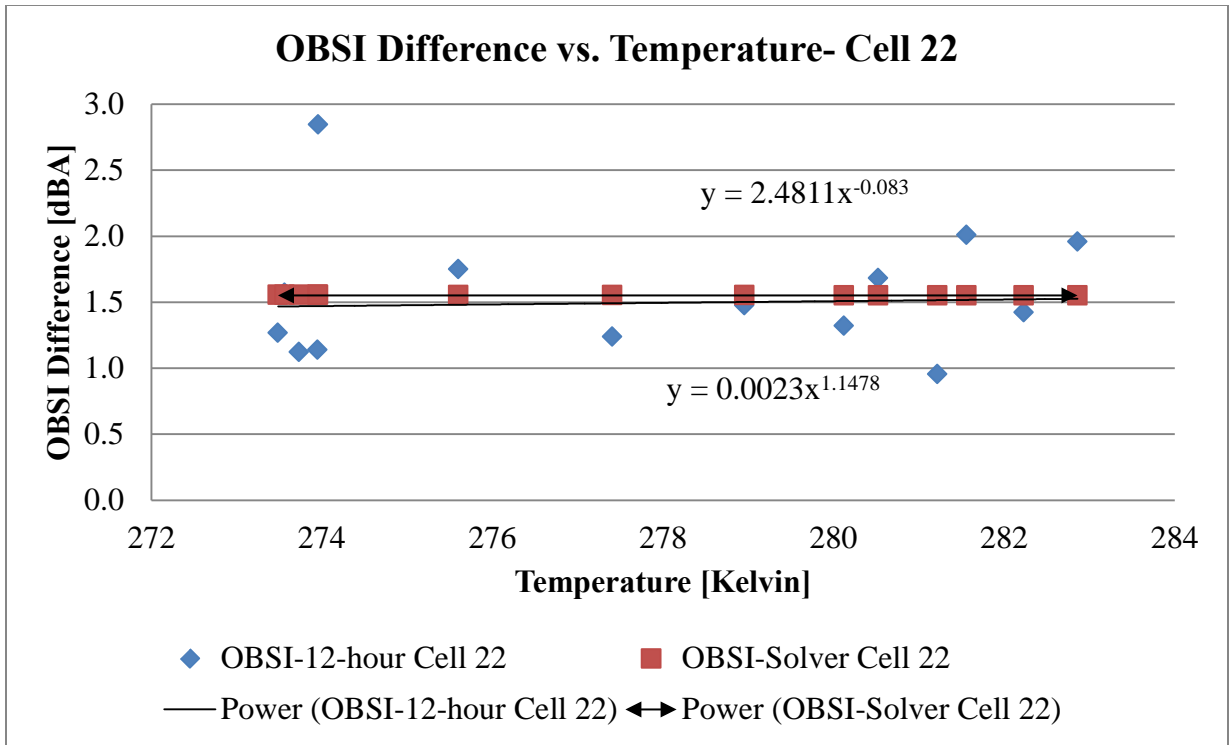
Figure 4.23 Plot of OBSI Difference versus Temperature for cell 22
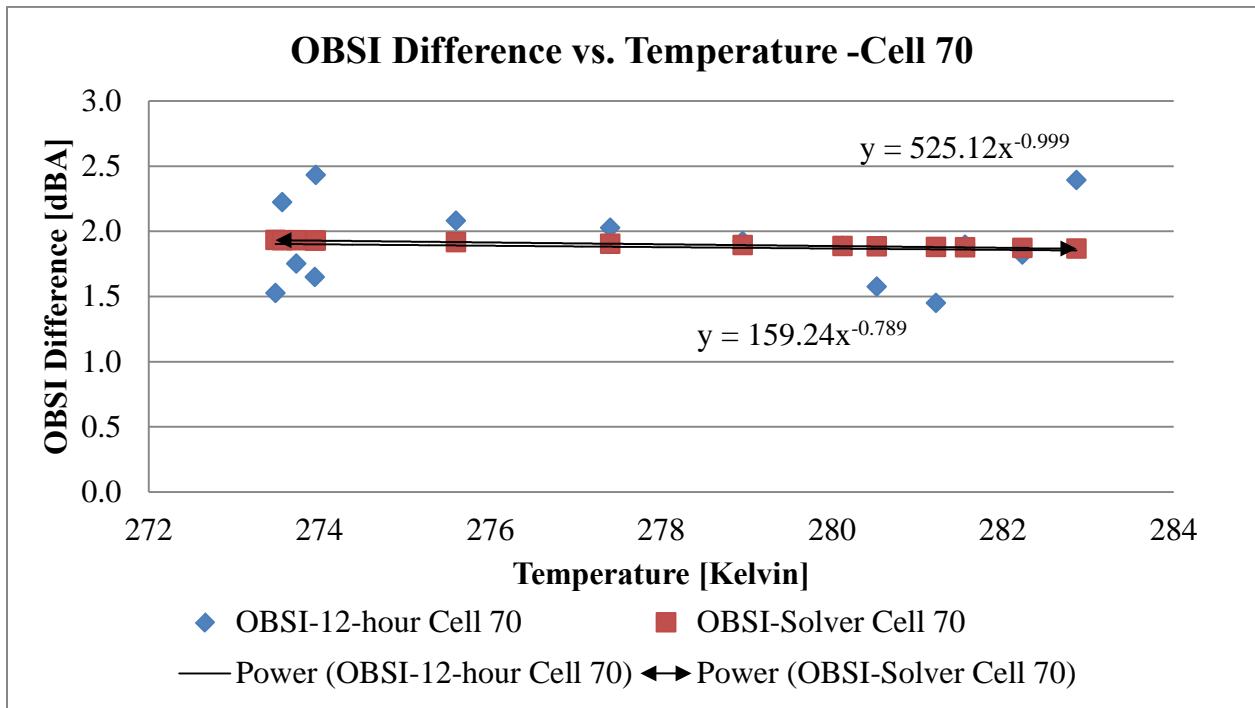
Figure 4.24 Plot of OBSI Difference versus Temperature for cell 70
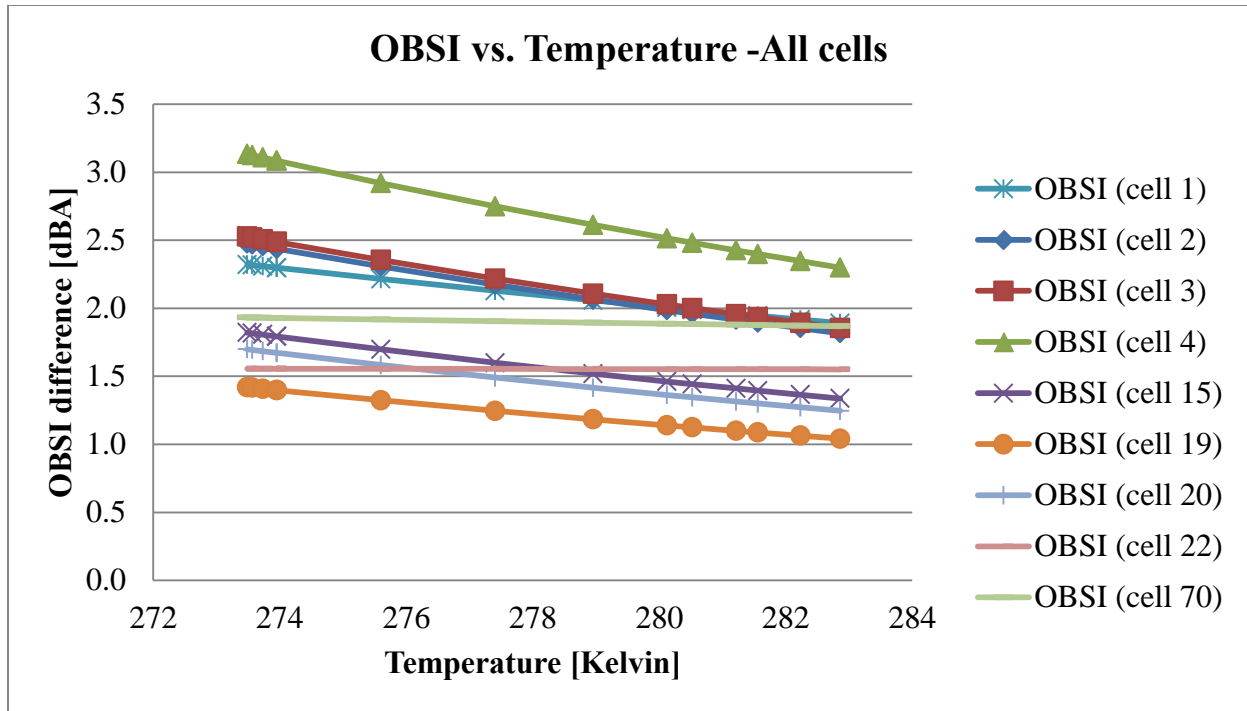
Figure 4.25 Data for 9 Test Cells

The table summarized all equations that are computed by using power trend line.

Table 4.2 Power trend line equation for all cells

Cell	Equations
	OBSI- Solver
1	$y = 2E+15x^{-6.092}$
2	$y = 6E+22x^{-9.185}$
3	$y = 6E+22x^{-9.174}$
4	$y = 8E+22x^{-9.183}$
15	$y = 4E+22x^{-9.179}$
19	$y = 4E+22x^{-9.188}$
20	$y = 4E+22x^{-9.187}$
22	$y = 2.4811x^{-0.083}$
70	$y = 525.12x^{-0.999}$

Table 4.2 summarizes the equations generated by using solve r to minimize the residuals According to cell description in appendix B, most of the test cells have a different thickness and

119

type, other than test cell 2 and 3. It is possible α-value simply varies with different asphalt mixes and in-service condition.

EFFECT OF TRAFFIC ON OBSI

The following table shows the summary for results of T-test on the effects of traffic on sound intensity. Parallel lanes of the low volume road and Mainline asphalt cells receive different levels of traffic. The low volume road receives no traffic in the outside lane and 80 trips per day of the 80 kip 5 axle semi 5 days a week in the inside lane. A 2- Sample T-test was used to analyze the effect of traffic on OBSI. The P-values shown in Tables 4.3 and 4.4 indicates that in both mainline and LVR the null hypothesis may be accepted thus, indicating that both driving and passing lane (or inside and outside lane for LVR) are have significantly different OBSI. The traffic does not seem to affect the sound intensity between the interaction of tire and pavement within the age range of the pavements and the material types as well at 95% confidence level. The test was repeated for the Wilcoxon Rank Sum Test and the Wilcoxon Sign Rank Test and gave the same result.

Table 4.3: Summary for Effect of Traffic on OBSI (Statistical Hypothesis Tests)

		T-TEST	WILCOXON SIGNED RANK TEST		WILCOXON RANK SUM TEST	
MAINLINE CELLS	Alpha	0.05	Normal Approximation	0.489	Normal Approximation	0.069
	Two-tailed P-value	0.326294923	Two-tailed P-value	0.6247	Two-tailed P-value	0.9447
LVR CELLS	Alpha	0.05	Normal Approximation	0.21	Normal Approximation	0.562
	Two-tailed P-value	0.873563915	Two-tailed P-value	0.8339	Two-tailed P-value	0.5738

Table 4.4: Results for Effects of Traffics on OBSI Difference

	T-TEST	WILCOXON SIGNED RANK TEST	WILCOXON RANK SUM TEST
MAINLINE CELLS	SIMILAR	SIMILAR	SIMILAR
LVR CELLS	SIMILAR	SIMILAR	SIMILAR

FRICTIONAL PROPERTIES ON ASPHALT PAVEMENT SURFACES

INTRODUCTION

This section examines the differences between friction number of smooth and ribbed tires to possibly identify hysteresis phenomenon and to determine how frictional resistance changes in asphalt pavements. Fragmentation of Friction al forces into hysteresis and adhesion forces is expected to characterize frictional properties better.

Cells 1 through 4 were used to observe the behavior of frictional properties between smooth tires and ribbed tires. Cell 3, 4, 19, and 22 were used to compare the coefficient of friction at the speed of 40km/hr.; and observation is made based on the type of asphalt pavement. The type of pavements for all these cells are: cell 1 has original hot-mixed asphalt; cell 2, 3 and 4 have stabilized full depth reclamation asphalt; cell 19 has recycled unbound base, warm mix asphalt; and cell 22 has low temperature cracking, fractionated reclamation asphalt. Data were retrieved from year 2007 to year 2012.

The purpose of the study for behavior of frictional properties between two types of tires is to identify the occurrences of hysteresis phenomenon on asphalt pavements; while the comparison of the coefficient of friction at the speed of 40km/hr. is to observe the differences in pattern of the frictional properties based on the type of asphalt pavements.

Friction is the force resisting the relative motion of surfaces. It moves in the opposite direction of the motion. The measurement of friction varies based on the coefficient of friction depending on the surface, which will be discussed in next Section.

Frictional properties play an important role in the analysis of pavement performance. The two main component of friction in tire-pavement interaction comprises of adhesion and hysteresis. Adhesion force, F_a is produced by the actual contact area between tire and pavement surface. Theoretically, energy that resists breakage of surface-to-surface contact forces in the direction of motion is friction and plane of contact is the frictional resistance. This energy is the work done by the adhesion force. On the other hand, hysteresis exists when there is deformation of rubber tire due to pavement surface asperities [58]. Hysteresis occurs when the rubber is alternately compressed and relaxed when travelling in an uneven pavement surface [58]. Hysteresis can be explained in such a manner: the "relaxing" process did not happen right after "compression" process because of a phenomenon called suction. Suction forces the tire to adhere to the pavement surface due to the differences in external and internal pressures. It depends on

the past environment and the current environment. Figure 4.26 illustrates the concept of both components discussed above.
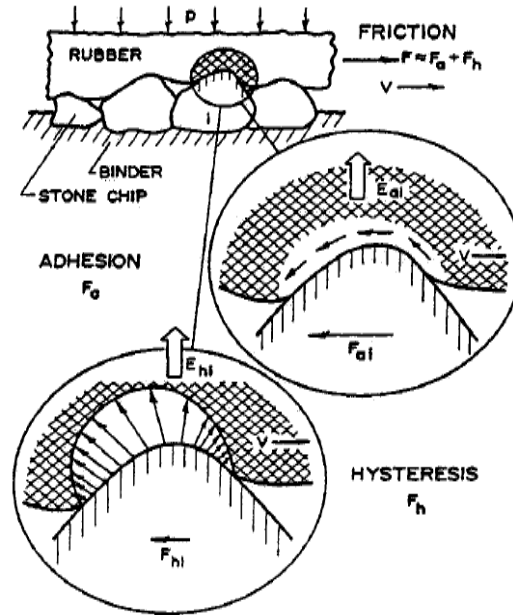
Figure 4.26 Schematic of adhesion and hysteresis component of rubber friction [58]

Friction Number:

Friction Number (FN) is a value representing friction of a surface obtained from using the KJ Law (Dynatest) skid trailer. It serves as an indication of friction level of pavement surface.

Coefficient of Friction:

Coefficient of Friction, often represented by Greek letter μ is the ratio of the frictional force between two surfaces (F_f) and the force pressing them together (normal force, N). Figure 4.27 and equation (18) explains the definition of μ.
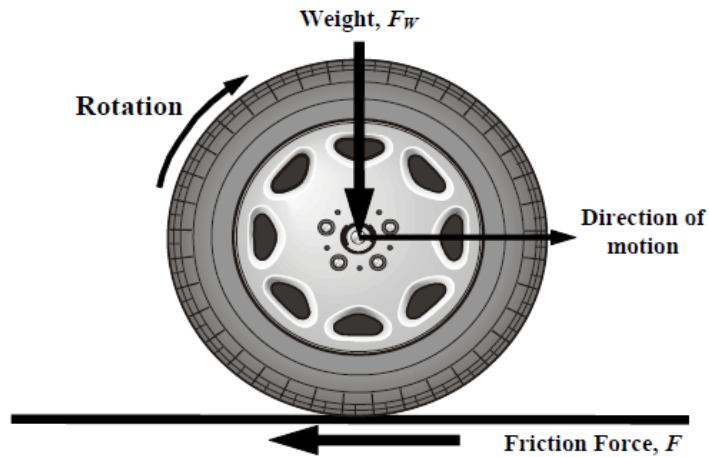
Figure 4.27 Forces on a rolling tire

The coefficient of friction can be expressed in the following equation:

$$\mu = \frac{F_f}{F_w} \qquad (18)$$

where μ = coefficient of friction

F_f = Frictional force

Fw = Normal Reaction.

Based on equation (18), frictional force is directly proportional to the μ-value of the material.

Friction Number vs. Time:

Data collected from Cells 1, 2, 3 and 4 at MnROAD was analyzed. The plots for friction number vs. time of each of cells are shown in Figure 4.28 through Figure 4.31.

- **Cell 1 –Driving Lane**

The differences in friction number of smooth tires and ribbed tires are listed in Table 4.5. It can be observed that both types of tire have a great difference in term of friction number.

124
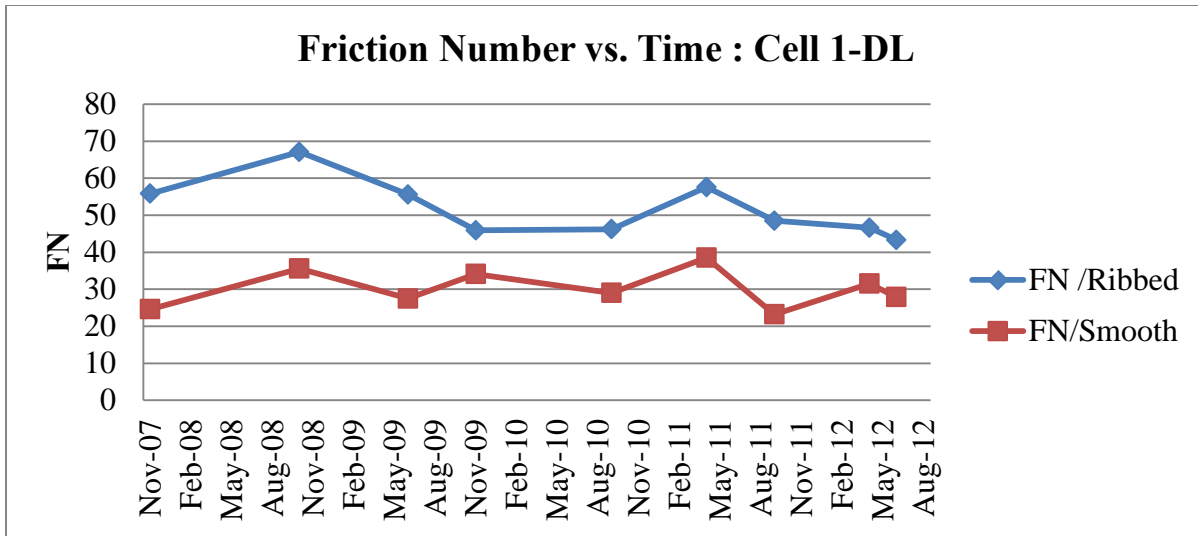
Figure 4.28 Friction Number vs. Time for Cell 1 Driving Lane

Table 4.5 Data Tabulation of FN Ribbed and Smooth for Cell 1 Driving Lane

Cell 1 DL	FN /Ribbed	FN/Smooth	FN difference
Nov-07	55.8	24.6	31.2
Oct-08	67.1	35.6	31.5
Jun-09	55.6	27.5	28.1
Nov-09	45.9	34.1	11.8
Sep-10	46.2	29	17.2
Apr-11	57.6	38.5	19.1
Sep-11	48.5	23.2	25.3
Apr-12	46.6	31.5	15.1
Jun-12	43.3	27.9	15.4

- **Cell 2 –Driving Lane**

The differences in friction number of smooth tires and ribbed tires are listed in Table 4.6. It can be observed that the FN for smooth tires and ribbed tires has a similar FN during the year of 2008 to 2011.
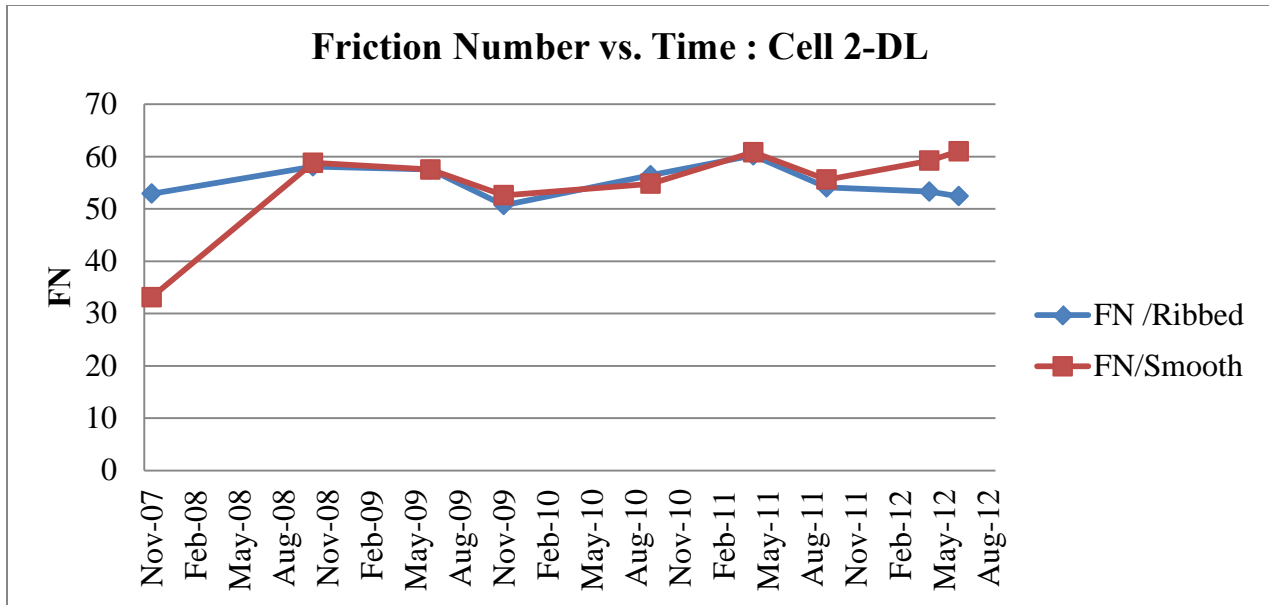
Figure 4.29 Friction Number vs. Time for Cell 2 Driving Lane

Table 4.6 Data Tabulation of FN Ribbed and Smooth for Cell 2 Driving Lane

Cell 2 DL	FN /Ribbed	FN/Smooth	FN difference
Nov-07	52.9	33.1	19.8
Oct-08	58.1	58.8	-0.7
Jun-09	57.5	57.5	0
Nov-09	50.7	52.6	-1.9
Sep-10	56.4	54.8	1.6
Apr-11	60.2	60.8	-0.6
Sep-11	54.1	55.6	-1.5
Apr-12	53.3	59.2	-5.9
Jun-12	52.4	61	-8.6

- **Cell 3 –Driving Lane**

The differences in friction number of smooth tires and ribbed tires are listed in Table 4.7. It can be seen that the FN of smooth tires and ribbed tires are much similar in the year of 2009. The FN for smooth tires increased tremendously from 38 to 52 in 11 months apart from November 2007 to October 2008. There has been no tenable explanation for this scenario.
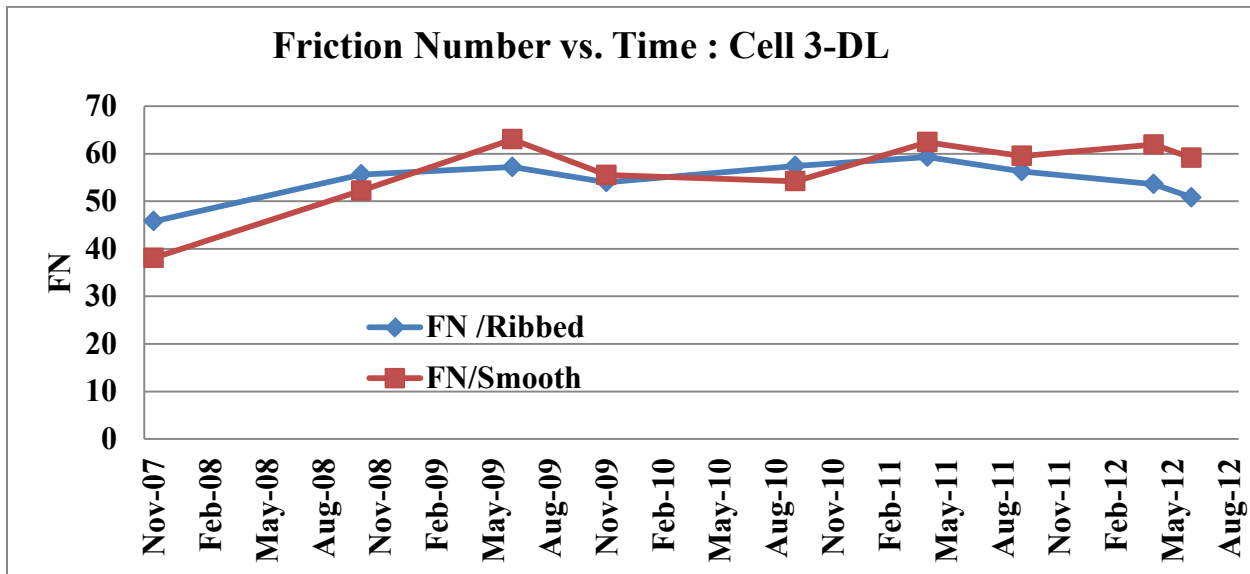
Figure 4.30 Friction Number vs. Time for Cell 3 Driving Lane

Table 4.7 Data Tabulation of FN Ribbed and Smooth for Cell 3 Driving Lane

Cell 3 DL	FN /Ribbed	FN/Smooth	FN difference
Nov-07	45.8	38.1	7.7
Oct-08	55.6	52.2	3.4
Jun-09	57.2	63.0	-5.8
Nov-09	54	55.5	-1.5
Sep-10	57.4	54.2	3.2
Apr-11	59.3	62.4	-3.1
Sep-11	56.3	59.5	-3.2
Apr-12	53.6	61.9	-8.3
Jun-12	50.8	59.1	-8.3

127

- **Cell 4 –Driving Lane**

The differences in friction number of smooth tires and ribbed tires are listed in Table 4.8. It can be seen that the FN of smooth tires and ribbed tires are much similar in the year of 2012.
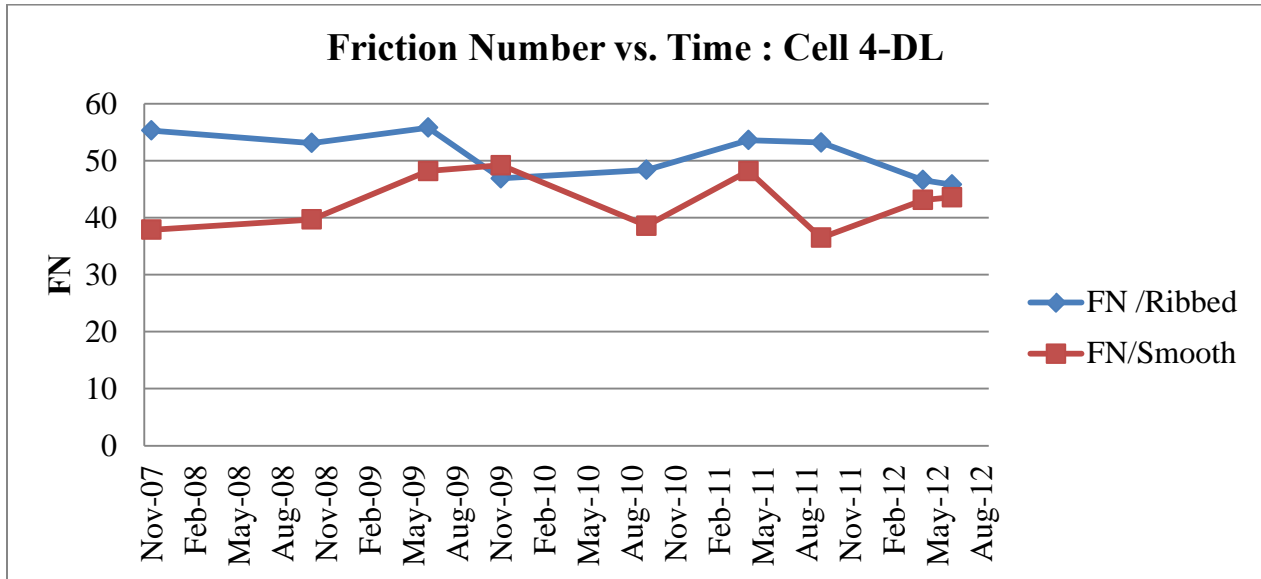
Figure 4.31 Friction Number vs. Time for Cell 4 Driving Lane

Table 4.8 Data Tabulation for FN Ribbed and Smooth for Cell 4 Driving Lane

Cell 4 DL	FN /Ribbed	FN/Smooth	FN difference
Nov-07	55.3	37.9	17.4
Oct-08	53.1	39.7	13.4
Jun-09	55.8	48.2	7.6
Nov-09	46.9	49.2	-2.3
Sep-10	48.4	38.6	9.8
Apr-11	53.6	48.2	5.4
Sep-11	53.2	36.5	16.7
Apr-12	46.6	43.1	3.5
Jun-12	45.8	43.6	2.2

Comparison of Coefficient of Friction at the Speed of 40km/hr.:

The comparison of coefficient of friction for cell 3, 4, 19 and 22 is plotted in Figure 4.32 to illustrate the frictional properties based on different type of asphalt pavements. Cell 3 and 4 has a stabilized full depth RAP; cell 19 has recycled unbound base, warm mix asphalt pavement, and cell 22 has low temperature cracking, fractionated RAP. The range of μ value for each cell is tabulated in Table 4.9.
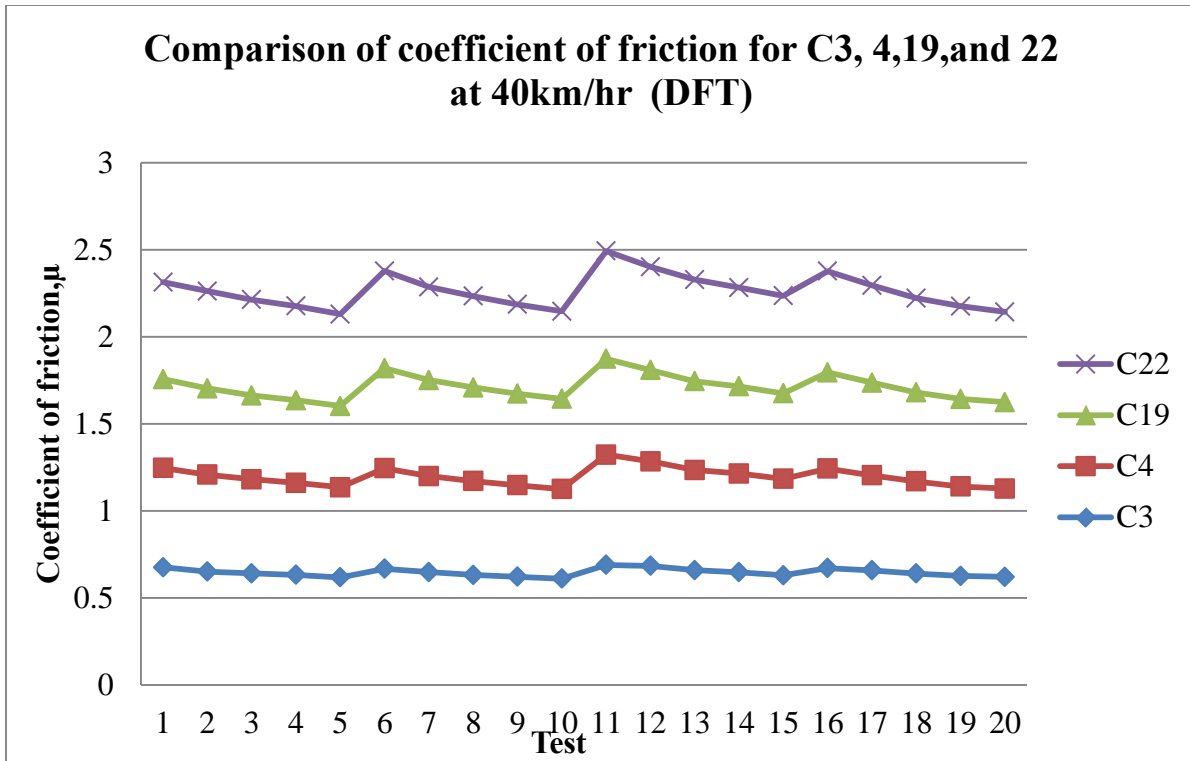
Figure 4.32 Comparison of Coefficient of Friction With DFT for C3, 4, 19, 22 at 40km/hr.

Table 4.9 Range of Coefficient of Friction for cell 3, 4, 19, 22

Cell	Range of μ value
3	0.61-0.69
4	0.50–0.63
19	0.47-0.57
22	0.50-0.62

Effect of Traffic on Friction Number:

The following table shows the T-test for both ribbed and smooth tire on both mainline and low volume road to determine the effect of traffic on friction number.

129

Table 4.10: P-values for Friction Number at 95% Confidence Level

Ho: There is no Effect of traffic on FN

	P-values			
	Ribbed		Smooth	
Mainline	0.05328	Reject	0.01205	Reject
LVR	0.034623	Reject	0.00598	Reject

Effect of Traffic on Skid Resistance:

A 2- Sample T-test was used to analyze the effect of traffic on OBSI. The P-values shown in Tables 4.10 indicates that both mainline and LVR accepted the null hypothesis for the test thus indicating that both driving and passing lane (or inside and outside lane for LVR) have significantly different frictional response. The traffic does not seem to affect the sound intensity between the interaction of tire and pavement within the age range and the material types at a 95% confidence level.

Table 4.11: Summary for Effect of Traffics on FN: (Statistical Hypothesis Tests)

		T-TEST	WILCOXON SIGNED RANK TEST		WILCOXON RANK SUM TEST	
			MAINLINE CELLS			
FN/RIBBED	Alpha	0.05	Normal Approximation	1.687	Normal Approximation	0.924
	Two-tailed P-value	0.05	Two-tailed P-value	0.092	Two-tailed P-value	0.356
FN/SMOOTH	Alpha	0.05	Normal Approximation	3.075	Normal Approximation	1.462
	Two-tailed P-value	0.01	Two-tailed P-value	0.002	Two-tailed P-value	0.144
			LVR CELLS			
FN/RIBBED	Alpha	0.05	Normal Approximation	2.178	Normal Approximation	1.051
	Two-tailed P-value	0.04	Two-tailed P-value	0.03	Two-tailed P-value	0.293
FN/SMOOTH	Alpha	0.05	Normal Approximation	2.65	Normal Approximation	1.084
	Two-tailed P-value	0.006	Two-tailed P-value	0.008	Two-tailed P-value	0.279

Table 4.12: Results for Effects of Traffic on Frictional Resistance

	T-TEST	WILCOXON SIGNED RANK TEST	WILCOXON RANK SUM TEST
		MAINLINE CELLS	
FN/RIBBED	DISSIMILAR	DISSIMILAR	DISSIMILAR
FN/SMOOTH	DISSIMILAR	DISSIMILAR	DISSIMILAR
		LVR CELLS	
FN/RIBBED	DISSIMILAR	DISSIMILAR	DISSIMILAR
FN/SMOOTH	DISSIMILAR	DISSIMILAR	DISSIMILAR

"Dissimilar" implies that driving and passing lanes have dissimilar frictional numbers to a 95% confidence level. Outside and inside

lanes have dissimilar frictional numbers to a 95% confidence level.

Friction Number vs. Time:

The difference of FN between both types of tires in cell 1 is significantly large. This indicates that from 2007 to 2012 hysteresis effect may be infinitesimal. In cell 2, a huge gap of FN between smooth and ribbed tires occurred only from November 2007 to September 2008. The main reason behind this occurrence is that cell was reconstructed on October 2008, therefore the differences of FN for both tires from October 2008 to September 2011 falls in the range of 0 to 1.5. Hysteresis as discussed earlier on the Chapter is a system where it depends on the past and current environment, so that is the reason why the difference of the newly reconstructed cell on October 2008 has a low difference in FN. The differences of FN between both tires increases after August 2011, indicates that hysteresis occurs.

Cell 3 shows a different pattern as compare to cell 2 even though cell 3 was reconstructed at the same time as cell 2 and has similar type of asphalt pavement. The differences of FN fluctuate throughout year 2007 to year 2012. The largest difference of FN occurs in year 2012, which has a difference of 8.3 between ribbed and smooth tire friction.

Cell 4 is observed to have a large difference in friction number from November 2007 to October 2009 and fluctuate into a smaller gap in difference at the end of year 2009. However, the differences in friction number increases from September 2010 to March 2012. The differences then decreases gradually from April 2012 to June 2012.

Comparison for Coefficient of Friction of Cells at 40km/hr:

The comparison of coefficient of friction for cell 3, 4, 19 and 22 can be found in Figure 4.32 in the results section. The trends in all four cells are similar to each other. However, it is obvious that the range of the μ value for cell three is much higher than the other cells. This is due to the type of asphalt pavements (Appendix 4.A, Figure 4.A.2). Even though cell 3 and 4 are stabilized full depth reclamation asphalt, cell 3 has an ultra-thin-bonded wearing course (UTWBC) on the top layer of the pavement. UTWBC is a material does not seem to experience aggregate rapid polishing or aggregate loss, therefore it provides excellent adhesion properties and friction on pavement. It can be proven with the differences in range of μ value between cell 3 and 4. Other than that, cell 3 has the higher range of coefficient of friction among the four cells, which is in the range of 0.61- 0.69. Cell 4 as mentioned above has a second highest friction value, which falls in the range of 0.50 – 0.63.

Cell 19 has recycled unbounded base and warm mix asphalt pavement has a μ range of 0.47 to 0.57. Cell 22 has a similar friction factor with cell 4. It may be due to the type of pavement surface of cell 22. Its range of μ value falls in between 0.50 to 0.62. Two-Sample T-test was used to analyze the effect of traffic on friction number. The P-values shown in Table 4.3.6 in the results section indicates that both mainline and LVR rejected the null hypothesis for both ribbed and smooth tires. This means that both driving and passing lane (or inside and outside lane for LVR) is significantly different. It can be deduced that the traffic does affect the friction number based on the preliminary study on effect of traffic on friction number. The heavy traffic on driving lane may cause an increment in deterioration of friction in comparison to passing lane.

Preliminary Half-life Friction Extrapolations:

This section depicts the relationship between the rate of friction degradation and friction number. It is hypothesized that the friction degradation will follow a pattern of decay, similarly to the half-life equation. A preliminary analysis was conducted on test cell 2, 3, 4 and 27. Test cell 2, 3 and 4 are stabilized full depth reclamation pavement first constructed on September 28, 1992. Both cell 2 and 3 were reconstructed with added ultra-thin bonded wearing course in October 2008. As for test cell 4, it was covered with dense graded SuperPave during the reconstruction in October 2008. Test cell 27 was built on August 15, 1992 and the double chip seal was added on August 15, 1999. The analysis was done based on the decay equation:

$$FN_t = FN_o e^{-\lambda t} \tag{19}$$

Where FN_t = friction number at year t

$\quad$ FN_o = friction number immediately after construction (at the zeroth year)

$\quad$ λ = decay constant

$\quad$ t = time (Yrs)

$$\ln\frac{FN_t}{FN_o} = -\lambda t \tag{20}$$

The slope of $\ln\frac{FN_t}{FN_o}$ versus time graph is the decay constant, λ-value based on equation 38. The λ-value is used to find the half-life for each cell using the following equation:

$$t_{1/2} = \frac{\ln 2}{\lambda} \tag{21}$$

The table below shows the results of half-life analysis for the test cells by the described method.

Table 4.13 Summary of half-life analysis for test cell 2, 3, 4 and 27

Cell	Pavement Type	Lane	Tire Type	Half Life (yrs)
2	Ultra-Thin Bonded Wearing Course	Driving	Smooth	52
			Ribbed	40
3	Ultra-Thin Bonded Wearing Course	Driving	Smooth	22
			Ribbed	72
4	12.5 mm Dense Graded Superpave	Driving	Smooth	18
			Ribbed	19
27	Double Chip Seal	Outside	Smooth	18
			Ribbed	32
		Inside	Smooth	31
			Ribbed	41

The half-life analysis is probabilistic and not deterministic but is indicative of the rate of friction survival. Table 4.13 shows significant disparity between ribbed and smooth tire FN half-lives in cell 3 which is the ultrathin bonded wearing course. This surface exhibits hysteretic friction with relatively high smooth tire friction and lower ribbed tire friction. The weakness of the half-life equation is portrayed when extrapolations are needed for hysteretic friction and adhesion friction. Since the bifurcation of friction is still a matter under investigation, the half-life predictions are at best based on friction numbers alone. The inherent errors are thus accentuated.

CHAPTER 5: CONCLUSION & RECOMMENDATIONS

CONCLUSION

This report presents results of the research that was conducted on various asphalt pavement surfaces in the MnROAD facility. Construction of Various Test Cells and initial monitoring provided useful results Seasonal Measurements of surface was conducted and annual reports were rendered as tasks of this project. However the 4th year performance and advanced data analysis and results in addition to the construction and initial monitoring are reported in this final report. It also discussed the fundamentals of surface profilometry, described the construction of the textures and performance trends of the various surface parameters. The variables examined include friction, measured with the lock wheel skid truck, smoothness, measured with the light weight profiler, mean profile depth measured by the circular track meter, sound absorption measured by the acoustic impedance tube and Tire-Pavement-Interaction-Noise measured by the on board sound intensity device. All surface textures examined were isotropic in the micro and macrotexture regimes although paving is in a given direction. This report performed advanced data analysis and accentuated intrinsic relationships between important variables.

Construction of the test cells and monitoring for 4 years prior to advanced analysis accentuated some notable trends. The research constructed different surface types with a wide range of mix designs and materials in close proximity to each other, to provide a valuable insight into the influence of mixture, environmental and traffic factors on various surface characteristics. The following are general inferences and comparisons that can be made about the influence of the mixture properties on the surface characteristics of the various mixture types at MnROAD.

- The porous asphalt mixtures (Cells 86 and 88) show a substantial amount of raveling, which is most likely due to a combination of construction defects, snowplow damage, and wear from heavy truck traffic.
- The largest rut depth on the Mainline is about ¼" while rut depths on the Low Volume Road are approaching ½" on some cells.
- The 4.75 mm taconite mixture (Cell 106) showed the lowest rut depths, closely followed by some of the dense graded mixtures (Cells 22, 24, and 87).
- The porous asphalt surfaces show the greatest rut depths.

- The UTBWC surfaces (Cells 2 and 3) are the smoothest over time. The porous asphalt surfaces (Cells 86 and 88) are the roughest over time. Ride quality tends to be worst in the spring with frozen or thawing conditions and better in the summer and fall when the subgrade materials dry out.

- Aggressive, open graded surfaces (porous asphalt, chip seal, UTBWC) have the highest mean profile depth, while the 4.75 mm taconite mixture has the lowest profile depth.

- Texture values can be variable when measured at different stations and offsets within a cell.

- Friction numbers measured by the skid trailer were generally very good with the exception of Cell 24, which has received a fog seal treatment just before friction measurements the last three years. For the dense graded asphalt surfaces (Cells 4, 106, 19, 22, 24, and 87) the ribbed tire has significantly higher friction numbers than the smooth tire. For the more open, aggressive asphalt surfaces (Cells 2, 3, 27, 86, and 88) the ribbed and smooth tires give more similar values, with the smooth tire often exhibiting a higher friction number. In general the passing/outside lane has a higher friction number than the driving/inside lane, showing the effect of traffic on friction. The UTBWC (Cell 3) and 4.75 mm taconite (Cell 106) surfaces had the highest coefficient of friction values measured with the dynamic friction tester. The dense graded Superpave surfaces (Cells 4, 19, and 22) had approximately equal coefficients. On Cell 24 the coefficient of friction decreased with each successive application of fog seal, indicating that a light sanding or chip seal may be considered to maintain a safe driving surface.

- The porous asphalt surfaces (Cells 86 and 88) are the quietest, while the chip seal (Cell 27) and some of the dense graded asphalt mixtures (Cells 4 and 24) are the loudest. OBSI levels are lowest in the summer when the pavement surface is warm; they are highest in cold weather. There is a general upward trend of noise levels over time with the porous asphalt showing a more gradual trend and dense graded surfaces showing a sharper increase. In some cases (e.g., NovaChip) the difference between cool and warm weather results is remarkable, while in other cases (e.g. porous asphalt) the differences in OBSI levels between seasons are much less.

- Porous asphalt surfaces (Cells 86 and 88) exhibited the highest sound absorption coefficients; UTBWC surfaces (Cells 2 and 3) are a distant second. Dense graded asphalt mixtures have extremely low sound absorption coefficients, with the 4.75 mm taconite mixture (Cell 106) having the lowest. The sound absorption coefficients of the open graded surface textures (porous and UTBWC) decrease significantly over time, while this is not the case for the dense graded mixtures.

Advanced analysis accentuated some important findings.

OBSI- temperature correlation was found to be a negative polynomial relationship indicating high importance of temperature to OBSI relationship in asphalt. It was ascertained that texture mean profile depth was not as significant as texture skewness in predicting surface properties. Additionally, the frictional time series appears to follow the first order differential equation similar to half-life equation. Based on results obtained from annual monitoring the asphalt surfaces were not associated with laser-induced anomalous IRI reading errors.

Prior to this study, minimal reference to the skewness of asphalt surfaces was available. This study examined the importance of skewness from the traffic data in relation to friction and OBSI. This research showed that skewness or texture orientation is an important variable in the prediction of asphalt surfaces. It shows that skewness when compared to mean profile depth was a far better predictor of OBSI and friction than mean profile depth.

Traffic difference was found to be a significant variable in the friction trend of the asphalt surfaces when the low volume roads inside lane of the cells were compared to the corresponding outside lane and the mainline driving and passing lanes of the cells examined were compared in using the Wilcoxon Rank sum, Wilcoxon Sign Rank and the T-test. A similar test on (OBSI -100dBA) found traffic to be insignificant within the 5 years of monitored performance of the same test tracks.

Prior to this study, minimal reference describing the rate of degradation of friction or skid resistance of asphalt surfaces in relation to the skid resistance at the time of measurement was available. This study finds the relationship to be similar to the half-life probabilistic function. The half-life of the various texture types was therefore computed. This describes the practical high rate of polishing or skid resistance reduction when the value of skid is high. In pervious asphalt, degradation of the surface does not reduce frictional resistance because raveling

RECOMMENDATIONS

In the evaluation of asphalt surfaces, consideration should be given to texture orientation.

There is an effect of temperature on Tire-Pavement-Interaction-Noise of asphalt pavements. A correction algorithm based on the temperature correlation obtained in this research is recommended. In our current specification, as traffic levels increase, a more angular and durable aggregate is required. We vary PG grades by traffic conditions but it relates to rutting and cracking characteristics. Current specification may include a simple check for texture orientation to facilitate corrective action towards friction and noise without compromising other required characteristics.

Pervious asphalt shows good acoustic properties. Research should investigate a durability enhancement of porous asphalt for use as acoustic. In our current specification as traffic levels increase a more angular and durable aggregate is required. We vary PG grades by traffic conditions but it relates to rutting and cracking characteristics. Does this research provide any recommendations on how we should specify our materials based on skid resistance and noise. Since most of the observed delamination is associated with down drain, more viscous binders are recommended to minimize this phenomenon in pervious mixes.

Subsequent work on long-term performance should examine time series analysis so that the performance and seasonal trends will be built into the prediction / forecasting algorithm for OBSI, and ride quality.

REFERENCES

1. South African National Roads Agency. Pavement Management Site, accessed August 7, 2008. http://www.nra.co.za/live/content.php?Item_ID=185

2. Sandberg, U., Ejsmont, J. Tire Road Noise Reference Manual Informex. Handelsbolag Harg SE 59040 Kisa, Sweden 2002.

3. Henry, J. Evaluation of Pavement Friction Characteristics. National Cooperative Highway Research Program (NCHRP) Synthesis No. 291. Transportation Research Board, 2000, Washington D.C.

4. Summer, C.J. The Idiot's Guide to Highway Maintenance, accessed August 22, 2008. <http://www.highwaysmaintenance.com/skidtext.htm>

5. Flintsch, G., Al-Qadi, A., McGhee, K., Davis, R. Effects of HMA Design Properties on Pavement Surface Friction. Maintenance and Rehabilitation of Pavements and Technological Control: Proceedings of the 3rd International Symposium. University of Minho, Guimarães, Portugal, July 2003.

6. Cerezo, V., Gothie, M. Megatexture Measurement with a Non-Contact Profilometer: Accuracy of the Method and Factors of Influence. Transportation Research Board Annual Meeting, Washington, D.C., 2008.

7. "Calculating Pavement Macrotexture Profile Depth," ASTM Standard Practice E-1845, IHS online ASTM Standards, American Society for Testing and Materials, West Conshohocken, PA, 2005.

8. The Study of Maintenance Repairs: The Effect of Maintenance on IRI Values. Unpublished MnDOT Report, 1998.

9. International PIARC Experiment to Compare and Harmonize Texture and Skid Resistance Measurements, PIARC Report 01.04.T, The World Road Association, Paris, 1995.

10. "Calculating the Friction Index of a Pavement Surface," ASTM Standard Practice E-1960, IHS online ASTM Standards, American Society for Testing and Materials, West Conshohocken, PA, 2007.

11. "Skid Resistance of Paved Surfaces Using a Full Scale Tire," ASTM Standard Practice E-274, IHS online ASTM Standards, American Society for Testing and Materials, West Conshohocken, PA, 2006.

12. "Measuring Pavement Macrotexture Depth Using a Volumetric Technique," ASTM Standard Practice E-965, IHS online ASTM Standards, American Society for Testing and Materials, West Conshohocken, PA, 2006.

13. "Measuring Pavement Macrotexture Properties Using the Circular Track Meter," ASTM Standard Practice E-2157, IHS online ASTM Standards, American Society for Testing and Materials, West Conshohocken, PA, 2006.

14. Smit, A., Waller, B. Evaluation of the Ultra-Light Inertial Profiler (ULIP) For Measuring Surface Texture on Pavements. Federal Highway Administration. National Center for Asphalt Technology, NCAT Report No. 07-01, June 2007, Auburn, Alabama.

15. Perera, R., Kohn, S., Soils and Materials Engineers, inc., Plymouth, MI. Issues in Pavement Smoothness: A Summary Report. National Cooperative Highway Research Program, Transportation Research Board, National Academies, Web Document No. 42 (20-51[1]) Contractor's Final Report, March 2002.

16. Berengier, M., Anfosso-Ledee, F. State of the Art Prediction and Control of Road Traffic Noise in France. Transportation Research Board of the National Academies, Transportation Research Record 1629, pp. 71-77.

17. Descornet, G., Goubert, L. Noise Classification of Road Pavements. European Commission Directorate General Environment, Task 1: Technical Background Information Draft Report, June 2006.

18. Boscaino, G., Pratico, F.G., Vaiana, R. Texture Indicators and Surface Performance in Flexible Pavements. Surf 2004, Fifth Symposium on Pavement Surface Characteristics, June 6-10, 2004, Toronto, Ontario, Canada.

19. Nagelhout, M., Wennink, P.M., Gerristen, W. Detection of Raveling. Surf 2004, Fifth Symposium on Pavement Surface Characteristics, June 6-10, 2004, Toronto, Ontario, Canada.

20. Izevbekhai, B. Report on Pavement Surface Characteristics Mini-Rodeo (MnDOT Test Data and Data Comparison). Minnesota Department of Transportation, Unpublished Report, 2008.

21. Jackson, M. Measuring Pavement Friction Characteristics at Variable Speeds for Added Safety. University of North Florida, Division of Engineering. Florida Department of Transportation, FDOT Order # DO-51684, Final Report, July 2005.

22. Maurer, P. The Influence of Different Measuring Tires, Measuring Speed and Macrotexture on Skid Resistance Measurements. Surf 2004, Fifth Symposium on Pavement Surface Characteristics, June 6-10, 2004, Toronto, Ontario, Canada.

23. Khasawneh, M., Liang, R. Correlation Study Between Locked Wheel Skid Trailer and Dynamic Friction Tester. Transportation Research Board Annual Meeting, Washington, D.C., 2008.

24. De Roo, F., Gerretsen, E. Modelling of Acoustical Road Surface Characteristics with RODAS (Road Design Acoustic Simulation). AIPCR/PIARC, 2000.

25. Lee, Y., Yurong, L., Ying, L., Fwa, T, Choo, Y. Skid Resistance Prediction by Computer Simulation. Association of Asphalt Paving Technologists (AAPT), 2004.

26. Trifiro, F., Flintsch, G., Giovanni, G., de Leon, E., McGhee, K. Comparison of Friction Measuring Devices and Preliminary Evaluation of the International Friction Index. Transportation Research Board Annual Meeting, Washington, D.C., 2008.

27. McGhee, K., Flintsch, G., de Leon Izeppi, E. Using High Speed Texture Measurements to improve the Uniformity of Hot-Mix Asphalt Pavements. Virginia Transportation Research Council in cooperation with: U.S. Department of Transportation, FHWA, Final Report No. VTRC 03-R12, May 2003.

28. Ongel, A., Kohler, E., Lu, Q., Harvey, J. Comparison of Surface Characteristics and Pavement/Tire Noise of Various Thin Asphalt Overlays. Transportation Research Board 86th Annual Meeting, Washington, D.C., 2007.

29. A. Johnson, Clyne, T. R., Worel, B. J. "2008 MnROAD Phase II Construction Report". Minnesota Department of Transportation, June 2009.

30. "Measuring Pavement Macro texture Depth Using a Volumetric Technique," ASTM Standard Practice E-965, IHS online ASTM Standards, American Society for Testing and Materials, West Conshohocken, PA, 2006.

31. "Measuring Pavement Macro texture Depth Using a Volumetric Technique," ASTM Standard Practice E-965, IHS online ASTM Standards, American Society for Testing and Materials, West Conshohocken, PA, 2006.

32. "Measuring Pavement Macro texture Properties Using the Circular Track Meter," ASTM Standard Practice E-2157, IHS online ASTM Standards, American Society for Testing and Materials, West Conshohocken, PA, 2006.

33. Abe, H., Henry, J.J., Tamari, A., Wambold, J. C., "Measurement of Pavement Macro texture using Circular Texture Meter (CTMeter)," Transportation Research Board Annual Meeting, Washington D.C., 2001.

34. Descornet, G., Goubert, L. Noise Classification of Road Pavements. European Commission Directorate General Environment, Task 1: Technical Background Information Draft Report, June 2006.

35. Henry, J. Evaluation of Pavement Friction Characteristics. National Cooperative Highway Research Program (NCHRP) Synthesis No. 291. Transportation Research Board, 2000, Washington D.C.

36. Izevbekhai, B. Report on Pavement Surface Characteristics Mini-Rodeo (MnDOT Test Data and Data Comparison). Minnesota Department of Transportation, Unpublished Report, 2008.

37. Izevbekhai, B. "Report of Pavement Surface Characteristics Mini Rodeo (MnDOT Test Data and Data Comparison)". Minnesota Department of Transportation, Project MPR 6-(012) and TPF 5-(134), July 2008.

38. "Skid Resistance of Paved Surfaces Using a Full Scale Tire," ASTM Standard Practice E-274, IHS online ASTM Standards, American Society for Testing and Materials, West Conshohocken, PA, 2006.

39. Hanson, D, James, R., NeSmith, C. Tire/Pavement Noise Study. Sponsored by Federal Highway Administration, National Center for Asphalt Technology, NCAT Report No. 04-02, August 2004.

40. Johnson, A., Clyne, T. R., and B. J. Worel, *2008 MnROAD Phase II Construction Report*, Minnesota Department of Transportation, Final Report MN/RC 2009-22, 2009.

41. Watson, M., Clyne, T. R., Izevbekhai, B., and B. J. Worel, *HMA Surface Characteristics Related to Ride, Texture, Friction, Noise and Durability*, Task 2 Report: Construction and Initial Monitoring, Unpublished Report, Minnesota Department of Transportation, September 2009.

42. Watson, M., Clyne, T. R., Izevbekhai, B., and B. J. Worel, *HMA Surface Characteristics Related to Ride, Texture, Friction, Noise and Durability*, Task 4 Report: First Year

Monitoring and Performance Report, Unpublished Report, Minnesota Department of Transportation, June 2010.

43. Watson, M., Clyne, T., and B. Izevbekhai, *HMA Surface Characteristics Related to Ride, Texture, Friction, Noise, and Durability*, Task 5 Report: Second Year Monitoring and Performance Report, Unpublished Report, Minnesota Department of Transportation, February 2011.

44. "Measuring Pavement Macro texture Properties Using the Circular Track Meter," ASTM Standard Practice E-2157, IHS online ASTM Standards, American Society for Testing and Materials, West Conshohocken, PA, 2006.

45. Abe, H., Henry, J.J., Tamari, A., and J. C. Wambold, "Measurement of Pavement Macro Texture using Circular Texture Meter (CTMeter)," Transportation Research Board Annual Meeting, Washington D.C., 2001.

46. Surface Texture for Asphalt and Concrete Pavements, June 17, 2005. Federal Highway Administration, http://www.fhwa.dot.gov/pavement/t504036.cfm, Accessed 2/29/2012.

47. "Concrete Texture Specifications" Minnesota Department of Transportation, http://www.dot.state.mn.us/materials/concretedocs/texturespec.pdf, Accessed 2/29/2012.

48. "Standard Test Method for Measuring Skid Resistance of Paved Surfaces Using a Full-Scale Tire," ASTM Standard Practice E-274-06, IHS online ASTM Standards, American Society for Testing and Materials, West Conshohocken, PA, 2006.

49. Technical Advisory: Pavement Friction Management, June 17, 2010. Federal Highway Administration, http://www.fhwa.dot.gov/pavement/t504038.cfm, Accessed 2/29/2012.

50. D. Janisch, An Overview of MnDOT's Pavement Condition Rating Procedures and Indices. Minnesota Department of Transportation, Saint Paul, MN, May 2006.

51. B. I. Izevbekhai, Report of Pavement Surface Characteristics Mini Rodeo (MnDOT Test Data and Data Comparison), Minnesota Department of Transportation, Project MPR 6-(012) and TPF 5-(134), July 2008.

52. Descornet, G. and L. Goubert, *Noise Classification of Road Pavements*, European Commission Directorate General Environment, Task 1: Technical Background Information Draft Report, June 2006.

53. Miller, J. and W. Bellinger, *Distress Identification Manual for the Long-Term Pavement Performance Program (Fourth Revised Edition)*, Federal Highway Administration, FHWA-RD-03-031, June 2003.

54. http://www.dot.state.mn.us/materials/pvmtmgmtdocs/Rating_Overview_State.pdf, Accessed February 28, 2012.

55. http://www.dot.state.mn.us/materials/manuals/pvmtmgmt/distressmanual.pdf, Accessed February 28, 2012.

56. Rutting, http://pavementinteractive.org/index.php?title=Rutting, Accessed February 28, 2012

57. Abe, H., Henry, J.J., Tamai, A., and Wambold, J.C., "Measurement of Pavement Macrotexture Using the Circular Texture Meter (CTMeter)," *Transportation Research Board Annual Meeting*, Washington DC, 2001.

58. Izevbekhai B.I. & Voller V.R. (2013): Development and validation of a tenable process for quantifying texture spikiness for pavement noise prediction, International Journal of Pavement Engineering, 14:2, 190-205

59. Bazlamit, Subhi M., and Reza, Farhad. "Changes in Asphalt Pavement Friction Components and Adjustment of Skid Number for Temperature." Journal of Transportation Engineering 131 (2005): 470-476

APPENDIX

APPENDIX A

Mix Design Worksheets

ULTRATHIN BONDED WEARING COURSE

NOVACHIP JOB MIX FORMULA

SemMaterials Laboratory   6502 South Yale Avenue   Tulsa, Oklahoma 74136

AGENCY - MnDOT	WORK ORDER - US.MN.NC.2008.0221
AGENCY PROJECT - N/A	ACCOUNT MANAGER - Kevin Kosobud
PROJECT LOCATION - Wright County, MN	DESIGN ENGINEER - Adam Meeks, E.I.
CONTRACTOR - Hardrives	FIELD ENGINEER - Tom Wood
DATE COMPLETED - 7/26/2008	PHONE - 952.905.9914

BINDER INFORMATION -

SUPPLIER - Flint Hills Resources
SUPPLIER FACILITY - Savage, MN
PG GRADE - PG64-34
MIXING TEMP - 286 - 278 °F
COMPACTING TEMP - 264 - 256 °F
SPECIFIC GRAVITY (Gb) - 1.030

ANTI-STRIP INFORMATION -

SUPPLIER - N/A
PRODUCT - N/A
RATE (%) - 0

AGGREGATE GRADATIONS & TESTING -

	AGGREGATE GRADATIONS - INDIVIDUAL & BLEND								
TYPE	3/8" Chip	MfgS	#8 Mesh						
SOURCE	NUQQ@N, MN	HDBP@S, MN	NUQQ@N, MN						
ORIGIN	Quartzite	Granite	Quartzite						
STOCKPILE #	S2008.0458	S2008.0523	S2008.0631						
% IN BLEND	69.0	17.0	14.0					0	Type B
SIEVE SIZES								BLEND	SPECS
3/4" 19.0 mm	100.0	100.0	100.0					100.0	100 - 100
1/2" 12.5 mm	100.0	100.0	100.0					100.0	100 - 100
3/8" 9.5 mm	100.0	100.0	100.0					100.0	85 - 100
#4 4.75 mm	16.0	85.0	100.0					39.5	28 - 42
#8 2.36 mm	2.0	57.0	100.0					25.1	22 - 32
#16 1.18 mm	1.0	42.0	80.0					19.0	15 - 23
#30 0.600 mm	1.0	32.0	57.0					14.1	10 - 18
#50 0.300 mm	1.0	23.0	38.0					9.9	8 - 13
#100 0.150 mm	1.0	16.0	21.0					6.4	6.0 - 10.0
#200 0.075 mm	0.8	11.1	10.9					4.0	4.0 - 5.5

Gab (T85 & T84)	2.627	2.688	2.603		2.634	Specification
FAA (T304)*		49.1	48.5		47.7	40 min (b)
Sand Equivalency (T176)		72	65		56	45 min (b)
Meth Blue (T330)*		10	2		7	10 max (b)
F & E (D4791)	11.3					25 max (b)
Micro-Deval (TP58)*	10.1					18 max (i)
LA Abrasion (T96)	15					35 max (i)
Crushed Faces (D5821)*						
Single Face (%)	100					85 min (b)
Two Faces (%)	100					85 min (b)

MIXTURE PROPERTIES -

Pb	Gmb	Gmm	% Air Voids	Gse	VMA	VFA	Surface Area	D/A	Pba
5.1	2.178	2.467	11.7	2.667	21.5	45.5	4.18 20.9	0.9	0.5

TSR (%) -	88.7	80 % min	Film Thickness -	11.3 microns 11.1 Adj.APT
Draindown (%) -	0.03	0.1 % max	Max Emulsion Shot Rate -	0.19 gal/yd²
Ignition Oven Calibration -	N/A		Min Emulsion Shot Rate -	0.14 gal/yd²

*This test is not covered by current AAP accreditation.

Test data herein has been secured by reliable testing procedures. As we have no knowledge of, or control over, the conditions that may affect the use of materials from which the samples were taken, we assume no responsibility in furnishing this data other than to warrant that they represent reliable measurements of the properties of the sample recieved and tested.

Figure A.1: Ultrathin Bonded Wearing Course (UTBWC) Cells 2 & 3

BITUMINOUS PLANT MIX DESIGN REPORT
Minnesota Department of Transportation
Office of Materials
1400 Gervais Avenue
Maplewood, MN 55109
Phone (651) 366-5459
FAX: (651) 366-5580

 # 0-2008-183

Date: 7/28/2008

THIS MIX DESIGN REPORT IS NOT VALID UNTIL PLANT NO. INDICATED BELOW IS CERTIFIED.

SPEC	2360
SPEC YEAR	2008
MIX TYPE	SPWEB440
AC GRADE	PG 64-34

TO BE FILLED IN BY CONTRACTOR	
ENGINEER	FOR
PROJECT NUMBER 8680-157 (Mn/RD)	

THIS MIXTURE HAS BEEN REVIEWED FOR VOLUMETRIC PROPERTIES ONLY, IT DOES NOT ASSURE THAT FIELD PLACEMENT AND COMPACTION REQUIREMENTS HAVE BEEN MET.

PLANT NO. 932051 -

JOB MIX FORMULA

Begin With Test Number

SP	WE	401
- -	- -	- - -

Sieve Size (mm) (in.)	Composite Formula	JMF LIMITS			For Information Only Virgin Formula
37.5 (1 1/2)			-		
25.0 (1)			-		P E R C E N T
19.0 (3/4)	100	100	-	100	P A S S I N G
12.5 (1/2)	93	86	-	100	
9.5 (3/8)	81	74	-	88	
4.75 (#4)	62	55	-	69	
2.36 (#8)	51	45	-	57	
0.075 (#200)	3.8	2.0	-	5.8	
Spec. Voids	4.0	3.0	-	5.0	%AC (NEW)
Spec. VMA	14.0	13.7			
% AC	5.4	5.0			
(TOTAL)					

TM # 3A-TM06-0025 Indicates a Gyratory Density of 148.5 (lbs/ft3) at 90 Design Gyrations
Use of anti-strip agent required:

Proportions		Pit	Source of Material	Sp.G
30	%	71063	VONCO II BA SAND	2.626
10	%	73006	MARTIN MARIETTA ST CLOUD WASHED SAND (GRANITE)	2.676
20	%	73006	MARTIN MARIETTA ST. CLOUD CA-50 (GRANITE)	2.748
40	%	73006	MARTIN MARIETTA ST CLOUD 3/4" UNWASHED (GRANITE)	2.702
	%			
	%			
	%			
	%			

Mix Aggregate Specific Gravity at the Listed Percentages = 2.685

Remarks   MINUS #4 AGGREGATE SPG AT THE LISTED PERCENTAGES = 2.664

Mix Design Reviewed by:

Mix Design Specialist

cc:
Contractor - HARDRIVES, INC
METRO INSPECTION

Cells 2-4

Figure A.2 12.5mm Dense Graded Superpave Cell 4

BITUMINOUS PLANT MIX DESIGN REPORT
Mn/DOT - Office Of Materials and Road Research
1400 Gervais Avenue Maplewood, MN 55109
Phone: (651) 366-5459 FAX: (651) 366-5580

THIS MIX DESIGN REPORT IS NOT VALID UNTIL PLANT NO.
INDICATED BELOW IS CERTIFIED.

#0- 2008-196

Date:	7/29/08
SPEC	**2360**
SPEC YEAR	**2008**
MIX TYPE	4.75mm
AC GRADE	PG 64-34

TO BE FILLED IN BY CONTRACTOR

ENGINEER		FOR
PROJECT NUMBER 8680-157 (Mn/RD)		
CONTRACTOR SIGN.		

THIS MIXTURE HAS BEEN REVIEWED FOR VOLUMETRIC PROPERTIES ONLY, IT DOES NOT ASSURE THAT FIELD PLACEMENT AND COMPACTION REQUIREMENTS WILL BE MET.

PLANT NO. **9 3 2 0 5 1** -   JOB MIX FORMULA

Begin With Test Number   **- 0 0 1**

Sieve Size (mm) (in.)	Composite Formula	JMF LIMITS		For Information Only Virgin Formula
9.5 (3/8)	100	95 - 100		P P
4.75 (#4)	92	90 - 100		E A
2.36 (#8)	72	-		R S
1.18 (#16)	51	30 - 60		C S
0.60 (#30)	34	-		E I
0.30 (#50)	21	-		N N
0.15 (#100)	12	-		T G
0.075(#200)	7.7	6 - 12		
Spec. Voids	4.0	3.0 - 5.0		%AC (NEW)
VMA	20.3	16.0		

%AC **7.4** (TOTAL)   7.0 -

TM# 0- 2008-110 Indicates a Gyratory density of 152.9 lbs/ft³ at 75 Design Gyrations.

Use of anti-strip agent required NO

Proportions		Source of Material	Sp.G
55	%	MIN TAC TAILINGS	2.948
10	%	ISPAT TAILINGS	2.908
35	%	LOKEN MAN SAND PIT # 05056	2.687
	%		
	%		
	%		
	%		

Mix Aggregate Specific Gravity at the Listed Percentages = 2.847
Minus #4 Aggregate Specific Gravity at the Listed Percentages = 2.856.

Remarks:

Mix Design Reviewed by:

cc:
METRO INSPECTION
Contractor – HARDRIVES

Cell 6

Figure A.3 4.75mm Taconite Cell 6

A3

BITUMINOUS PLANT MIX DESIGN REPORT
Minnesota Department of Transportation
Maplewood Materials Lab
1400 Gervais Avenue
Maplewood, MN 55109
Phone (651) 366-5459
FAX: (651) 366-5580

 # 0-2008-210

Date: 8/13/2008

THIS MIX DESIGN REPORT IS NOT VALID UNTIL PLANT NO. INDICATED BELOW IS CERTIFIED.

			SPEC	2360
TO BE FILLED IN BY CONTRACTOR			SPEC YEAR	2008
ENGINEER	FOR		MIX TYPE	SPWEB440(R)
PROJECT NUMBER	8680-157 (Mn/RD)			WARM MIX
			AC GRADE	PG 58-34

THIS MIXTURE HAS BEEN REVIEWED FOR VOLUMETRIC PROPERTIES ONLY, IT DOES NOT ASSURE THAT FIELD PLACEMENT AND COMPACTION REQUIREMENTS HAVE BEEN MET.

PLANT NO. 932051 - [ ]   JOB MIX FORMULA

Begin With Test Number

| SP | WE | 401 |
| SP | RM | - - - |

Sieve Size (mm) (in.)	Composite Formula	JMF LIMITS		For Information Only Virgin Formula
37.5 (1 1/2)		–		P E R C E N T (PERCENT)
25.0 (1)		–		P A S S I N G (PASSING)
19.0 (3/4)	100	100 – 100		100
12.5 (1/2)	92	85 – 99		90
9.5 (3/8)	85	78 – 90		82
4.75 (#4)	63	56 – 70		60
2.36 (#8)	46	40 – 52		42
0.075 (#200)	2.8	2.0 – 4.8		1.5
Spec. Voids	4.0	3.0 – 5.0		%AC (NEW) 4.2
Spec. VMA	14.0	13.7		
% AC	5.2	4.8		
(TOTAL)				

TM # 2008-138   Indicates a Gyratory Density of 147.8 (lbs/ft3) at 90 Design Gyrations
Use of anti-strip agent required: N

Proportions	Pit	Source of Material	Sp.G
40 %	73006	MARTIN MARIETTA ST CLOUD WASHED SAND (GRANITE)	2.682
25 %	73006	MARTIN MARIETTA ST. CLOUD 1/2" WASHED CHIPS (GRANITE)	2.731
15 %	05056	LOKEN 3/4 ROCK	2.742
20 %		Mn/RD CRUSHED MILLINGS	2.630
%			
%			
%			
%			

Mix Aggregate Specific Gravity at the Listed Percentages = 2.692

FOR LAB INFORMATION ONLY: LAB MIXING TEMP. RANGE = 235-245 °F   LAB COMPACTION TEMP. RANGE = 235-240 °F
Remarks   MINUS #4 AGGREGATE SPG AT THE LISTED PERCENTAGES = 2.676
WARM MIX DESIGN

Mix Design Reviewed by:

Mix Design Specialist

cc:
Contractor - HARDRIVES, INC
METRO INSPECTION

Figure A.4 Warm Mix (WMA) Cell 19 and WMA Control Cell 24

BITUMINOUS PLANT MIX DESIGN REPORT
Minnesota Department of Transportation
Office of Materials
1400 Gervais Avenue
Maplewood, MN 55109
Phone (651) 366-5459
FAX: (651) 366-5580

 # 0-2008-198

Date: 8/1/2008

THIS MIX DESIGN REPORT IS NOT VALID UNTIL PLANT NO. INDICATED BELOW IS CERTIFIED.

SPEC	2360
SPEC YEAR	2008
MIX TYPE	SPWEB440(R)
AC GRADE	PG 58-34

TO BE FILLED IN BY CONTRACTOR

ENGINEER		FOR
PROJECT NUMBER	8680-157 (Mn/RD)	

THIS MIXTURE HAS BEEN REVIEWED FOR VOLUMETRIC PROPERTIES ONLY, IT DOES NOT ASSURE THAT FIELD PLACEMENT AND COMPACTION REQUIREMENTS HAVE BEEN MET.

PLANT NO. 932051 -   JOB MIX FORMULA

Begin With Test Number

SP	WE	401
--	--	---

Sieve Size (mm) (in.)	Composite Formula	JMF LIMITS		For Information Only Virgin Formula
37.5 (1 1/2)		-		P E R C E N T
25.0 (1)		-		
19.0 (3/4)	100	100 - 100		P A S S I N G 100
12.5 (1/2)	91	85 - 98		88
9.5 (3/8)	85	78 - 90		81
4.75 (#4)	65	58 - 72		59
2.36 (#8)	49	43 - 55		42
0.075 (#200)	3.5	2.0 - 5.5		1.5
Spec. Voids	4.0	3.0 - 5.0		%AC (NEW) 3.7
Spec. VMA	14.0	13.7		
% AC	5.2	4.8		
	(TOTAL)			

TM # 2008-121 Indicates a Gyratory Density of 149.7 (lbs/ft3) at 90 Design Gyrations
Use of anti-strip agent required: N

Proportions		Pit	Source of Material	Sp.G
35	%	73006	MARTIN MARIETTA ST CLOUD WASHED SAND (GRANITE)	2.682
20	%	73006	MARTIN MARIETTA ST. CLOUD 1/2" WASHED CHIPS (GRANITE)	2.731
15	%	05056	LOKEN 3/4 ROCK	2.742
20	%		Mn/RD FRAP FINES	2.595
10	%		Mn/RD FRAP COARSE	2.632
	%			
	%			
	%			

Mix Aggregate Specific Gravity at the Listed Percentages = 2.677

Remarks MINUS #4 AGGREGATE SPG AT THE LISTED PERCENTAGES = 2.658
FRACTIONATED RAP DESIGN

Mix Design Reviewed by:

Mix Design Specialist

cc:
Contractor - HARDRIVES, INC
METRO INSPECTION

wear
Cell 22

Figure A.5: Fractionated RAP Cell 22

BITUMINOUS PLANT MIX DESIGN REPORT
Mn/DOT - Office Of Materials and Road Research
1400 Gervais Avenue Maplewood, MN 55109
Phone: (651) 366-5459   FAX: (651) 366-5580

THIS MIX DESIGN REPORT IS NOT VALID UNTIL PLANT NO.
INDICATED BELOW IS CERTIFIED.

#0- 2008-195

Date:	8/5/08
SPEC	2360
SPEC YEAR	2005
MIX TYPE	POROUS
AC GRADE	70-28

TO BE FILLED IN BY CONTRACTOR

ENGINEER   FOR

PROJECT NUMBER   8680-157 (Mn/RD)

CONTRACTOR SIGN.

THIS MIXTURE HAS BEEN REVIEWED FOR VOLUMETRIC PROPERTIES ONLY, IT DOES NOT ASSURE
THAT FIELD PLACEMENT AND COMPACTION REQUIREMENTS WILL BE MET.

PLANT NO. **9 3 2 0 5 1** -   JOB MIX FORMULA

Begin With Test Number

P O R - 0 0 1

Sieve Size (mm) (in.)	Composite Formula	JMF LIMITS			For Information Only Virgin Formula
37.5 (1 ½)			-		P P E A R S C S E I N N T G
25.0 (1)			-		
19.0 (3/4)	100	100	-	100	
12.5 (1/2)	87	85	-	91	
9.5 (3/8)	62	58	-	66	
4.75 (#4)	15	12	-	18	
2.36 (#8)	6	5	-	9	
0.075 (#200)	2	2	-	4	
Spec. Voids	18.0	17.0	-	19.0	%AC (NEW)

%AC **5.5** (TOTAL)   5.5 - 5.9

TM# 0- 2008-077 Indicates a Gyratory density of 127.7 lbs/ft³ at 50 Design Gyrations.
Use of anti-strip agent required NO

Proportions		Source of Material		Sp.G
45	%	MARTIN MARIETTA ST. CLOUD CA-50	PIT # 73006	2.736
45	%	MARTIN MARIETTA ST CLOUD CA-70	PIT # 73006	2.715
10	%	MARTIN MARIETTA ST CLOUD ¾" UNWASHED	PIT # 73006	2.702
0.3	%	FIBER STABILIZER		
	%			
	%			
	%			

Mix Aggregate Specific Gravity at the Listed Percentages = 2.723
Voids in the Coarse Aggregate - Dry Rodded Condition (VCA$_{DRC}$) = 42.5

Remarks: + #4 AGGREGATE SPECIFIC GRAVITY AT THE LISTED PERCENTAGES = 2.725. MIXING TEMPERATURE = 309-322°F ; COMPACTION TEMPERATURE = 271-280°F

Mix Design Reviewed by:

cc:
METRO INSPECTION
Contractor – HARDRIVES

Cells 86, 88

Figure A.6: Porous HMA Cells 86 and 88

BITUMINOUS PLANT MIX DESIGN REPORT
Minnesota Department of Transportation
Office of Materials
1400 Gervais Avenue
Maplewood, MN 55109
Phone (651) 366-5459
FAX: (651) 366-5580

0-2008-192

Date: 7/30/2008

THIS MIX DESIGN REPORT IS NOT VALID UNTIL PLANT NO. INDICATED BELOW IS CERTIFIED.

TO BE FILLED IN BY CONTRACTOR				SPEC	2360
				SPEC YEAR	2008
ENGINEER		FOR		MIX TYPE	SPWEB340(R)
PROJECT NUMBER	8680-157 (Mn/RD)				
				AC GRADE	PG 58-28

THIS MIXTURE HAS BEEN REVIEWED FOR VOLUMETRIC PROPERTIES ONLY, IT DOES NOT ASSURE THAT FIELD PLACEMENT AND COMPACTION REQUIREMENTS HAVE BEEN MET.

PLANT NO. 932051 - _____ JOB MIX FORMULA

Begin With Test Number

SP	WE	301

| - - | - - | - - - |

Sieve Size (mm) (in.)	Composite Formula	JMF LIMITS		For Information Only Virgin Formula
37.5 (1 1/2)		-		PERCENT PASSING
25.0 (1)		-		
19.0 (3/4)	100	100 - 100		100
12.5 (1/2)	89	85 - 96		87
9.5 (3/8)	83	76 - 90		80
4.75 (#4)	69	62 - 76		66
2.36 (#8)	61	55 - 65		59
0.075 (#200)	4.6	2.6 - 6.6		3.9
Spec. Voids	4.0	3.0 - 5.0		%AC (NEW) 4.5
Spec. VMA	14.0	13.7		
% AC	5.5	5.1		
(TOTAL)				

TM # 2008-122 Indicates a Gyratory Density of 147.5 (lbs/ft3) at 60 Design Gyrations

Use of anti-strip agent required: N

Proportions		Pit	Source of Material	Sp.G
40	%	71063	VONCO II BA SAND	2.626
20	%	05056	LOKEN MAN SAND	2.688
20	%	05056	LOKEN 3/4 ROCK	2.742
20	%		VONCO II MILLINGS	2.630
	%			
	%			
	%			
	%			

Mix Aggregate Specific Gravity at the Listed Percentages = 2.662

Remarks MINUS #4 AGGREGATE SPG AT THE LISTED PERCENTAGES = 2.639

Mix Design Reviewed by:

Mix Design Specialist

cc:
Contractor - HARDRIVES, INC
METRO INSPECTION

Cell 87

Figure A.7: Coarse, Dense Graded SuperPave Cell 87

APPENDIX B

Continuous Ride Plots
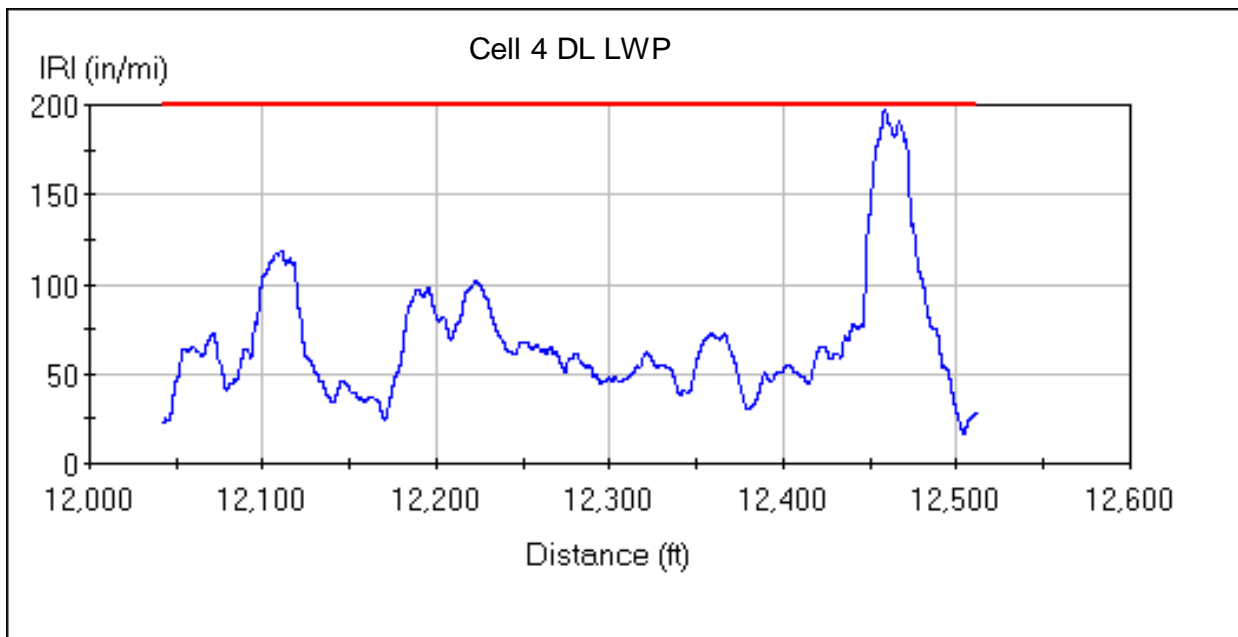
Figure B.1 October 2008 Continuous Ride Results, Cell 4 (Driving Lane, Left Wheel Path)
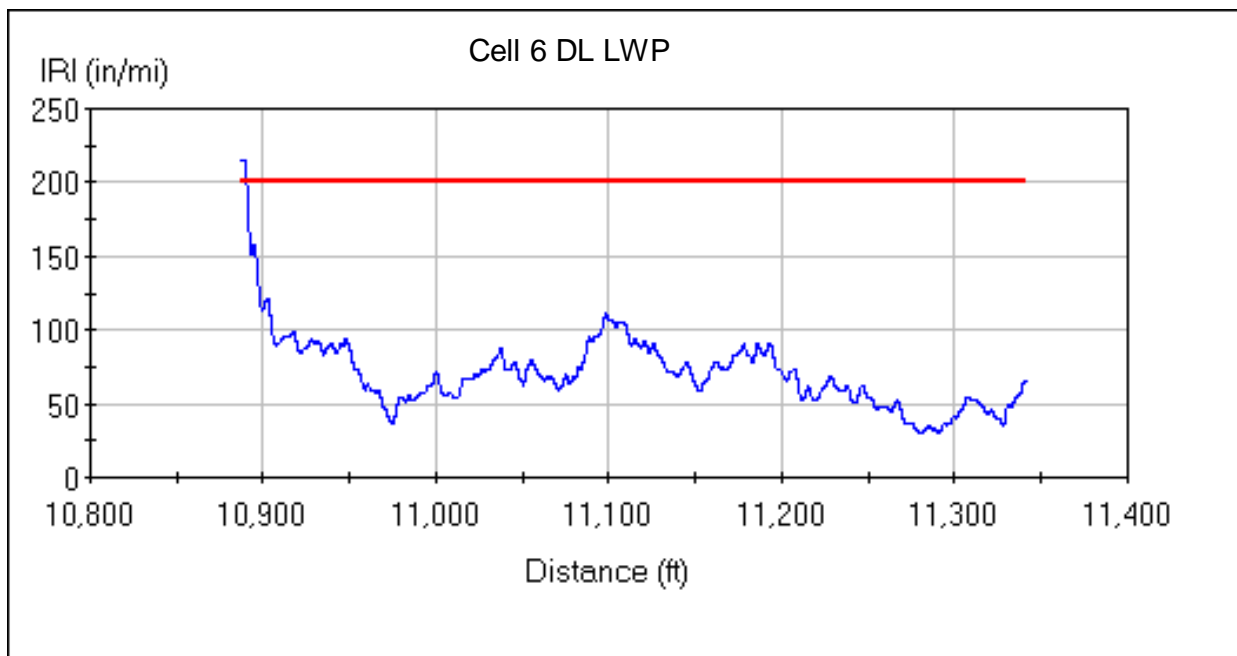
Figure B.2 October 2008 Continuous Ride Results, Cell 6 (Driving Lane, Left Wheel Path)
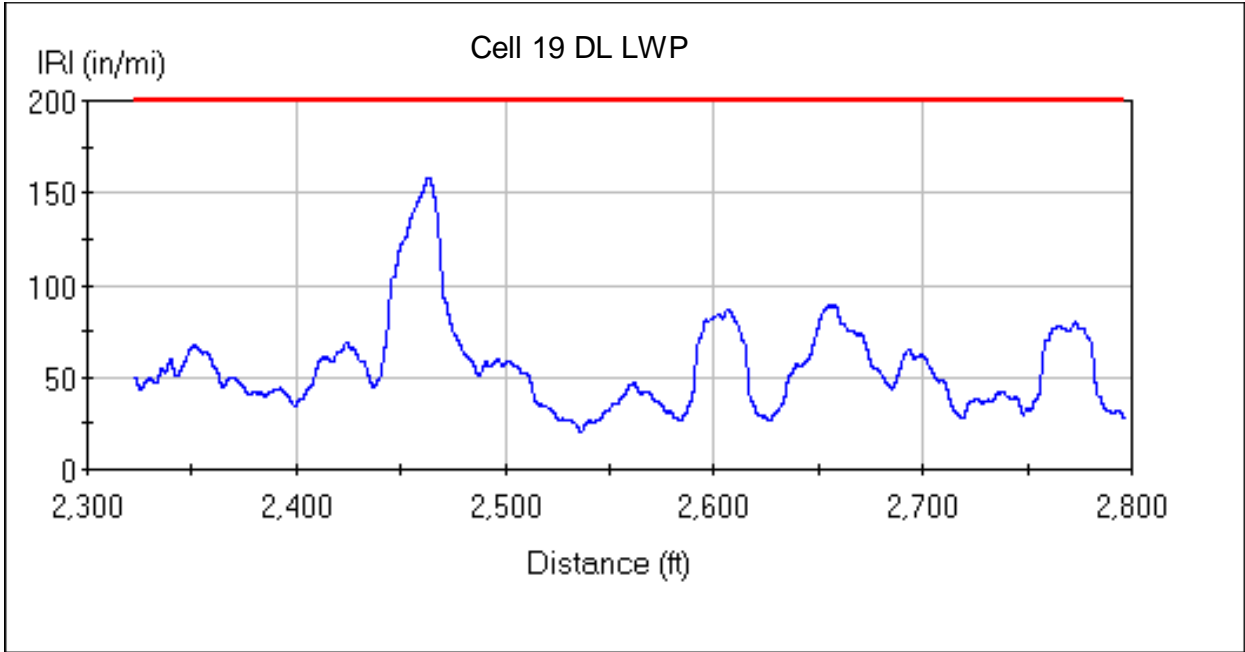
Figure B.3 October 2008 Continuous Ride Results, Cell 19 (Driving Lane, Left Wheel Path)
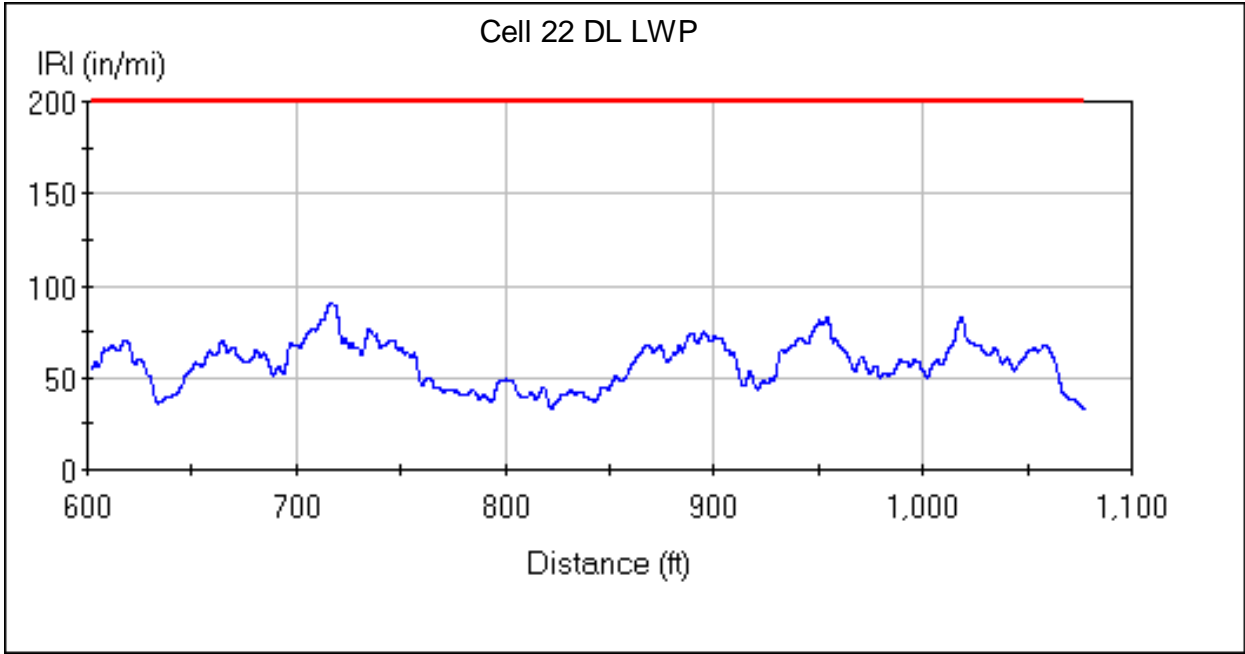
Figure B.4 October 2008 Continuous Ride Results, Cell 22 (Driving Lane, Left Wheel Path)

APPENDIX C

CT Meter Plots
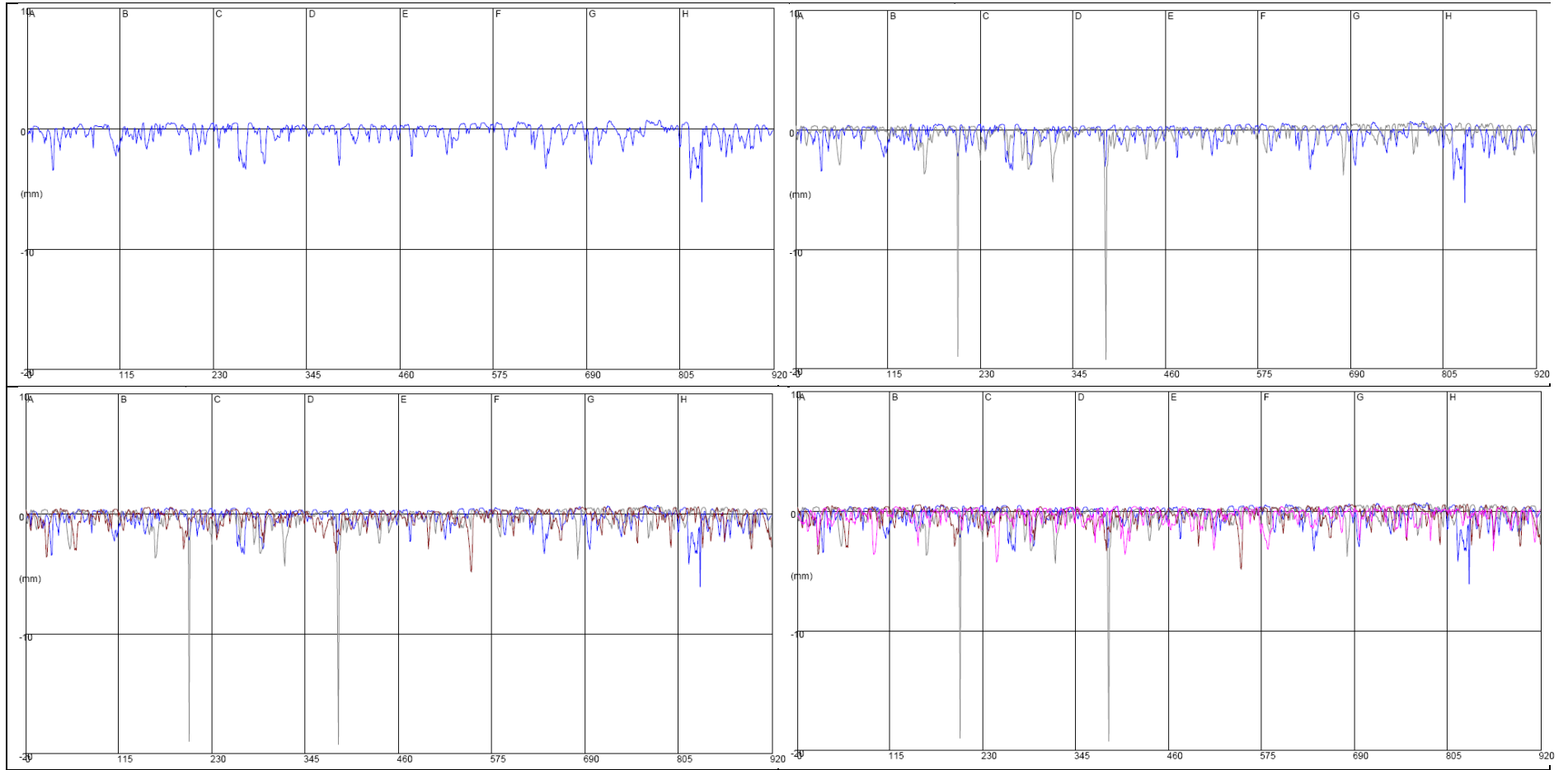
Figure C.1 Cell 3 (2, 4, 6 and 8' from fog line)

C1
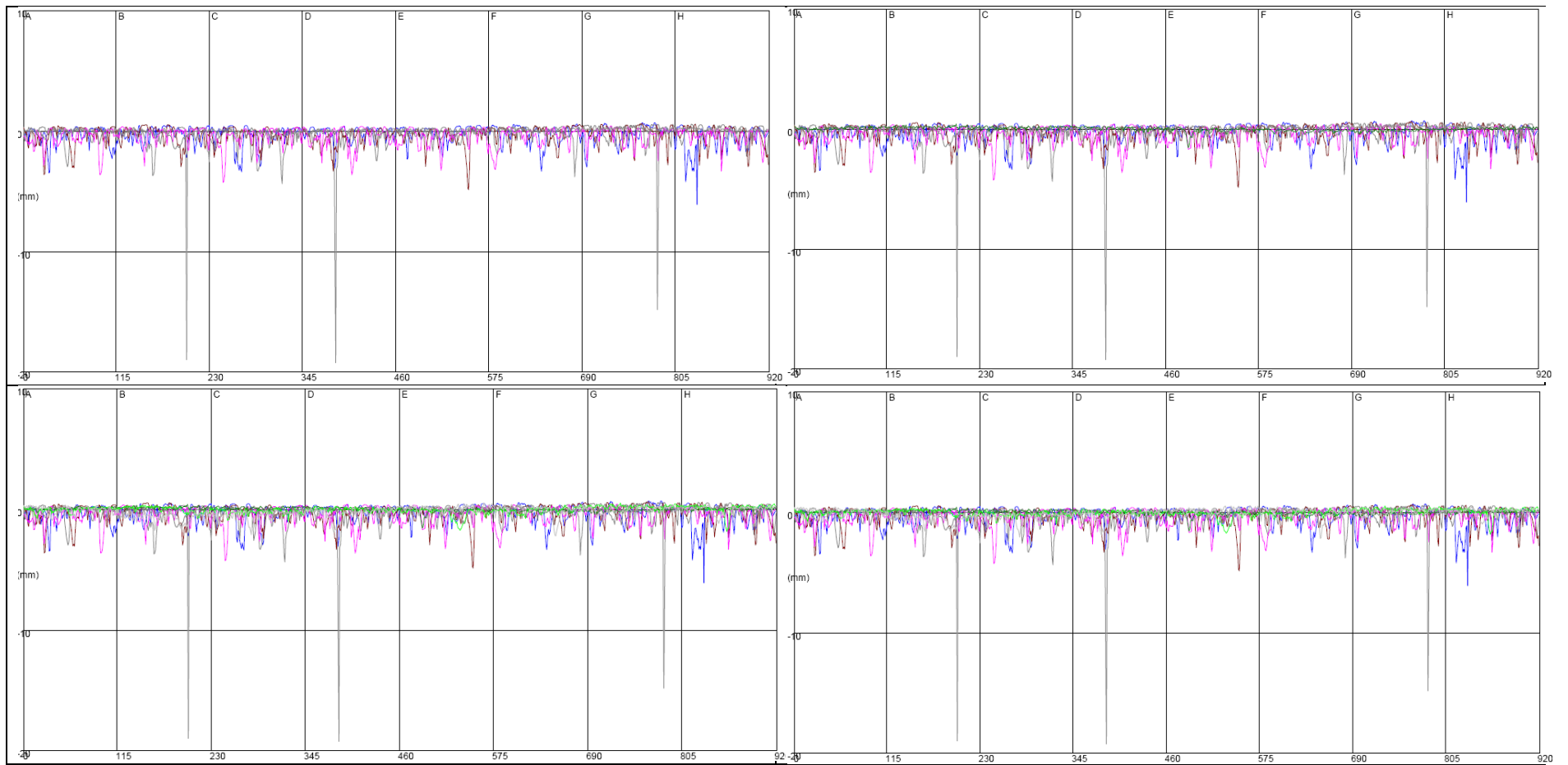
Figure C.2 Cell 4 (2, 4, 6 and 8' from fog line)
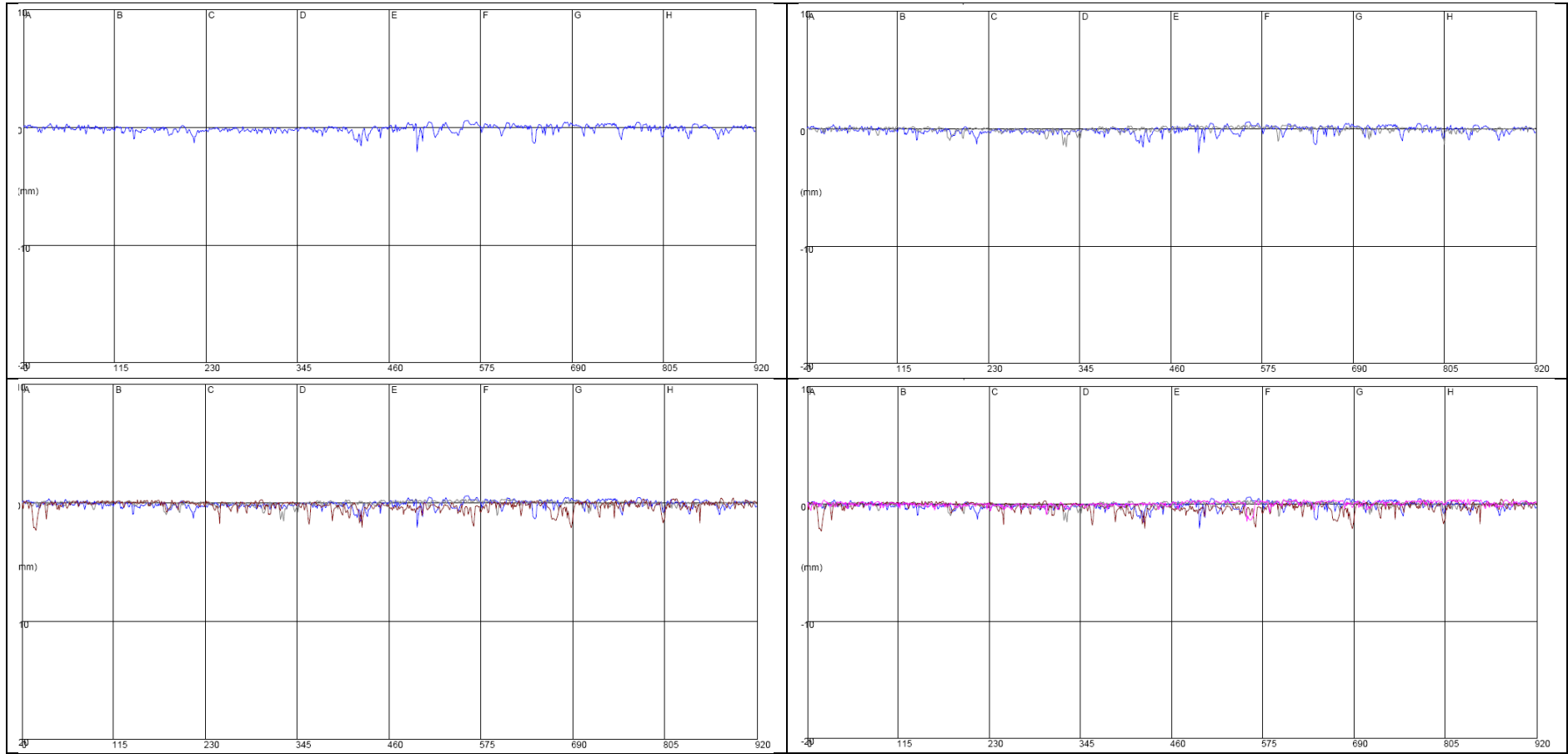
Figure C.3 Cell 19 (2, 4, 6 and 8' from fog line)

C3
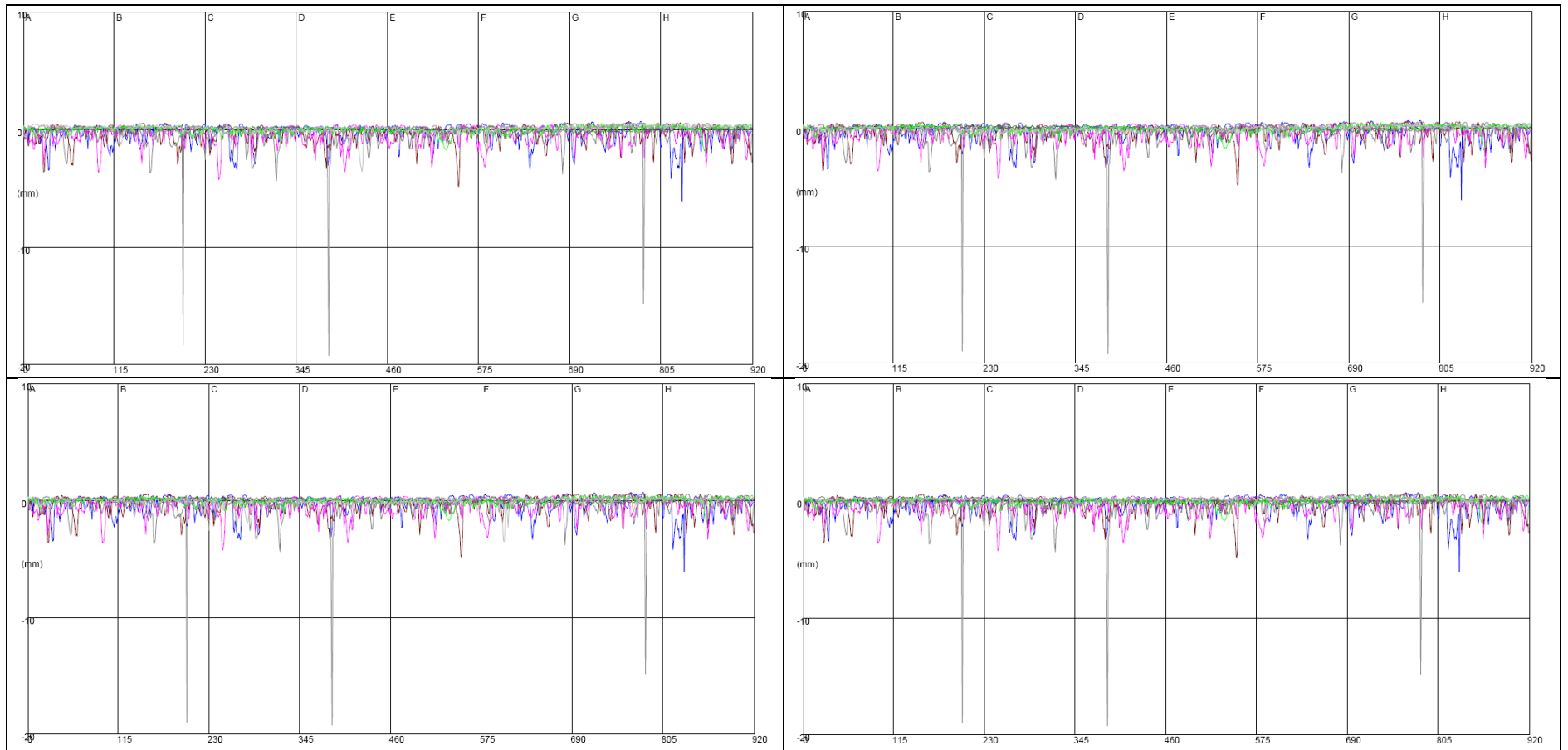
Figure C.4 Cell 22 (2, 4, 6 and 8' from fog line)

C4
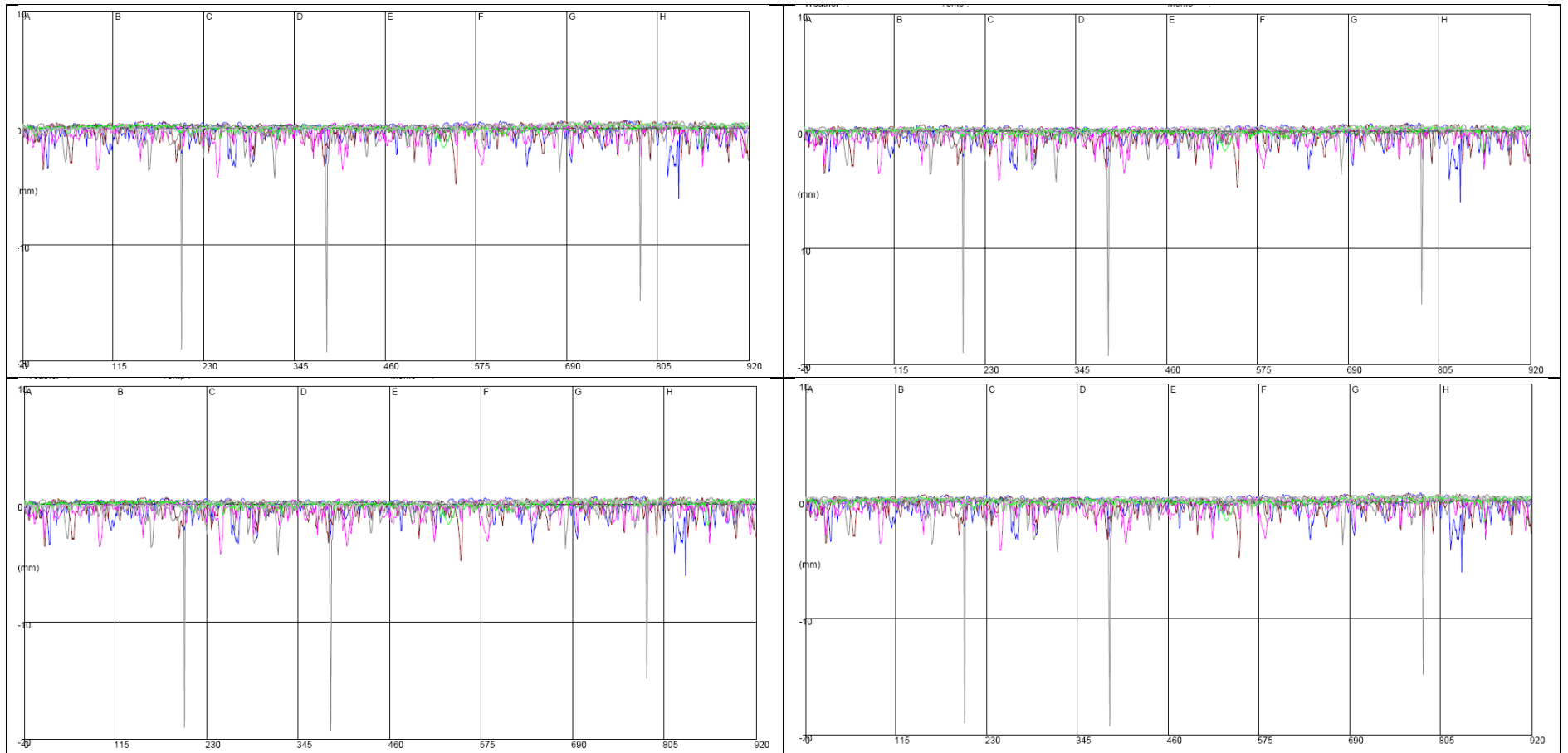
Figure C.5 Cell 24 INSIDE (2, 4, 6 and 8' from fog line)
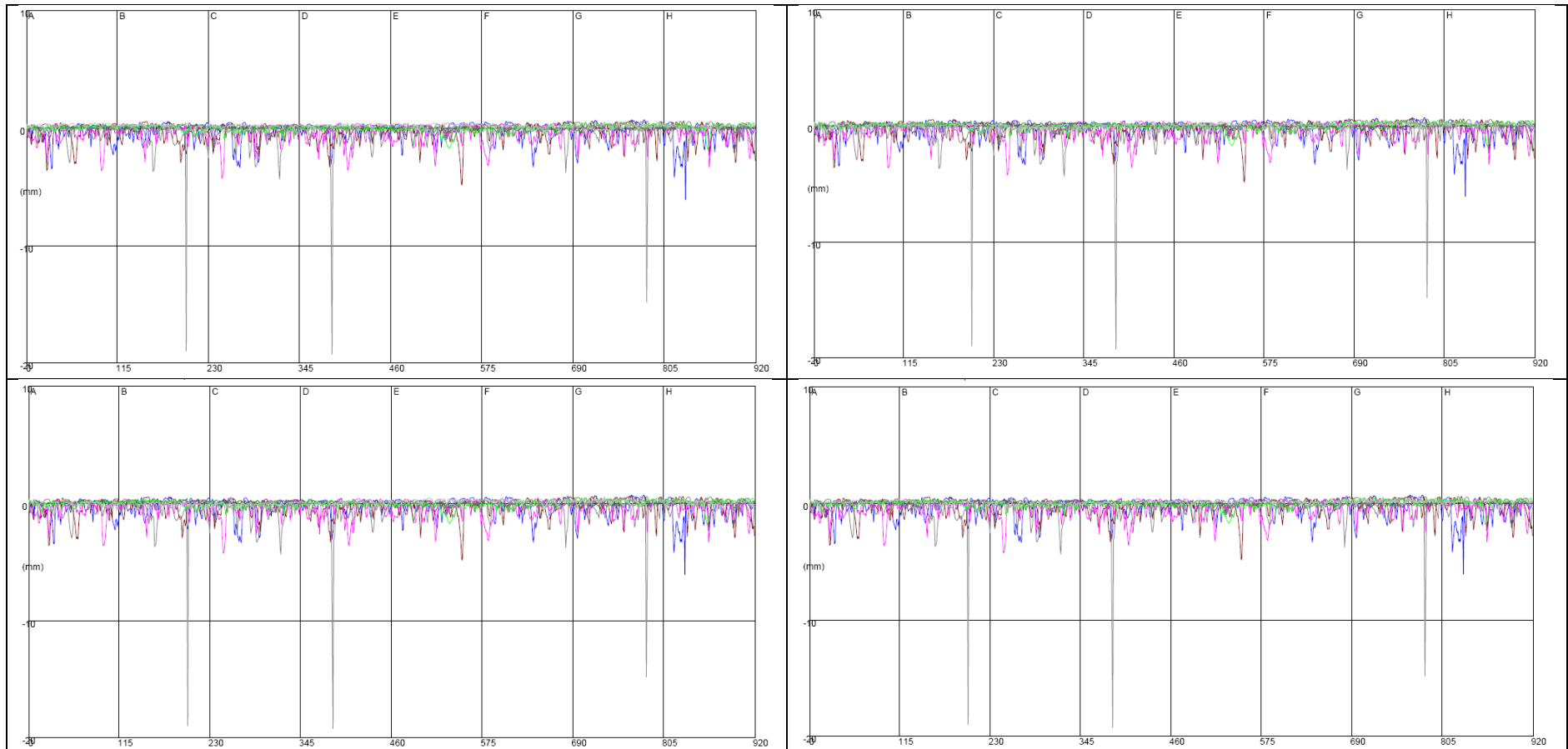
Figure C.6 Cell 24 OUTSIDE (2, 4, 6 and 8' from fog line)

C6
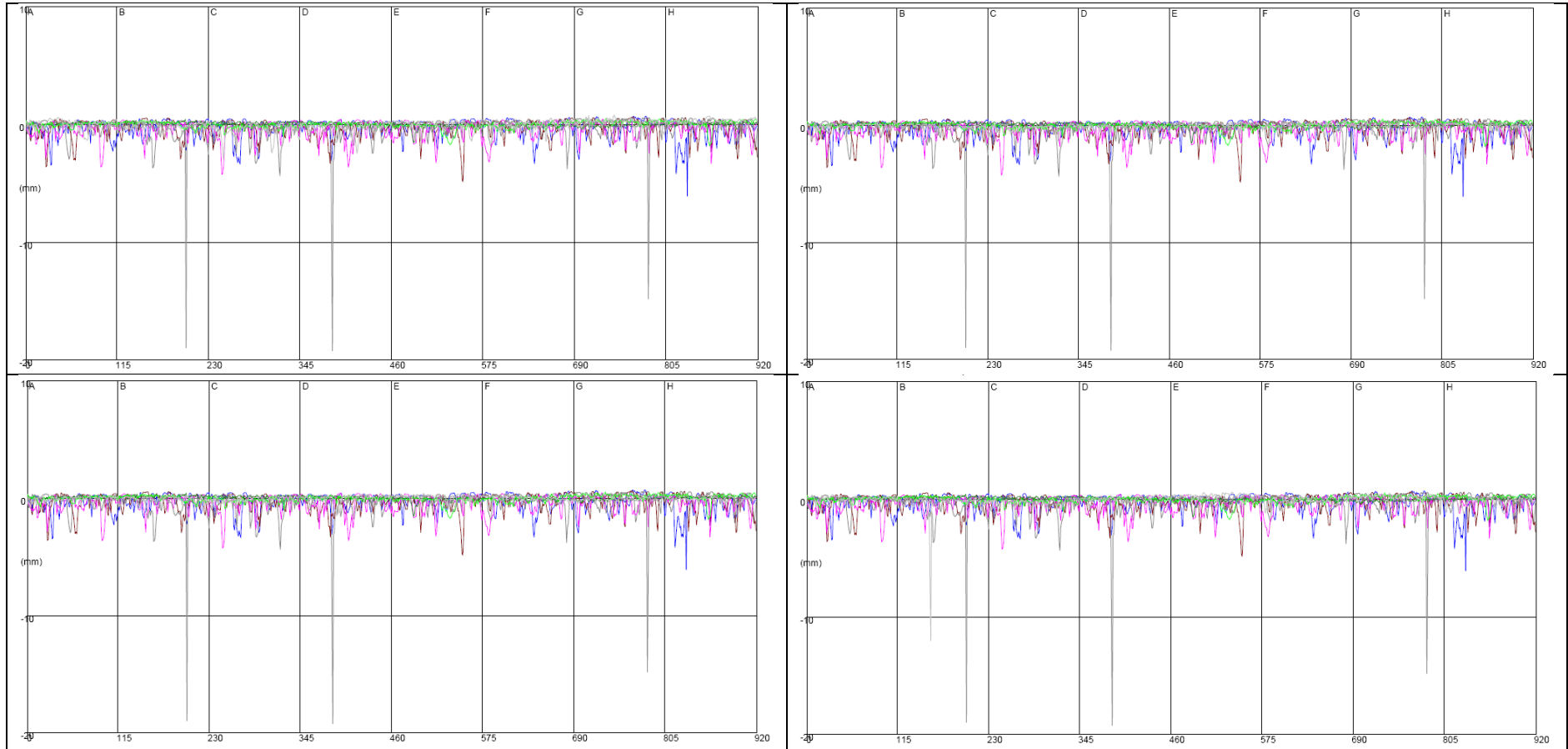
Figure C.7 Cell 86 (2, 4, 6 and 8' from fog line)

APPENDIX D

OBSI Plot
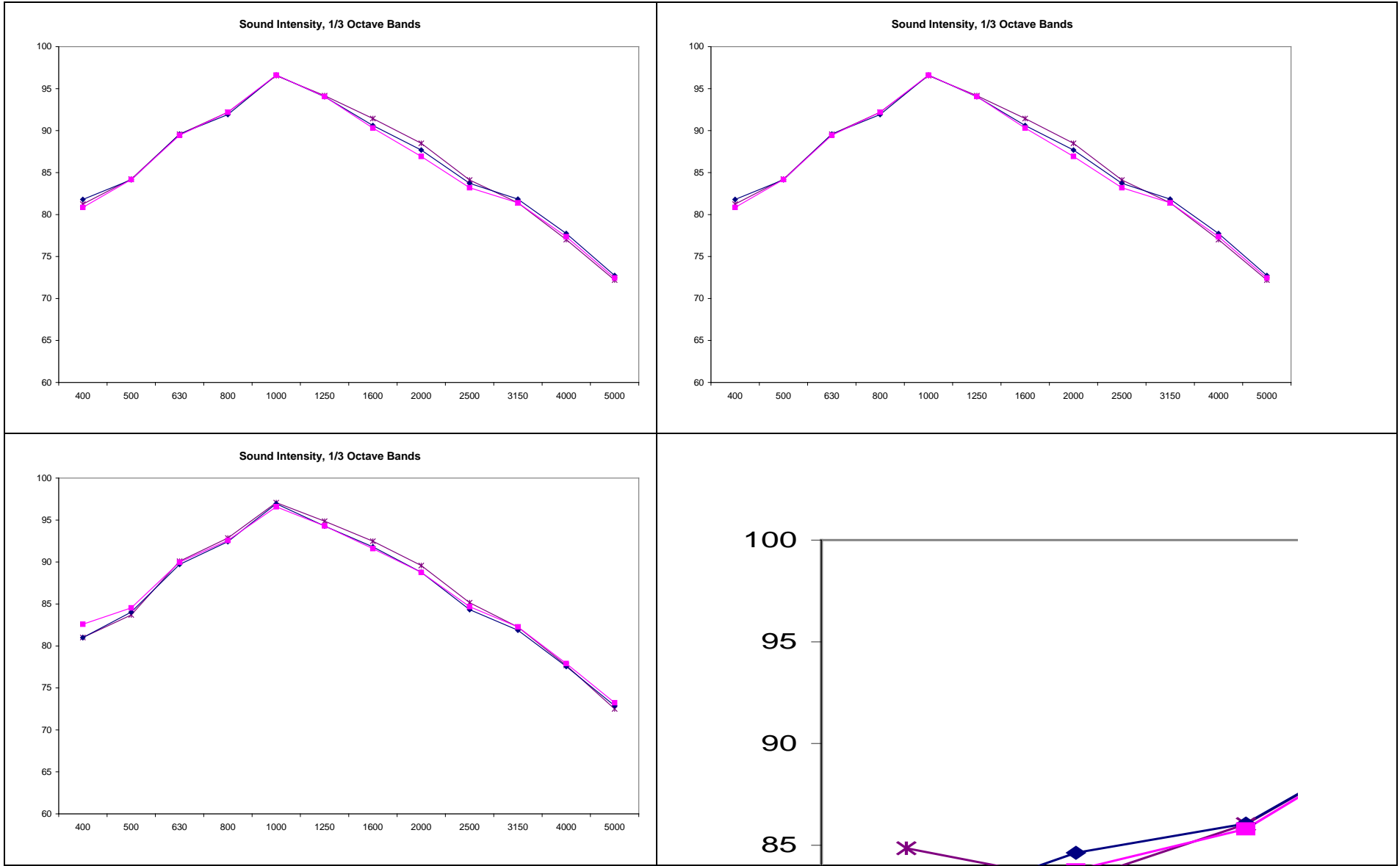
Figure D.1. Cell 2 (TOP), Cell 3 (BOTTOM); DRV LN (LEFT), PASS LN (RIGHT)

D1
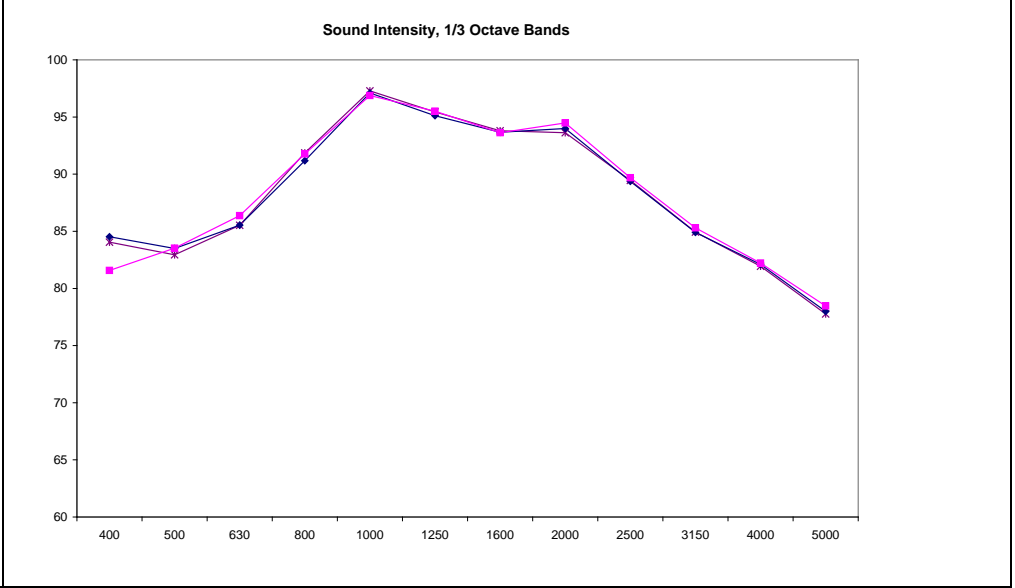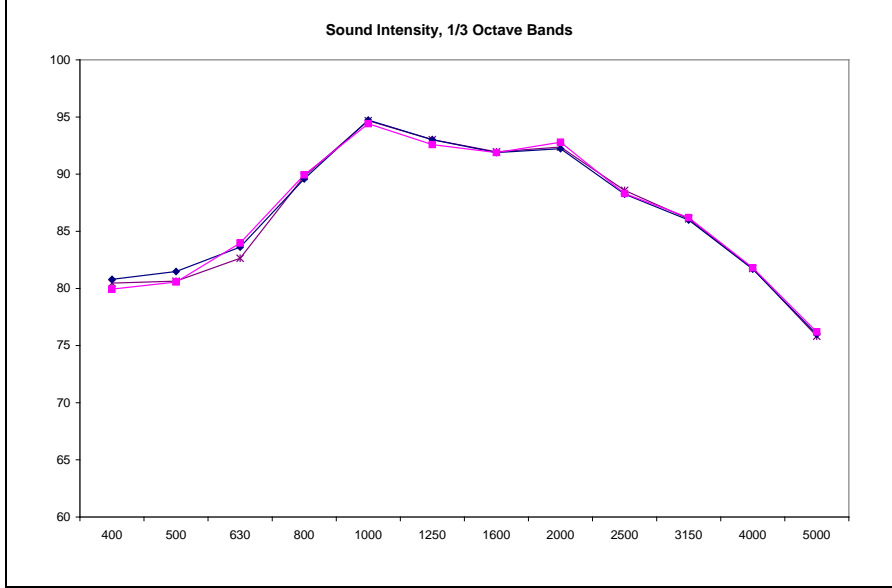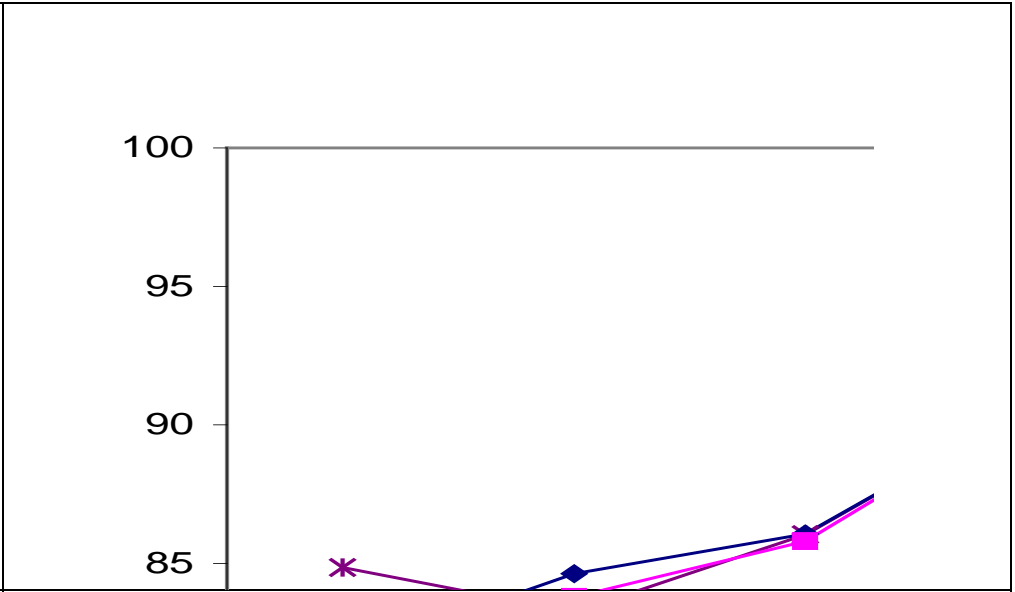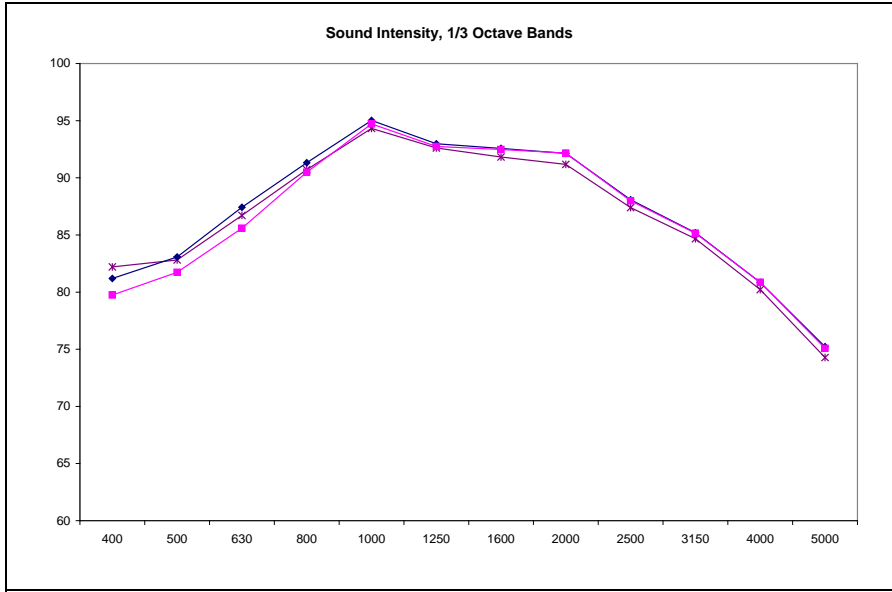
Figure D.2. Cell 4 (TOP), Cell 6 (BOTTOM); DRV LN (LEFT), PASS LN (RIGHT)

D2
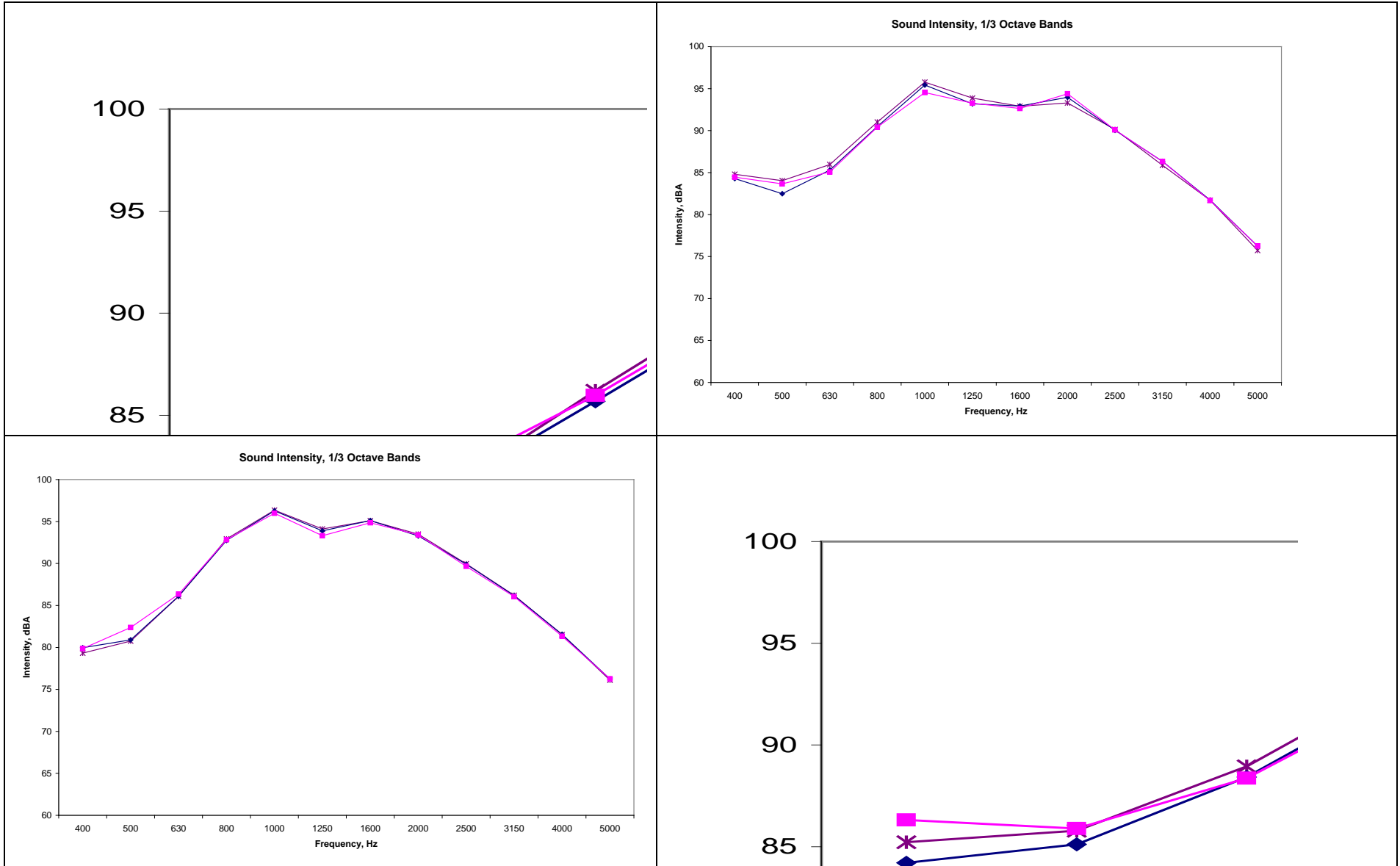
Figure D.3. Cell 19 (TOP), Cell 22 (BOTTOM); DRV LN (LEFT), PASS LN (RIGHT)

D3

APPENDIX E

1	2	3	4	15	19	20	22	70
6" 58-28 75 blow	1" TBWC 2"64-34	1" TBWC 2"64-34	1" 64-34 2"64-34	3"WM 58-34	5" WM 58-34	5" 58-28	5" 58-34	3" 64-34 Saw/Seal
	6" FDR + EE	6" FDR + EE	8" FDR + EE					6" PCC Recycle
	6" FDR	2" FDR		11" 64-22 1993 HMA	12" Class 5	12" Class 5	12" Class 5	
33" Class 4		2" Cl 5	9" FDR + Fly Ash					8" Class 7
		33" Class 3	Clay	Clay	12" Class 3	12" Class 3	12" Class 3	Clay 15'x12'
Driving Lane 1.5" 52-34 HMA inlay 2006	26" Class 4				7" Select Gran	7" Select Gran	7" Select Gran	1.25" dowels driving none passing
Clay	Clay				Clay	Clay 30% Non Fract RAP	Clay 30% Fract RAP	
		Clay						
Sep 92 Current	Oct 08 Current	Oct 08 Current	Oct 08 Current	Sept 08 Current	Sept 08 Current	Sept 08 Current	Sept 08 Current	May 10 Current

Figure E.1 Cell description for test cells 1-4, 15, 19, 20, 22 and 70

Original HMA	Stabilized Full Depth Reclamation			Recycled Unbound Base, Warm Mix Asphalt				Low Temperature Cracking, Fractionated RAP		
1	2	3	4	16	17	18	19	20	21	22
6" 58-28 75 blow	1" TBWC 2"64-34	1" TBWC 2"64-34	1" 64-34 2"64-34	5" WM 58-34	5" WM 58-34	5" WM 58-34	5" WM 58-34	5" 58-28	5" 58-28	5" 58-34
33" Class 4	6" FDR + EE	6" FDR + EE	8" FDR + EE	12" 100% recycle PCC	12" 50% RePCC 50% Class 5	12" 100% RAP	12" Class 5	12" Class 5	12" Class 5	12" Class 5
	6" FDR	2" FDR	9" FDR + Fly Ash							
		2"Cl 5								
Driving Lane 1.5" 52-34 HMA inlay 2006	26" Class 4	33" Class 3	Clay	12" Class 3	12" Class 3	12" Class 3	12" Class 3	12" Class 3	12" Class 3	12" Class 3
Micro Surface Aug 2012				7" Select Gran	7" Select Gran	7" Select Gran	7" Select Gran	7" Select Gran	7" Select Gran	7" Select Gran
Clay	Clay			Clay	Clay	Clay	Clay	Clay 30% Non Fract RAP	Clay	Clay
		Clay							30% Fract RAP	30% Fract RAP
Sep 92	Oct 08	Oct 08	Oct 08	Sept 08	Sept 08	Sept 08	Sept 08	Sept 08	Sept 08	Sept 08
462	500	454	500	500	500	500	500	500	500	500
97	60	156	75	50	70	70	50	90	80	80

Figure E.2: MnROAD Test Cells

E2